"Analysis and evaluation of efficiency criteria of modern high pressure injection systems under special consideration of future CO_2 targets"

DISSERTATION

To obtain the degree Doctor of Engineering

Submitted by Dipl.Ing. (FH) Stephan Revidat

submitted to the School of Science and Technology

of the University of Siegen

Siegen 2021

Supervisor and first appraiser

Prof. Dr. Ing. Thomas Seeger

University of Siegen

Second appraiser

Prof. Dr. Ing Michael Wensing

Friedrich-Alexander University of Erlangen-Nuremberg

Date of the oral examination

12. January 2022

„Analyse und Beurteilung der Effizienzkriterien moderner Hochdruckeinspritzsysteme unter besonderer Berücksichtigung zukünftiger CO_2 Ziele"

Inhalt: „Die Mobilität der Zukunft fährt elektrisch" – ein Satz, der die vergangenen Jahre geprägt hat. Der Schritt zu einer regenerativen Verkehrswirtschaft erfordert, aber global nicht nur den Einsatz von Batterien, sondern wird auch mittelfristig den Verbrennungsmotor benötigen. Die Komplexität einer rein elektrisch basierten Infrastruktur ist an vielen Orten nicht realisierbar, daher müssen synthetische Kraftstoffe als Alternative angewendet werden. Daraus resultiert jedoch ein Flickenteppich verschiedener Kraftstoffe, die unterschiedliche Einflüsse auf den Motor haben.

Der notwendige Wandel des Verbrennungsmotors als mittelfristige Antriebslösung bedarf nicht nur „klassischer" Optimierungen -wie Reibungsreduktion- sondern neuer Brennverfahren oder die Verwendung neuer künstlicher Kraftstoffe. Das Kraftstoffsystem fungiert hierbei als Bindeglied zwischen einem neuen Kraftstoff und dem Motor. Optimierungen in diesem System bewirken, aufgrund des niedrigen Gesamtwirkungsgrades von im Mittel 15%, signifikante CO_2 Emissionsverringerungen von bis zu 5 g/km im NEDC Zyklus.

Novum: Durch Zerlegen der Einflussfaktoren für die Gesamteffizienz leiten sich neue Möglichkeiten ab. So kann mit dieser dargestellten Methodik der zu erwartende CO_2-Emissions Einfluss vorausgesagt werden oder auch der veränderte Reibungseinfluss durch Kraftstoffe für Motorsimulationen verwendet werden. Ein simplifiziertes Kompressibilitätsmodel erlaubt zum einen die Anwendung auch bei unbekannten Kraftstoffen oder Gemischen (sogenannten „Blends"), zum anderen erlaubt es auch eine Rückrechnung zur Identifizierung des Kraftstoffes.

Um dies zu erreichen wird ein generisches Simulationsmodell parallel mit einer präzisen Leistungsbestimmung in einem passend konfigurierten „Design of Experiment" angewendet. Die Simulation liefert hierbei das Umgebungsszenario für das Einspritzsystem und wird zur exakten Leistungsbestimmung genutzt anhand der Messdaten genutzt. Dabei kann die Zustandssimulation des Einspritzsystems als „Vorarbeit" auf wenige Parameter reduziert werden und hinreichend genau der Leistungsbedarf im Motorbetrieb über einfache Interpolationen bestimmt werden.

Das Verfahren ist durch seinen generischen Ansatz vom Motor und Kraftstoffart unabhängig. Eine zusätzliche Zerlegung in mechanischen Einfluss und hydraulischen Einfluss erlaubt eine „Umrechnung" in andere Kraftstoffe.

Anwendung: Dies unterstützt die Auslegung eines Motors für länder- oder kraftstoffspezifische Applikationen jeder Leistungsklasse, um hier bestmöglich auf eine hohe Varianz im Markt vorbereitet zu sein. So können Emissionseinflüße neuer Brennverfahren durch veränderte Motorreibung bestimmt werden, mechanische Anwendbarkeit neuer Kraftstoffe geprüft werden, Regelstrategien verbessert werden und den Einfluss veränderter Hardware nachgewiesen werden.

Ferner lässt diese Methode es zu eine Effizienzgeführte „Raildruckregelung" zu. Diese würde nicht wie ein heute angewendeter PI –Regler auf einen Solldruck regeln, sondern es erlauben die energetisch sehr aufwendige Verdichtung des Kraftstoffs weiter zu optimieren.

„Analysis and evaluation of efficiency criteria of modern high pressure injection systems under special consideration of future CO_2 targets"

Content: „The future mobility will be electrified"– a phrase which has a significant impact on last year's development. Indeed, the steps to a sustainable society requires not only the application of novel high power battery technologies, furthermore will combustion engines play an important role to achieve this sophisticated target. Due to its high complexity, an infrastructure based on an electric energy only supply is in many locations not applicable. Thus, synthetic fuel solutions have to be applied as an alternative sustainable energy source. As a consequence, a huge variety of fuels may be brought into local markets with their own impact on the combustion engine.

The mandatory change of the combustion engine requires more than friction reduction, but also novel combustion approaches as well as the application of novel fuels. Herein, the fuel injection system acts as interface between the fuel and the mechanical engine operation. Nevertheless, this system suffers typically in its operation by its low total efficiency of ~15%. Therefore, optimization has shown that CO_2 emission benefits of up to 5 g/km in cycles are possible.

Novum: By separation of the total efficiency influencing parameters, new applications become possible. This method allows to predict the CO_2-emission impact by fuel injection systems as well as an application in a simulation environment to validate powertrain friction by fuel properties. Furthermore, a simplified compressibility model allows an application also with unknown fuels and possible blends. On the other hand, an identification of a fuel type is also an additional feature.

To achieve this goal, a generic simulation model of an injection system has been applied in combination with an accurate power demand measurement in a well-matching design of experiment. Herein, the simulation generates results of operative conditions data while the measurement allows an accurate determination of fuel systems power consumption. The operation condition simulation can be reduced to a minimum of initial parameters as a pre-processing, to calculate the power demand of the fuel injection system by an interpolation in real-time.

In principle, the method is by its generic approach independent of engine and fuel type. An additional separation in mechanical and hydraulic influence allows a processing of measurement and layouts in different fuels becomes possible.

Application: The novel approach has the intention to support the development to be prepared in best way for upcoming high fuel varieties in the market. Therefore, it supports the layout and dimensioning of engines to country or fuel specific application in every performance class. This allows the prediction of emission impact by novel combustion impact by changed engine friction, mechanical application performance by new fuels, influence by rail pressure control strategies and the impact by exchanged injection hardware.

In addition, this new method opens the possibility to a novel efficiency-based rail pressure control strategy. It differs from a today typically used „simple"PI-Controller by application of efficiency as parameter to achieve a lowest power consuming high pressurization of fuel.

Contents

0. Abstract

With focus on CO_2 reduction of combustion engines, several steps have been taken into account to achieve global targets. One notable step is the improvement of subcomponents. As one in today's major engine families, fuel injection equipment has, by means of its high pressure levels, a significant impact on total power consumption. Pre-executed measurements showed high impact in reducing 1% of the entire vehicle fuel consumption in driving cycle by simple parametric modification such as modification of springs. To understand these phenomena and utilize knowledge as none or low cost fuel consumption improvement, investigation has been initialized. Since pressure levels nowadays increase on gasoline direct injection engines, high pressure system impact becomes a higher priority.

This particular analysis contributes as first step an analysis on physical boundaries during pressurization as well as listing all parts contributing to fuel system demands. Hardware analyses of applied components build foundation for this analysis, including engines mechanics interfaces. Also a generic simulation model utilized for gasoline injection systems and Diesel injection systems, supports in investigation of actual conditions during engine operation. A new simplified model to describe compression of fuel has been created, to explain impact by altering fuel on system efficiency.

For confirmation and to create background data for further investigation or possible improvements, measurements from component test bench, engine test bench and chassis dyno for entire vehicles were applied and executed. In total, entire evaluation contains analysis of several fuel injection systems for Gasoline engines, passenger diesel engines and commercial engines. In addition, to have a higher focus on integrational parameters, a study on engine interface has been executed including own unique setup. Data acquisition and handling for fuel injection system front load data has been generated. A commissioning of all above mentioned features was compared to all measurement data.

Ultimately, given analysis opens doors to estimate impact of new combustion methods, new fuel types including fuel quality and conventional component impact, whereby by parameter optimization becomes reasonable. Therefore, integration into simulation models or complete cycle investigations support future engineering in higher fleet complexity as forecasted by today's global market development.

As future perspective, a novel controller type has been created as well as new parameters for intelligent engine controls, which allows to adapt engine calibration online to its sourcing fuel.

1. Introduction

In nearly all industrial countries across the world, the combustion engine maintained itself as a reliable tool for personal and commercial mobility. Long distances with heavy goods or traveling across the land are possible since the first car was developed by Carl Benz in 1885 [1]. From that day on, the automobile industry grew very strongly to become one of the worldwide major industries.

Due to the wide spreading of automobile across the world, the industry today has to encounter different challenges. Exhaust gas regulations for carbon-monoxide (CO), nitrogen oxide (NO_X), soot and far more unwanted combustion products are already regulated by different exhaust gas emission laws all around the world. A newer target and also one direct measurable parameter for the customer is the regulation of Carbon-dioxide (CO_2). Therefore, governments set up CO_2 emission targets for the automobile industry. The last one for the European market is 95 g/km in 2020. With 56% less greenhouse gas, like CO_2 from combustion of crude oil, until 2030 for the transportation sector, the German governments set up a hard milestone for the entire German industry [2].

At first glance, this regulation offers a good way to spare money for the customer and to preserve the environment as well as the rare oil resources of the earth. Especially the customer has significant benefit by lowered fuel cost. Unfortunately, reaching those goals is connected to the introduction of more complex powertrain technologies, e.g. hybrid vehicles, or other types of powertrain concepts with significant demerit(s), e.g. battery electric vehicle. Both key points are connected to higher costs for the customer, up to 12000,- $ [3]. This fact may be acceptable for first world countries, but for margin markets (e.g. South America or India) this is barely acceptable and affordable.

Also the medium and heavy duty transportation as well as off road application encounter lower potential for CO_2 reduction by Hybrid powertrain concepts and battery electric driven trucks will not be adequate in driving range, power output for transport and cost of ownership until 2030. Although, costs for alternative fuel have to decrease from today approximately 4,50 € per liter to a suitable cost range. Approaches in fuel have a wider range. Therefore, algae based diesel, oxygenated or hydrated vegetable oil could replace today's fossil fuels. One major parameter remains in legislation and their acceptance of alternative CO_2 calculation than today tank to wheel approach [4].

1.1. Next developments in powertrain technologies

Not even since the "Dieselgate" in 2015, but years before strong discussion to new powertrain technologies arose within society and industry. As a result, our current level of technology for powertrain developed since 1881. The first electric vehicles, built by Gustaf Trouve and later Werner Siemens in 1882, drove earlier than Carl Benz Motorwagen in 1885 [1]. Until the early 20th century, the sales number of electric vehicles and internal combustion engine vehicle were at similar level. After the two world wars, the internal combustion engine revealed itself as the most practical solution. Not only in terms of range, but also in terms of handling [5]. The electric vehicles were always under development, also parallel to internal combustion engine. One famous example is the Ford Concept in 1982 as it was also shown in the movie Blade Runner.

Later fuel cell vehicles and hybrid vehicles started as alternative for the internal combustion engine [6]. But even the hybrid vehicle requires a combustion engine, at least as generator. And on commercial and heavy duty side, hybrid or even electric vehicle are currently not relevant options for the market [7].

Even when powertrain technologies are still under discussion and strong development, the internal combustion engine will be the major technology in the near and wider future [2].

1.2. The necessity of fuel injection equipment in modern powertrains

The circumstance of "decarbonized" future, as it is proposed by nearly all large industrial countries, leads to the scouting for new approaches in mobility. The simplest idea is still to exchange fuel production from crude oil to alternative fuels made from reproducible sources. Also it is a concept which can be taken into account in nearly all countries over the world. The cost for replacing a fluid in a gas station are far lower than building up new electric sources including all wiring for full electric vehicles. Additionally, heavy duty approaches can still be taken into account.
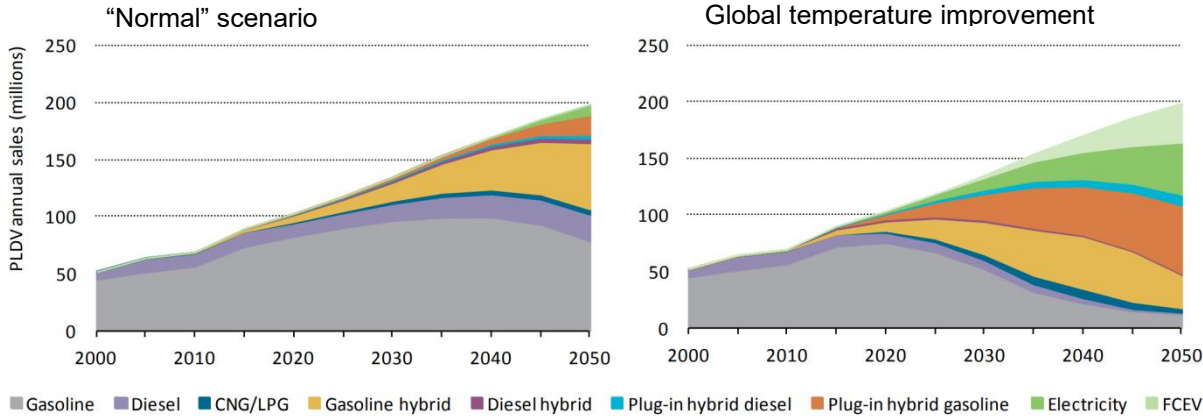
Figure 1: Share of alternative light duty sales up to 2050 [8]

As shown by the International Energy Agency (IEA), the worldwide major mobility concept for passenger light duty vehicle (PLDV) will be based on a combustion engine passenger, despite if global economy behaves "normally" and allows a global temperature increase by 4°C in 2050 or improves global temperature level [8]. Even in "improved" cases, the worldwide peak production of combustion engines for light duty vehicles is expected between 2035 and 2040 [8].

To ensure a proper function of engines, which running with crude oil products up to new engines with next generation (Bio)fuels, the fuel injection equipment (FIE) needs to be adopted for those fuels or – at least- need to be very robust.

One conclusion of the IEA study is fuel economy improvement by energy saving and emission reduction [9]. Reviewing costs for integration of new technologies into the powertrain, the automobile industry accepts up to 50,- € [10] per gram CO_2 saving in the New European Driving Cycle (NEDC) [12].

Especially in countries with low income (e.g. margin countries like India) high cost build obstacles, which leads to a rejection by society. Reviewing up to 2050, especially in India large

growth of road occupation (= sales in transportation) is expected [11]. Due to its infrastructure condition, India cannot achieve this high amount by battery electric driving. Lowered cost approaches for fuel consumption reduction -like engine optimization- have higher potential for acceptance [11].

Furthermore, pressurizing fuel for direct injection consumes a significant amount of power, which is a loss for the entire powertrain. By category, those losses are defined as frictional losses with same potential for low cost optimization. This can be applied to all types of combustion engines independent from size and fueling. Also small gasoline based engines with direct injection in a hybrid powertrain are affected and will achieve lower fuel consumption, as well as large size commercial Diesel engines have herein room for optimization. In addition, alternative fuels require in some circumstances a modification of the FIE to maintain proper function under all condition in all countries.

1.3. Next goals for future fuel injection equipment

The combustion engine in any type of integration will be also for the next 30 years the driver of the world wide mobility [11]. The goal for lower fuel consumption was since the beginning of this technology one major technology driver and will remain in the future as one major goal. Therefore, the FIE -with its high power demand for pressurization- also needs review in terms of lowered power consumption. Especially the direct Diesel injection was in the past in focus for optimization. The Gasoline Direct Injection (GDI) –with pressures of 350bar in serial production- starts today to get into focus for power consumption optimization. Herein particulate number of GDI engines have to achieve stronger limits by new upcoming legislations word-wide.
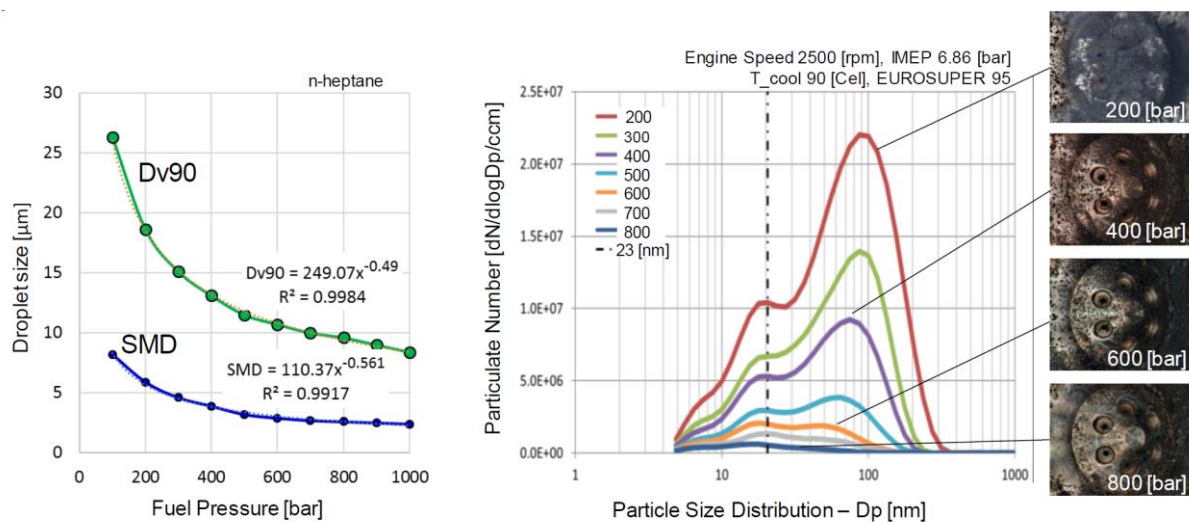
Figure 2: Impact by GDI pressure level on Particulate Number [12]

The illustrated counter measure for increasing particulate number in *Figure 2* demonstrates one focus in automotive industry development: Reaching ideal pressure levels for highest cost efficient products [12]. Therefore, utilization of higher pressure targets the reduction of other components to achieve legislation levels, such as Gasoline Particulate Filters [12]. This development also targets the improvement in real vehicle usage conditions as they are introduced into the US SULEVIII certification.

Exhaust gas limits for SULEVIII Bin20 (for FTP cycle)				Test range	
#	Specification	NMOG + NOx	CO	PM	Milage	Special
1	„Standard"	0.02 g/mile	1 g/mile	0.003 g/mile	150.000 mi or 15yrs.	Any US fuel quality
2	„High altitude"	0.03 g/mile	Same as „standard"			E0
3	„Low temperature"	0.3 g/mile	10 g/mile		50.000 mi	-7°C (20°F)

Table 1: US SULEVIII exhaust gas emission regulation as binding from 2021 [14]

The legislation targets mentioned in the table above represent future targets of new legislation, which will come up all over the world. Not only strict exhaust emission in laboratory conditions have to be achieved, also usage condition and severe test ranges above 200.000 km with unregulated fuel quality has to be considered for operation [14]. Especially aging of exhaust gas emission system and operation ranges of such systems increase vehicle cost significantly. As a result, providing low raw emission levels support achieving sophisticated emission targets.

A new demand, as a reaction of the "decarburization", is to analyze the impact of new type of fuels. Due to different heat values of different fuels, different required pressures for clean combustion and different viscosities of new fuel mixtures, new types for pressure generation are required. Qualified knowledge for these new fuels and their impact on old and new systems are not given. Especially the basic information of power consumption for the engine and therefore for the complete vehicle were only vaguely given.

HMETC reviewed in the past 5 years FIE's by different suppliers and realized the strong impact of the pressure generation to engine fuel consumption, especially for modern Common Rail Diesel engines. By this experience, HMETC decided to analyze the physical boundaries of fuel properties, pressure generation and pumping method and engine integration for lower fuel consumption of future powertrains by lower costs. Measurement of the impact instead of commonly used simulation methods forms focus of this analysis. Former strong differences between measurement and simulation build background of this decision.

1.4. Challenges and targets

Driven by its change to encounter future worldwide legislation and will to build a sustainable mobile society, conventional and novel fuel injection systems require a deep understanding. Therefore interaction and interfaces between combustion engine and its components have to be revised. Not only to identify losses or additional approaches for optimization, also to support the possible change from fossil fuels to carbon neutral fuels.

One limitation today is the availability of information about fuel injection system energetics, due to lower priority within the scope of research and development activities in the automobile industry. This leads to missing information on detailed impact by equipment composition, fuel

type and quality as well as final engine integration [15]. An analysis in this particular field shall enhance knowledge and understanding to predict loads and frictional impact by the FIE. This includes detailed impact by components (e.g. pumps and injectors), as well as calibration and impact of altering fuel type. In addition, the enhanced knowledge shall also predict operation ranges for novel engines modes and alternative fuels. As emission results within specific test cycles determine the "standard" in among automotive industry, effects on the entire vehicle in such driving cycle have to be evaluated for final results. Thus, CO_2 emission is a final marker for evaluation result. Also, as this included method shall focus on a generic approach, elements and models for simplification have to be defined.

As procedure in an analysis for the fuel injection equipment related losses, first step leads to hardware review and their designated operation systems. As a first approach, related engine are separated in passenger size gasoline engines, passenger size diesel engines and commercial diesel engines. Therefore chapter *2* describes as introduction the detailed engines as detailed content of analysis. The following chapter *2.1* explains common automotive understanding and basic boundaries on standardized evaluation principles, as driving cycles.

A detailed review on hardware for fuel injection, the FIE, is listed up up chapter *2.2* including all sub-chapters. Since core features of such systems are implemented in today's hardware approaches, a detailed review by each component type becomes necessary. This leads to next major item for analysis, the fuel itself. The chapter *2.3* and its sub-chapters explain therefore necessary boundaries in worldwide used fuel types and qualities. To finalize the background review, mathematical as well as engineering approaches used today are listed in chapters *2.4* and *2.5.*

As analysis requires non-standard tools and methods, the individualized methods and campaigns have to be described in detail. Therefore, the chapters *3.1* to *3.5* describes all related test bench build ups and measurement procedures for especially all power consuming components within the FIE. Also test procedure on engine dyno and chassis dyno are explained. Nevertheless, as some effects and boundaries are hardly measurable, generic simulation models have been established in order to support the analysis. The applied simulation models in LMS AMESIM and their purpose are explained in chapter *3.6* and all sub-chapters.

The entire chapter 4 reviews measurement results on selected systems in an order from "small" sub-component to the "large" entire vehicle. The chapter *4.1* gives an overview on performance aspects especially high pressure pumps and item wise selected samples. This shall mean basic geometry and operation modulus remains as state, but performance differs among the samples. In this review, also a specialized measurement campaign on integrational parameters is located in chapter *4.2.* as well as the measurement on supply systems in chapter *4.3*. As finalization on measurement campaign, the chapters *4.4* and *4.5* contain the measurement results on engine and chassis dyno.

The entire chapter *5* evaluates the measurements results of chapter *4* and utilizes generic simulation models of chapter *3.6* to understand the measurement results. Herein, also a structure from "small" component to "large" vehicle entities is applied. The chapter *5.1* evaluates the impact caused by performance differences of the sub-components. The following chapter *5.2* evaluates the impact of the FIE on the entire vehicle. Thus, this chapter focuses mainly on impact of supply system and its contribution to entire power consumption. Since fuel has a special interest as todays fuel are changing fast, the chapter *5.3* evaluates impact on

FIE system performances based fuel abilities. Herein a novel and patented method to determine fuel type, blend and quality on board is explained.

The chapter *6* sums up the measurement and evaluation results based on the three target aspects of component performance in chapter *6.1*, calibration and combustion process related impact in chapter *6.2* and fuel type and quality related impact on *6.3*. On each aspect, the most relevant achieved result is summed up. As finalization of the analysis, the chapter 7 contains future possibilities based on the result. Therefore, new approaches and possible optimization of independent fuel pressurization for the entire vehicle performance is shown.

2. Fuel injection equipment and its impact on engine performance losses

Despite their combustion concept, power generation (torque and speed) as a major task defines every internal combustion engine, from smallest single cylinder engine for multipurpose up to large scale engines for marine application. Thus, correct sizes and working principle defines the appropriate engine for a specific application [16]. Since this analysis is focused on "On-Road" application or vehicles, engine sizes from 1 liter up to 6.3 liter displacement for Diesel and Gasoline 4-stroke engines are analyzed. This selection also fits into the Hyundai Motor Company engine portfolio, which represents engine families for evaluation as shown in following *Figure 3* [17].

Figure 3: Hyundai Motors engine portfolio [17]

In this portfolio range, especially Theta and R-engine have high sales number and therefore special interest for CO_2 reduction measures in countries with challenging CO_2 targets. Both engines meet Euro 6 legislation and are sold across the globe. Thus, these engines represent "mean" engine for their specific combustion concept and will be referred in more details. Nevertheless, also commercial engines encounter strong CO_2 targets. Especially "cost of ownership" plays major role for commercial engines, which also includes the fuel consumption as one mandatory parameter for sales. The G – engine, as one of the large engines in the vehicle market, will also be taken into account for CO_2 emission analysis.

Engine family	Theta-engine [18;19]	R-engine [20]	G-engine [21]
Picture			
Displacement	2.0 ℓ	2.0 ℓ 2.2 ℓ	6.3 ℓ
Max. power	202 kW @6000 rpm	135 kW @4000 rpm 145 kW @3800 rpm	220kW @2500 rpm
Max. torque	378 Nm @1750-4200 rpm	392 Nm @1800 -2500 rpm 436 Nm @1800 – 3500 rpm	1070 Nm @1200 rpm
Legislation level	Euro 6	Euro 6	Euro 6
Injection type	Gasoline Direct Injection	Common Rail Diesel Direct Injection	Common Rail Diesel Direct Injection
Max. rail pressure	200 bar	2000 bar	2000 bar

Table 2: Base engines for investigation

All engines provide fuel direct injection as common injection type with rail pressure level in medium state of the art pressures. Currently, 350bar for gasoline engines and 2500bar injection pressure for Diesel engines maintain the "high end" applications in on-road mass production. Injection pressure up to 1800bar for gasoline [22] and above 3000bar for Diesel application [23] are in focus for current research projects.

Similar to other auxiliaries, like oil pump or alternator, in engine build up, the fuel injection equipment (FIE) feed the engine with critical supply for its function. Modern engines with direct injection require additional power for pressurizing the fuel to current high levels. By increasing the pressure and flow demand, which is depending on the engine power output, the power demand of FIE is also increasing.

2.1. Basic boundaries on fuel and testing

Fuels used today are mainly based on crude oil and therefore have a fossil base. During development over the last 100 years, crude oil generates majorly four different fuel types for multiple purposes. For passenger and commercial purpose, Diesel and gasoline fuels become major powering source. For maritime purposes, such as ships, heavy oil becomes major source of energy. For flights, Kerosene delivers power to airplanes' jet engines [24].

From a chemical perspective, fuel combines carbon and hydrogen chains in different chain lengths, defining their physical properties.

Name	Density [kg/m³]	Heat value [MJ/Kg]	Chain length	Combustion Specific	International standard
Gasoline [25] (E5 & E10)	720 – 775	40,1 – 41,8	Methanol (CH_4O) *Up to* i-Butanol ($C_4H_{10}O$)	RON min. 95	DIN EN 228
Diesel [26] (B7)	820 - 845	43,0	$C_9 – C_{26}$	Cetan min. 45	DIN EN 590
Heavy Oil [26] (Bunker C)	960 - 1010	-	C26 - ~C70	Cetan min. 40	Residuals as in ISO 8217
Kerosin [27] (Jet A1)	750 - 845	42,8 – 43,5	$C11 – C12$	-	Military F35

Table 3: Exemplary fuel products in today fuel markets [25;26;27]

The principle of today's crude oil refinery process utilizes the complete bandwidth of molecules. Basic distillation process allows production for several different target applications, as exemplary stated in *Table 3* [26]. In general, the C-H molecule length determines basic abilities, in terms of density and distillation, while heat value remains overall in range of 41 MJ/kg. Best fitting combustion concept analysis utilizes "artificial" measurement by reference elements, which represent the individually required properties for each combustion concept. Thus, "Research Octane Number" (RON) represents number of reaction unwilling molecule Octane within fuel blend. "Cetan" index instead represents reaction willing molecule Cetan within the fuel mix. Both numbers are measured on a specific type of engine as defined in each standard [28].

As determination of vehicle power consumption, international standards have utilized specific full vehicle test cycles. In particular, a total vehicle performs certified velocity profiles on a chassis dyno, while all vehicle emissions are collected and evaluated in mass. The emitted pollutants are evaluated and compared against official restrictions as typically in NOx, HC, CO, particle number and mass (see chapter *1.3*). In addition, CO_2 emissions represent total vehicles power consumptions. Today approach in CO_2 emission follows the "tank to wheel" review. Herein, the evaluation follows the direct emission form the exhaust pipe. Thus, battery electric vehicles have also 0 emissions while in contrast non-fossil fuels have by law CO_2 emission. In opposite, the "well to wheel" approach reviews which source provides energy. Herein also battery electric may emit CO_2, if fossil fuels are utilized for providing energy, while also combustion engines may have no CO_2 emissions, if fuel crude stock utilizes "alternative" sources. As worldwide common method, test cycles on chassis dyno established in past years as major evaluation and certification background. The European Union certificates until 2018 the "New European Driving Cycle" (NEDC) [29] and beyond the "Worldwide Harmonized Light Vehicles Test Procedure" (WLTP) [30]. Both cycles are shown in following illustration.

Despite performance parameters such as average speed required power increase, *Table 4* review of cycle shape reveals the most significant change from NEDC to WLTP. WLTP cycle has higher dynamic in its profile with higher gradient in ramps and lower stabilized dynamic portion. This indicated a closer realization to real road driving, but complicates deep analysis.

In perspective for fuel injection system analysis, vehicles FIE controller will stabilize seldom. To find identical position between two tests is therefore an unpractical approach. Therefore, the "old" NEDC advantage for this type of analysis is the given stabilization time. Herein a fair comparison between two setups becomes possible.
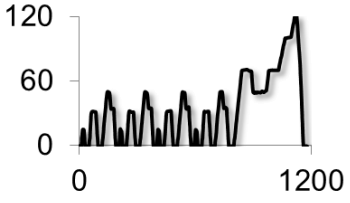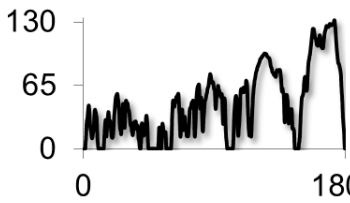
Cycle	NEDC [29]	WLTC [30]
Profile		
Average speed [kph]	34	46,5
Maximum speed [kph]	120	131
Stop time [s]	267	242
Length [km]	11,0	23,25
Average power [kW]	7	11
Maximum power [kW]	34	42

Table 4: Comparison between NEDC and WLTP cycle for passenger vehicles

Today's utilized test cycles for passenger sized vehicles represent a change in type and also approach. While dyno test cycle becomes more dynamic to ensure higher accuracy to physical appearance in all day usage, also real driving emissions on real streets getting more in focus and relevance for testing and evaluation, not only by original equipment manufacturer (OEM) but also by governmental authorities.

Commercial vehicles have to fulfil a different certification program. Herein a separation between transient application and stationary application determines each certification type. The "Worldwide Harmonized Transient Test Cycle" (WHTC) is a drive cycle closer to real road driving, due to its dynamic and transient nature. In difference to WLTC, the vehicle speed does not build performance targets, rather than relative engine load for a selected application [30]. In opposite to the WHTC, the "Worldwide Harmonized Stationary Cycle" (WHSC) represents certification in stationary duty cycle in relative engine load condition. This cycle includes full load operation points for emission quality evaluation [31].

2.2. Modern fuel injection equipment in combustion engines

As state of the art, Common Rail established itself as most used FIE for internal combustion engines (see *Figure 4*). Gasoline as well as Diesel engines equipped with direct injection technologies become mandatory due to several political and customer demands.
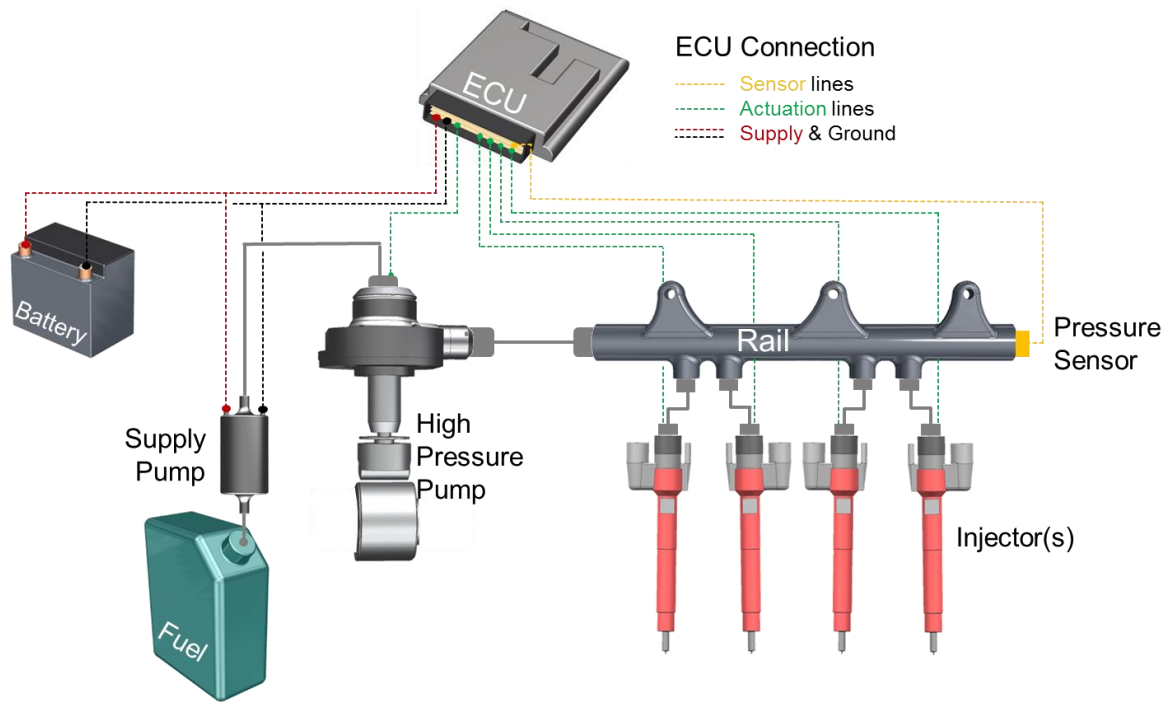
Figure 4: General schematics of fuel injection equipment

The common accumulator for all injectors ("Rail") builds the center of this common rail technology. Due to its large volume compared to injection quantity, rail pressure remains almost stable during injection. Especially Diesel FIE require stable pressure over a complete injection process for up to 7 injections, while Gasoline FIE focus on constant spray over the complete injection process. Nevertheless, also gasoline FIE inject up to 3 times per cycle. In both cases, the injectors perform the injection process. Their nozzle tip leads into the combustion chamber of the ICE. Therefore, they build the connection between power output of the engine and fuel pump as well as pressurization.

Until today, high injection pressure of 350 bar for gasoline and 2500 bar for Diesel engines cannot be realized with simple pump modules. Special high pressure pumps are required to generate high pressurized fuel for injection and combustion. Especially for Diesel engine purposes, high pressure pump shows high variety in features and parameters. Basic specification, like maximum flow, maximum pressure and fuel type, are sufficient to define the high pressure pump.

Fuel demands in engine operation and therefore required fuel flow by high pressure pump vary mainly by operation condition such as engine speed and engine load. Also, environmental temperature, fuel temperature, engine aging and fuel pump aging determine fuel pump load condition per cycle as illustrated in *Figure 5*.

This generalized illustration demonstrates one major obstacle to encounter for high pressure pump selection. State of the art engine, with high low end torque levels, have fuel systems highest possible delivery rate not at engines rated power, but in low end torque area. This circumstance requires additional precaution, when engineering in line with engine aging.
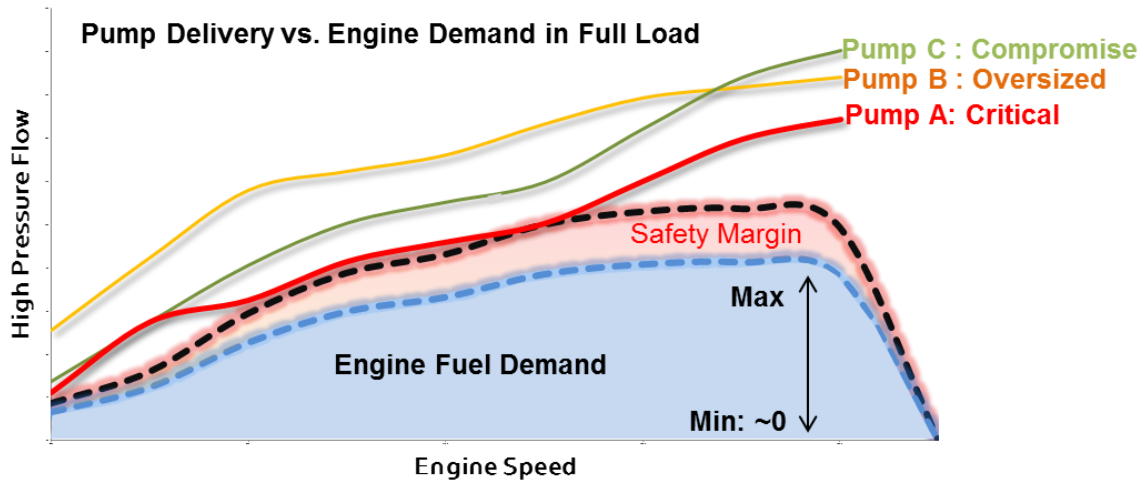
Figure 5: Generic review of engine fuel demand vs. pump delivery [32]

Passenger vehicle drivers reach seldom rated engine power over total lifetime, but acceleration with full torque demand may happen frequently over lifetime and may therefore be recognized also during aging of the vehicle. In case of commercial engine and their always high torque requirements, this may even lead to high amount of customer complaints and engine malfunctions due to lack of fuel delivery by also aged FIE.

2.2.1. Rail design and rail pressure control

The "Common Rail" builds the base for modern injection systems. Its volume supports stable injection over complete engine cycles and stabilizes the rail pressure within the system. Rail equipment and setup depends on type and control strategy of the FIE. Pre-controlling of the high pressure pump's pressurized quantity is the most efficient way. The resulting system schematics are shown in *Figure 6*. This FIE type appears in gasoline direct injection engines mainly, but also a minor share of common rail diesel engines are equipped in this configuration.
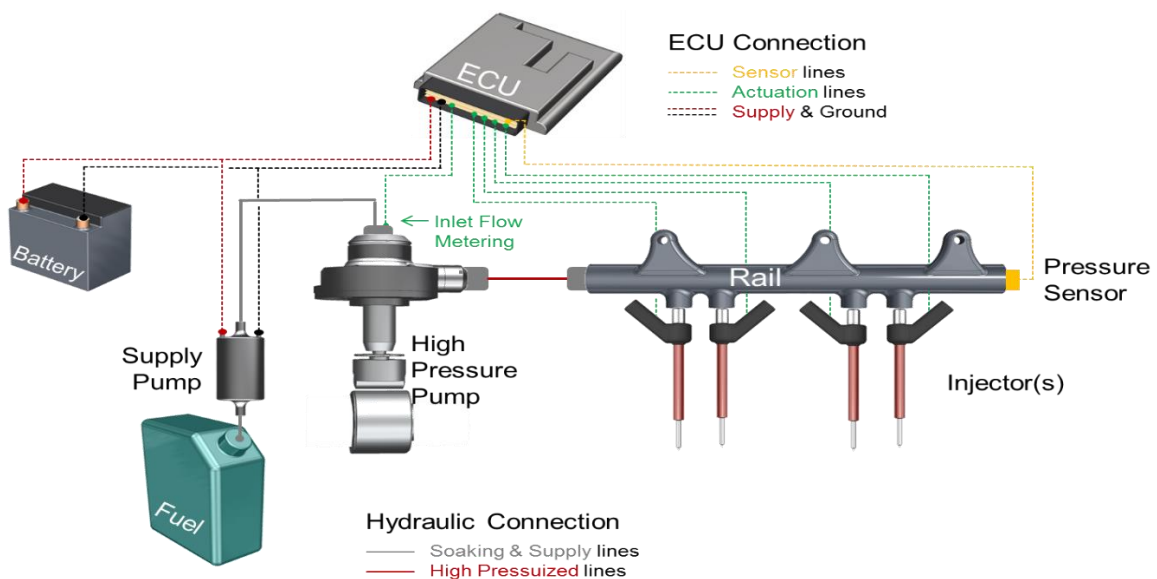
Figure 6: Gasoline direct injection system

Within this approach, only the quantity of pressurized fuel controls the actual rail pressure. Therefore, a precise volume flow control into the high pressure pump head becomes mandatory to realize sophisticated high accuracy. As a consequence, digital inlet valves (DIV) control nowadays the GDI high pressure pumps flow and pressure generation. Prior used metering units (MeUn), which are basically proportional valves, are still used in many Diesel applications and rarely used in gasoline engines. *Table 5* illustrates and lists differences between both pre-control hardware concepts.
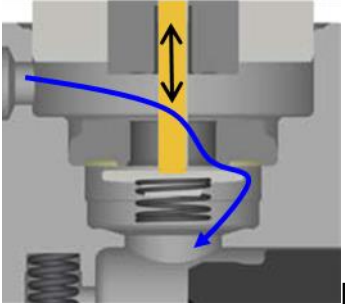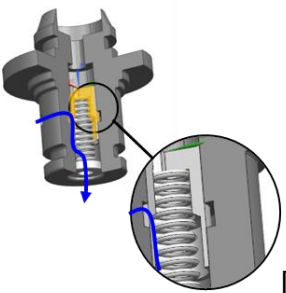
Type	Digital inlet valve	Metering unit
Picture	[33]	[33]
Principle	Pump synchronous activated valve	Adjustable inlet flow throttle
Advantages	- Precise metering for even smallest volume flow	- Low noise emission during function - Simple control handling - Fail safe functionality
Disadvantages	- Higher controlling complexity due to synchronization - Sensitive for aging - Loud and rough function noise	- Unprecise fuel metering in especially low flow

Table 5: High pressure pump metering control types

Since pre-control concepts have by principle low control leakage for rail pressure stabilization, this control type demonstrates best efficiency. Nevertheless, to reduce rail pressure quickly, as it may be mandatory during high dynamic driving, pressurized fuel needs to be released or even evacuated out of the rail. Fuel injection during engine running fulfills this task, but the pressure decrease inside the rail is connected to injection quantity and engine rpm.

This obstacle plays minor role in case of gasoline systems with comparably low pressure level of today up to 350 bar. Today diesel FIE, with a pressure level of 2500 bar, requires additional pressure regulation in order to maintain fast pressure decrease. Therefore, the diesel FIE architecture integrates a rail pressure control valve into the rail, as shown in *Figure 7*. If e.g. the current rail pressure is higher than desired, it opens and the fuel amount necessary for reaching the desired rail pressure flows into the fuel tank.

Typical diesel FIE does not only have one line back to the tank for rail pressure control. To realize high actuation forces within the injectors for injecting the diesel fuel, the injector works in a servo-hydraulic principle. Thus, every injection event releases additional leakage into the tank. Both leakages of injector actuation and rail pressure control sum up to nearly all hydraulic losses in diesel FIE. Since those systems reach high pressure levels, these leakage losses impact significantly the total efficiency of the entire FIE and lead to fuel heat up.
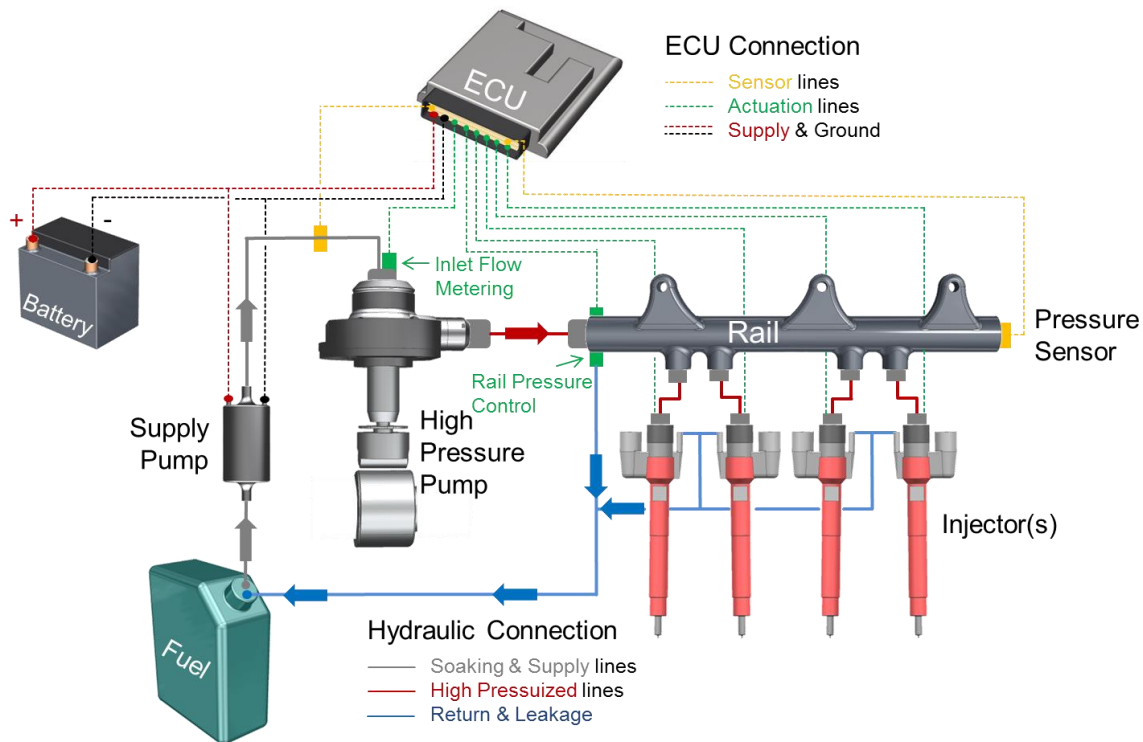
Figure 7: Diesel fuel injection equipment

Anyhow, this demerit is useful in winter time to unblock the vehicle's fuel filter. By pressurization of too high fuel amount, the "unused" energy of highly pressurized fuel heats up. The hot fuel melts the paraffin on filter surface to maintain proper function of the FIE and therefore the entire vehicle.

The design of the rail itself is mainly impacted by the two rail pressure control methods, mentioned above. Gasoline engine designated rails differ from diesel engine rails and their pressure control method (see *Table 6*). Nevertheless, the rail serves as an accumulator mainly to stabilize pressure pulsation or even to prevent pressure drop during long injections. Today's most used shape is a long pipe reaching over all cylinders.

Type	Gasoline direct injection	Diesel common rail
Picture	[34]	[35]
Pressure range	~500 bar	~4.000 bar
Addition	Pressure sensor	- Pressure sensor - Pressure control valve - Throttle(s)
Advantage	Cost effective	- Very robust - High dynamic rail pressure
Material	- Aluminium - Steel	- Forged steel - Casted steel
Manufacturing method	Bar extruding & soldering of injector ports	- Casting & laser welding - Forging & hard drilling

Table 6: Fuel injection equipment rail features

The above mentioned features describe mainly constructive features. Of course rail volume, geometrical dimension, number of injector connectors depend on designated engine and preferences by the original equipment manufacturer (OEM). This also implies the layout and number of throttles inside the rail. To ease handling in case of V-type engines, the rail usually splits up into two separated rails, connected via a pipe (see *Figure 8*). Depending on size of the engine, one or two high pressure pumps pressurize the rail.

Figure 8: V-type engine fuel injection equipment [36]

Furthermore a far higher rail separation is also possible, especially for heavy duty Diesel engines with 12 cylinders and power output of 1 MW and higher [37], as exemplary shown in *Figure 9*.

Figure 9: Heavy duty fuel injection equipment by Liebherr [36]

Since engines with such rated power and torque require a high amount of highly pressurized fuel, resulting rail size is difficult to apply. Thus, a separation of the entire rail volume becomes the most practical solution for a hardware realization. With an own large accumulator per injector, the pressure waves inside the "rail" are stabilized to maintain a constant pressure "in front" of the injector. Nevertheless, this concept increases costs significantly and therefore is only used in rare cases or in engine with lower cost priority.

2.2.2. High pressure pump for common rail systems

To achieve high pressures for injection and combustion nowadays, a special pump type for generating high pressure is included in every FIE. Thus, the high pressure generation still

challenges the equipment design. Higher demands on lifetime and fuel pressure for diesel and gasoline engines lead to an increased stress on those components as well as their interfaces to the engine. To optimize the performance of the pump for an entire powertrain, high pressure pumps show large variety in their principle. Nevertheless, all high pressure pumps, applied in state of the art FIE, have a common working principle: Nowadays a radial piston pump (see shown hardware principle in *Figure 10*), in which a plunger (or piston) generates pressure and flow by forced movement. A cam shaft or an eccentric shaft drives this mechanics. Due to the resulting high loads on the plunger and furthermore high stress on all materials, those parts are in most cases highly expensive due to high graded steel types. Also bearings and all other interior mechanics components are engineered to sustain these sophisticated conditions.

Herein also the pressurized fluid has impact on the design. The applied coating on plunger or liner surface fits to the viscosity abilities of the fluid. Also the usage as lubricant and coolant fluid becomes an option for high pressure pump, as it is applied in majority of diesel high pressure pump.
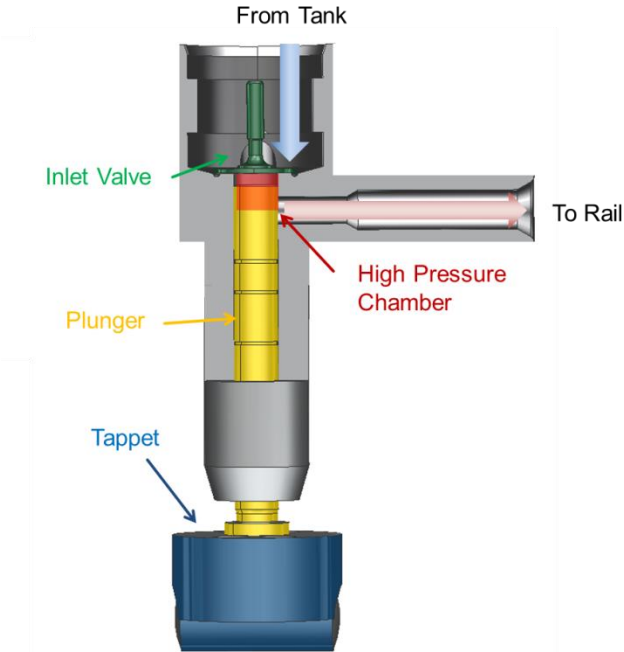
Figure 10: Radial piston pump schematic

One pumping cycle can be divided into two phases. During first phase, down movement of the plunger soaks in fuel from tank until plunger has reached bottom dead center (BDC). Due to high pumping frequency of the high pressure pumps (especially in GDI application up to 100Hz), external supply pressure (3.5 to 5 bar relative) maintain a proper filling of the high pressure chamber. With beginning of the plunger upward movement, the inlet valve closes and seals the high pressure chamber. At this moment, the pressurization phase starts. Continuous upward movement increases pressure until the pressure inside the high pressure chamber reaches levels above rail pressure. Then the outlet valve opens for the flow from the high pressure chamber towards the rail and therefore, pressurizes the rail for the next injection cycles. This phase ends when the plunger reaches top dead center (TDC). A cam or eccentric shaft drives the plunger and the upwards movement. Strong spring(s) initiate downward movement and keep contact between tappet and shaft.

As a rough summary, especially fuel and target engine define the high pressure pump design features. Desired engine power output and the within related maximum fuel flow defines displacement and number of plungers. The vehicle's supply circuit design requires adaptation on high pressure pump and engine integration as well as maximum pressure determines cam lobe and plunger geometry.

This has to be considered to engine fuel demand and maximum pump delivery (see *Figure 5*). Depending on pump characteristics, maximum engine torque or maximum rated power defines final geometry. Maximum torque is a major criterion when the maximum injected quantity has to be covered by the high pressure pump flow.

Since modern engines' torque characteristics targets high "low end torque", this leads to large pumping geometry. A higher pumping frequency than the injection frequency supports a smaller pump geometry additionally. Thus, this approach causes a possible demerit in rail pressure stability from injection to injection. Another demerit and also criteria for pump geometry selection is the engine maximum fuel demand at high engine speed, which means rated engine power. When the pump reaches its maximum fuel flow rate too early, a larger geometry or higher supply pressure becomes mandatory.

Radial piston pumps have limited self-soaking or priming abilities. In order to maintain proper fueling at start up and high rpm, an additional supply for the high pressure element becomes mandatory. A major criterion is enough flow for the high pressure demands and enough static pressure to maintain proper high pressure filling. Either an electrical external supply pump from tank to high pressure pump provides pre-pressurized fuel or a self-suction internal pump attached to the high pressure pump soaks from tank to the high pressure pump.
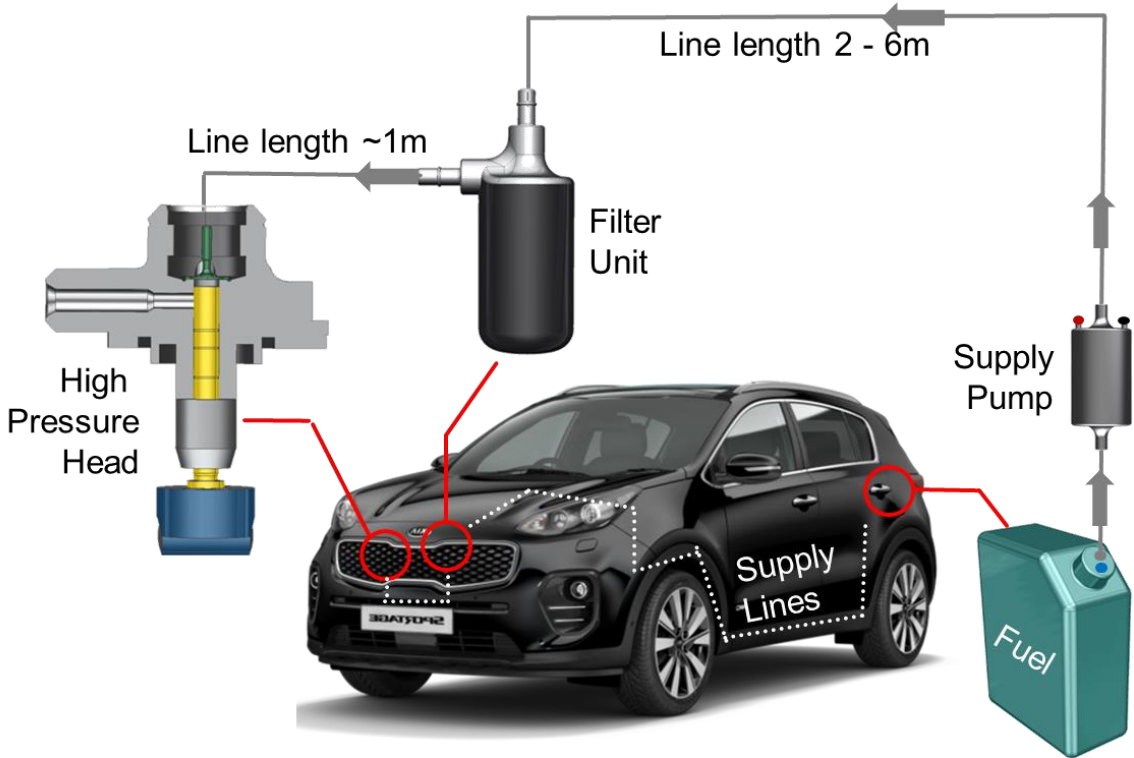
Figure 11: Illustration of the supply system integration into the vehicle architecture

Due to such physical boundaries, the vehicle architecture and the low pressure system follows to assure proper working system. The illustrated system in *Figure 11* shows most common

configuration for today passenger vehicles. Those vary in position of the filter and the application of fuel heating system, in particular for self-sucking pumps attached to the high pressure system.

Also the type of integration to the engine assembly impacts the plunger features. Therefore, the engine mechanics limits the high pressure pump peak torque. Especially in production cost driven passenger vehicle sized engines, high pressure pumps encounter an engineering limit for the maximum torque. One possibility to reduce the peak torque is the reduction of plunger diameter, which causes an increase of the plunger lift to maintain flow requirements. This action often reduces the benefit by diameter reduction. "Slow" plunger lift with slight offset also reduces peak torque. The following *Figure 12* illustrates this parameter effect.
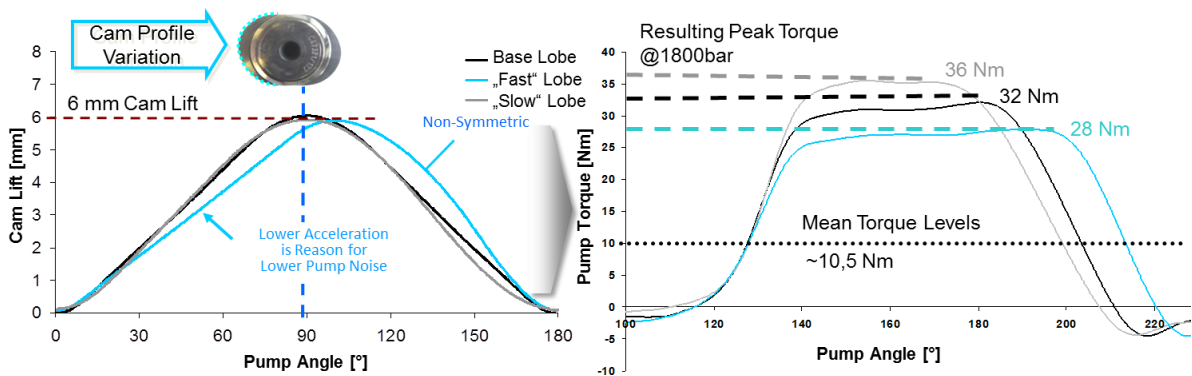
Figure 12: Cam lobe impact on Bosch CP4 pump [38]

The "slow" plunger lift causes not only a lowered peak torque, but also noise emissions by high pressure pumps are also impacted positively. Due to the longer time with high pressure, leakage losses of the high pressure pumps increase, as well as load on the pump mechanics, which has to encounter the force initiated by the pressure [38].

The position within engine assembly depends in most cases on the engine design already given. Nevertheless, three typical positions are summed up in *Table 7*.
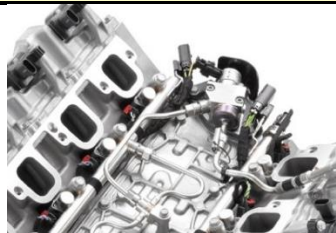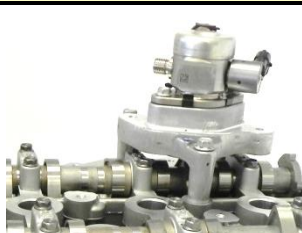
Position	Crankshaft	Additional shaft in belt / chain	Camshaft
Describing picture	[39]	[38]	[33]
Short description	Most effective way for high power consuming pumps or engine with high number of auxiliaries	Cost attractive solution for external lubricated pumps with higher torque	Integration at the end of camshaft or as pumping element integrated into the camshaft
Typical application	-Commercial engines -Off-Road applications	-Passenger diesel engines	- GDI engines - "low budget" engines - small auxiliaries engines

Table 7: Typical high pressure pump engine integration approaches

The integration on already given shaft gives the engine manufacturer benefit in terms of costs due to fewer parts, but mechanical stress on those parts increases significantly. Especially large scale Diesel high pressure pumps consume high power and therefore, require a high torque level. Thus, durability of the complete engine mechanics can be affected by high pressure pump negatively.

Since especially passenger vehicles are also sold by emotional factors, noise emission of the vehicle plays a significant role. High pressure pumps themselves emit high mechanics noise levels, which need to be dampened and isolated as well as possible. In this juncture, high pressure pumps mounting impacts final vehicle noise emission strongly.

2.2.2.1.   Gasoline direct injection high pressure pump

GDI high pressure pumps design reduces the pump to its minimum. Today, it is only a build up by a simple 1-plunger pump head which is supplied via an external supply pump from the vehicle tank, as illustrated in *Figure 13*. In first rail applications, GDI systems reached pressures of 50 bar. Since the beginning of 2017 OEM's start the production of engines with rail pressures of 350 bar.
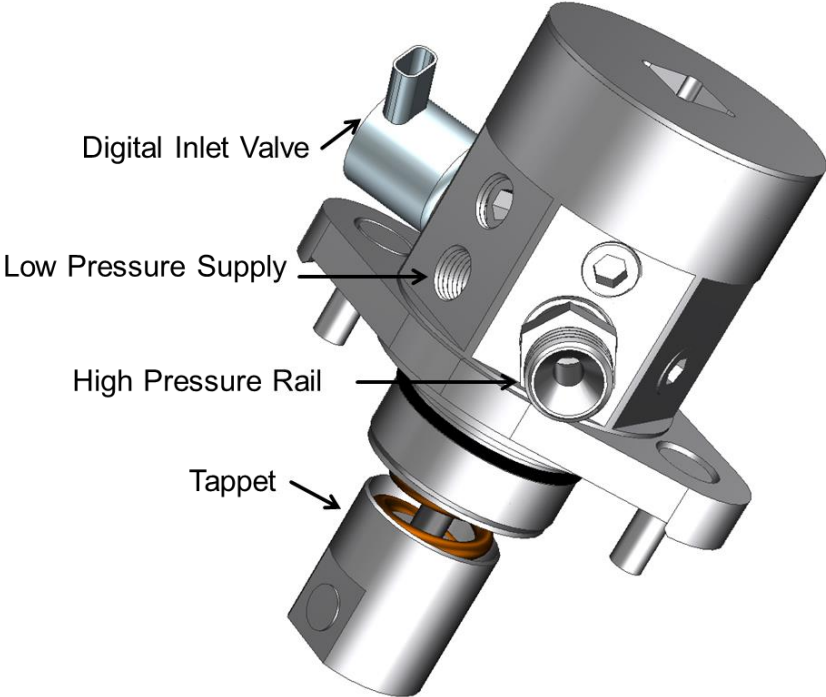
Figure 13: GDI High Pressure Pump (HMETC's parameter test pump) [40]

Cost, weight and noise nowadays defines GDI high pressure pump features. Especially in respect due to fact of the gasoline engines worldwide spreading, simple and cost efficient design for cost efficient gasoline engines drive most built high pressure pump types. Also, since gasoline has very low lubrication abilities, engine oil lubricates nearly all GDI high pressure pumps. Therefore, OEM's integrate those pumps into the engine's cam drives as a cost efficient solution. As an example *Figure 14* shows a GDI high pressure pump integration as applied in HMC Theta II engine.
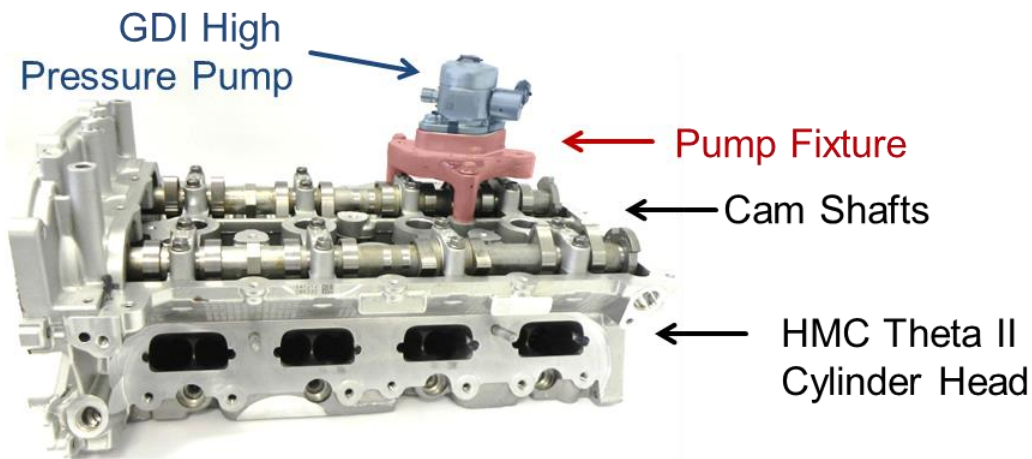
Figure 14: GDI high pressure pump integration onto HMC Theta II engine [33]

The upper position of the high pressure pump leads to a higher noise emission tendency in this mounting. Depending on the target market additional noise insulation provides a good noise coverage but brings in additional cost and also stores heat. OEM's for passenger vehicles as well as Tier 1 supplier invest significant effort to reduce noise emission of the high pressure pump. Resulting shaft and chain or belt design lead to additional issues, which needs to be countered by the optimization of the pump and its integration [41].

For integration analysis purpose, special development pumps are applied. Since serial production pumps are welded and not dismountable, such approaches become mandatory. A utilized GDI special parameter high pressure pump, as illustrated in Figure 15, support engine integration parameters such as noise emission, mechanics loads and hydraulic performance.
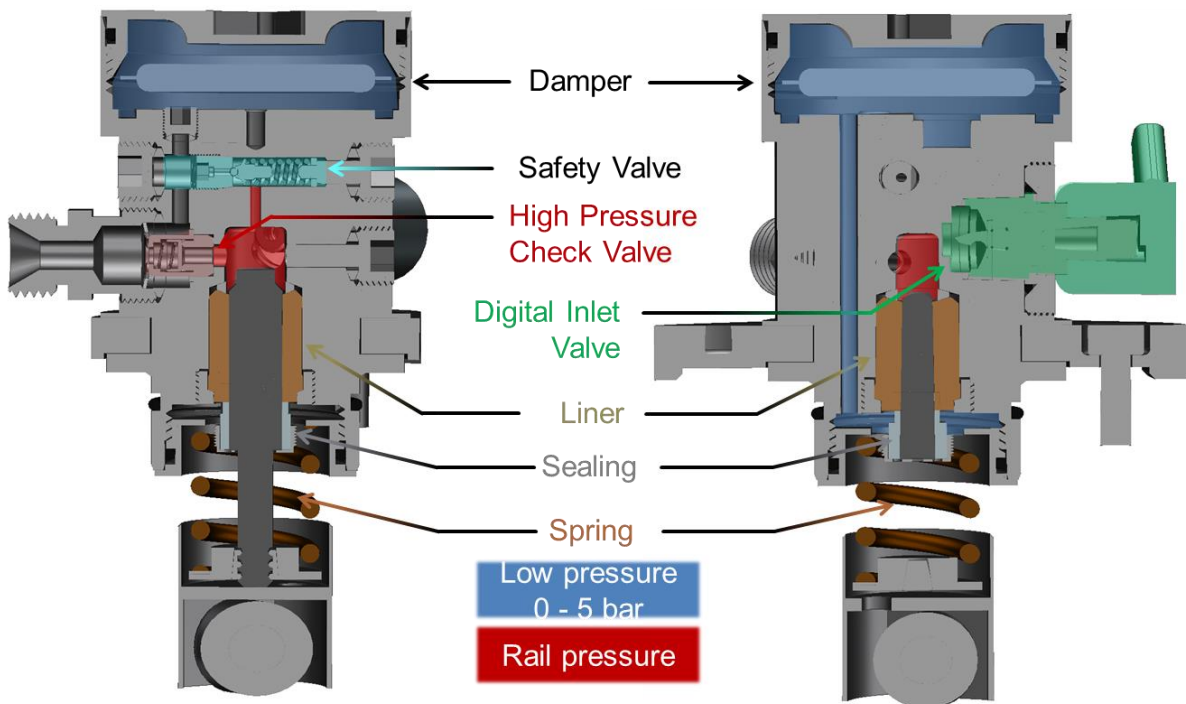
Figure 15: Gasoline direct injection high pressure pump schematics [33]

The GDI high pressure pump's functional core remains within the high pressure chamber. Similar to other radial high piston pumps, the GDI high pressure pump can be split into low and

high pressure areas. Low pressure areas receive supply from an external source. In most cases, a pump inside the fuel tank provides 3.5 to 5 bar pressurized fuel to achieve a full high pressure chamber filling also at high engine rotation speed and pumping frequency. State of the Art GDI high pressure pumps use a Digital Inlet Valve (=DIV) for precise rail pressure control over complete speed, rail pressure and injection quantity range. To ensure stable pressure inside the high pressure pump and therefore precise rail pressure control, special damper are enclosed into the GDI high pressure pumps. State of the Art GDI high pressure pumps use a Digital Inlet Valve (=DIV) for precise rail pressure control [42].

To avoid fuel ingress into the engine oil, an additional sealing below the liner separates the pump fuel circuit against the engine. This sealing increase pumps friction significantly, but become mandatory due to the fact that small leakages from the high pressure chamber creep along the plunger to the exterior. Without a sealing, fuel dilutes the engine oil and causes engine damage [33]. Also the oil inside fuel impacts on combustion negatively and needs to be avoided. Nevertheless, small fuel leakages cool down liner and plunger surfaces and therefore maintain pump functionality over lifetime. Thus, GDI high pressure pumps have a small accumulator for stabilization of the inlet supply, which collects the leakage between plunger and liner [42].

GDI high pressure pumps are equipped with a safety valve to mitigate possible exceeding rail pressure. In principle, this valve is a check valve with predefined load. When pressure inside the high pressure chamber exceeds maximum allowable pressure, this valve opens and the pressurized fuel flows into high pressure pump supply line. Without safety valve, a too high pressure damages the injectors and causes, in the worst case, even a bursting of the rail.

2.2.2.2. Common rail Diesel high pressure pumps

Two major differences compared to GDI high pressure pumps allow a changed approach for providing highly pressurized fuel for Common Rail Diesel engines: Fuel type and the target rail pressure. Diesel like fuel has abilities of light oil, including viscosity of 2,0 mm²/s - 4,5 mm²/s, which allows some lubrication of mechanics parts. Therefore, fuel itself lubricates most modern passenger vehicle sized Diesel engine high pressure pumps which requires an own housing for the pumping unit [43]. An exemplary approach is shown in *Figure 16*.
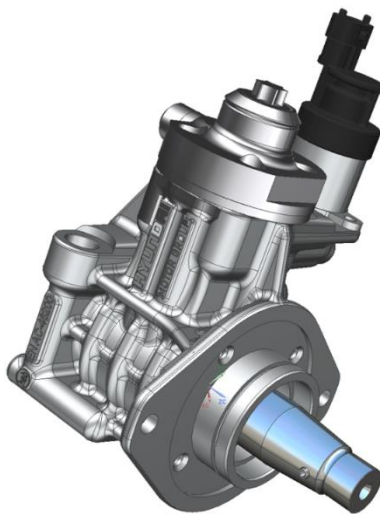
Figure 16: HMETC diesel high pressure pump concept HEFP Gen.2 [38,44]

State of the art passenger sized high pressure pumps are based on a very similar design concept: one plunger which is driven synchronously to engine speed. This means, one pumping event before injection event to maintain a nearly static rail pressure. For cost & weight optimization, the OEM's and supplier reduce the pumps to minimum configuration. As a result, one plunger pumps are common today. Only for high-powered or V-type engines, they receive a second plunger [44].

Figure 17: Bosch CP4 diesel high pressure pump with one plunger and two plungers [45]

The inner build up (see *Figure 18*) differs among serial productive pumps only in details. Most parts and build ups are developed over each technology step and are following simplification consequently. The durability of high pressure pumps becomes more important, especially due to large numbers of high powered diesel engines and increasing rail pressure demand for a clean combustion.
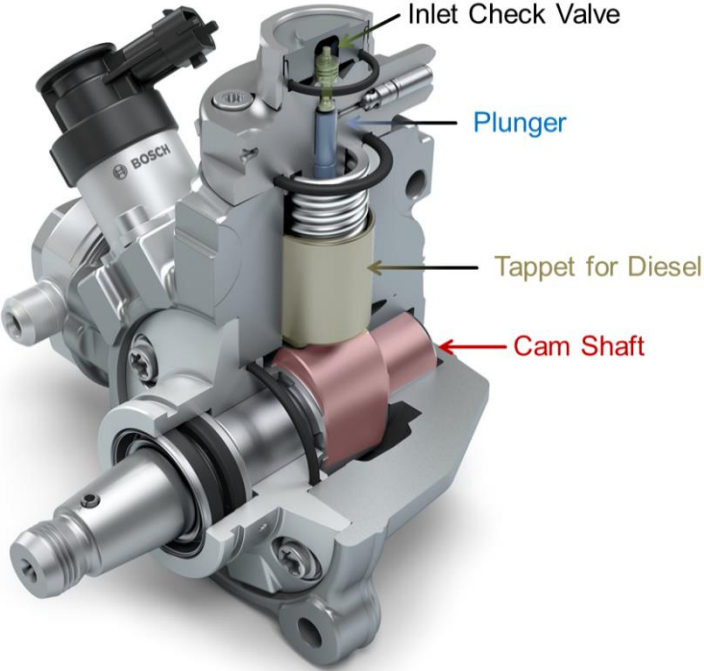
Figure 18: Cross section of Bosch CP4s1 [modified from 45]

Therefore parts like springs, tappet and bearings, which carry the major load of pump function, are designed for high loads. Since typical build in bush bearings require constant pressure and to maintatin a proper filling of the high pressure head, the system pressure inside the complete pump volume reaches levels of 3.5 bar to 5 bar relative to atmosphere. A pressure valve controls outlet (leakage) flow of the high pressure pump. This stabilizes the internal pressure and as well regulates constant flow out for cooling [46].

Furthermore the entire high pressure pump setup requires well defined parameters in order to achieve best integration performance. Therefore, in order to tailor the high pressure pump to an engine setup, especially cam lobe design and plunger geometry have significant impact on high volumetric efficiency as well as low noise emission [46]. The specific priority determines the subsequent tasks. High pressure pumps for commercial engines require a higher efficiency with less focus on noise emission. To encounter durability issue, engine oil lubricates commercial high pressure pumps typically. Especially in commerical application, robustness of the function of critical componenets reaches highest priority. Thus, usage of engine oil lubrication instead of diesel supports the final lifetime of the FIE. But also margin markets with very low fuel quality, often require engine oil lubricated pumps for a proper function of the engine over lifetime. Herein unit pumps are a cost reduction option for fuel pressurization (see *Figure 19*).
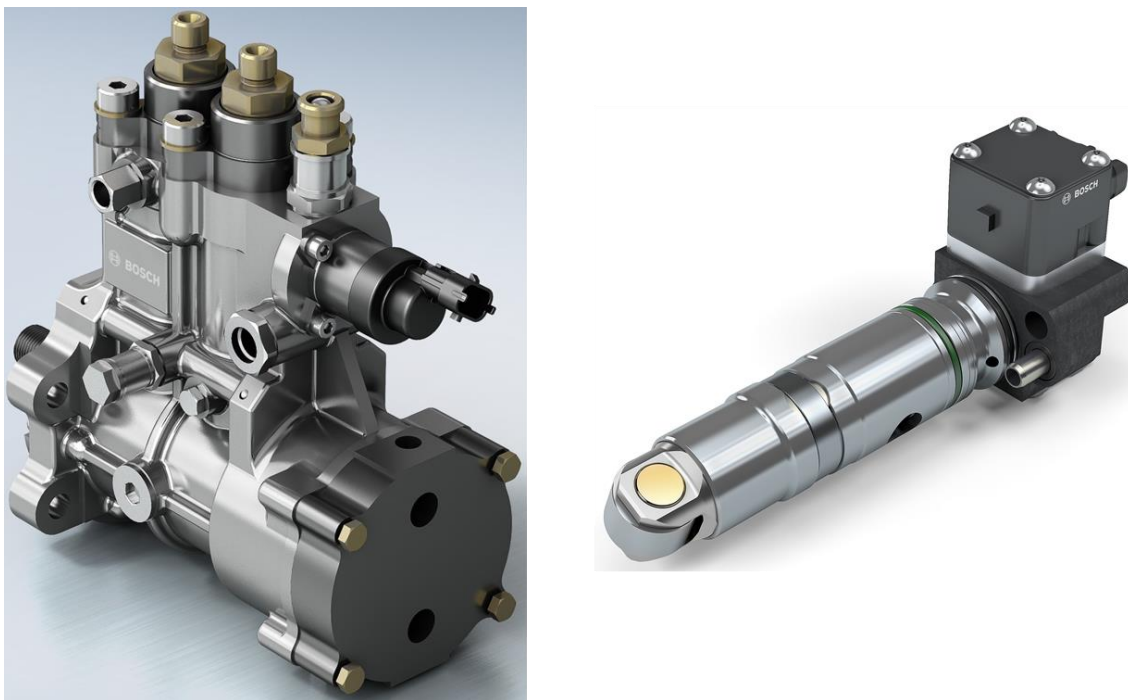
Figure 19: Bosch CP5 (left) and Unit Pump for heavy duty application (right) [45]

This approach of engine oil lubrication brings benefits in durability of the complete system, but increases the system complexity. Usage of Unit Pumps simplifies the constructional effort by engine integration. Nevertheless, a common disadvantage of this system is the possible close contact between engine oil and fuel which has to be avoided strictly. Special seals, which are also used in GDI high pressure pumps, ensure a separation between both media. Also heat transfer by hot oil into fuel increases the fuel aging and needs to be considered before selecting the high pressure pump type [47].

2.2.3. Injector technology for modern engines

In terms of combustion quality and therefore emission quality, the injector remains as a major part. In principle, fuel atomization and distribution into the cylinder describes the target of all injectors, regardless of their intended fuel or combustion type.

Their working principle depending on the target rail pressure. Since gasoline pressure nowadays rises up to 350bar and higher in development, direct acting and simple injectors are assembled into those engines for substantial cost benefit. On the opposite, the diesel injectors require support of injector internal servo-hydraulic, due to today's very high system pressure.

2.2.3.1. Gasoline direct injector

Gasoline direct injectors are a simple hardware for injection technology. Today's engine concepts a system pressure of up to 350 bar, which does not require cost intensive servo-hydraulic actuated injectors (see *Figure 20*). As additional cost reduction support, the gasoline engines feature a quantity correction by lambda control already. This corrects injector drifting during aging as well as sample to sample differences by production process. Therefore, gasoline injector hardware development targets maintain on cost and noise reduction [48].

Figure 20: Continental XL3 GDI injector [49]

The length of the injector as well as the electric and hydraulic connection can be modified by OEM to fit for their specific application. Core for a significant engine performance enhancement in terms of emission quality builds the injection nozzle. The injected spray penetrates through the nozzle into the engine's combustion chamber with the target to achieve a homogenous mixture of fuel and air for a clean combustion. In the case of improper injector layout, fuel may hit the cylinder wall causing oil fuel mixtures with a low emission quality and increased oil dilution [50]. Since injected fuel quantity itself can be controlled via lambda sensor in the exhaust gas, and pressure range is low enough for direct acting, gasoline injectors design results in very consequent simplified hydraulic for cost reduction, as the illustration in *Figure 21* shows.

A basic functional element is the ball sealing at the nozzle, which is acting like a valve. The coil triggers its opening via a piston inside the injector, while a spring pushes the ball back into the seat again. A damper between the piston and the spring supports closing and reduces a second opening by needle bouncing. Those injection systems are reduced close to a minimum of parts for a proper function and therefore they are cost efficient. Since GDI injectors do not require servo hydraulic actuators for proper function, they achieve a better efficiency by nearly no leakage of high pressure flow at all.
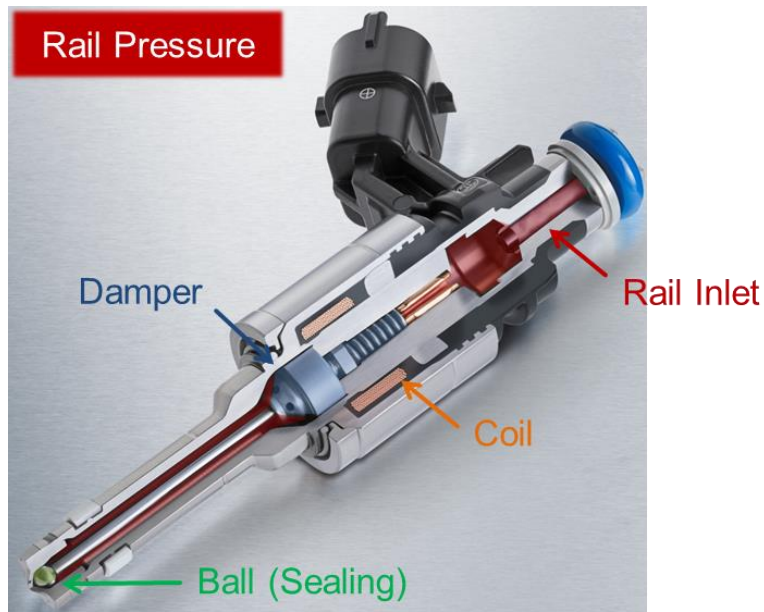
Figure 21: Cross section of Bosch HDEV5 GDI injector [modified from 45]

In principle, gasoline injectors -based on the solenoid principle- react on a triggered signal by ECU. It sends a pulse to the injector with a calculated length, which represents the duration of the injection event. The resulting relation is shown in *Figure 22*. Therefore, the injected quantity respects to energizing timing and rail pressure.
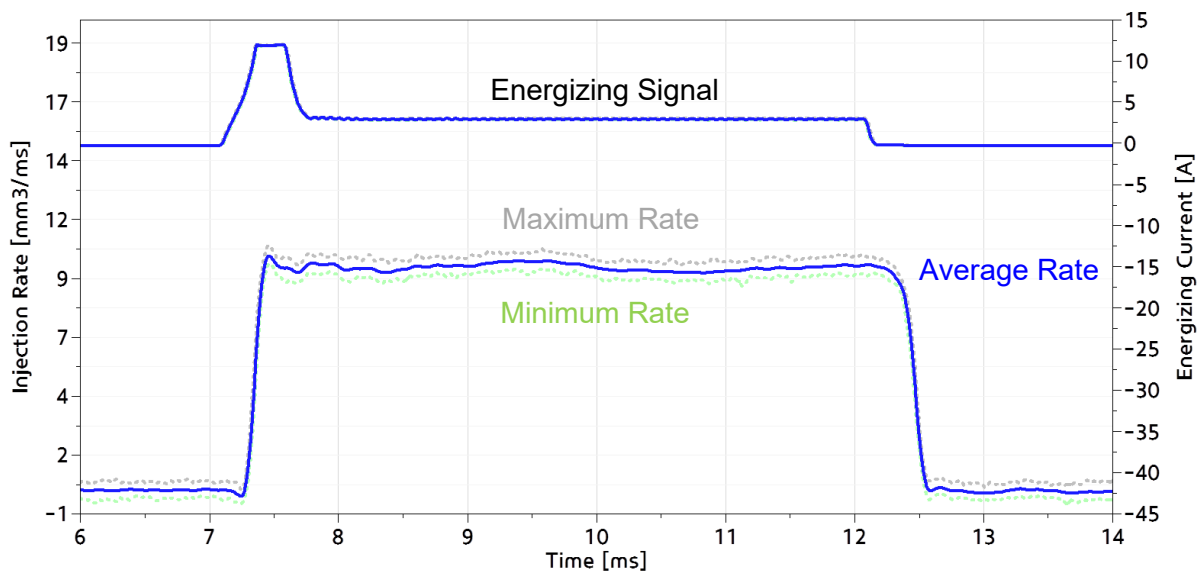
Figure 22: Exemplary gasoline direct injection at 200bar including shot to shot dispersion [38]

in most cases, the energizing consists two different phases: The first phase is the so called „Boost" or „pull-in" in which the complete armature including needle lifts. Thus, the ball at the end of the needle opens the seal and pressurized gasoline flows through the holes into the combustion chamber. During the following "Hold" phase, the complete armature stays in open position. As long as armature, needle and ball are lifted in open, gasoline still flows through hole into the combustion chamber. When energy cuts off, armature, needle and ball return into closing position, forced by spring, which pushes on the armature. To reduce bouncing of needle and therefore additional small injections, a damper between spring and needle reduces

29

upcoming oscillations. Additionally, this measure reduces mechanical noise emissions by the injection process. In addition, modifications and intermediate steps may be operated, as they are required by the mechanics or by a system wise utilized unique feature. This can be additional approaches for quantity correction. Nowadays, one injector performs 1-3 injections per cycle for clean combustion [50].

A well-defined spray shape in the combustion is one very important criterion for modern GDI injectors. The so called targeting takes into account the maximum length of injection, as well as the fuel vaporization for a homogeneous mixture at ignition.
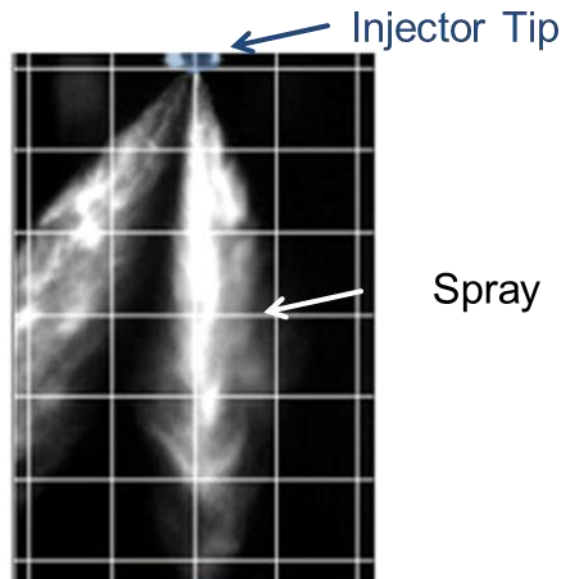
Figure 23: Gasoline spray at 100bar rail pressure [51]

As visible in Figure 23, the spray injected into the chamber penetrates a certain length into combustion chamber before it breaks up and the fuel vaporizes to generate a homogenous mixture for the combustion. Especially the rail pressure remains a major driver for the vaporization and therefore improves raw exhaust gas emissions. On the other hand, the increasing rail pressure requires higher durability and higher power demand of the high pressure pump. The "trade off" for optimized performance vs. above mentioned demerit is currently under research by nearly all OEM's.

2.2.3.2. Common rail Diesel injector

Diesel direct injectors encounter in most cases higher pressures than gasoline systems. Nowadays, on one hand, a target pressure of 2000bar and up to 3000bar requires robust technology. Simultaneously the injector requires high stability and accuracy due to low pilot quantities of 1 mm³/strk. by up to three pilot injections during one cycle. As a result, diesel injectors, as shown in *Figure 24*, are not cost efficient as a gasoline injectors. This intensifies in commercial application, because the requirements in durability, fuel quality and accuracy are higher as for a passenger vehicle application [52].
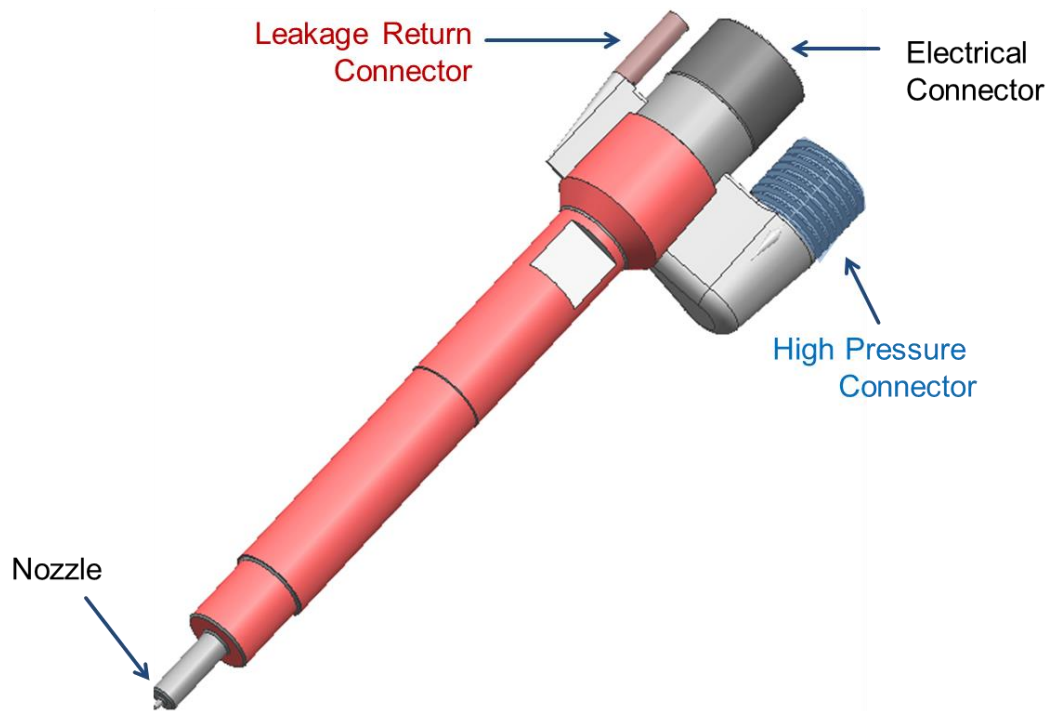
Figure 24: Common rail diesel injector

On the other hand, high system pressure utilized within the common rail system makes servo-hydraulic actuators mandatory for proper injection stability and low electrical power. By principle of a servo-hydraulic circuit, the injector actuates due to a pressure difference between upper side and lower side of the internal needle. The utilized approach is by controlled discharge via an internal valve, which leads to reduce static pressure on the top side of the needle or rod. This leads to a static leakage, caused by the sealing ability valve as component itself, and a dynamic leakage due to actuation of the valve. Since high pressurized fuel of the rail supplies this leakage amount, it states as one element of the FIE related losses. Additionally, integration of servo-hydraulic actuator increases complexity of the entire component, as illustration in *Figure 25* shows. As a result, modern common rail diesel injectors become a cost intensive part with high contribution to emission quality of an entire engine. To overcome or reduce impact by such servo-hydraulic actuators, Tier1 suppliers develop new valve concepts, e.g. 3-way valves, and improve performance continuously. Modern injectors have further features integrated, which allow adjustable injection rates by so called "Digital Rate Shaping" or close loop quantity control [52].

Depending on costs, target engine and supplier preferences, servo-hydraulic actuator of injectors are actuated by a solenoid or a piezo stack. The illustrated cut in Figure 25 goes through a typical solenoid actuated diesel injector. Even if the assembly and position of each specific part in diesel injector may be different between suppliers and actuation type, all modern diesel injectors have servo hydraulic actuator connected via a rod with a needle. Trials of suppliers to also implement direct acting diesel injectors without a servo-hydraulic system showed low durability in field. Further developed direct acting diesel injectors suffered from cost intensive approaches. In concluding, direct acting diesel injector approaches are nowadays not applied anymore, despite minor highly specialized applications.
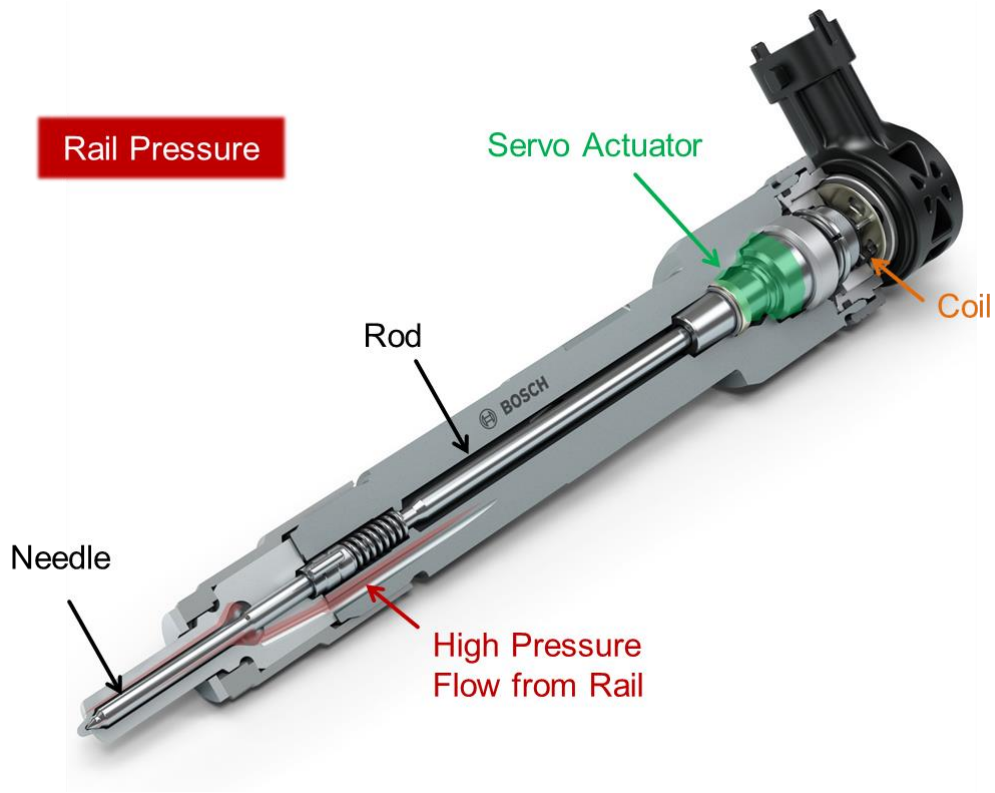
Figure 25: Cut through Bosch CRI2.25 [modified from 45]

Since the combustion principle of Diesel engines is based on self-ignition by the fuel, the time range for the injection shortens with increasing engine speed. As engineering target point, usually the point of rated power or maximum engine output remains as point with highest injection quantity in shortest period of time during engine duty. At this point the injector flow rate has to cover required amount at given rail pressure. Therefore, higher rail pressure encounters lack of flow rate, but intensified FIE power consumption as well as durability of the entire engine. As low end, pilot injection quantities still have to be precise in order to achieve pollutant emission targets. The following *Figure 26* shows the spreading in injection rate for a typical passenger vehicle application including tolerated sample to sample and shot to shot dispersion.
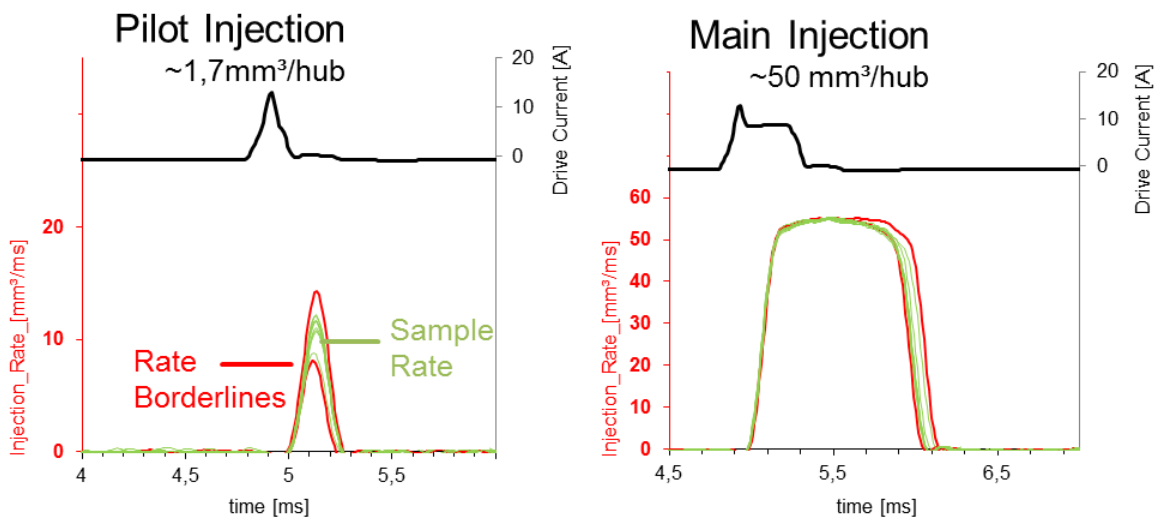
Figure 26: Diesel injector rate spreading from highest to lowest amount and their dispersion [38]

Injection rate itself has also a significant impact on the combustion quality as well as the spray shape itself. Which type of shape gives highest potential for combustion, cannot be generalized. In fact all FIE suppliers and OEM follow own approaches with success. Nevertheless, future approaches have as common target more precise and more stable injections. Ranges for stable quantity and even control depend again on OEM and supplier's approaches, as well as target engine.

.

2.3.   Fuel boundaries and properties for hydraulic systems

For reviewing energy amount and power consumption of the FIE, physical properties of the fluid impact the entire system. Not only combustion concept influences power demand, also fluid density and viscosity have significant impact. Due to this fact, base fuels are standardized in several engineer standards, as EN 590 which describes Diesel fuel in Europe.

2.3.1. Fuel in respect of their physical properties

In a simplified reflection of FIE influences, the density impacts especially the flow volume. Since engines have specific fuel consumption in mass flow, lower density increases power consumption. The viscosity has an impact which can be described as "hydraulic friction". With lowered viscosity, the internal pumping losses by the flow are reduced, but leakage losses increase without countermeasures.

Parameter	Diesel B7 EN 590	Paraffinic diesel EN 15940	OME-1 [55]	OME-3 [60]	BtL (HVO) [58;59]
Cetane No.	51	53	50	75	75 - 99
Density [kg/m³]	820-845	835	873	1070	780
Kinematic viscosity [mm²/s]	2 - 4 @40°C	2,92 @40°C	0,33 @20°C	0,71 @20°C	-
Heat value [MJ/kg]	43,8	43,8	22,4	22,5	44
Boiling point [°C]	250 - 350	210 - 302	42	157 - 259	180 - 320
HFRR [µm]	250	260 @60 °C	759 @20 °C	278 @20 °C	-

Table 8: Fuel properties of selected "alternative" fuels based for self-ignition combustion [55, 58, 59, 60]

Parameter	Gasoline (E5) EN 858	LPG [57]	DMC [54]	MeFo [54]	Ethanol [56]
Octane No.	95	111			
Density [kg/m³]	747,5	540	1079	957	789,3
Kinematic viscosity [mm²/s]	0,7 @20°C	-	0.625 @40°C	0,361 @20°C	
Heat value [MJ/kg]	43,6	46	18,73		
Boiling [°C]	25 - 210	-42 - (-5)	157		78
HFRR [µm]	639 @40°C				

Table 9: Fuel properties of "alternative" fuels for spark ignited engines [54, 56, 57]

As visible in Table 8 and Table 9, properties of novel fuel types differ from specified fuels in high variety. In some cases, all necessary information is still not available. Reasons vary from not ready defined mixtures due to not given standardization to protected intellectual property of (petro-) chemical companies. Also incompatibility of the fuels to standardized test procedure results in a lack of information. Nevertheless, from today's perspective those fuel types mark future possibilities for mobility and therefore need to be considered.

2.3.2. Fuel in respect of country and region specific boundaries

Countries and regions all over the world encounter different issues in terms of fuels. Root causes can be politically motivated, like reducing fossil component in sold fuels, or may have logistical reasons like aging due to long storage time of the fuel on the countryside. Of course also misuse, like dilution or wrong mixing, has impact on fuel quality in some regions. Fuel quality mapping supports engineering for proper FIE layout and design. Fuel traders as well as scientific organizations investigate world-wide fuel quality and mixtures to establish those mappings [61].

Especially "Bio components" content of fuel rises significantly among the world [61]. Diesel as well as gasoline fuels have increased renewable content, not only in industrial countries, but also in margin markets as visible in *Figure 27* and *Figure 28*.
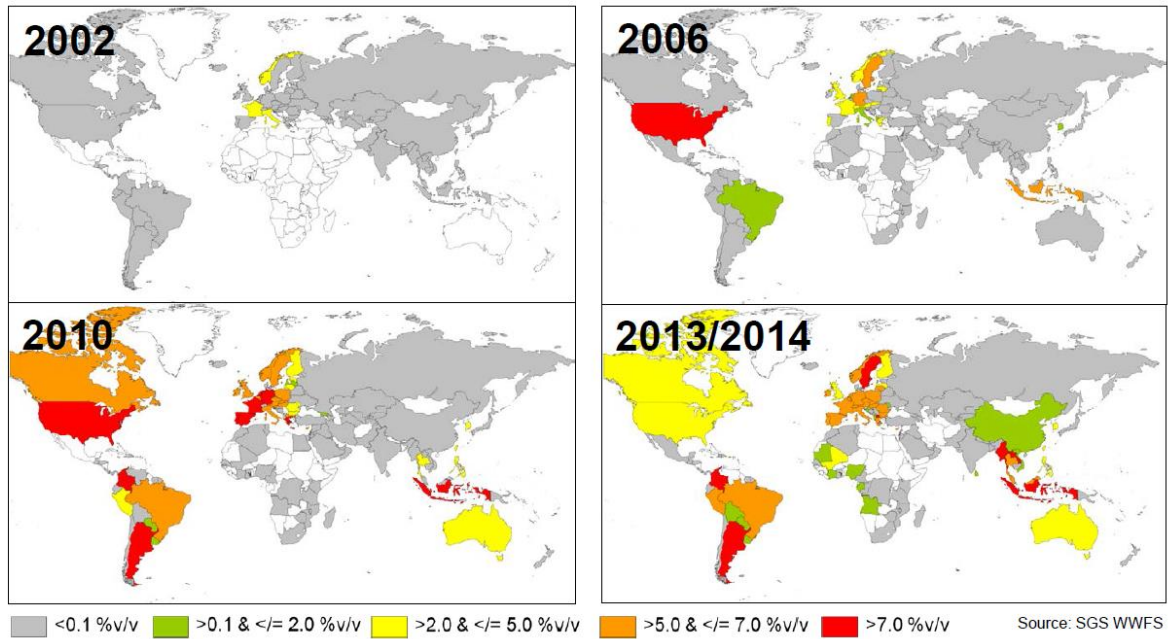
Figure 27: Timeline on Biodiesel relative volume to volume (%v/v) content by company SGS [59]
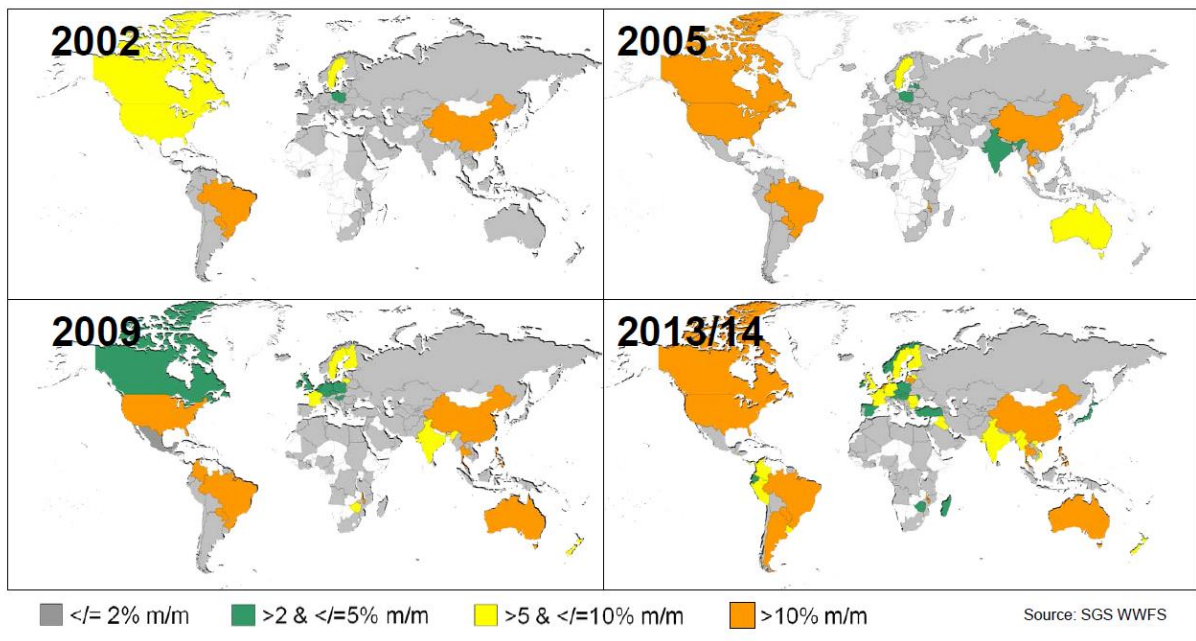
Figure 28: Timeline of ethanol relative mass to mass (%m/m) content in gasoline by company SGS [61]

As mentioned in chapter *2.3.1* especially molecule contribution of fuels has major impact on their fluid properties. Therefore, increasing numbers of fuel mixtures and future fuel mixtures with artificial fuels unknown today, review of certain parameters becomes mandatory. For a simplified view, only major fuel types are listed in *Table 10* together with physical properties.

Table 10: List of selected Diesel qualities [62]

Diesel fuels data from 2014	Germany	Finland	USA (Midwest)	South Korea	India	Brazil
Density@15°C [kg/m³]	836	802	844	823	832	847
Cetane index	55	63	45	51	54	50
Boiling point [°C]	204 - 348	200 - 309	209 - 338	181 - 356	188 - 366	208 - 356
Viscosity [cSt]	2,68	2,12 @40°C	2,62	2,61	2,57	2,8
Biodiesel content [%]	5	0	3	2	0	5
HFRR [µm]	250	341	378	328	432	198

Even if mean values of such physical properties differ among several countries in each point, increasing differences may occur within one country. Fuel quality at the gas station depends mainly on consumption frequency, additives used and crude oil quality in local refinery. As a result, quality spreading shows high deviations especially in countries with a poorly developed infrastructure [61]. The *Figure 29* illustrates the fuel quality spreading among selected countries.
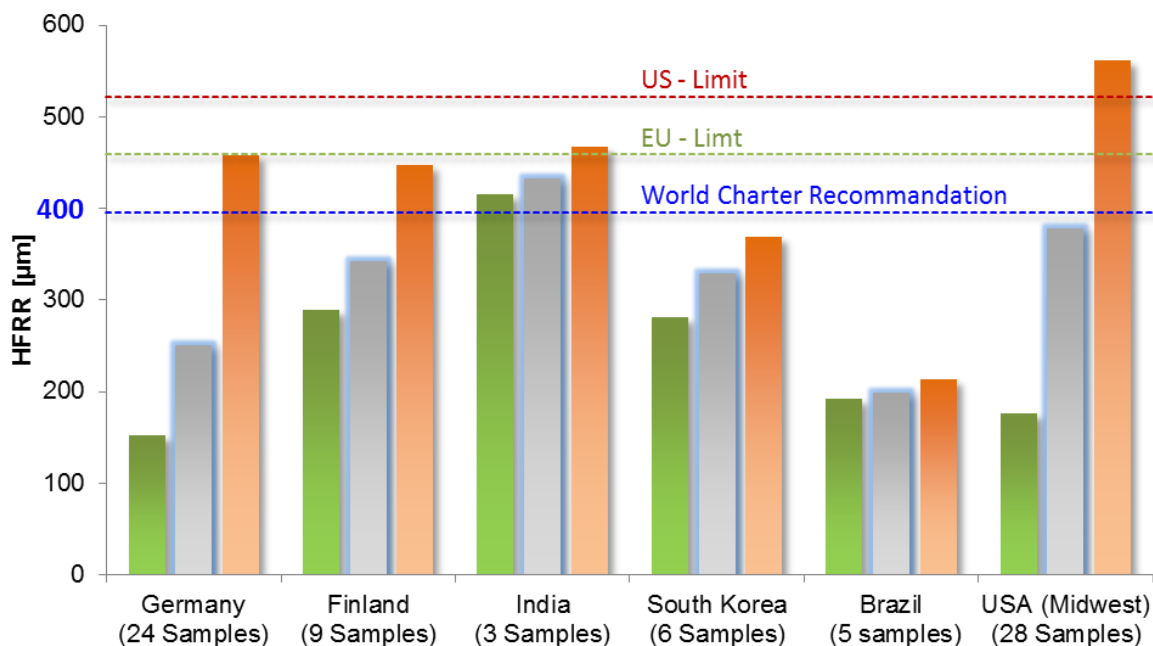
Figure 29: Diesel fuel quality range shown by the high frequency reciprocating rig (HFRR) over selected countries [62]

Three generalized market types reveals the review in *Figure 29*: high quality markets with low outlier in quality (Germany, Finland), countries with low quality crude fuel and therefore resulting borderline fuel quality (India, South Korea) and countries with high quality crude fuel but high quality differences (USA).

2.4. Calculation of mandatory provided power for direct injection

Looking at the physical energy inbound into the FIE, high pressure generation takes a major part of the complete demand. A simplified approach by a calculation of the hydraulic energy leads to a first assumption [46]:

$$P = \dot{V} \, \Delta p = \frac{\dot{m}}{\rho} (p_{outlet} * P_{inlet}) \tag{1}$$

P: power; $\dot{V}$: volume flow; Δp: pressure difference; $\dot{m}$: mass flow; ρ: media density; p_{outlet}: system outlet pressure; P_{inlet}: system inlet pressure

This basic equation *(1)* shows a linear increase in power consumption. Also flow and generated pressure share the same level of importance for the power consumption. In case on an entire FIE, the system border for using equation *(1)* includes fuel tank as inlet conditions and ends with the combined outlet of the injectors, as following *Figure 30* illustrates.
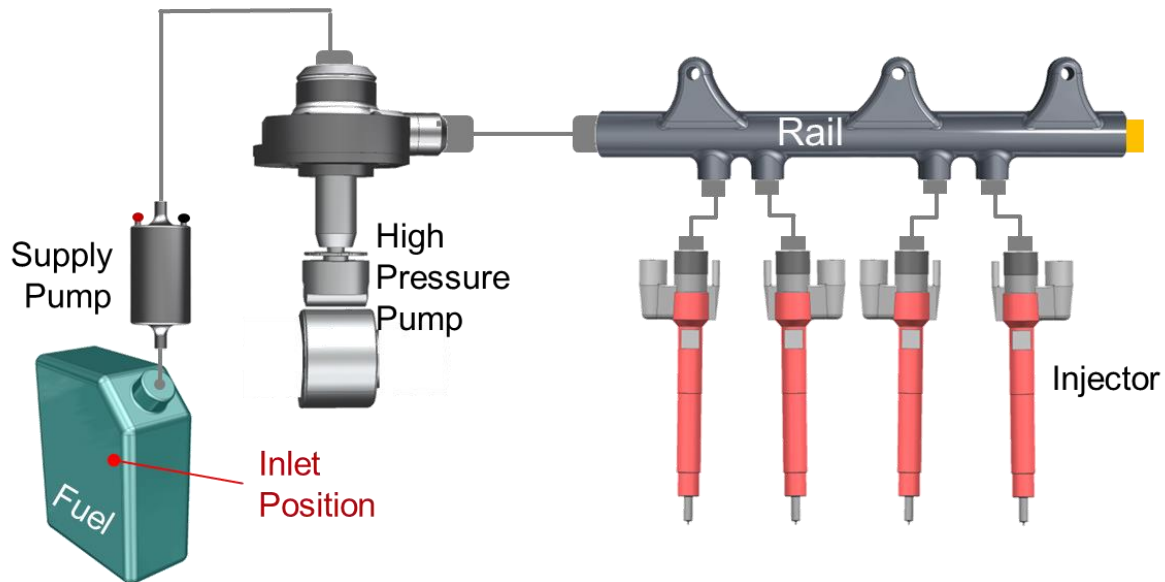
Figure 30: Simplified FIE for power consumption review

Since the injectors provide fuel for injection and therefore for the combustion process, the required volume or mass flow describes the fuel consumption in engine operation. Atmosphere at fuel tank and rail pressure defines differences between inlet pressure and outlet pressure [46].

$$P_{hyd} = \frac{\dot{m_{Fuel}}}{\rho_{Fuel}} (p_{Rail} * p_{tank}) \tag{2}$$

P_{hyd}: hydraulic power; $\dot{m_{Fuel}}$: fuel mass flow for engine duty; ρ_{Fuel}: fuel density; p_{Rail}: actual rail pressure; p_{tank}: pressure in fuel storage

Since m_{fuel}, represents the idealized engine fuel consumption and p_{rail} the regulated pressure at tip of the injector for combustion, the resulting power consumption shows minimum hydraulic power demand from FIE.

The technical effort to realize this for FIE shows a different picture. Modern GDI systems have in principle this kind of architecture, but high pressure levels of todays Diesel FIE require at

least, as mentioned in chapter *2.2.3.2,* a servo hydraulic injector architecture, which leads to additional leakage losses.
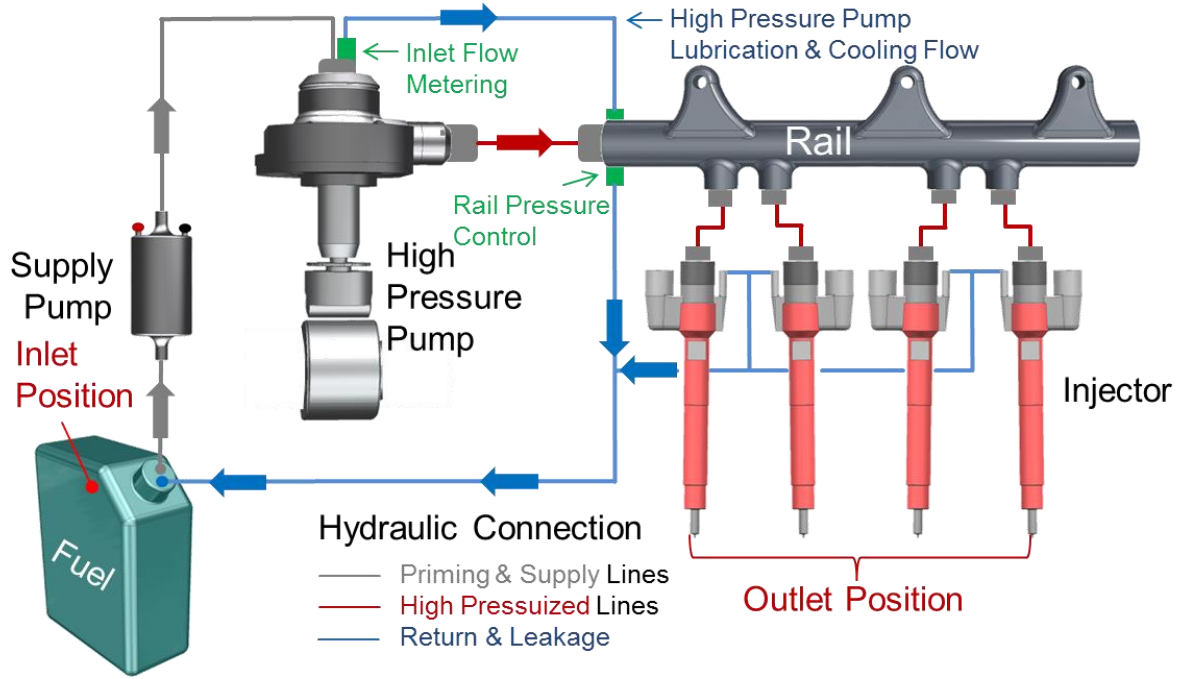
Figure 31: Diesel FIE hydraulic schematics

The hydraulic circuit, shown in *Figure 31*, illustrates additional losses for the complete FIE, as it is typically used in diesel FIE. The first is caused by the high pressure pump. Modern fuel lubricated high pressure pumps flush the complete pump to lubricate bearings as well as cool the entire pump. As second loss, also the rail pressure controller and already mentioned injector leakage sum up to a loss for the complete system:

$$\dot{m}_{total} = \dot{m}_{Fuel} + \dot{m}_{Pump\_leak} + \dot{m}_{Injector\_leak} + \dot{m}_{Rail\_control} \qquad (3)$$

$\dot{m}_{total}$: entire FIE fuel mass flow;
$\dot{m}_{Pump\_leak}$: fuel mass flow for high pump leak and coolant;
$\dot{m}_{Injector\_leak}$: fuel mass flow for injector servo circuit actuation;
$\dot{m}_{Rail\_control}$: fuel mass flow for rail pressure correction leakage

Later the complete FIE hydraulic power consumption is not only impacted by the mass flow, but also by a pressure increase per stage. Modern common Diesel FIE require, due to lubrication and cooling (see chapter *2.2.2.2*), at least two stages: the supply pump and the high pressure pump.

$$P_{hyd\_total} = \left[\frac{\dot{m}_{total}}{\rho_{Fuel}} \left(p_{supply} - p_{tank} \right) \right]$$
$$+ \left[\frac{\dot{m}_{Fuel} + \dot{m}_{Injector\_leak} + \dot{m}_{Rail\_control}}{\rho_{Fuel}} \left(p_{rail} - p_{supply} \right) \right] \qquad (4)$$

P_{hyd_total}: entire FIE hydraulic power demand;
p_{supply}: supply system pressure;

The supply pump needs to pump the fuel to the high pressure pump, which also requires supplying a high mass flow through the filter and the heater. Depending on the high pressure pump type, nowadays supply pressures are rising up to a relative pressure of 8 bar.

Injector leakage by its servo hydraulic (see chapter 2.2.3) determines the second loss of the complete FIE ($\dot{m}_{Injector\_Leak}$). Since the servo hydraulic utilizes high pressurized fuel, leakages have high energetic impact. In the same way, rail pressure control losses ($\dot{m}_{Rlyail\_control}$) may reach high values due to pressurization up to rail pressure levels.

2.4.1. A detailed review of the high pressure pump energy demand

The detailed high pressure pump function understanding requires a more fundamental review of its thermodynamic description. This can be described in equation *(5)*. To focus on mechanical power consumption, an adiabatic approach has been used [63].

$$P_{pump\_hyd} = \dot{m} * \Delta h_{Fuel} = \dot{m}\left[h_2 - h_1 + \frac{c_2^2 - c_1^2}{2} + g*(z_2 - z_1)\right] \qquad (5)$$

P_{pump_hyd}: hydraulic pump power;
Δh_{Fuel}: difference in enthalpy before and after pressurization;
h_x: generalized enthalpy;
c_x : generalized fluid speed;
g: gravity constant;
z_x: generalized height

The difference in enthalpy ($h_2 - h_1$) describes the energy stored within the fluid, while the specific change in flow speed $\left[\frac{c_2^2 - c_1^2}{2}\right]$ describes the change in kinetic energy within the fluid. The last term ($g*(z_2 - z_1)$) determines the change in potential energy due to the difference in height. Nevertheless, since for engines in passenger as well as commercial vehicles no significant changes in height occur, the last term has an insignificantly low value compared to pressure change and speed. Therefore it can be ignored for this application [16].

The difference in enthalpy ($h_2 - h_1$) can also be described as a fuel pressure increase. Assuming the incompressibility of liquids and an insignificantly low speed of fluid, leads to the equation *(6)*:

$$P_{pump\_hyd} = \dot{m}\Delta h_{Fuel} \approx \dot{V}(p_{rail} - p_{supply}) \;\; [16] \qquad (6)$$

$\dot{V}$: generalized volume flow;

Equation (6) is nowadays typically used to describe the hydraulic power consumption of high pressure pump. However, since volume and fluid density have to be static during compression, this equation is only valid up to ~150bar [15]. Even gasoline high pressure pumps, which reach pressure levels of 200bar – 350bar, exceed this borderline. Thus, the description for fuel injection equipment requires a correction for compressibility. A typical engineering approach

for calculation uses the bulk modulus of fuel for compression correction [64], as in equation (7) [64].

$$K = \frac{1}{E} = \frac{-1}{\Delta p} \frac{\Delta V}{V_0}$$

(7)

K: bulk modulus; E: elastic modulus;
Δp: change in pressure; ΔV: change in volume; V_0: initial volume

By solving this equation to a change in volume, the theoretical compression can be expressed by equation (8) [64].

$$-\Delta V = \frac{V_0 * \Delta p}{E}$$

(8)

Integration of equation (6) into equation (8) leads to a compression corrected equation of the hydraulic pump power.

$$P_{Pump\_comp} = \dot{V} * \left(p_{rail} - p_{supply} \right) - \frac{\dot{V}}{E} * \left(p_{rail} - p_{supply} \right)$$

(9)

P_{Pump_comp}: Compression corrected hydraulic power demand;

The correction for compressibility in equation (9) is a major difference for a technical calculation approach of high pressure pumps compared to pumps in most industrial applications. Nevertheless, industry typically uses equation (6) as common and simple approach. But also equation (9) has its importance within detailed high pressure pump efficiency review.

To predict final pressurized density, the equation of Huang and O'Connell is recommended by Bruce E. Poling within "The properties of Gases and Liquids" [65].

$$\frac{(p-p_0)}{RT} = (1 - C'b_1)(\rho - \rho_0) - C' \left[b_2 V' \frac{(\rho^2 - \rho_0^2)}{2} + b_3 V'' \frac{(\rho^3 - \rho_0^3)}{3} + b_4 V''' \frac{(\rho^4 - \rho_0^4)}{4} \right]$$

(10)

p : actual pressure; p_0: initial pressure; R: universal gas constant; T: temperature;
C': Compression parameter; b_i: coefficients for reduced temperatures

In equation (10), most of the values b_i for pure fluids with a minor temperature dependence according equation (11) can be expressed by constants [65]:

$$b_i = a_{1i} + a_{2i}\tau + a_{3i}\tau^2 \quad \text{with } \tau = \frac{T}{T\prime} < 1$$

(11)

a_{ji}: Constants by Huang and O'Connell

The entire approach in equation (10) and equation (11) has an error in range of 1.5%, if well fitted parameters are used [63]. Since those very detailed values are typically not given for fuels, especially new type of fuels, this approach is not satisfying for a general review of FIE performances.

2.4.2. A detailed review of high pressure pump efficiencies

For a comparison of high pressure pumps in terms of their losses, two major efficiencies describe the high pressure pump performance. The most used efficiency type is the volumetric efficiency, which describes the ratio of the actual flow compared to the maximal geometric flow [64].

$$\eta_{vol} = \frac{\dot{V}_{fuel}}{A_{Plunger} * s_{lift} * n_{hub} * n_{rpm}} = \frac{\dot{V}_{fuel}}{\dot{V}_{Geom}} \qquad (12)$$

η_{vol}: volumetric efficiency; $A_{Plunger}$: plunger effective surface;
s_{lift} : plunger lift; n_{hub} : number of lifts per rotation; n_{rpm}: number of rotations

As feasible in equation *(12)* volumetric efficiency describes itself as the ratio between actual volumetric flow and geometrical abilities by the high pressure pump. This equation targets flow losses, like leakages or an improper filling. Especially for quality and function check of high pressure pumps, this equation is widely spread amongst industry.

One major disadvantage of this measurement method remains in necessity to measure the high pressure pump in maximum capacity. Due to the fixed geometric approach, partial filling of high pressure pump cannot be correctly applied by this test, as well as digital inlet valves (=DIV) controlled pumps. Thus, another test method is based on the high pressure pumps mechanical power consumption measurement [64].

$$\eta_{tot} = \frac{\dot{V}_{fuel} * (p_{rail} - p_{supply})}{T_{mean} * 2 * \pi * n_{pump}} = \frac{P_{pump\_hyd}}{P_{pump\_mech}} \qquad (13)$$

η_{tot}: total efficiency; T_{mean}: mean torque;
n_{pump} : pump rotation speed; P_{pump_mech}: mechanicsal power consumption;

The total efficiency, as stated in equation *(13)*, describes the ratio between mechanical power consumption and idealized hydraulic power consumption. Since all required values are based on measurements, this review allows the analysis of high pressure pump performance, during metering. Additionally, high pressure flow and torque are two direct interfaces between engine duty and the high pressure pump as "power loss". In other words, high pressure total efficiency indicates as scalar value impact on engine fuel consumption performance [64].

2.5. Friction impact on the complete engine powertrain

Finally, impact on engine emission and fuel consumption requires a detailed review of the energetics as well as the mechanics. As described within chapter 2.4, all parts within the FIE contribute to the complete power consumption by providing pressurized fuel flow for the combustion process and therefore require a hydraulic power demand. However, high pressure system flow direct interfaces to the engine via the high pressure pumps mechanics power consumption and the low pressure pumps electric power consumption. Additionally, indirect influence is given by increasing the fuel temperature. Depending on fuel and FIE type, this influence can have major impact on durability of FIE and therefore for the entire engine.

2.5.1. Reduction of the required hydraulic energy by the FIE

In most cases, a hydraulic power demand reduction means to reduce flow ($\dot{m}_{total}$) and supply pressure (p_{supply}). Since the fuel flow for combustion process is mandatory to provide proper engine function, fuel flow reduction approaches leakage of injectors ($\dot{m}_{injector\_leak}$) and coolant flow for high pressure pump ($\dot{m}_{pump\_leak}$).

All those mentioned parameters, which reduce total system flow, impact the hydraulic friction [64]

$$\Delta p = \left[\xi * \frac{\overline{c^2}}{2}\right] + \left[\frac{64 * \nu}{\overline{c} * D} * \frac{L}{D} * \frac{\overline{c^2}}{2}\right] \tag{14}$$

ξ:resistance coefficient; $\overline{c}$: average fluid speed;
ν : dynamic viscosity; D: effective diameter; L: effective length

Especially, the fuel filter and the fuel heater increase system friction significantly. As the pressure difference calculation in equation *(14)* show, the internal resistance (ξ) remains in low pressure systems in high value since net size is around 10µm. On the other hand: typical used steel pipes for high pressure connection feature low roughness levels, which leads to low friction levels. Thus major beneficial impact results from lower flow in low pressure system [66].

Therefore, new low pressure systems focus on reduction of pressure levels and flow levels. Beneficial for this effect remains the low total efficiency of low pressure pumps. Also a demand controlled or a pressure controlled low pressure circuits have the ability to reduce the hydraulic power demand significantly [65].

From equation *(4) [66]*:

$$P_{LP\_hyd} = \left[\frac{\dot{m}_{total}}{\rho_{Fuel}} * \left(p_{supply} - p_{tank}\right)\right] + \left[\frac{\dot{m}_{total}}{\rho_{Fuel}} * \left(\Delta p_{supply}\right)\right] \tag{15}$$

P_{LP_hyd}: hydraulic power demand in low pressure circuit;

As visible in equation *(15)*, the flow as well as the pressure have proportional impact on the power consumption reduction. In case of a low pressure system, the value of the target system pressure is compared to the high pressure target low value. Anyhow, since the supply pressure supports the high pressure generation, the low supply pressure impacts the high pressure pump power consumption. Total system fuel flow reduction achieves higher benefits. Additionally to the reduced power by lower volume flow, lowered flow speed in hoses and pipes reduce hydraulic friction.

In case of the high pressure circuit, the engine demands by its calibration fuel quantity and rail pressure in order to achieve performance and emission targets. The realization of lowered power consumption becomes feasible by reducing the systems leakages or changing the combustion strategy leading to lower rail pressure or lower number of injections [67].

$$\Delta P_{HP\_hyd} = \left[\frac{\Delta\dot{m}_{combustion} + \Delta\dot{m}_{leakage} + \Delta\dot{m}_{Rail\_control}}{\rho_{Fuel}} * \left(p_{supply} - p_{rail}\right)\right] + \left[\frac{\dot{m}_{fuel}}{\rho_{Fuel}} * \left(\Delta p_{rail}\right)\right] \tag{16}$$

P_{Pump_hyd}: hydraulic power demand in high pressure circuit;

Equation *(16)* demonstrates the expected differences in power demand, due to changes on the high pressure system, since technical application differs amongst the industry. Especially the injector technology build major driver for a high pressure system demand reduction. The diesel FIE with servo injectors and multi injection for clean combustion and high rail pressure levels achieves higher differences in total power consumption and therefore higher potential than the GDI FIE. Nevertheless, this review respects required hydraulic energy and neither reflects mechanics interaction nor potential improvement in combustion process.

2.5.2. Total efficiency increase of low and high pressure pump

Despite the power demand for actuators and injectors energizing, low and high pressure pump consume together nearly complete energy of the engine FIE. Therefore, by increasing the efficiency in these components, the FIE friction influence on the engine improves overall. Also, all required energy demands reflect ideal technical solution with no mechanics impact at all. Anyhow, as described in chapter *2.4.1,* the fuel pressurization by high pressure pump as well as low pressure pump suffer mechanical losses.

Since both systems have different functional background, their efficiency levels as well as their contribution to the total power consumption differ from each other. The low pressure pump supplies highest flow but on low pressure levels. Nowadays technical solution reaches total efficiency of about 15% - 25% [67]. Even if this value is quite low, an efficiency increase significance suffers from comparably low required hydraulic energy amount to supply entire FIE [66]. Also modern low pressure systems control flow and pressure levels, which reduce hydraulic energy consumption [66]. This optimization towards smaller volume flows reduces required energy amount of the low pressure system, but leads to a altering in the low pressure pumps total efficiency. This is shown in *Figure 32*.
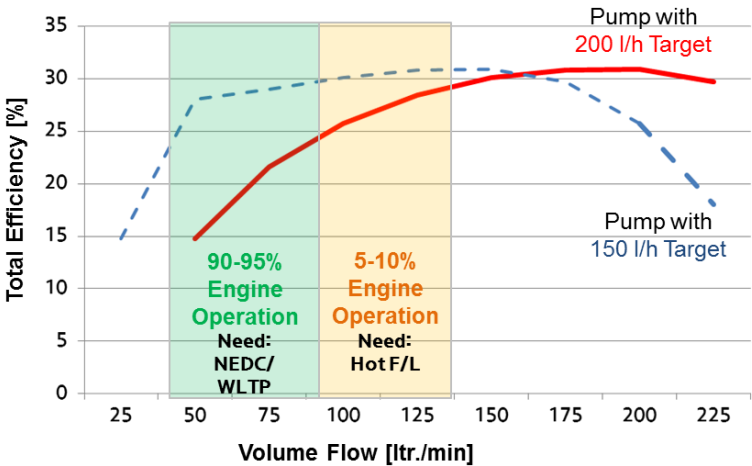
Figure 32: Total efficiency of low pressure pump according to their target flow [67]

Nevertheless, in times when OEM start to review for even smallest portion in CO_2 reduction, this aspects also get into focus. State of the art low pressure systems therefore applied by two different methods to increase the low pressure system efficiency. The first approach targets on a well-defined low pressure circuit including demand controlled fuel pumps. In this case low pressure pump works in similar total efficiency range as before, but hydraulic demand is reduced. Impact can be calculated by following idealized approach equation *(17)* [66]. Herein temperature range of component and fluid is assumed to be in operational nominal condition.

$$P_{LP_{Elec}} = \frac{P_{LP_{Hyd}}}{\eta_{LP_{tot}}(\dot{V}, p_{supply})}$$ (17)

$P_{LP_{Elec}}$: electric power consumption of low pressure pump;
$\eta_{LP_{tot}}$: low pressure pump total efficiency

By reviewing the efficiency level as in *Figure 32* in combination with equation *(17)*, the reduction of hydraulic power demand may improve electrical power consumption. Since efficiency states as a function of volume flow and final pressure level, also operational areas with no final improvement are feasible [66].

An alternative approach targets to improve the low total efficiency levels generally. This is feasible by review of equation *(17)*. Since the total efficiency differs amongst its operational range, increasing or optimization frequently used areas' total efficiency lead to lower electric power consumption [66].

On high pressure side, equational background remains on the same principle, (see equation *(18)* [46]) thus hydraulic energy reaches far higher levels than on low pressure side. As an advantage against low pressure side, high pressure pumps reach higher total efficiency, mostly driven by their hydraulic losses or pump internal leakages.

$$P_{HP_{mech}} = \frac{P_{HP_{Hyd}}}{\eta_{HP_{tot}}(\dot{V}, p_{rail})}$$ (18)

$P_{HP_{mech}}$: mechanical power consumption of high pressure pump;
$\eta_{HP_{tot}}$: high pressure pump total efficiency

Nevertheless, also a high pressure pump requires sustainable mechanics, since internal forces are very high. As a result, high pressure pumps may achieve a comparable high total efficiency against a low pressure pump, but only in full load and ideal speed range. By lowered plunger filling and lowered pressure levels, total efficiency may reach very low levels, comparable to low pressure pump as following *Figure 33* illustrates.
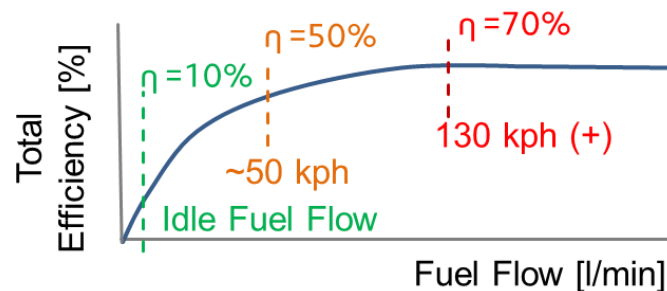
Figure 33: Qualitative total efficiency characteristic according to vehicle speed [68]

This *Figure 33* demonstrates the decreasing efficiency of high pressure pumps and therefore increasing engine loss. Thus, depending on the injection and combustion strategy, the hydraulic energy reach high level, leading to necessity to review pump total efficiency mapping very carefully [66].

Since the low pressure and the high pressure pump together consume nearly all power demanded by FIE, full system total efficiency calculation remains as final step [66]. Depending

44

on review from combustion process or hydraulic system side, different subsystems need to be included. Especially spray as interface between "hydraulic system" and "combustion systems", have different type of efficiencies. As assumption, the spray interaction will be seen as quasi constant and therefore ignored.

$$P_{FIE} = \frac{P_{HP_{Hyd}}}{\eta_{HP_{tot}}\left(f:\frac{\dot{m}}{\rho_{Fuel}},p\right)} + \frac{P_{LP_{Hyd}}}{\eta_{LP_{tot}}\left(f:\frac{\dot{m}}{\rho_{Fuel}},p\right)} \qquad (19)$$

P_{FIE}: entire fuel injection equipment power consumption;

Combined with equation *(4)* and equation *(13):*

$$\eta_{FIE} = \frac{\left[\frac{\dot{m}_{total}}{\rho_{Fuel}}*\left(p_{supply}-p_{tank}\right)\right]+\left[\frac{\dot{m}_{Fuel}+\dot{m}_{Injector\_leak}+\dot{m}_{Rail\_control}}{\rho_{Fuel}}*\left(p_{rail}-p_{supply}\right)\right]}{T_{mean}*2*\pi*n_{pump}+U_{Bat}*I_{LP\_Pump}} \qquad (20)$$

η_{FIE}: entire fuel injection equipment total efficiency;

The equation *(20)* gives the possibility to get an overview of impact by each component on total system efficiency. All adjustable and measurable parameters are listed and support engineering approaches to identify losses.

2.5.3. Impact on the engine's fuel consumption

Final analysis target remains on the impact in terms of engine loss and therefore FIE impact on engine's fuel consumption. As ended in chapter *2.5.2*, FIE power consumption sums up from low pressure pump, high pressure pump, injector and rail. Nevertheless, also fuel abilities like density and viscosity impact the total system efficiency and therefore power consumption.

As usual practice among engine engineers, friction or engine efficiency determines the equation for specific fuel consumption.

$$b_e = \frac{\dot{m}_{Fuel}(T_{Eng},n_{eng})}{P_{eng_{out}}(T_{eng},n_{eng})*h} \qquad (21)$$

b_e: engine specific fuel consumption; $P_{eng_{out}}$: engine power; h: hour;
T_{eng} : engine torque; n_{eng}: engine speed

Since the described value *b_e* uses an hour based timeframe, specific fuel consumption within equation (21) [16] follows often used engineering review per hour. It therefore remains as index for engine efficiency at certain positions on the engine map.

Table 11: Example specific fuel consumption of HMC engines [38]

Engine Type	Gasoline engine (Theta Engine 2,0 ℓ)	Passenger diesel (R-Engine, 2.0 ℓ)	Heavy duty diesel (G-Engine , 6.8 ℓ)
Idle / lowest operation ($P_{eng} = min$)	$609\ \frac{g}{kWh}$	$393\ \frac{g}{kWh}$	$721\ \frac{g}{kWh}$
Rated torque ($T_{eng} = Max$)	$278\ \frac{g}{kWh}$	$204\ \frac{g}{kWh}$	$196\ \frac{g}{kWh}$
Rated power ($P_{eng_{out}} = Max$)	$311\ \frac{g}{kWh}$	$210\ \frac{g}{kWh}$	$219\ \frac{g}{kWh}$

As visible in *Table 11,* with increasing torque and power output, engines become more and more efficient. On the other hand, engines which only use a small share of their capacity, suffer in efficiency. Nowadays, engine design and management targets to optimization of use and test ranges.

Unfortunately, in case of passenger vehicles, loads are usually in low range of flow and pressure demand, which is followed by the typical test cycles as NEDC with 7 kW [29] and WLTP with 11 kW average power output [30]. Thus, engine components energy consumption has significant high share in specific fuel consumption (b_e). OEM use also b_e to calculate this portion of each engine auxiliary in engine losses.

$$\dot{m}_{fuel\_sub}(T_{Eng}, n_{eng}) = b_e * P_{loss}(T_{eng}, n_{eng}) * h \text{ [16]} \qquad (22)$$

$\dot{m}_{fuel\_sub}$: sub-component fuel consumption share; P_{loss}: sub-component power consumption

Equation (22) calculates mandatory fuel consumption on complete engine to power the subsystem or auxiliary. In order to receive correct information from this equation, it is mandatory to have detailed knowledge of power consumption. In case of a high pressure pump, not only the power consumption of the components has to be taken into account, also the installation and the integration into the engine mechanics impact this auxiliary fuel consumption.

Anyhow, engine test benches and chassis dyno as final stage of evaluation with pre-defined test cycle perform such evaluation as a common tool for fuel consumption and exhaust gas emission quality analysis. The consumed fuel within this cycle sums up by the engine losses and fuel required to move the vehicle. Thus, improvements or demerits result by difference in complete fuel consumption over complete cycle. To calculate fuel consumption and differences, the summation over complete mapping shows precise changes by different components

$$\begin{aligned} m_{fuel} &= \sum \dot{m}_{fuel\_sub}(T_{Eng}, n_{eng}) * X \\ &= \dot{m}_{fuel\_sub}(T_{Eng1}, n_{eng1}) * X_1 + \dot{m}_{fuel_{sub}}(T_{Eng2}, n_{eng2}) * X_2 \\ &\quad + [\ldots] + \dot{m}_{fuel\_sub}(T_{Engn}, n_{engn}) * X_n \end{aligned} \qquad (23)$$

m_{fuel}: total fuel consumption ; X_n: test point share to entire test

The factor X_n in equation *(23)* represents share of each point during testing. In this manner also resolution of measurements on engine dyno or calculation can be adjusted. To achieve a highest accuracy, a numerical approach over a recorded or simulated measurement becomes mandatory. However, since such operation is time consuming and not often proper for all types of test cycles, this factor can be adopted to the share of each point. This allows an estimation for first review or measurement clustering to speed up calculation time to achieve real time calculation [69].

3. Methods to determine the power consumption of the fuel injection equipment

As part of the engine auxiliaries, the Fuel Injection Equipment (FIE) consumes mechanics power and electrical power. Even when the hydraulic power shows higher power consumption compared to other engine auxiliaries, the total loss for the engine is determined by the final power consumption of the engine. Therefore, knowledge about the integration into the engine assembly is of the same importance as the correct total power consumption of the FIE.

Typically, high pressure pumps as one major "consumer" of FIE power demand are mounted in three positions in the engine assembly:
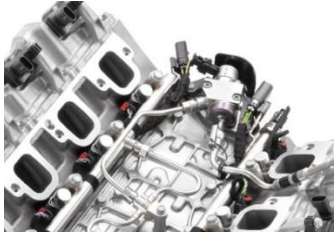
Position	Crankshaft	Additional shaft in belt / chain	Camshaft
Describing picture	[39]	[38]	[33]
Short description	Effective way for high power consuming pumps or engine with high number of auxiliaries	Cost attractive solution for external lubricated pumps with higher torque demands	Integration at the end of camshaft or as pumping element integrated into the camshaft
Typical application	-Commercial engines -Off-road applications	-passenger diesel engines	- GDI engines - Cost efficient solution - Small auxiliaries engines
Effect on torque / power consumption	$T_{eff} = T * \eta$	Details in 4.2.2	$T_{eff} = T * \eta_{chain}$

Table 12: High pressure pump engine integration with respect to the estimated physical impact

In respect to the mentioned background in *Table 12*, friction losses due to engine integration are determined by the mechanical interface and its efficiency. The integration into the chain (or belt) is a special case, since the physical boundaries needs to be reflected for the specific design approach [68]. Taking into account the high amplitudes in dynamic torque of modern high pressure pumps, measurements in an entire assembly becomes mandatory.

Anyhow, first direct torque measurement on high pressure pump samples is a possible start for analysis. But this operation requires measurement in high sampling rate in order to receive plausible results. Herein, simulations can support the understanding of internal processes and its interfaces for the entire FIE as well as for the combustion process. In addition the measurement of drive train implementation losses completes the full analysis of the high pressure pump impact on engine performance.

3.1. Direct measurement of mechanical power consumption of the high pressure pump

For achieving a detailed analysis of losses caused by the high pressure pump, direct measurement procedures are required. Thus, OEM's as well as Tier 1 typically test such equipment in special test benches for the FIE analysis.

High pressure pump power consumption measurement are therefore performed on a Bosch Moehwald CA4000 test bench with a setup specially designed at HMETC (Hyundai Motor Europe Technical Center).

Performance and equipment data overview of HMETC FIE-Rig 04 in Rüsselsheim	
Maximum power output [69]	35 kW
Maximum torque [69]	240 Nm at 2000 rpm
Maximum speed [69]	6000 rpm
Fueling and lubrication	ISO 4113 (Diesel substitute) Engine oil (Shell Helix 5W30) 1-Octanol (Gasoline substitute)
Temperature conditioning range [69]	20° - 60° (40°C "Standard" measurement temperature)
Maximum rail pressure (setup during examination)	500 bar – 3500 bar (safety limitation)
Rail pressure control hardware and software	Bosch EDC 17 (Software for Diesel) Kefico HnB (Software for Gasoline) IAV FI2RE (Rapid Prototype Controller)
Measurement auxiliaries	16 Analog measurement channels (Temp, pressure, etc...) Drive torque measurement flange Kistler 4504B500 Oscilloscope LeCroy Waverunner 44Xi Coriolis mass flow meter (Siemens Sistrans F)

Table 13: Overview of FIE test bench equipment

In principle this test bench can be used for multiple purposes, but it is configured in its build up to measure and analyze high pressure pumps [45]. To measure the torque of the pump with a high precision, the pump is directly connected to the drive torque measurement flange via a steel flange without any coupling. By this rigid build up, noise and oscillations are suppressed to a possible minimum. Also the short connection allows very low torsional oscillations, which enhance precision. The measurement accuracy for the total efficiency achieved in the measurement described below is within ±1,2%. The value is a result by a CP-test, as this test is frequently executed to ensure measurement precision. Details are listed in *Appendix D-1*. *Figure 34* shows the simplified hydraulic circuit utilized for the measurement. Since it only contains the high pressure fluid circuit, all supply fluids and secondary supplies (e.g. temperature condition and motor coolant) have been removed from this illustration, as they are not part of the measurement subject. An additional engine oil supply is available for the pumps and measurement setup.
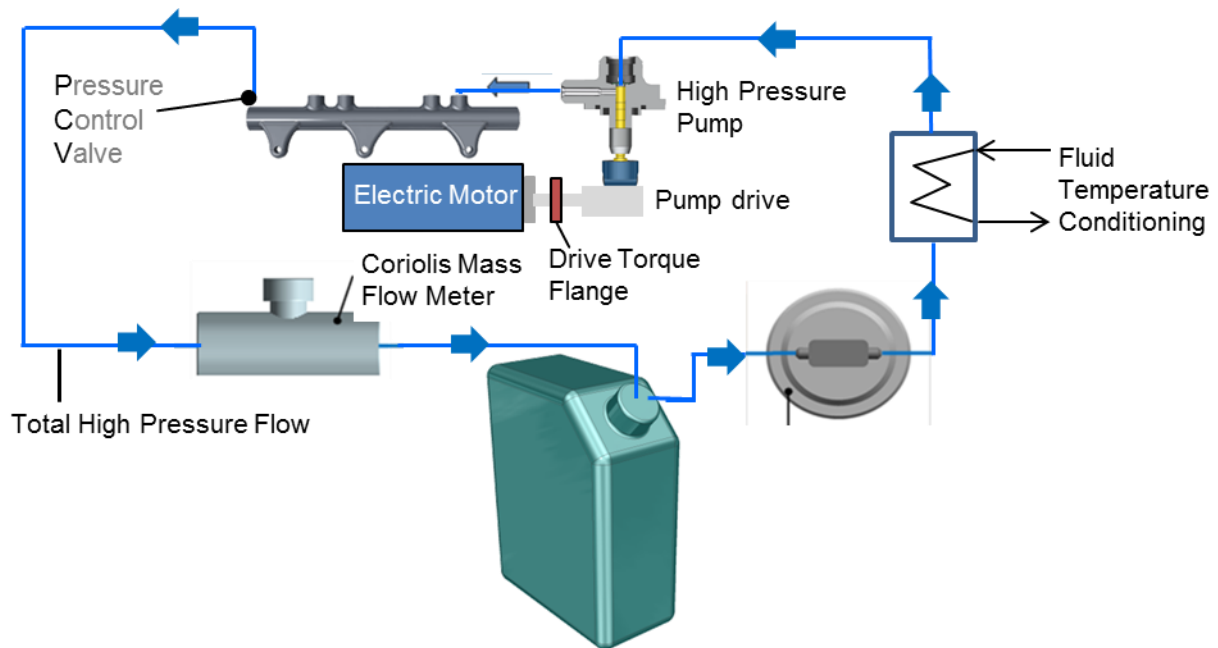
Figure 34: Schematic of the hydraulic test bench setup

Residual impacts by misalignment or unequaled screw tightening contribute to a virtual load in partial areas of the drive torque flange. By rotation, they are visualized as a sinus curve, which has the mean value of 0 after one rotation. The offset level has been scanned prior to measurement after a run in phase of 2h [46].

During measurement operation, it is possible that this self-equilibrating stress may change. This would lead to a change in the measured drive torque offset. Since changing of the offset is clearly noticeable by a "jump" in the drive torque values, such measurements have to be deleted during analysis process.

The pump samples with primer pump have a fuel supply at low pressure to maintain the priming feature. Also pump samples with a special fuel supply pressure demand, receive the adjustments in the setup as required by its specification. Nevertheless, the majority of all tested samples require a relative fuel supply pressure of 3.5bar. As test fluids, substitutes were applied during measurement at the FIE rig. Diesel type, ISO 4113, or gasoline type, 1-Octanol were used. To maintain clean supply lines, the conditioning for gasoline fuel is done by an external fuel conditioning unit with own storage and supply system.

The high pressure circuit differs by type of control and fuel. In the standard configuration, the high pressure pump connects to the high pressure rail via a steel pipe. The rail itself controls the adjusted rail pressure via a pressure control valve (PCV). The injectors themselves are not connected, therefore the complete high pressurized mass flow leave the rail via the PCV. After the PCV, the Coriolis mass flow meter measures the outgoing flow of fuel which returns into the tank. A fuel temperature sensor is positioned between PCV and Coriolis mass flow meter, to correct results by the fuel temperature. This measure increases the flow measurement precision significantly and also gives redundant information for the correct adjusted rail pressure. The flow through the pump is controlled via the metering unit (MeUn) mounted on pump side [46].

In case of a Digital Inlet Valve (DIV) controlled high pressure pump, as they are common for GDI systems or several diesel high pressure pumps, two ways to achieve a proper rail pressure

controlling are applied. The first approach utilizes the complete FIE including rail and injectors, as shown in *Figure 35*.

Figure 35: Build up gasoline high pressure pump test build up

This test setup provides a rail pressure control which is close to a full engine setup. This leads also to high flow control accuracy under realistic condition. In addition, a GDI ECU controls the rail pressure. Limiting factor of this setup is the capability of the injectors' flow rates. This limits the high flow areas and may exceed the controllers calibrated flow limits. Therefore, another rail pressure control strategy for measurement in a wider mass flow range with DIV controlled pumps is necessary.

The second approach targets especially the analysis for commercially sized Diesel engine or high performance gasoline engine (>500HP), where a wider fuel flow range becomes mandatory. Similar to the high pressure pump testing with the MeUn, the PCV controls rail pressure also in this case. A rapid prototyping controller (e.g. IAV FI2RE) adjusts the actuation angle of the DIV. The range from the pump cams top dead center to the bottom dead center regulates the high pressure flow between 0% and 100% of the high pressure pump flow capacity. Since the pump manufactures have strict boundaries for the actuation signals, the rapid prototyping controller receives a voltage and current profile as specified by the manufacturer.

3.2. Design of experiment approach used to determine the power consumption of the high pressure pump

Since not only the proper measurement approach plays a major role for correct power consumption, also a well-defined data matrix becomes necessary for the measurement and analysis capability. Since the system analysis targets not only one specific engine configuration, but also all possible configuration scenarios, a measurement of this kind requires too much time and generates too much data. Thus, pump characteristic described by a data matrix, which allows calculating HPP power consumption among its physical capability, is more efficient in application. Such data matrix (or "mappings") provides performance data such as the mass flow as function of high pressure pumps speed and pressure.

A major performance mapping describes pumps in their full delivery characteristic (see *Figure 36*). Running high pressure pump in full load and within its pressure capability generates a shell of maximum performance, assuming that total efficiency lowers when the pump is operating at part load condition. In case of DIV actuated pumps, a well prepared scanning for

the maximum delivery points becomes necessary in order to achieve the correct shell curve data.
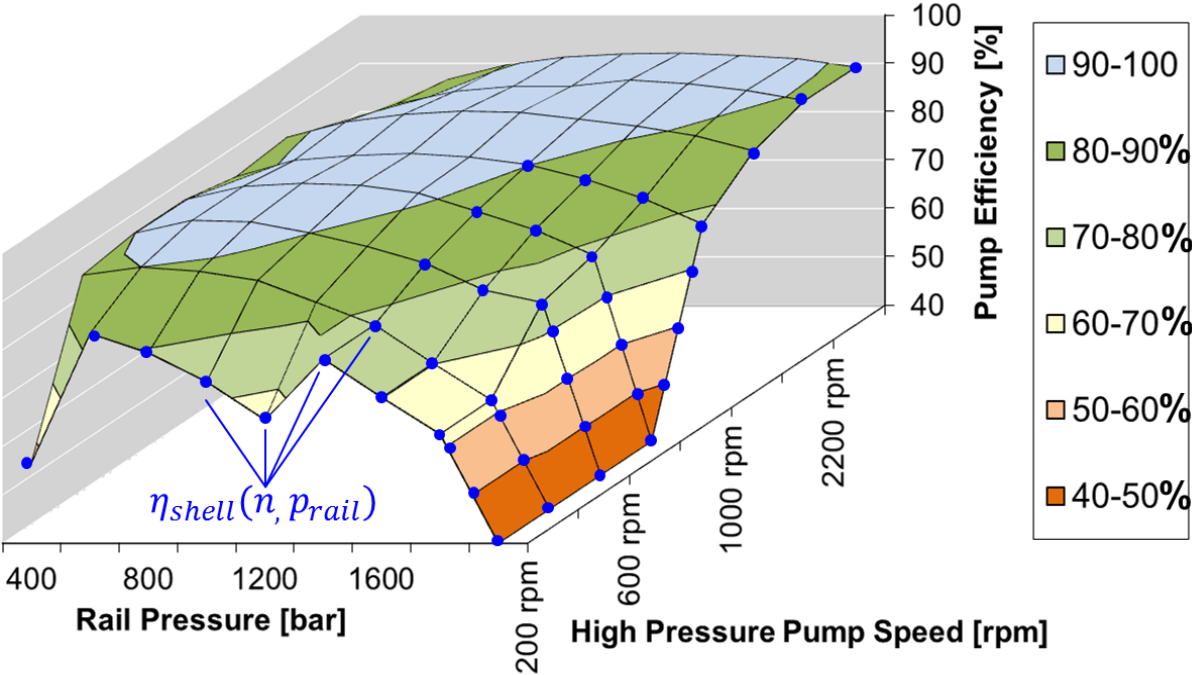
Figure 36: Illustration of the full fuel flow efficiency shell, exemplary for a Bosch CP4s1 high pressure pump

In contrast to old or low cost system rail pressure control architecture, high pressure pumps are usually operated with reduced delivery to deliver the fuel demand for engine duty only. Thus, the power demand of the high pressure pump is reduced by this metering. Since friction differs in load and rotation speed condition, mathematical linear load reduction does not give adequate results. Furthermore detailed knowledge of the high pressure pump down ramping characteristic becomes necessary to achieve detailed information of the high pressure pump power demand (see *2.2.2.*)

In case of MeUn metered high pressure pumps, reduce the inlet flow to the high pressure chamber. This impacts not only hydraulic performance of the pump, but also mechanics performance by different stress level on moving components. Thus, throttled or metered drive torque characteristic differ by load and speed conditions, as *Figure 37* illustrates.

Not every possible speed and load combination is reasonably reflected in the real engine duty. Therefore well-defined down ramping steps, which reflect later pump duty in the engine cycle, are suitable to calculate high pressure pump power consumption. Herein, a separation between a passenger and a commercial application is necessary, since operation ranges of both applications differ significantly. As a consequence the selection of measurement points and its boundaries has to be adapted to the engine or the high pressure pump operation range.
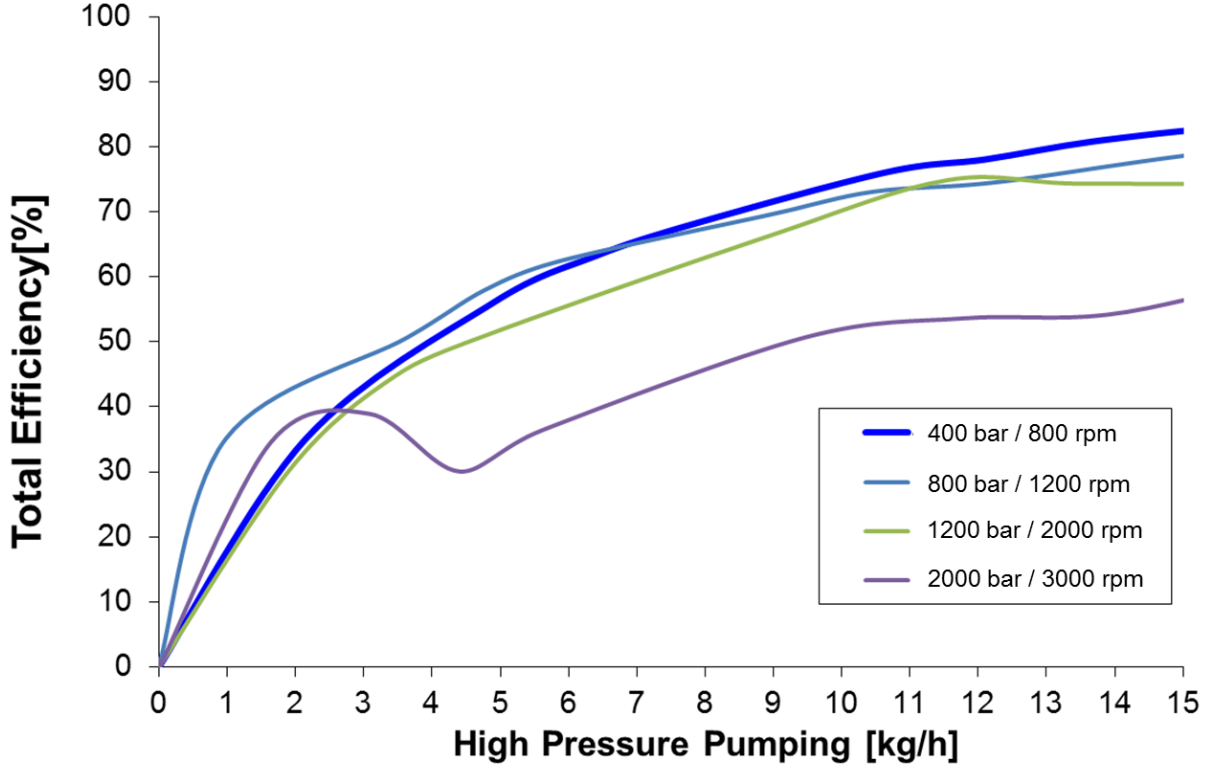
Figure 37: Exemplary metering from zero flow to 15 kg/h mass flow of a Bosch CP4s1 high pressure pump

The afterwards following operation is an interpolation between those measured characteristic points of the former measured shell. This interpolated value is then multiplied by a regression factor for reduced torque by metered pump operation. Those operation points to calculate metered operation impact are herein called "pivot" operation points. This measurement is executed as a ramping from full flow to zero flow as in *Figure 37* .

$$T_{pump}\left(n_{pump}, \dot{m}_{fuel}\right) = \left[\left(\frac{T_{shell1} - T_{shell2}}{n_{shell1} - n_{shell2}}\right) * \left(n_{pump} - n_{shell2}\right) + T_{shell2}\right] * r(\dot{m}_{fuel}) \qquad (24)$$

T_{pump} : high pressure pump mean torque;
T_{shellx}: torque on corresponding position on "shell of maximum performance";
n_{shellx} : pump speed on corresponding position on "shell of maximum performance

With $r(\dot{m}_{fuel})$ as regression factor for load reduction defined as:

$$r_x\left(\dot{m}_{fuel}\right) = \frac{\left(\frac{T_{pivot1} - T_{pivot2}}{\dot{m}_{pivot1} - \dot{m}_{pivot2}}\right) * \left(\dot{m}_{act} - \dot{m}_{pivot2}\right) + T_{pivot2}}{T_{pivotmax}} \qquad (25)$$

T_{pivotx}: torque on corresponding position on "pivot" line for metered pump efficiency;
$\dot{m}_{pivotx}$: mass flow on corresponding position on "pivot" line for metered pump efficiency;
$\dot{m}_{fuel}$: actual requested mass flow of high pressure pump;
$r_x\left(\dot{m}_{fuel}\right)$: regression factor corresponding to speed range of pump

Since reviewed operation point may be between steps of the measured load reduction operation ramps, an interpolation between two ramps is mandatory:

$$r\left(\dot{m}_{fuel}\right) = \left(\frac{r_1\left(\dot{m}_{fuel}\right) - r_2\left(\dot{m}_{fuel}\right)}{n_{pivothigh} - n_{pivotlow}}\right) * \left(n_{pivothigh} - n_{pivotlow}\right) + r_2\left(\dot{m}_{fuel}\right) \qquad (26)$$

$n_{pivothigh}$: pump speed during regression measurement in higher range;
$n_{pivotlow}$: pump speed during regression measurement in lower range

T_{shellx} , the torque on corresponding position on "shell of maximum performance", as well as corresponding parameter n_{hullx}, the pump speed on corresponding position "hull maximum performance", represent closest values for interpolation in full fuel flow hull (see *Figure 36)*. Based on this value the actual power consumption by FIE in each engine cycle becomes feasible. Since typically FIE integrate deep into engine mechanics, also embedding of hardware needs revision and analysis.

3.3. Measurement of chain drive embedded losses of the high pressure pump

The integration of the high pressure pump into the engine impacts also the power consumption of the FIE. While the direct connection to an already given shaft (like cam shaft) or connection via gears (like crankshaft gear in large engines) contributes as efficiency factor for the entire compound. In contrast the integration of the high pressure pump into the chain depends on the assembly and connection boundaries. As one of the most common connection, the integration into the chain between crankshaft and camshaft is in special focus of analysis, as presented here.
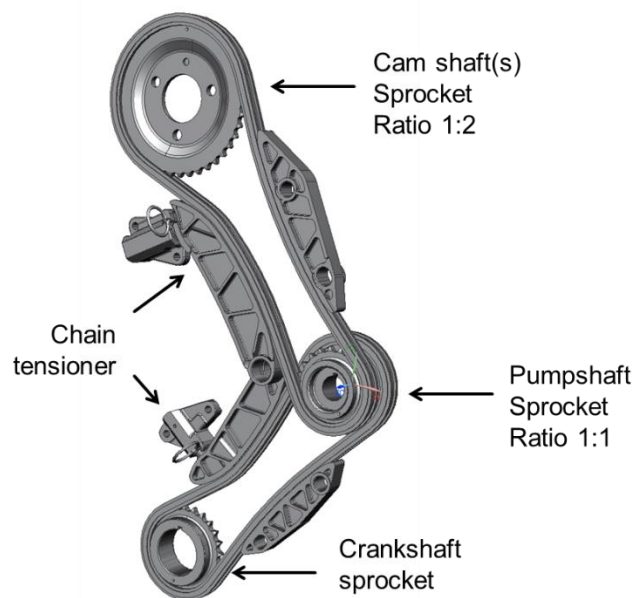
Figure 38: Exemplary passenger diesel engine chain drive [68]

For the integration impact analysis, a R-Engine chain drive has been applied for this analysis. The R-Engine chain drive represents a common approach in the automobile industry for passenger diesel engines. Its transmission ratio between crank shafts to high pressure pump shaft is 1:1 and therefore 1:2 between high pressure pump shaft to camshaft (see *Figure 38*). This configuration represents the preferred configuration by Tier 1 suppliers, due to synchronous pumping to injection events within one combustion cycle.

For an analysis of the entire compound, a special test rig is applied as illustrated in *Figure 39*. It includes serial chain, including support and periphery, sprockets and cam shaft.
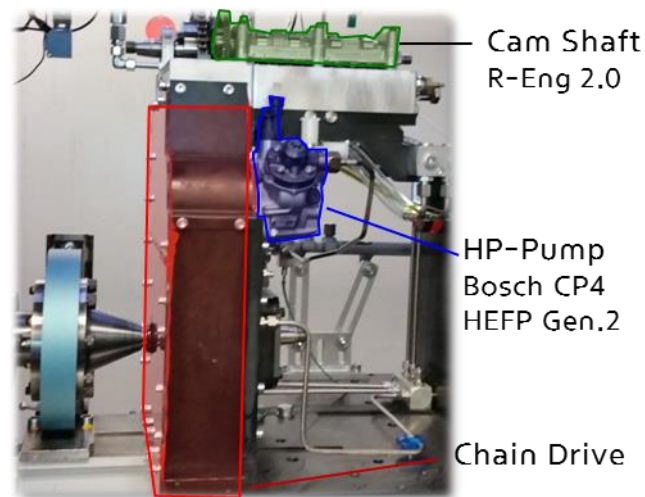
Figure 39: Chain drive torque measurement build up with Bosch CP4S1 on a test bench

An oil lubrication circuit of same type as in production R-Engine supplies chain and cam shaft with engine oil. Also valves and complete mechanics as well as cam shafts bearings allow conditions close to serial engine. An external oil supply adjusts pressure levels to typical conditions in real engine (0,3 bar to 3 bar relative).

For these investigations of the chain load impact, the camshaft simulates two cylinders. By this measure, one high pressure pump rotation demonstrates the condition in real engine, while the other turn demonstrates only the load by bearing and chain. Thus, impact of a full engine setup and a pump only setup can be executed at the same time. Major focus on this review is on analysis of the high pressure pump as major part of the engine bearing and not as an attached auxiliary. Due to high rotating masses mounted on the test bench, speeds higher than 3000rpm are not tested for safety reason.

The mechanical connection to the test bench is established via a direct connection to the drive torque measurement flange without a coupling to avoid torsional frequencies impacting the measurement activities. Internal and external conditioning units supply the high pressure pump sample with diesel or gasoline substitute fuel. Further information is available in chapter *3.1*.

3.4. Measurement of the electrical power demand

Substantial losses are also caused by the FIE due to its electric power consumption. The actuators as well as the driving current for valves and injectors require a high current from the battery. Therefore, two components in typical engine are of interest in electrical architecture:

battery, which is drained by power consumption and alternator, which consumes mechanical power to charge battery.

In a complete picture both components need to be analyzed for complete engine duty. As approximation, the discharging from the battery results of the electrically consumed power of the auxiliaries [16].

$$\Delta Q = \frac{P_{elec}}{U_{bat}} \times t \text{ With: } P_{elec} = U_{bat} * I_{cons} \tag{27}$$

ΔQ: difference in battery charge; P_{elec}: system electrical power; U_{bat}: system (battery) voltage; t: discharge time; I_{cons} : system current

For the complete vehicle energy consumption, the discharging of the battery is a summation of all draining power consumptions. Thus, measurement at the battery gives most accurate result for power consumption determination. The impact on fuel consumption and therefore CO_2-emission results finally from mechanical impact during the charging of the battery via the alternator. Over long term, the alternator has to charge battery with a certain amount of energy since the vehicle's auxiliaries discharge the battery [66].

$$P_{alt} = U_{bat} * I_{alt} * \eta_{alt} \text{ With: } \eta_{alt} = f(n_{eng}, I_{alt}) \tag{28}$$

P_{alt}: power consumption alternator; U_{bat}: battery voltage; I_{alt} : alternator current; η_{alt}: alternator total efficiency

Nowadays, alternators and battery are following an "energy management system" or "battery management system" depending on the type of ECU. Equation *(28)* does not respect such charging strategies behavior, as those charging strategies impact cycle and real road emissions. Nevertheless, if the charging conditions of the engine are known or simulated on test bench, this equation can be used to calculate the actual power demand [66].

A method which respects those facts is a measurement on chassis dyno with the full vehicle including defined electrical consumers and their operation mode. In case of this analysis, the difference in electrical power consumption by the FIE impact the entire cycle, when only FIE components are changed. This requires a base measurement for comparison with a defined base configuration. To respect charging strategies by the ECU, the battery has to be charged and discharged as it is intended. To ensure comparable measurements, the state of charge (SOC) has to be in function window of the implemented logic. Since the calibrated windows differ by vehicle type, each window has to be selected based on the calibrated parameters. For this analysis, the window of a SOC between 70% and 76% and begin of testing has been applied [66].

In case for a lower SOC of the battery after the test cycle, the drained capacity is caused by the higher energy consumption by electrical power. The "lost" percentage in battery SOC is proportional to the CO_2 emission and is reflecting the vehicle energy management optimization.

To support the CO_2 emission impact analysis, a prior study on well-known electrical consumers can be executed. Herein, a steady consumption and well known part is activated during the entire test, such as a head lamp. This causes the same effect as if a component has different electrical power consumption.

3.5. Evaluation for a complete engine and vehicle

For a direct comparison of high pressure pumps, equation *(24)* is useful for a calculation of the total efficiency of pump samples in part load area. This equation allows calculation of every duty cycle within the engine operation and therefore allows calculating the correct torque of the high pressure pump. Especially frictional effects contribute to the analysis outcome and therefore also respected in the engine specific fuel consumption analysis. Therefore, the specific fuel consumption calculation is building a foundation for each engine related analysis (see equation *(21)*).

The following equation describes the mechanical component specific fuel consumption of the high pressure pump as a target component.

$$be_{pump} = be_{engine} * \frac{P_{HPmech}}{P_{eng\_out}} \qquad (29)$$

be_{pump}: specific fuel consumption by high pressure pump;
be_{engine}: engines specific fuel consumption at operation point;
P_{HPmech}: actual power consumption by the high pressure pump at operation point;
P_{eng_out}: engines power output at operation point

In order to consider an electrical power consumer, the approach of equation *(30)* follows an identical approach, in principal. The electrical efficiency of the alternator needs to be considered, since the alternator impacts the engine performance also by mechanical losses [66].

$$be_{electrical} = be_{engine} * \frac{P_{LPhyd} x \, \eta_{LP}}{P_{eng\_out}} \qquad (30)$$

$be_{electrical}$: specific fuel consumption by the supply pump;
P_{LPhyd}: actual power consumption by the supply pump at operation point;
η_{LP}: efficiency of supply pump at operation point

The total FIE power consumption at a certain engine load and speed condition is the sum of the $be_{electrical}$ and the be_{pump}. The total impact in fuel consumption within a specific cycle (NEDC, WLTP, etc.) is the sum over all inherit duty engine cycles (see equation *(31)*) [66].

$$m_{fuel\_duty} = \sum_{t=0}^{t=x} \left[\frac{be_{pump} + be_{electrical}}{P_{engine} * t} \right] \qquad (31)$$

m_{fuel_duty}: total fuel consumption of FIE during cycle;
t: cycle time

Shown equation *(31)* allows summation of the entire fuel consumption by FIE. This is useful for the analysis of test cycles measured in an engine dyno in a "Hardware in the Loop" setup (HIL). By nature of a HIL setup, recorded data from a prior test cycle in real condition is mandatory. These so called front load data require data of engine operations and vehicle data, such as speed. Otherwise reasonable engine duty conditions for analysis can also be used. Those front load data can be assumed by a vehicle simulation in early development states or as it would be an applicable approach for analysis of WHTC points in on- and off-road commercial applications. Especially commercial applications, with a high grade of individual application, cannot generate these front load data.

Following information from chapter *2.,* a proper way to receive adequate measurement is to run a full vehicle on the chassis dyno, following a certified cycle. This is especially reasonable in case of passenger vehicles, whereas higher dynamics and high idle time are requiring a full vehicle setup for realistic boundaries. Since complete vehicles are giving a possibility for high disturbances by variety of their interacting systems, uniform test cycle becomes mandatory in order to measure smallest effects. Therefore, test preparations as regulated in NEDC or WLTP cycle are not enough. Also, battery charging, fuel and vehicle preparation have high impact on all measurement results. Therefore, a strictly defined test preparation has to be applied, which prepares the entire vehicle every time in an equally way and guarantees same test conditions.

3.6. Supportive measures by simulating the injection system

Modern simulation approaches enable a deeper analysis of systems and allow a more efficient optimization without prototyping. They also allow an analysis of dynamic behavior and a first optimization of duty cycle strategies. Therefore, a very accurate and detailed model is required. Such simulation models, may lead to high computing requirements, especially memory and time. In addition, physical models and databases are often at the edge of the applied knowledge or even out of the available data boundaries. Especially non-linear specifications are often based on empirical data and not on a certain equation or model. As mentioned in *2.4.1* characteristics in high pressure areas lead to large deviations between the measurement value in experiments and calculation based on today's used equation *(10)* and equation *(11) [72]*. Especially for fuels, Robert Bosch GmbH established adiabatic property tables under high pressure based on empirical data [73].
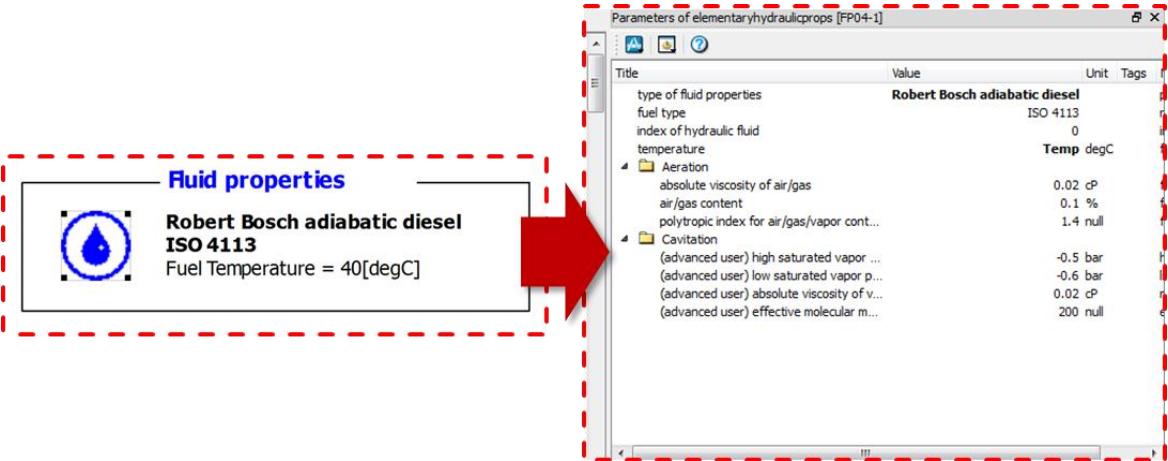
Figure 40: Screen print of base Robert Bosch fluid properties in LMS. Amesim simulation software [73]

Figure 40 lists the available properties for modification. Compared to all physically possible abilities, the number of options is limited. A highest detail grade would also allow mixture levels of different fuels. In typical engineering approaches only the temperature and the fuel type itself receive modification: system simulation focusing cavitation effects, as in supply lines and pumps, often use air/gas and saturated vapor properties adjustment to identify effects. The available properties match for such tasks. Anyhow, simulation systems which focus high pressure analysis do not require adjustments in saturation properties [74]. The high-pressure range impacts viscosity and compressibility, which is not fully reflected by available properties. Since data background is empirical, viscosity abilities and compressibility are reflected by the measurement, but cannot be modified for analysis by simulative parameters [73].

3.6.1. Introduction into simulation system approaches

Depending on the desired target of an analysis or on the following evaluative step, engineers often utilize simplified simulation models to achieve fast results in sufficient accuracy. An individual level of abstraction therefore needs to be considered in order to achieve the accuracy demands and analyze the effects in focus of activity. Especially Hardware in the Loop (HIL) simulation requires practical and simplified solutions to allow a real time handling [75]. Another suitable situation for using simplified and abstracted systems is the analysis of unknown constellations. Then these simplified systems can give a first overview of the system and helps for a first understanding [76].

As shown in *chapter 2.2* the FIE complexity increases depending on the system type and the depth of investigation. In *Table 14* an overview is given of different simplified model approaches utilized in the 0D and 1D simulation software "LMS.AmeSim" for a FIE.
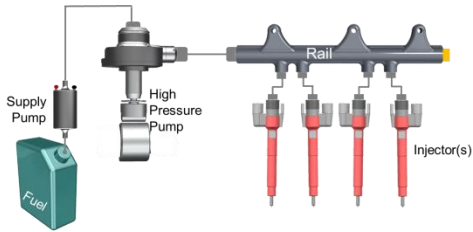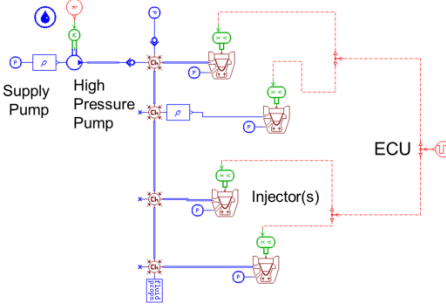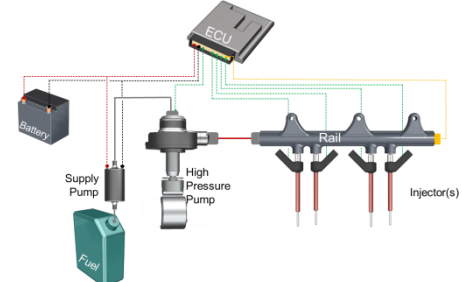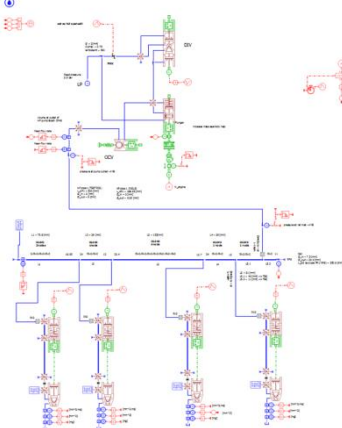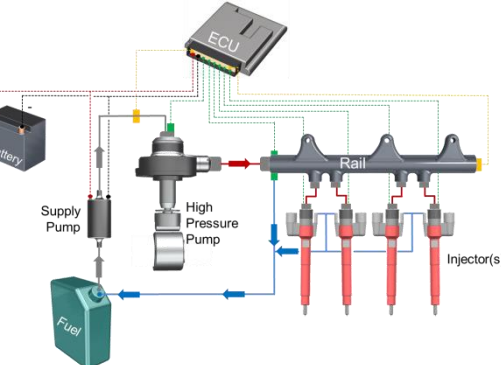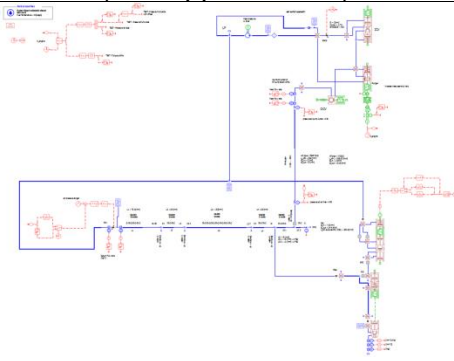
Type	System Layout	Simulation Layout
"Very simple" Model		
Generic Gasoline Model		 *(see Appendix D-3)*
Generic Diesel Model		 *(see Appendix D-4)*

Table 14: FIE layout and related simulation layout in LMS.AmeSim simulation software

As demonstrated in *Table 14,* each simplified system approach requires a unique simulation model to receive proper results [77]. Since very simple approaches only respect the main

feature of a FIE, its complexity remains on a low level. On this simplified level, basic fuel performances and rudimentary energetics are analyzed in this system. Such systems can be used in very early development stages, where only performance targets are given [77].

A generic gasoline FIE considers major boundaries for a plausible hardware setup. As state of the art GDI systems have a radial piston high pressure pump, a rail and direct acting injectors, those components need to be implemented in a simulation system (see chapter *2.1.* and chapter *2.2*). In addition, a rail pressure controller is required too, since high pressure pumps' power consumption in realistic condition is of special interest to the entire examination. The injector hardware of a GDI injector is simple compared to following diesel injector. A generic injector model, which contains needle geometry, masses and volumes of major GDI injectors, provides enough information for analysis. Herein, pressures and pressure waves of the entire GDI system is of special interest.

A generic diesel FIE simulation model differs in its complexity to a gasoline FIE, as described in chapter *2.2*. Since diesel injectors have a servo-hydraulic actuator concept, an increased number of system components are mandatory to simulate correct total quantities or to perform pre-dimensioning of hydraulic components. The servo-hydraulic actuators of a common rail diesel injector are based on the injector internal ratio of throttles, control volumes, masses and actuation force [78]. Thus, a too simplified model (sometimes also called functional model) [79] cannot simulate a diesel injector accurately enough for an analysis of energetics by internal pressures and flows. Furthermore, a detailed "generic" model, which contains all functional elements of a diesel injector, is mandatory.

3.6.2. Detailed fuel injection equipment component model definition

For hydraulic simulation activities, the system suppliers usually define detailed models based on their known physical attributes and features of their individual parts of such layouts. To support the development activities among collaborative companies, they create black box models (or also called "super component" [77]) for their individual components to support their customers. Those customers are typically OEM's, which use such systems to optimize the complete powertrain hydraulics or powertrain entities. Therefore, to ensure proper results, suppliers and Tier1 manufacturers validate such single components models on their own.
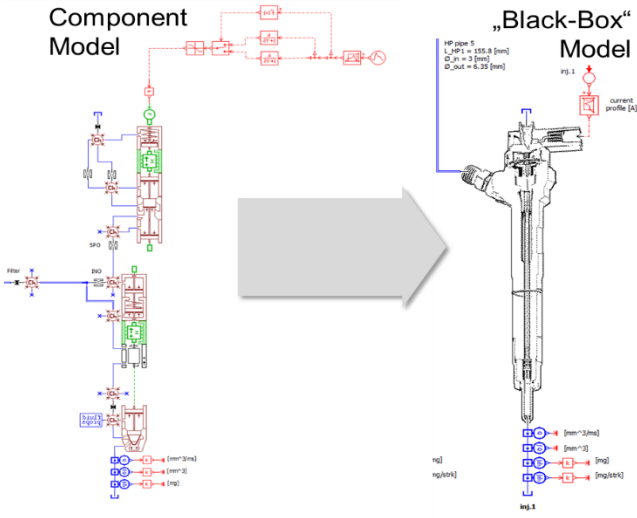
Figure 41: Illustration of component model vs. black box model in LMS.AmeSim

A generic simulation model provides a basis to analyze the interaction between components (see chapter *3.6.1)* and also to run a first parameter optimization. With increasing level of detail, simulation models are designed to match with an origin component and therefore loses its generic character. As an alternative approach, also simulation of small subsystems within its components builds a background for analysis and optimization [72].

To create and use a generic model, a minimum of physical information is required. Especially when the components in the available portfolio do not differ much between each type, parameters can be standardized for generic simulation purposes. In the case of a gasoline direct injector, common injectors in the market have a low variance in its masses and volumes. Therefore, a generic injector model for gasoline direct injector contains a comparably low number of elements, as the following illustration shows.
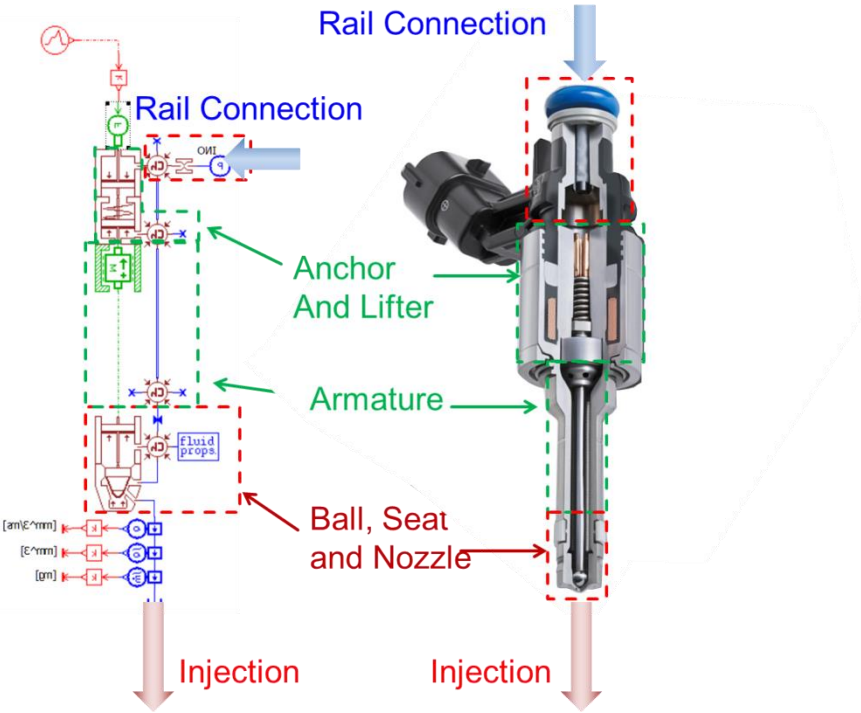
Figure 42: Generic 1D-Injector simulation model and its real components counterparts [including 45]

The generic injector model, as illustrated in *Figure 42,* provides a basis for analysis and reflects also necessary physical abilities. In order to achieve adequate results, a generic simulation model contains simplified subcomponents.   Results of such simulations visualize all characteristics, but not component specific features. From a practical point of view, it is important to apply several different injector types on the same engine. Here this generic approach supports early development stages where not all components have been fixed yet.

An example of mandatory physical actuations of an injector and its simulated reaction in a generic system is shown in *Figure 43.* In this case injection rate ① demonstrates an ideal injection for injector without disturbance or measurement device impact. Only injection rising, plateau and falling slope occur in the simulation result, including a "needle bouncing" for the critical injector properties. Those parameters describe injection performance and include combustion negatively impacting injection features. Displayed from ③ to ⑥ displayed are injector are features impacting performance, which lead to the final injection rate. Thus, variation of injector internal parameters and its driving components supports Tier 1 suppliers to optimize for engine integration. Such adjustable parameters can be used to determine

60

maximum flow rate, the hydraulic minimum dwell time and the opening as well as the closing behavior (see to Chapter *2.2.3.1*). Anyhow, limitations of such systems are the description of injection characteristics or in a performance analysis. E.g. a pressure wave correction analysis or a tolerance field analysis cannot be done, since the required sub-components and definitions are not given or "standardized" in the generic model.
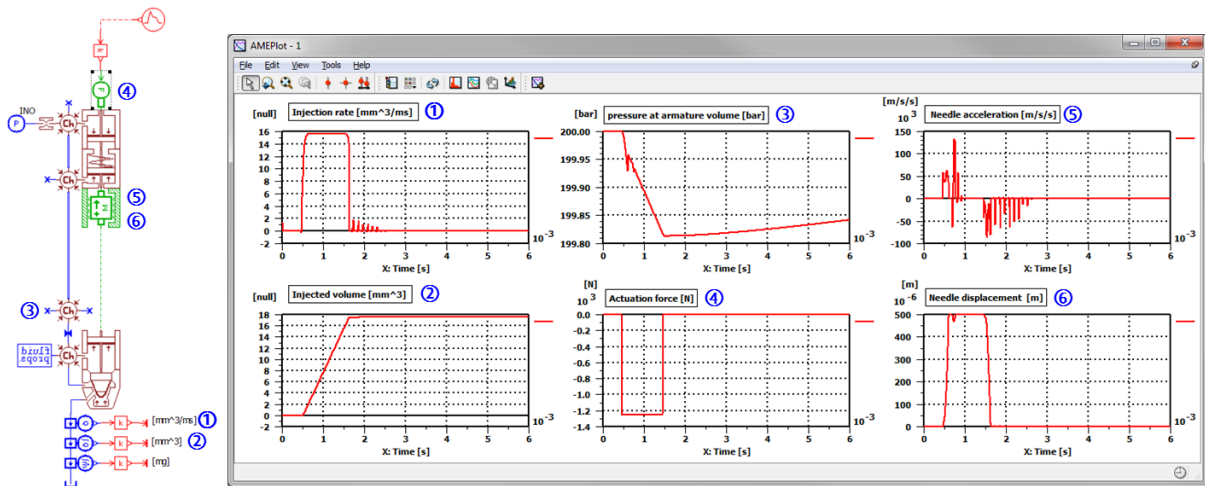
Figure 43: Example simulation results of generic injection model by AmeSim

Since *Figure 42* and *Figure 43* refer to gasoline injectors, an additional servo hydraulic actuator has to be implemented for a generic diesel injector model. Unfortunately, this part has high variance among the TIER 1 suppliers, due to their different approaches in avoiding leakage. Also, achieved dynamics differ significantly due to the suppliers' unique approaches. Anyway, to support simulation result for leakage tendency and therefore later CO_2 impact, also a generic approach, based on most common technology, remains adequate. The parametric model calibration focuses on correlation with injector leakage behavior and an accurate ratio between injection and leakage.
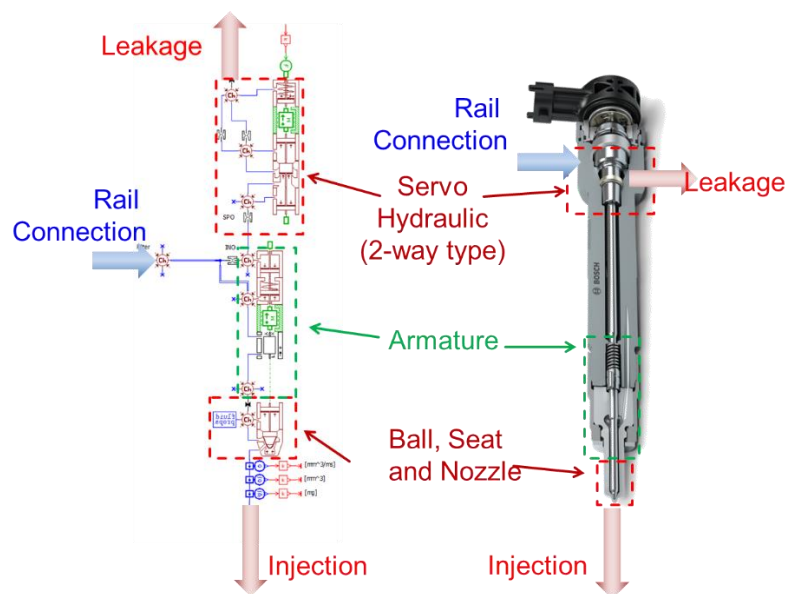
Figure 44: Generic diesel injector model in AmeSim and exemplary real counterparts [incl. 45]

To establish the higher forces, required for a stable injection at pressure above 1000 bar, a servo-hydraulic actuator realizes the injection process. Therefore, the difference between above shown *Figure 44* and *Figure 42* remains in a changed actuation principle. As described in chapter *2.2.3.2.* servo-hydraulic actuator has a dependence on the injector internal throttle ratios. This has to be included into a simulation to analyze the correct leakage amount and injector abilities. For analyzing such simulation results, a basic knowledge on the injectors function frame is mandatory in order to interpret correctly.
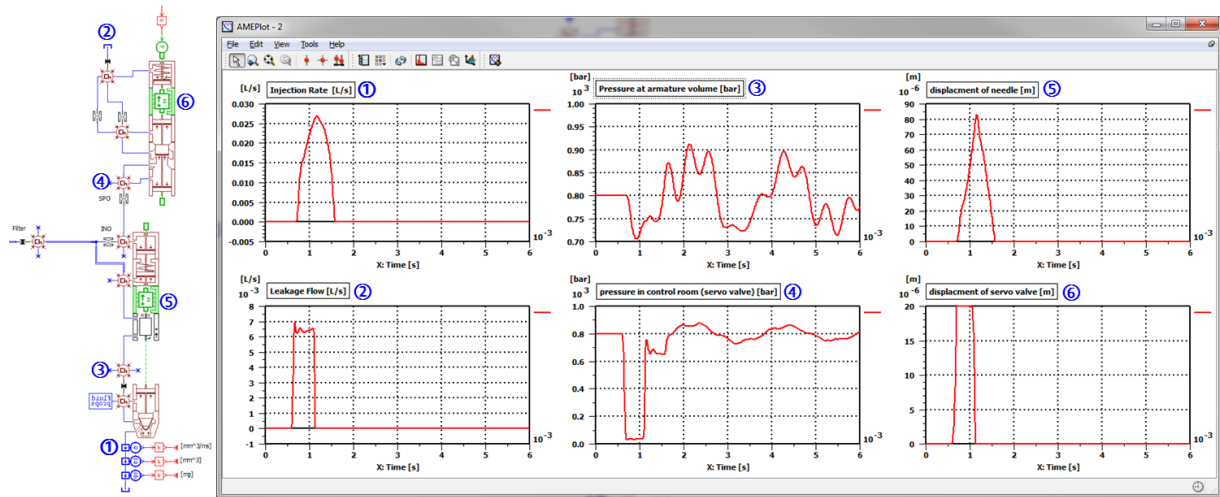
Figure 45: Example simulation result of generic 1D-Diesel servo-hydraulic model by AmeSim

The interaction between servo valve (④ + ⑥) and needle or nozzle seat (③+ ⑤) as well as ratio between injection ① and leakage ② determine performance impact on an engine [80]. *Figure 45* shows this configuration for diesel injection. Those results show simulated reaction of the needle ⑤ to the changed pressure in servo valve control chamber ④ by the lifting of the valve poppet ⑥. The resulting injection rate ① and the reaction by pressure waves inside the rail connector ③ have all typical characteristics for such injector type. The leakage flow ② also shows reactions due to actuation by the servo valve, but only during actuation. Thus, the simulation model does not provide enough background to simulate static leakage. However, since aging impacts static leakage most critically [81], this missing information has to be gained by measurement on the component test bench, but would leave the boundaries of a generic approach. The required data by measurement would be too individual for a specific sample.

In case of high pressure pumps, also generic models support analysis of component performance. Base performance parameters for high pressure pumps are drive torque and flow rate at given pressure levels for engine integration.

Similar to a generic diesel injector model, also a high pressure pump model requires specific properties to achieve representative results. The *Figure 46* shows such parts within a high pressure pump simulation model as well as important hydraulic flows. The illustrated leakage flow separates in two lower types: one driven by cooling and lubrication demand, the other one driven by loss of volumetric efficiency or static leakage between high pressure chamber and lower pressure area. While cooling and lubrication demand can be adjusted to an industry-wide standard value of about 100 to 200 l/hr [67], shows static leakage of plunger dependency on geometrical as well as fluid abilities. Therefore, same as for leakage of servo-hydraulic

injectors, measurement on a component test bench give information on leakage and therefore high pressure pump volumetric and total efficiency (see to chapters *2.2.2.*, *2.3.1.* and *2.4.1*) .
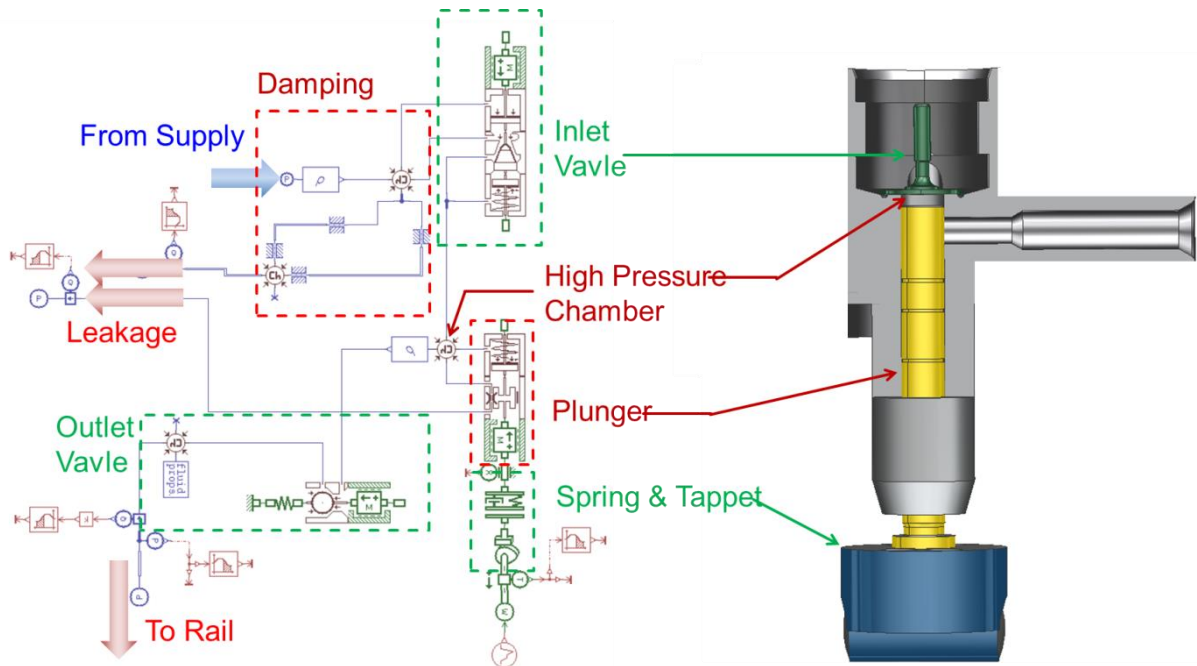
Figure 46: Generic high pressure pump model in AmeSim and its real counterpart [82]

Also mechanical impact needs to be reviewed in order to establish a useful generic model. Since the mean torque and the peak torque have high impact on engine mechanics, those results demand attention. Unfortunately, 1D simulation friction models suffer from low accuracy especially in mixed condition, as they are in high pressure pumps [83]. Thus, variations in pre-load, which are directly affecting friction, can only be determined by measured approach.
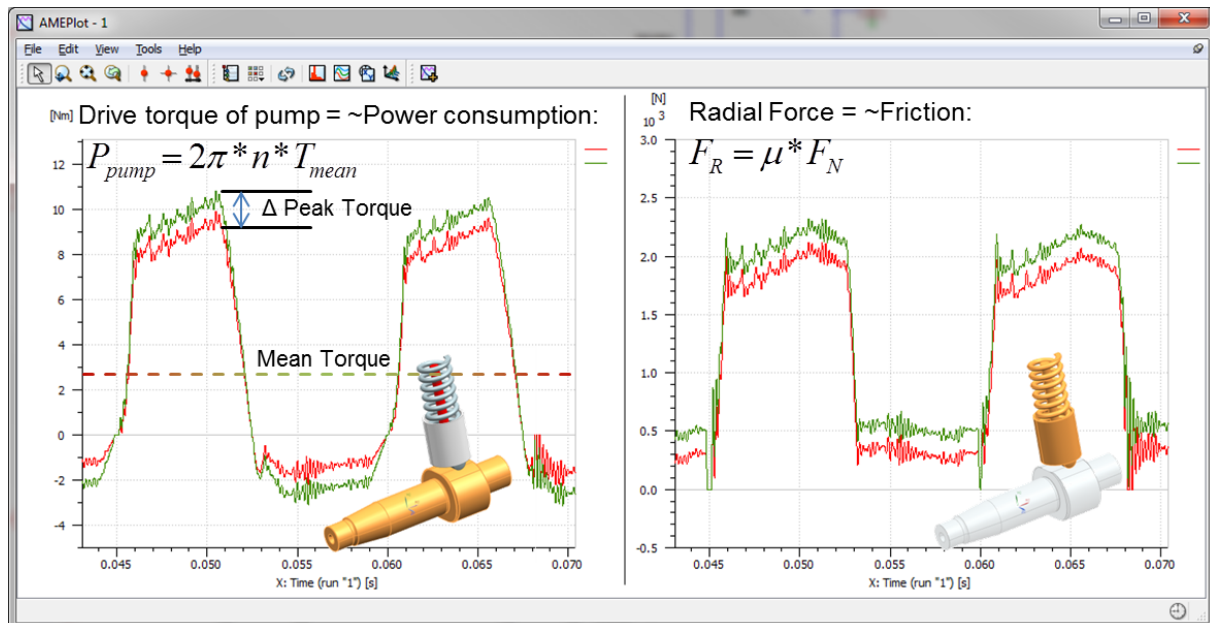
Figure 47: Impact by spring force modification on simulation, based on AmeSim 1D-model [84]

Reduction of spring force on the high pressure pump's cam shaft leads to nominal force reduction. *Figure 47* illustrates such impact as calculated by simulation. The peak torque shows reduction, as expected, but also the retaining torque is reduced, which leads to an equal mean torque. As a result, the nominal force reduction does not impact entire system friction, as it would be expected by measurement. This relation builds a conflict for future observation and comparisons between simulation and measurement [84].

3.6.3. Total fuel injection equipment simulation model

For a total evaluation, combination of the sub-models mentioned in chapter *3.6.2* to a complete system remains as last step. Due to the long processing time required by the simulation software, total evaluation usually takes place at the end of single component optimization. Depending on the evaluation target, simulation contains only a high pressure system or only a low pressure system or a injector or the total system for deep dive analysis. Another possibility remains in reduced model complexity to provide real time calculation for Hardware or Software in the Loop application [85].

Since simplified models are often based on upon pre-processed mappings, efficiency processing -as used in chapters 3.1, 3.3and 3.4.- can serve for an analysis. Anyhow, a deep dive analysis for possible optimization requires an understanding in the total process. Therefore, a full simulation model still remains as required. The following *Figure 48* shows an entire simulation model for a total FIE.
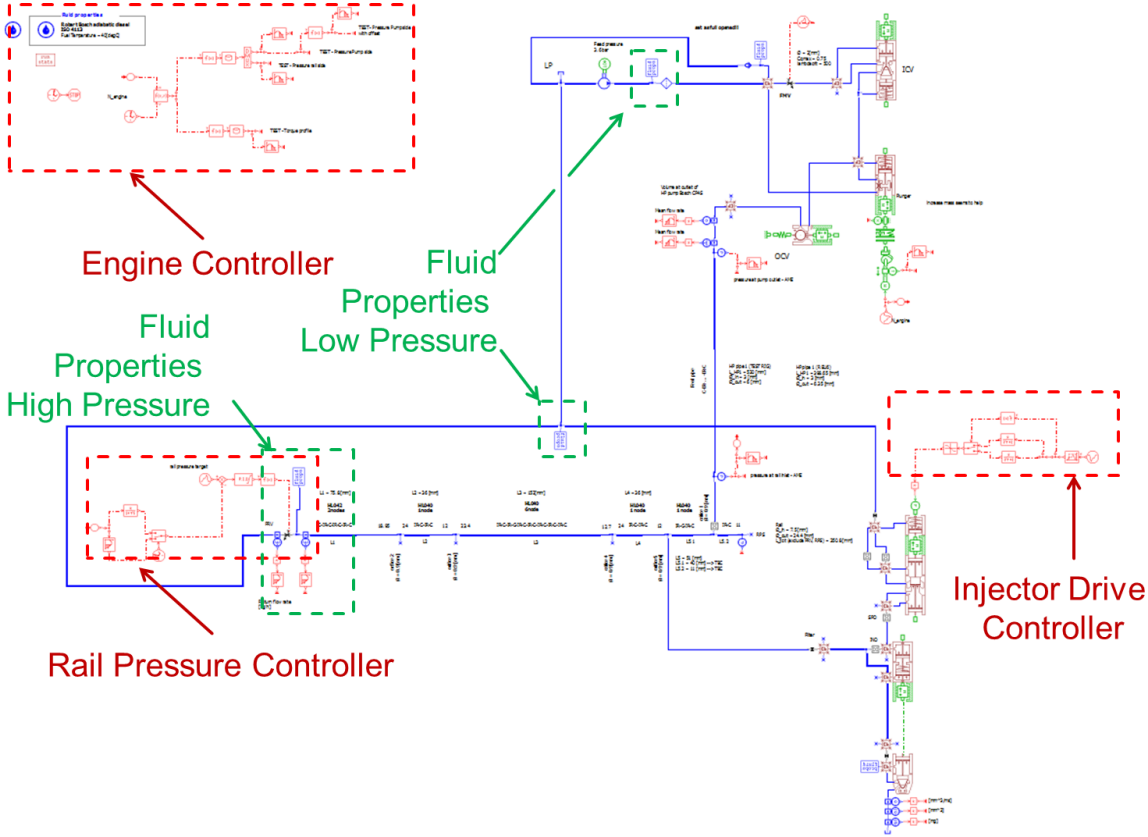
Figure 48: 1D Simulation model of total FIE System in LMS Amesim

Despite the system's subcomponents, also the controller parameters need to be applied, as well the interfaces between all components. As visible in *Figure 48 a* major interface is the

physical property of fuel between components, as well as controller parameters in particular. Since high dynamics have to be assumed in this simulation mode, the processing time for each simulation cycle will not reach real time performance. Furthermore, by its complexity, a long processing time of more than 10 minutes per operation point, can be assumed. Thus, a simulation of an entire driving cycle will take an impracticably long processing duration.

Due to its high details, this model supports the analysis of flow and inbound energy processing. Especially controller setup as well as orifice layout first optimization are executed in a time and cost efficient. For the purpose of hydraulic power demand evaluation, a deep simulation model allows deep insight into systems states during operation. This includes the actual rail pressure on the high pressure pumps plunger during pressurization and accurate leakage shares during operation. Therefore, *Figure 49* illustrates exemplarily a review of leakage distribution in one operation point (1000 bar rail pressure, 2 pilots 7mg each and 1 main at 30mg injection per shot) of a diesel FIE based on simulation evaluation. As remark, the shown measurement results require intensive and well organized test preparation for each measurement, since they are all located within the high pressurized circuit of the FIE.
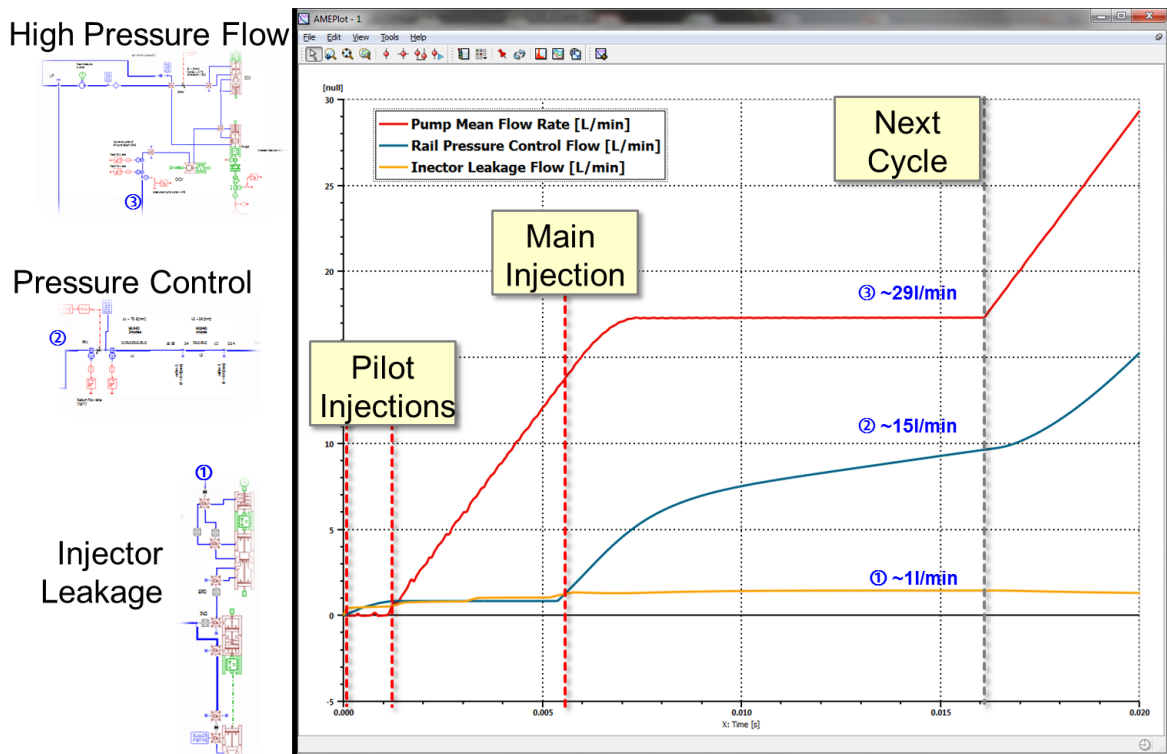
Figure 49: Mandatory system leakage vs. high pressure pump delivery of Diesel engine

Especially control leakages in dynamic behavior or controller misconfiguration can be evaluated in this type of simulation. The losses from rail pressure control (shown in *Figure 49*) result from a simulation of a fully delivering high pressure pump, which displays a worst case scenario in terms for efficiency. In late calibration processes on entire vehicles, the leakage composition is typically not evaluated in this depth. Since the implementation of sensors within return flow lines is unusual in vehicle assembly and mix up with pump coolant flow as well as injector leakage, such exemplary misconfiguration can hardly be analyzed, by measurement, but within a simulation environment.

4. Measurements and results

As mentioned in chapters *2.5* and *3.5* not only the physical properties need to be considered for power demand of a fuel injection equipment (FIE), but also integrational parameters and component performance. This becomes reasonable since the physical properties of high stressed fluids change significantly, while also high amount of energy are conducted. Due to inapplicability of standard "Bernoulli" equation for hydraulics (see to chapter *2.4.1*), final impacts are at this state mostly unknown.

In addition, since the operation mode and load condition influences the component efficiency significantly, detailed review of examined performance requires measurement of each component to verify its specific impact on engine performance. To complete this analysis, also interaction between the FIE and engine needs to be analyzed. Thus, mechanical integration parameter and impact on a total vehicle measurement are mandatory to verify the impact of the FIE on CO_2 emission and fuel consumption.

Especially to analyze vehicles impact, the system integration parameters have to be respected. Small GDI engine in hybrid powertrain infrastructure have a different load collective and operation range compared to commercial diesel engines for trucks or excavators. For an overview purpose, the presented measurement results focus on combustion engine concept only and will be divided in passenger vehicles and commercial vehicles, as described in entire chapter *2* and especially in chapter *2.2.3*. Also, for comparability reasons, all shown results are measured under "standard" test condition of 40°C fuel inlet temperature.

The mode of presentation increases in complexity and size of tested systems. Also, a comparison between a "standard" state of the art applied component and a modified or novel type will be shown. This comparison is performed from component level, over integration level up to engine and vehicle level. Also shown measurements represent a new level of content for analysis. All samples have been analyzed by the same method, but not all contents will be shown as long as no new information are embedded.

The chapter *4.1.* focuses on the analysis of performance on component level of the high pressure pump. Herein, chapter 4.1.1 shows the evaluated high pressure pump samples for this analysis. These pump samples presented in detail will be analyzed from component level analysis up to vehicle level analysis. Other types may appear as example, but will not be deeply analyzed. The chapter 4.1.2 analyzes GDI high pressure pump performance with specialized focus on parametric performance impact, as it appears by altering high pressure pump type. For an overview, an entire deep analysis will be performed as example for the analysis process. The Magneti Marelli PHP7 pump shown subsequently shall demonstrate as example the effect of pressurizing up to 1000bar. With increasing pressure level, the next step in chapter 4.1.3 is the analysis of high pressure pumps for diesel engines in passenger size. Focus is the difference in performance between high pressure pumps for diesel and for gasoline direct injection application. The following chapter *4.1.3.1* and chapter 4.1.3.2 analyze the mechanical boundaries and the influence by fuel type on component performance. Therefore, the Continental DHP1 is shown as example as only available Polyoxymethylendimethylether (OME) capable high pressure pump during period of testing. As last step in high pressure pump analysis, samples for commercial engine applications are presented in chapter *4.1.4.* Since power consumption of such components are comparably high in relation to former shown

samples, the friction modification possibilities on components and engine performance are in focus.

In the chapter *4.2* the mechanical interaction between high pressure pump and engine is analyzed. Since the integration in diesel applications for passenger cars is by an own shaft most sensitive, the influence will be shown on a chain drive build for the HMC R-Engine. The included chapter 4.2.1 and following chapter 4.2.2 deeply analyzes the part load effects and interaction between chain and high pressure pump.

To complete the interactions analysis between the FIE and the engine, chapter *4.3* focuses on the remaining components measurement. In particular, the chapter *4.3.1* focuses on the analysis of the low pressure system and the chapter *4.3.2* quantifies losses by injector hardware.

The next level of analysis is the entire engine and vehicle. Herein, measurements separate between commercial and passenger vehicle application. As shown in chapter *2.1,* commercial vehicles are typically evaluated for certification on engine dyno. The chapter *4.4* follows this circumstance and determines impact by high pressure pump on commercial engine performance. As a consequence, the chapter *4.5* determines impact on entire vehicles as they a certified on chassis dyno. This chapter is separated into chapter 4.5.1 for gasoline application and chapter 4.5.2 for diesel application for clarity.

4.1. High pressure pump measurement results

An analysis of each high pressure pump and its power consumption requires several measurement and setups, due to their variety. Especially pressurizing fuel into high pressure ranges for direct injection, mechanical performance plays a key role for entire engine friction. But also the influence of electrical power consumption by low pressure system is known to be relevant, as referred to chapter *2.5.1*.

To be as close as possible to serial application, the measurement of a high pressure pump requires at least serial ECU and rail for their specific engine type. Depending on the rail pressure controller type and fuel volume flow control type, also a full injector set operates to realize a rail pressure control as close as possible to serial engine.

Detailed test bench build up and setup focus for a precise drive torque, flow and high pressure pressure measurement are according to equation *(13)* in order to measure all necessary values to calculate the high pressure pump efficiency*.* The test bench and all inbound measurement devices are listed in chapter *3.1*.

4.1.1. Overview of deep analyzed high pressure pump samples

Major focus remains on the validation of injection system power consumption. Depending on the system type and the target pressure, the high pressure pump has a high impact on the final power consumption. To avoid cross system impacts, the focus of this analysis remains on today's common rail system architecture. Since there is variety also in a very wide range, selected measurements will be presented for clarity. Thus, analysis will show a "standard" high pressure pump in serial production, compared to a performance optimized pump. Several of

those utilized approaches are a "world first" approach within automobile industry. Nevertheless, they all follow explained principle as described in chapter *2.2*.

In terms of Gasoline high pressure pumps, high variety by manufacturer and individual layout for targeted engine type is given. For analysis purposes, discussed samples reduced to three samples with same duty area for 1.6 to 2.0 displacement engine within range of 136 HP to 240HP and significant differences in performance.

Parameter for gasoline high pressure pump	Hyundai Kefico GDI high pressure pump [38]	HMETC parameter carrier pump in "Best of Best" configuration[40]	Magneti Marelli PHP7 1000bar prototype[86]
Picture			
Maximum pressure	250 bar	350 bar	1.000bar
Plunger diameter	8,5 mm	8 mm	8 mm [85]
Sample type	Serial Production	Research Pump	A-Sample Prototype
Target engine	HMC Gamma I 1.6	-All-	-Research-
Remark	Wide spread usage in HMC cars	Defined in hardware matrix definition	Prototype for highest rail pressure level

Table 15: List of analyzed Gasoline Direct Injection Pumps [38, 40, 85, 86]

Especially HMETC parameter carrier pump in Table 15 has to be mentioned. Its intention targets to study integration effects and is therefore designed to be dismountable. The design approach and layout bases on the Kefico GDI high pressure pump shown in first the column. A deep analysis matrix of state of the art GDI high pressure pumps indicated design parameter and their impact on high pressure pump performance [33]. The system configuration, named "best of best" (= BoB), utilizes trade-off in performance for engine application. In the third column, the Magneti Marelli PHP7 GDI high pressure pump for 1.000 bar is shown. This sample targets the next generation of GDI high pressure pumps for new combustion approaches. Even though, the pump still consumes mechanical and electrical power, which has to be covered by the engine.

The diesel high pressure pumps analysis has to be split into two performance classes: passenger sized engines and commercially sized engines. This analysis is based on engine examples mentioned in Table 2.

Typical passenger vehicle sized Diesel pumps have one or two plungers, depending on the engine rated power and the maximum fuel demand within a complete engine mapping. The Bosch CP4s1 and HMC HEFP Gen2 pumps in *Table 16* mentioned, share, as designed for R-Engine, the same high pressure head and therefore the same geometry. Both pumps differ in their mechanical and supply system layout. While nowadays high pressure pumps like Bosch CP4s1 require 3.5 bar to 6 bar absolute pressure at a lubrication demand of 40 – 250ltr./h, the HEFP Gen.2 requires a lower lubrication amount of 20 ltr./h and a lower absolute supply

pressure of 1,1 bar to 3,5 bar to maintain functionality. As an additional feature, HEFP Gen.2 allows application with fuel and also with engine oil lubrication [44].
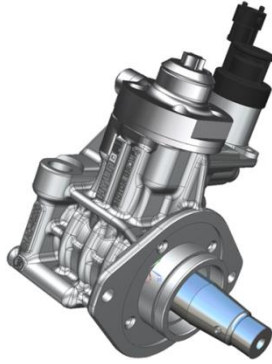
Parameter for diesel high pressure Pump	Bosch CP4s1 [45]	Hyundai HEFP Gen2 [44]	Continental DHP 1 [88]
Picture			
Maximum pressure	2000 bar	2500 bar	2500 bar
Geometric volume	0.398 cm³	0.398 cm³	0.48 cm³
Sample type	Serial Production	B-Sample	C-Sample
Target engine	HMC R-Engine	HMC R-Engine	HMC D4FIII
Remark	Most used Common Rail pump among Euro 6 cars	Optimized pump for lowest friction losses	Modified for OME study

Table 16: List of analyzed diesel high pressure pumps for passenger car engines [44, 45, 88].

As last remaining samples, the following high pressure pumps are applied for analysis of commercial engine high pressure pump performance.

Parameter for commercial diesel Pump	Denso HP4 [89]	Hyundai Modified Denso HP4
Picture		
Maximum pressure	1800 bar	1800 bar
Geometric volume	1.2 cm³	1.2 cm³
Sample type	Serial Production	Research Prototype
Target engine	HMC G-Engine	HMC G-Engine
Remark		For analysis purpose designed pump sample

Table 17: List of evaluated Diesel high pressure pumps for commercial vehicle sized [89].

The investigation background bases on in *Table 17* mentioned serial production applied Denso HP4 and a modified Denso HP4 high pressure pump for reduced friction. Both pumps are designed for HMC G-Engine. Due to outstanding effort in hardware and software integration for engine integration, analysis will focus on these samples. The focus for modification was to reduce the pump's internal friction without changing of pump's internal hydraulic. This supports in quantification of losses for commercial application. Therefore, new bearing concepts were applied to utilize this modified high pressure pump. As one major application, HMC G-Engine utilizes in serial production hose pumps on international markets. Due to application in commercial sized engine range, applied displacement by this pump is three times higher than in passenger sized Bosch CP4s1 pump. Therefore, Denso HP4 is an eccentric shaft driven pump with three plungers instead of one as in Bosch CP4s1.

Denso HP4 also differs from prior mentioned samples by an integrated supply pump. It does not require, as for all gasoline or diesel system mentioned before, supply pressure and lubrication flow. Therefore, integration requires suction line from pump inlet to fuel tank.

4.1.2. Measurement results of GDI high pressure pumps

All before mentioned samples tests are executed on Bosch Moehwald CA4000 test bench in HMETC laboratory in same setup. The test approach focuses on close to application measurement with full GDI system and ECU (see to *Figure 35*). Base setup for all tested samples on component test bench follow measurement setup as described in chapter 3.1.

Figure 50: Build up gasoline high pressure pump test build up with mounted Kefico 250 bar GDI pump

All pump samples are measured and analyzed in same way, but the full deep analysis will be demonstrated exemplarilly on the Kefico 250bar GDI high pressure pump, which is shown in *Figure 50* as mounted sample in the standard GDI test setup. Utilized and for test purpose standardized cam lobe for GDI measurement bases on HMC Theta 2.0 TGDI engine with 4 hubs and 4.5 mm lift per rotation. To adjust cam shaft speed, an increment of 500 rpm per step, starting from 400 rpm up to 2800 rpm, has been selected during entire measurement process. For illustration purpose, error bars will be shown for total efficiency in one line, but are valid for the entire mapping, as described in chapter *3.1*.
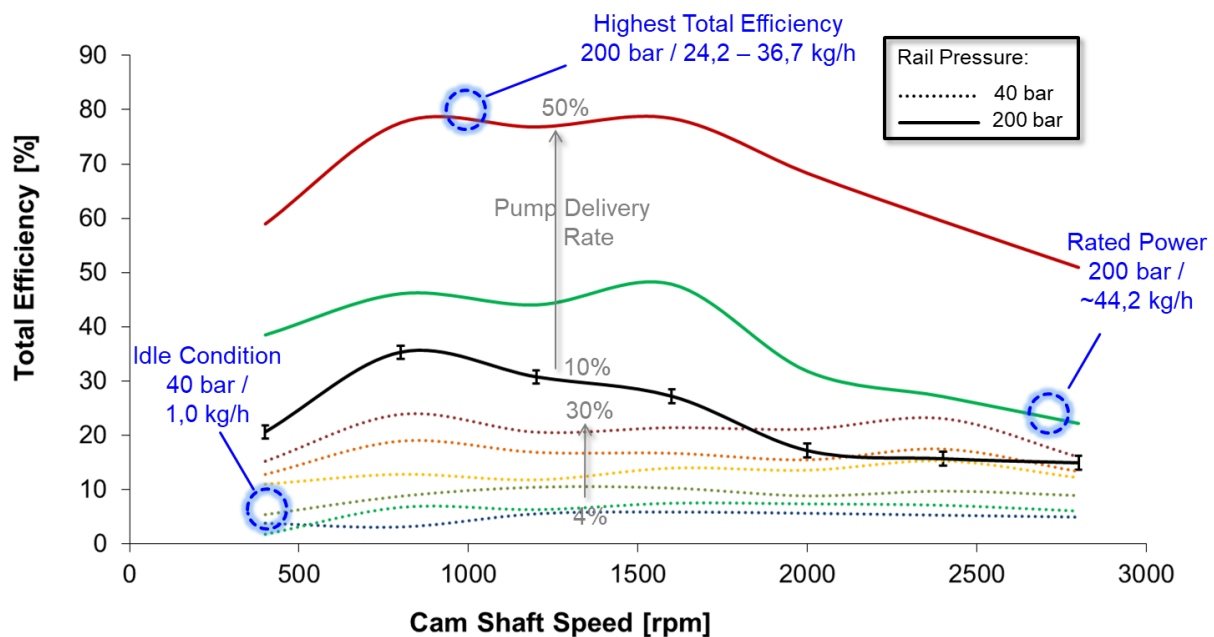
Figure 51: Total efficiency mapping of Kefico 250bar GDI pump according to equation 13

The shown pump efficiency of Kefico 250bar GDI HPP represents total efficiency among entire pump duty area. The engine conditions in *Figure 51* for illustration mentioned do not represent standardized areas for calculation and only guide for understanding in which conditions the mapping is located. Also features, characteristics and boundaries of high pressure pumps are shown. The delivery range of the test sample is limited by its setup of the installed injector type and speed range. This means that only 30% maximum delivery at 40bar are reached, because the injection would take too long at 5600 rpm engine crank speed. Also measurement density is increased for demonstration purpose, to shown significant impact by delivery rate on total efficiency, even by small changes. The area of highest total efficiency are highlighted for given configuration including Theta cam lobe and in HMC standard used Kefico ECU.

Performance measurement reveals in first assumption range of expected total pump efficiency. Lowest total efficiency levels found achieved levels of 5% and lower. While also major parts of total mappings utilized high pressure pump in areas of about 20% total efficiency. Also in low load areas, total efficiency is nearly constant with increasing values by higher delivery rates. As mentioned, high pressure pump performance has high sensitivity to flow by even small steps of 5 %. As also shown higher pressure levels increase efficiency over total mapping, but lowers by increasing cam shaft speed (or pump frequency). Related to included engine operation conditions, the total efficiency by GDI high pressure pump itself ranges in areas of 5% up 25%. Also, Kefico GDI high pressure pump has a high efficiency range of close to 80% total efficiency.

Each pump type has an individual performance mapping, but key performance features are similar. For demonstration purpose, other pump samples are shown in *Figure 52* and following *Figure 53*.
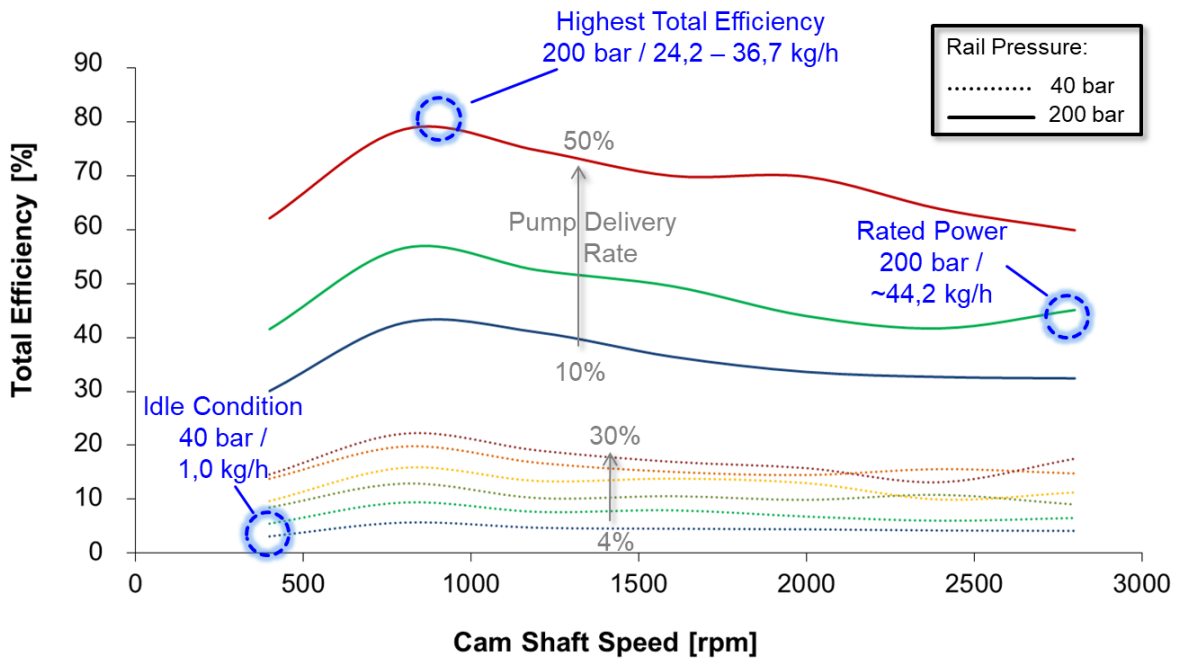
Figure 52: Total Efficiency Mapping of Continental GHP2-25 pump according to equation 13

The characteristics of this Continental GHP2-25 GDI high pressure pump sample show also total efficiency ranges of 5% up to 80%. Especially also part load area and low load areas achieve total efficiency of 20% and lower. In this particular sample, the total efficiency in rated power range shows higher values of 45 -50% as Kefico GDI high pressure pump sample.
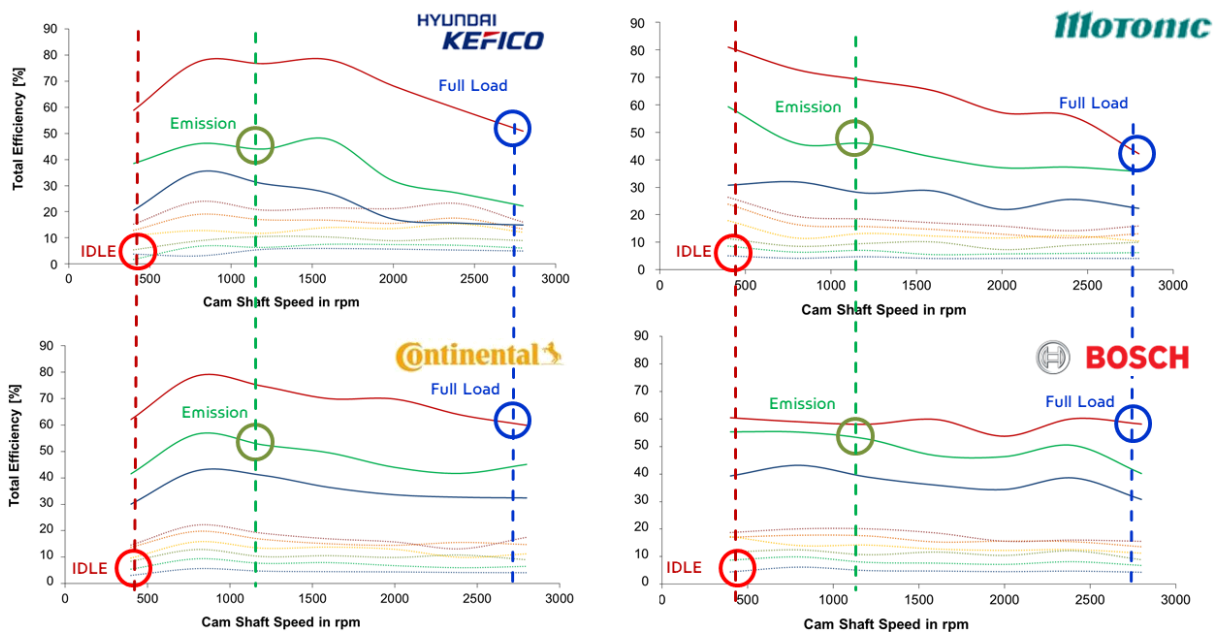
Figure 53: Performance mappings overview of 4 different 250bar GDI pump samples

As a result of several GDI pump samples analysis, as illustrated in *Figure 53,* all show performance in similar range as the deeply analyzed Kefico 250 bar GDI pump. All of them are

not reaching highest total efficiency in engine related duty cycles. When reviewing the area from "idle" to for this purpose applied "emission" operation point, total efficiency ranges in values 5 % - 50%. These are representing engine conditions comparable from 0 kph – 120 kph and contains major range of engine operation within passenger engines' life span.

To continue the analysis of the Kefico 250 bar GDI pump, the root cause for the total efficiency has to be taken into account. Most obvious root cause is the mechanical power consumption of the pump.
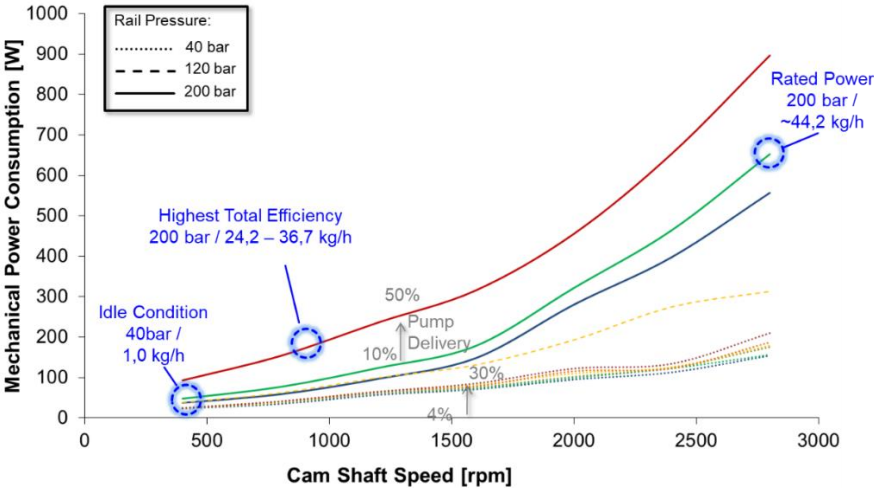
Figure 54: Mechanical power consumption of Kefico 250 bar GDI pump over total mapping

The GDI pump power consumption ranges from 20 W up to over 800 W in case for 200 bar systems, as illustrated in *Figure 54*. Although, since highest power consumption is outside of engine duty cycle, the engine is unlikely to encounter this highest power consumption. Usage in different engine derivate may enable such high power demands also in future applications. Since this illustration represents total mapping with low details in common passenger engine operation ranges, detailed review in lower load area is required. In particular, since differences in low speed areas from 40 bar up to 200 bar and 400 rpm to 1200 rpm are hardly recognized. Therefore, a more detailed illustration in reduced speed range is illustrated in *Figure 55*.
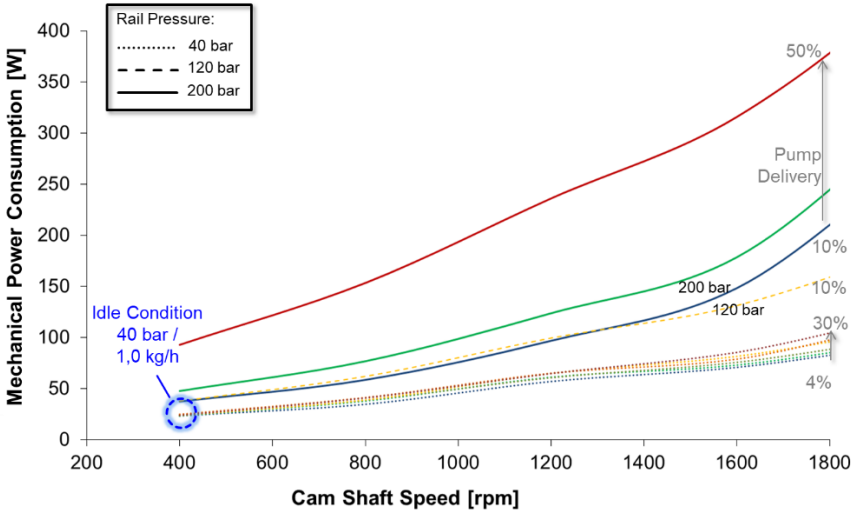
Figure 55: Detailed power consumption of Kefico 250 bar GDI pump for major used engine operation ranges

The major engine operation states, as utilized within NEDC or WLTP cycles, power consumption may reach 350 Watt during acceleration. A remarkable point is in pressure and flow as major influence for total power demand. Within the pressure range, the pump delivery influences in lower pressure range have minor influence, while in high pressure range influence has significant impact. The generated pressure itself has an always significant influence, even if a doubling of pressure does not cause a doubling of power demand. Also marked line of 120 bar and 200 bar with nearly same power demand from 400 rpm to 1400 rpm is also remarkable when reviewing effective flow rates in this particular configurations: both lines show nearly the same power consumption, at the same adjusted delivery rate, nearly the same mechanical power consumption.

To identify the second root cause for the total efficiency, a review of the flow is required. Since the mechanical power consumption at 120 bar and 200 bar with 10 % adjusted delivery rate are nearly on same level, this range is of special interest.
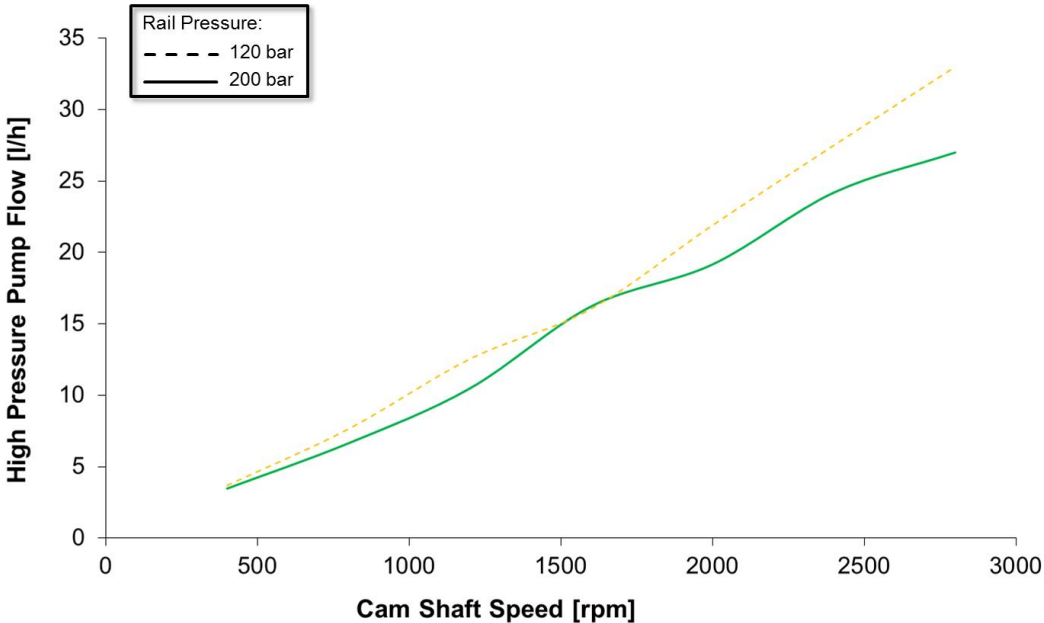
Figure 56: High pressure flow comparison on Kefico 250bar GDI pump

Not only does high pressure total mechanics power consumption shows nearly same behavior at 120 bar and 200 bar, but also high pressure flow has in this certain area nearly same flow results (shown in *Figure 56*). As a remark, this particular area reflects engine duty area in range of around 100 kph and higher in case for passenger cars. Thus, engine size and powertrain configuration as well as vehicle size changes particular range. Pressure range itself depends more on calibration and combustion strategy.

For further analysis, the GDI pumps drive torque measurement supports a deeper level of understanding. Following illustration demonstrates the pump's drive torque reaction on changing rail pressure levels.
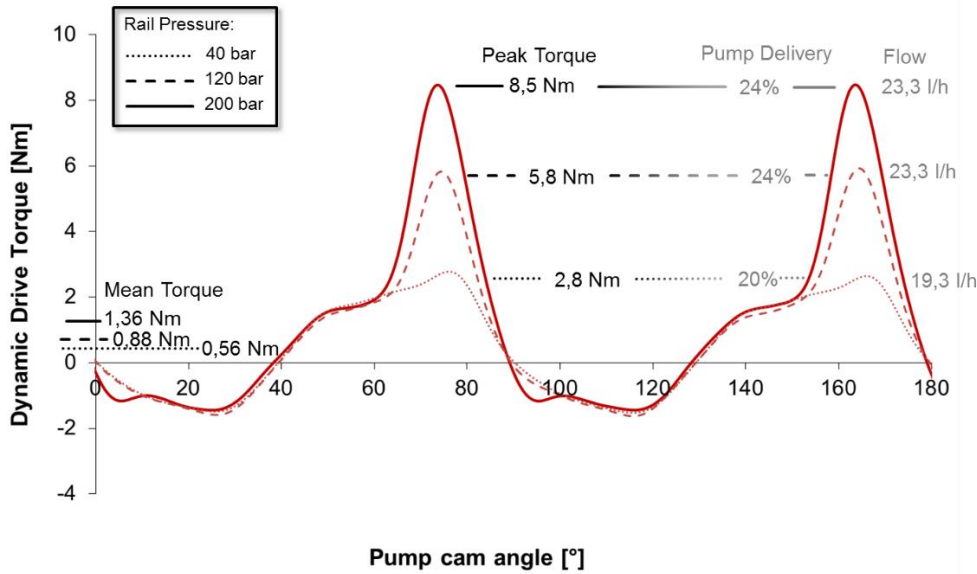
Figure 57: GDI Pump drive torque of Kefico 250bar pump at changing rail pressure

At same pump speed and same target delivery state, only difference due to rail pressure become visible. Therefore *Figure 57* targets visualization of this particular effect by changing rail pressure. The obvious outcome remains in peak torque development from 2.8 Nm up to 8.5 Nm, which is similar as for power consumption (*Figure 54*) and thus total efficiency mapping (*Figure 53*).

Two secondary reactions show their impact on drive torque on high pressure pump. The torque gradient during pressure generation increases by rising rail pressure levels, as well as start of pressure generation becomes earlier or pressure generation itself require longer stroke. Obvious change remains in reaching high pressure pump top dead center (TDC), when drive torque positive values cross x-axis and become negative value. Also here rail pressure levels affects drive torque gradients significantly. In addition, 200 bar pressure condition establish a second local minima after reaching bottom dead center (BDC).

The parameter carrier pump mentioned in *Table 15* has one major design difference to before mentioned samples. Since typical GDI high pressure pumps in serial application ensure lowest production cost by non-dissemble housing concept, a parameter replicable concept, as close as possible to serial application, has to be utilized for performance analysis. Therefore the parameter test pump mentioned in chapter *2.2.2.1* as well as in same chapter described parts explain in the detail approach of this designated pump.

The GDI pump illustrated in *Figure 13* orientates in concept and layout on Kefico 250bar serial pump. Nevertheless, its concept allows also pressure generation up to 350bar and higher. For purpose on later analysis, the parameter carrier pump will be used in "Best of Best" configuration. A study on identifying parts and setups for a best "engineering tradeoff", has been performed [33].

Variations	Kefico (Base)	Power Cons.	Peak Torque	Noise Emission	Media Separation	Cost Impact
Control		+16 %	+20%	-2 dB(A)	0	higher
Damper		0%	+5%	- 1dB(A) -> 0	0	0
Plunger		-15% -> +5%	-20% -> +10%	-0.5dB(A)-> +1,5dB(A)	0	0
Stroke		-4% -> +10%	-12%-> +24%	0 -> +2dB(A)	0 -> +5%	0
Spring		0%	-2%-> +2%	-0.5dB(A)-> 0	0	0
Preload		-1% -> +9%	-3%-> +2%	0-> +1,5dB(A)	0	0
Sealing		-4%	0%	0	+ 21%	Slightly lower

Table 18: Parameter study result summary for GDI high pressure pumps on parameter carrier pump [82]

Since a performance optimization contains a huge variety of possible combination, the summary shown in *Table 18* is a small cutout for clarity. The blue marked performance parameters are the by evaluation identified major performance impacting items. Some items exclude other features from proper integration. As example, the plunger diameter and stroke variance are limited, in order to achieve required fuel delivery for engine operation. The equipped "Best of Best" pump configuration for this analysis has major focus on reduced peak torque and noise emission, since these features can be modified most significant to serial produced Kefico 250 GDI high pressure pump [33]. As a performance summary, the peak drive torque is reduced by -0.5 Nm at 250 bar [38], total efficiency is in same level as "best in class" [82].

Novel gasoline engines combustion strategies to improve "cleanness" of exhaust gas utilize very high pressure levels for injection. The Magnetti Marelli's PHP7 GDI high pressure pump attempts as first pump a serial application in those high pressure levels.

Figure 58: Magneti Marelli PHP7 GDI High Pressure Pump [86]

This mentioned pump targets utilization to serial application and can be mounted in comparable way to today's common engine installation and is therefore in its principle common to the former measured pump samples. Therefore, the mechanical connection and synchronization is realized by cam shaft. This differs from former analysis for highest injection

pressures for GDI engines, whereas diesel high pressure pump pressurized the fuel to target level [88].

Another challenge is the rail pressure control logic. Since today's applied rail pressure controllers in serial ECU are not designed for higher pressures than 400 bar, a rapid prototyping controller has to be utilized in order to measure this pump type. Therefore, a total efficiency analysis has been controlled by an IAV FI2RE for rail pressure control and digital inlet valve actuation.
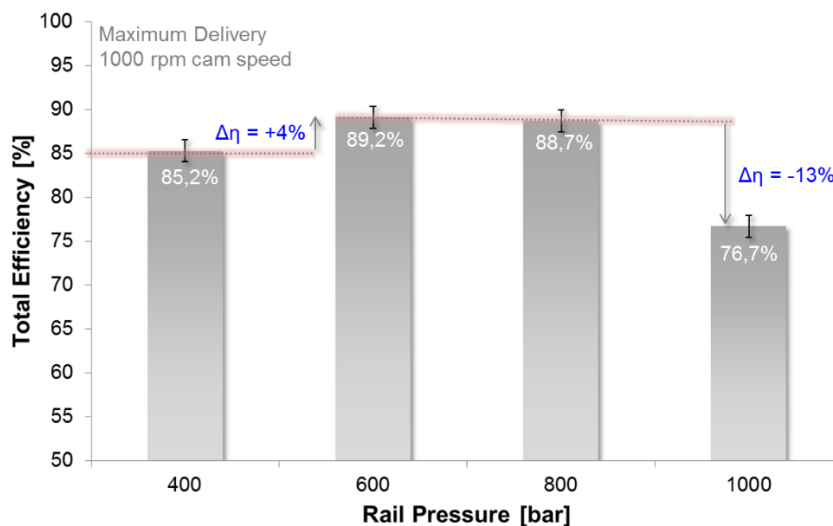
Figure 59: Total efficiency performance of Magneti Marelli PHP7 at 1000 rpm cam speed and full delivery

As this pump follows the similar performance characteristics as former shown high pressure pump samples, despite the maximum pressurization level, only major characteristic points are illustrated in *Figure 59* for overview purpose. For selected exemplary points of a full delivery at 1000 rpm cam speed and increasing pressure up to 1000 bar, change in high pressure pumps total efficiency becomes visible. Herein an optimized rail pressure range of 600 bar to 800 bar demonstrates an increasing dependency on reaching physical limits of this high pressure pump type. Furthermore, the increasing pressure and changing total efficiency leads to a difference of 705 W, from 548 W at 400 bar up to 1253 W at 1000 bar at a same time reduction of flow capacity of 11,3 kg/h. Initial starting condition in this setup are 47,3 kg/h at 400 bar. It should be noted that, the measurement tolerance has to be adjusted during the testing, due to the different rail pressure controller type to ± 2%.

4.1.3. Measurement results of diesel high pressure pumps for passenger vehicles

Diesel high pressure pumps differ from GDI high pressure pumps in two ways: volume and flow control is typically utilized via suction valve and the pump contains complete mechanics, as in chapter *2.2.2.2* described. For the most commonly used pump among passenger vehicles nowadays, the Bosch CP4s1, the initial total efficiency results represent full delivery mapping condition as described in chapter *3.1.* To adjust pump shaft speed, an increment of 200 rpm per step, starting from 400 rpm up to 4000 rpm, has been selected during entire measurement process. For illustration purpose, error bars will be shown for total efficiency in one line, but are valid for the entire mapping, as described in chapter *3.1.*
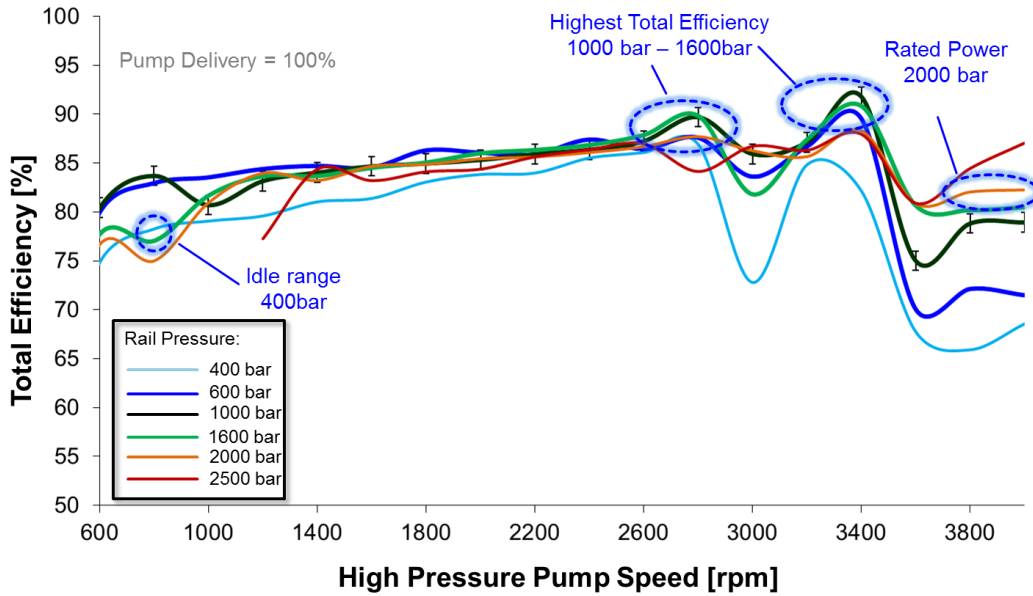
Figure 60: Total efficiency mapping of Bosch CP4s1 common rail pump for HMC R-Engine

The total efficiency mapping in full load of Bosch CP4s1 reveals two major information: Diesel high pressure pumps have a "corridor" in which they achieve nearly similar total efficiency of in this case 82 % - 85 % and increasing disadvantages in lowered pressure ranges, as illustrated in *Figure 60* on the 400 bar measurement line. As second occurrence, unsteady deviations appear with relation to the high pressure pumps speed range.

A pressure control valve mounted on the rail controls high pressure inside the rail. The analyzed pump runs in full delivery, which leads to higher flow rates than an engine may require. In contrast, running the pump in part load operation, information on internal leakage at an actual pressure are not shown sufficiently. Therefore, as an industry wide common performance criteria, the analysis of the pumps volumetric efficiency is performed especially by TIER 1 suppliers. The volumetric efficiency itself is defined according to *Equation 12*.
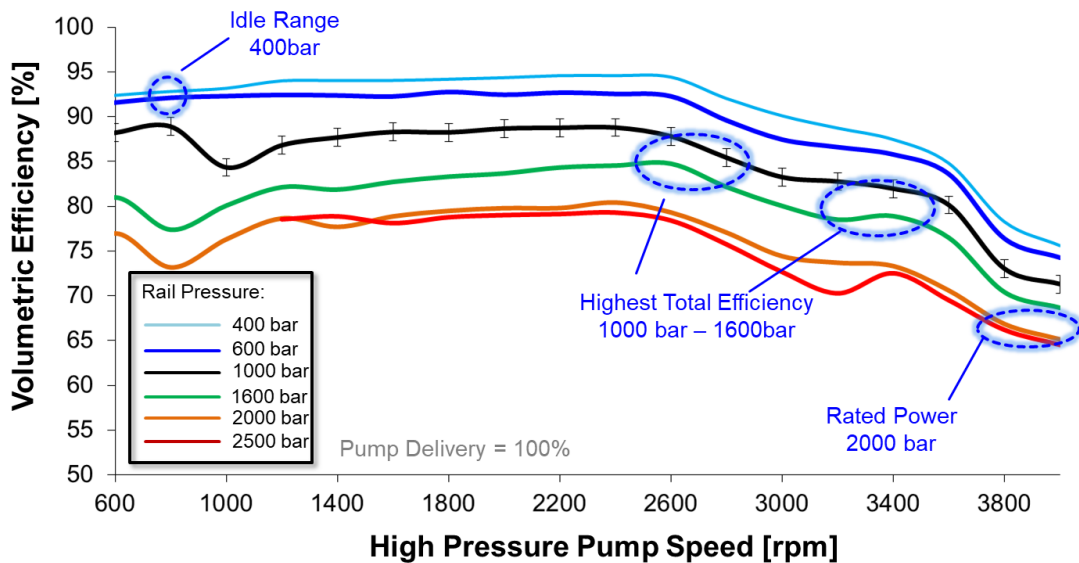
Figure 61: Volumetric efficiency of Bosch CP4s1 in full pump delivery according to equation 12

The graph shown in *Figure 61* demonstrate volumetric efficiency calculated as described in chapter *2.4.2* by comparison between geometrical delivery and measured pump flow. Two dependencies occur in analysis of volumetric performance of diesel high pressure pumps: first pressure range impacts in decreasing efficiency, while high pressure pump speed slightly improve volumetric efficiency but drop after 2600 rpm in case of shown Bosch CP4s1 high pressure pump.

The difference between 2000 bar and 2500 bar volumetric performance shows results within measurement tolerance (as shown in 1000 bar measurement line). Since the Bosch CP4 sample for R-engine is defined by its specifications a maximum pressure limit of 2000bar, it is obvious that the pump is generating pressure at its limit.

As an embedded information in total efficiency analysis, the mechanical power consumption by high pressure pump remains. Therefore, a detailed drive torque analysis for accurate power consumption analysis becomes mandatory, similar as before in chapter *4.1.2*. Especially peak and mean torque by high pressure pump have strong impact on final mechanical power consumption.
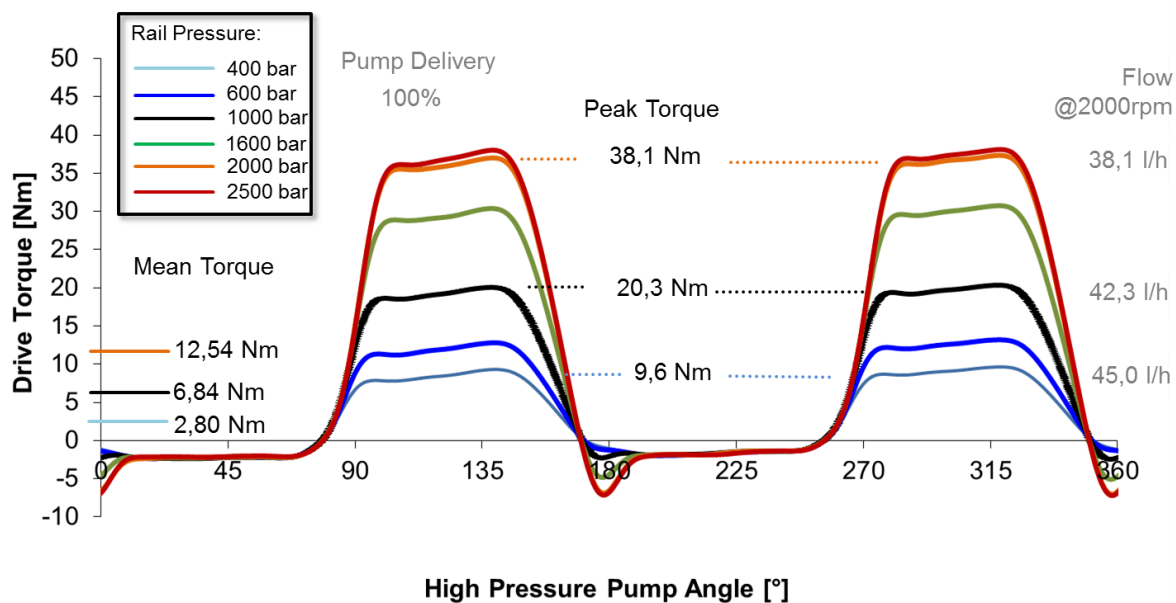
Figure 62: Dynamic drive torque of Bosch CP4s1 at full delivery and 2000rpm pump speed from 400bar to 2500bar

In contrast to GDI high pressure pumps, diesel high pressure pumps with their volume control dosing via a suction valve, are showing a flattened drive torque curve with a clear visibility of the pressurization stroke and the suction stroke. Further on, the comparison between *Figure 62* and *Figure 57* demonstrates impact by higher pressure on mean and peak drive torque levels by the high pressure pump type: while the peak torque level at 200 bar for a GDI high pressure pump reach typical values of 8,5 Nm, the Bosch CP4s1 pump reaches 38,1 Nm at 2000 bar.

This, at first glance, recognizable diversion from an expected linearity in peak torque is following the change of geometric parameters between a diesel and a GDI high pressure pump. Especially variation in plunger diameter and cam lobe profile has positive impact on

peak torque performance (see to chapter *2.2.2* and following). Also difference in flow from 400bar up to 2000bar needs to be remarked: while pressurization length remains identical, effective flow reduces by ~7 l/h or nearly 16%. As shown in *Figure 61*, the pump speed range of 2000 rpm is not affected by volumetric loss due to reduced filling rate. Also the shown dynamic drive torque is not in area of affiliates, when analyzing the mechanical power consumption over the entire speed range.
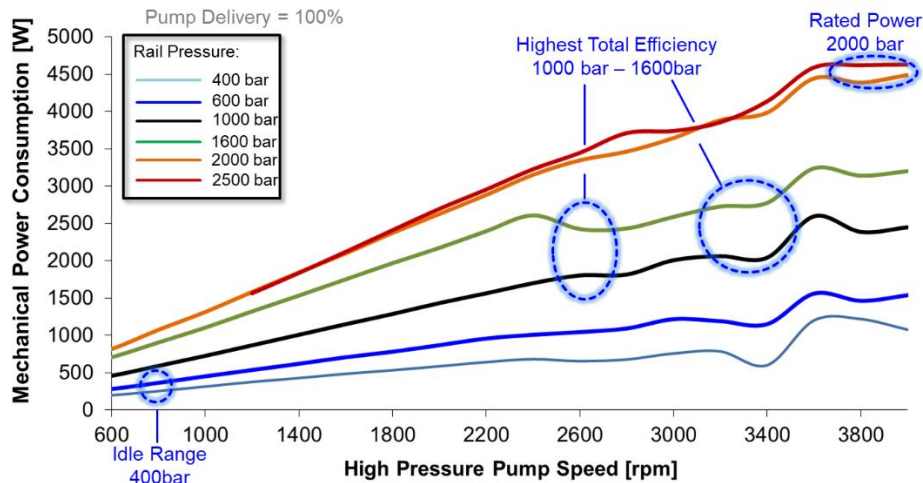
Figure 63: Mechanical power consumption performance of Bosch CP4s1 pump over total mapping

In major occurrence, the mean drive torque has a nearly flat behavior up to 2800 rpm, from then with increasing pump speed the power consumption and therefore the drive torque becomes unsteady (see *Figure 63*). This characteristic repeats by pressure steps up to 1600 bar rail pressure, but changes in intensity by increasing rail pressure.

The maximum flow capacity of the Bosch CP4s1 pump for R- Engine is 66 ltr./h at 2000 bar rail pressure. Since most engine operation, especially in passenger vehicle applications, does not require this high amount of fuel and pressure, a typically installed volume control valve or digital inlet valve doses the fuel demand before pressurization. Therefore, its total efficiency changes with changing of the fuel delivery.
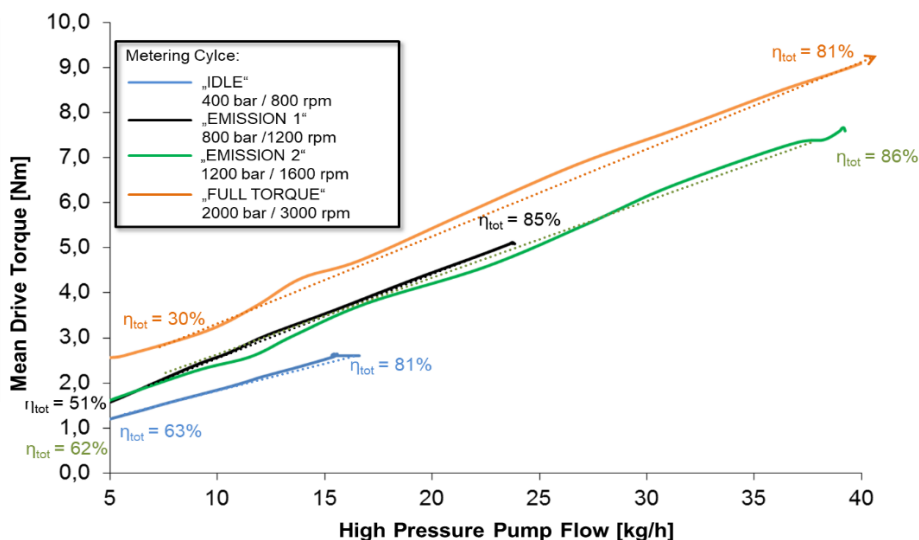
Figure 64: Part load operation performance of Bosch CP4s1 on "Pivot" points

Figure 64 shows that the part load delivery performance of Bosch CP4s1 high pressure pump leads to a reduction in total efficiency. Especially in range of 800 bar to 1200 bar rail pressure and part load conditions, drive torque demands remain nearly static. Herein given information for analysis on engine mapping requires a review corresponding to engine operation. Also by mentioned total efficiency, the rail pressure has an increasing disadvantage at decreasing flows. All information has to be taken into account for an analysis and evaluation over an entire operation cycle. The "pivot" test points are according to the procedure shown procedure for total efficiency analysis shown in chapter *3.2*.

4.1.3.1. Mechanical performance impact by measurement of HEFP Gen.2

As mentioned in chapter *2.2.2.2*, variation and modification in different mechanical parameters remains feasible within high pressure pumps. As a different mechanical and supply system approach instead of the Bosch CP4s1, a HEFP Gen2 high pressure pump can be utilized (see *Table 16*).

Following results base on a Bosch CP4s1 derivate of the HEFP Gen.2.: the high pressure head including geometry as well as cam lobe are utilized from Bosch CP4s1 pump similar type utilized before.

In an attempt to reduce the entire powertrain fuel consumption, the total efficiency builds a typical background for optimization. Therefore, the following figure shows the total efficiency mapping of a high pressure pump optimized for total efficiency.
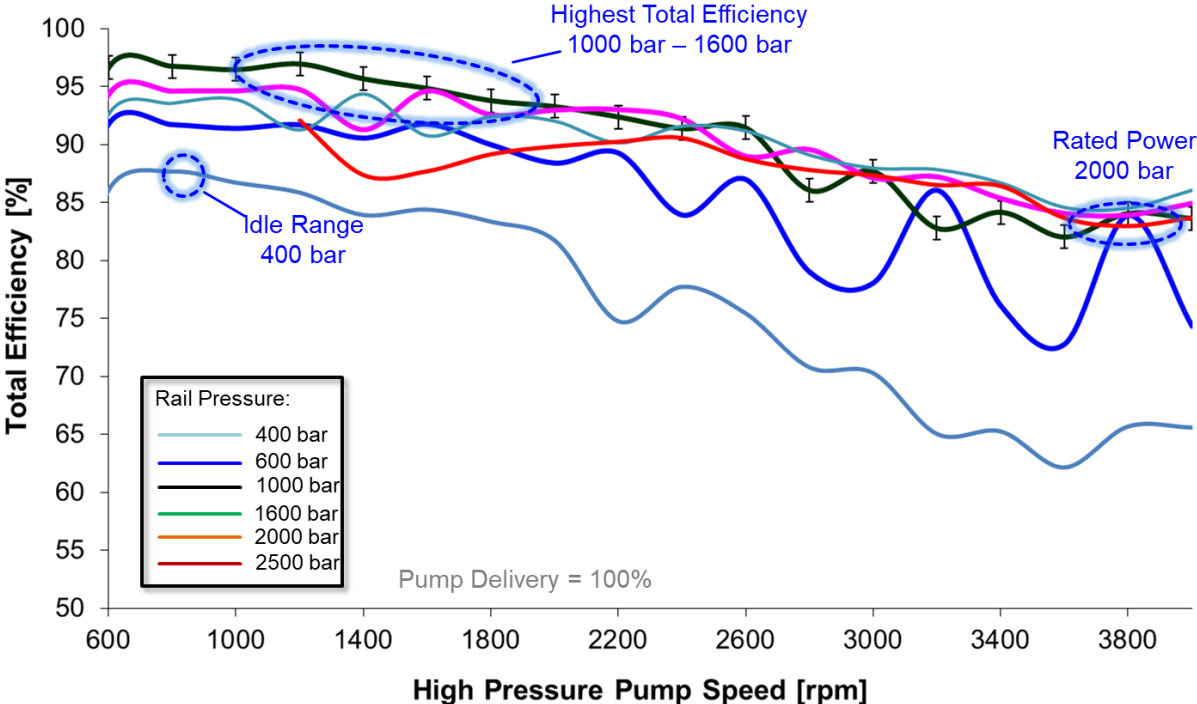
Figure 65: Total efficiency mapping by HEFP Gen.2 high pressure pump for HMC R-Engine

The here shown results reach on wider range a total efficiency level of 90 % and higher. Also lower pressure levels reach total efficiency levels of 87%, as displayed in *Figure 65*. In range of rated power, the total efficiency reaches levels of 83%-85%, depending on rail pressure levels. In case of the HEFP Gen.2 version shown here, the high pressure pump achieves pressure levels of 2500 bar.

The total efficiency level does not follow straight lines over total high pressure pump speed range. With increasing pump speed, the total efficiency reduces by up to 10 %. Since HEFP Gen.2 utilizes needle bearing as main bearing system, this performance is reasonable by roller bearing typical friction characteristic. The high total efficiency oscillation at 600 bar and 2400 rpm pump speed and increasing is a second "unusual" observation. Direct explanation remains at this certain point not available and will be discussed later in chapter *5.1.2.*, when utilizing operation point simulation.

As before, during those mappings the high pressure pump runs on full delivery performance. However, for analysis of in vehicle performance, where pump runs in part load operation, this analysis has also to be performed, as in following figure.
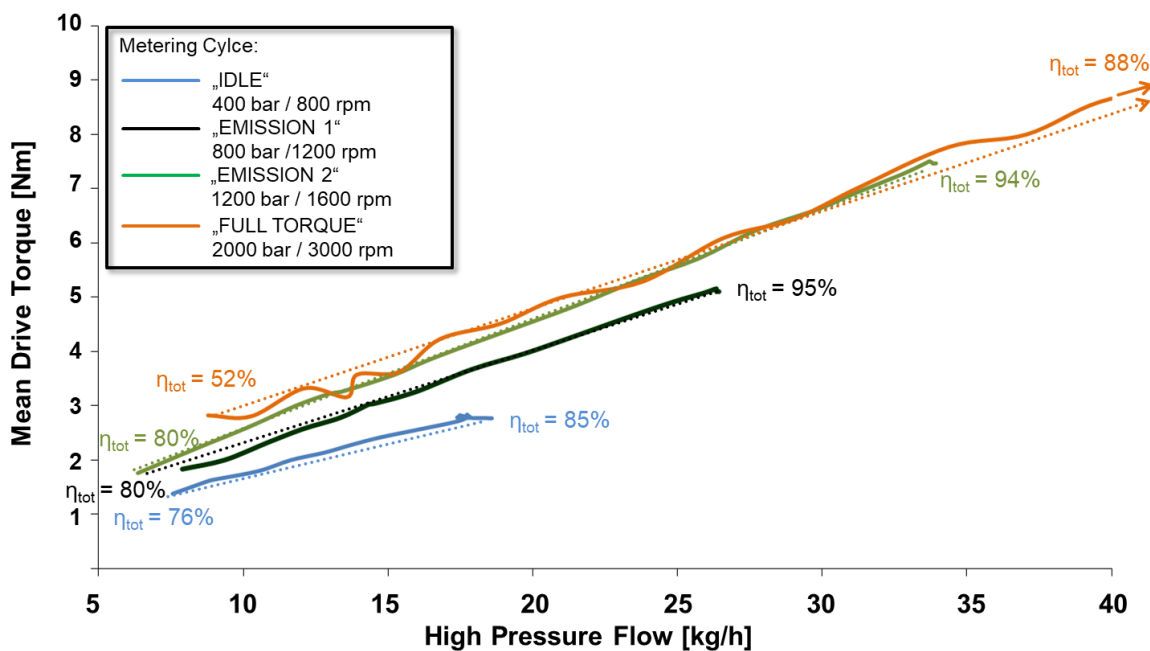
Figure 66: Metered duty performance of HEFP Gen.2 on "Pivot" test points

Reviewing drive torque impact and therefore also total efficiency over pump flow at fixed rail pressure and pump speed shows the impact by part load operation of high pressure pump. During a part load operation of 6 - 8 ltr. / h of pressurized fuel flow (see *Figure 66*), most operation points achieve total efficiencies of 76 % up to 80 %. Despite high loaded "Full Torque" metering cycle, where high rail pressure and high pressure pump speed are applied. As in same condition of decreasing efficiency with increasing high pressure pump speed, as visible in *Figure 65,* the needle bearings of HEFP Gen.2 suffer higher losses by higher speeds. Therefore, frictional impact has at this specific operation point higher influence. Also, the scale on x-axis for flow is shortened for illustrative purpose, to focus on more relevant ranges. At this point in particular, the pump is capable to deliver up to 55,7 ltr./ h.

When reviewing "Emission 1" and "Emission 2" metering cycle, the high pressure pump sample reaches nearly same total efficiency. Since measurement tolerance, as identified via CP-test described in *D-1 Appendix,* has a value of ± 1,2% of total efficiency, the difference of 1 % is within measurement tolerance. Remarkable for both conditions are the differences in set point: rail pressure level increases by 400 bar from 800 bar to 1200 bar and high pressure pump speed increases by 400 rpm from 1200 rpm to 1600 rpm and even reaching nearly same conditions at minimum displayed flow values.

4.1.3.2. Fuel type impact on pump performance by Continental DHP1

In most cases, utilized fuel follows strong regulation by authorities (see in chapter *2.1)*. In particular, most abilities mentioned in *Table 3* lead to generic assumptions for performance of fuel injection equipment. Also today's market situation changes for fuel by stronger implementation and blending of non-fossil and renewable fuels. Therefore, fuel abilities needs to be considered for full analysis (see chapter *2.3)*, which does include synthetic fuels such as OME, but also local fuel quality influence as in markets which suffers high quality differences.

Following measurement describes impact of OME on drive torque performance of a diesel high pressure pump. The results will focus on measurements executed with Continental DHP1 high pressure pump, as it is utilized for OME usage parametrized available pump. Base diesel substitute fuel is ISO4113 (see chapter *3.1)*.
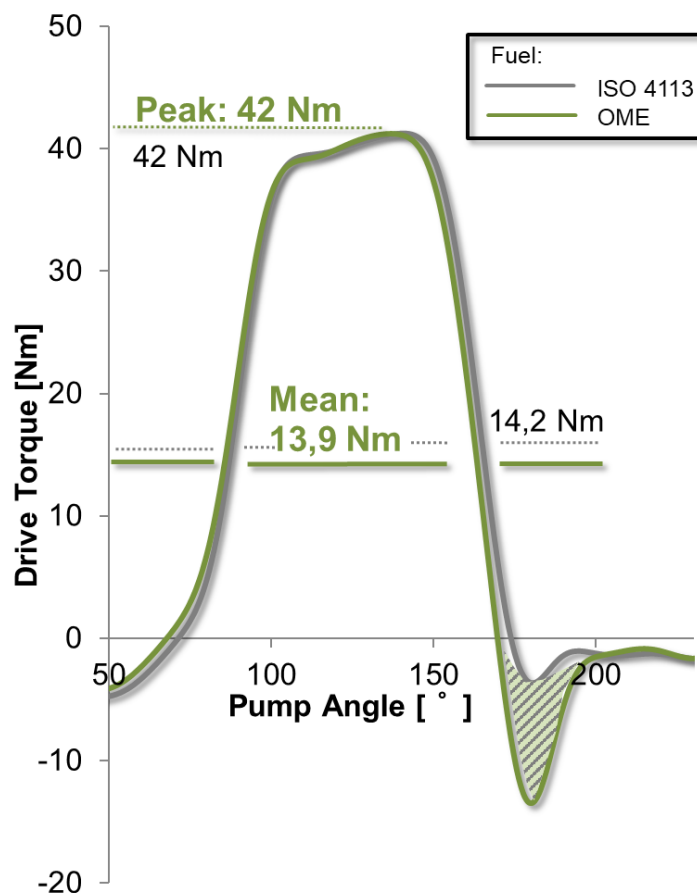
Figure 67: Impact by OME on dynamic drive torque of Continental at 2200bar and 2000rpm

Analyzing the dynamic drive torque impact on a detailed level, shows the impact on peak torque and minimum torque performance by high pressure pump. Especially minimum torque as shown in Figure 67 reduces from -3 Nm for diesel substitute pressurization to -13 Nm for OME pressurization. On positive torque side, especially peak torque characteristic share same properties between diesel substitute and OME. Due to lower minimum drive torque, the mean torque reduces by 0,3 Nm to 13,9 Nm when pressurizing OME.

Fuel properties not only impact high pressure pump drive torque performance, but also fuel flow performance. Therefore, *Figure 68* displays the resulting fuel flow when pressurizing OME.
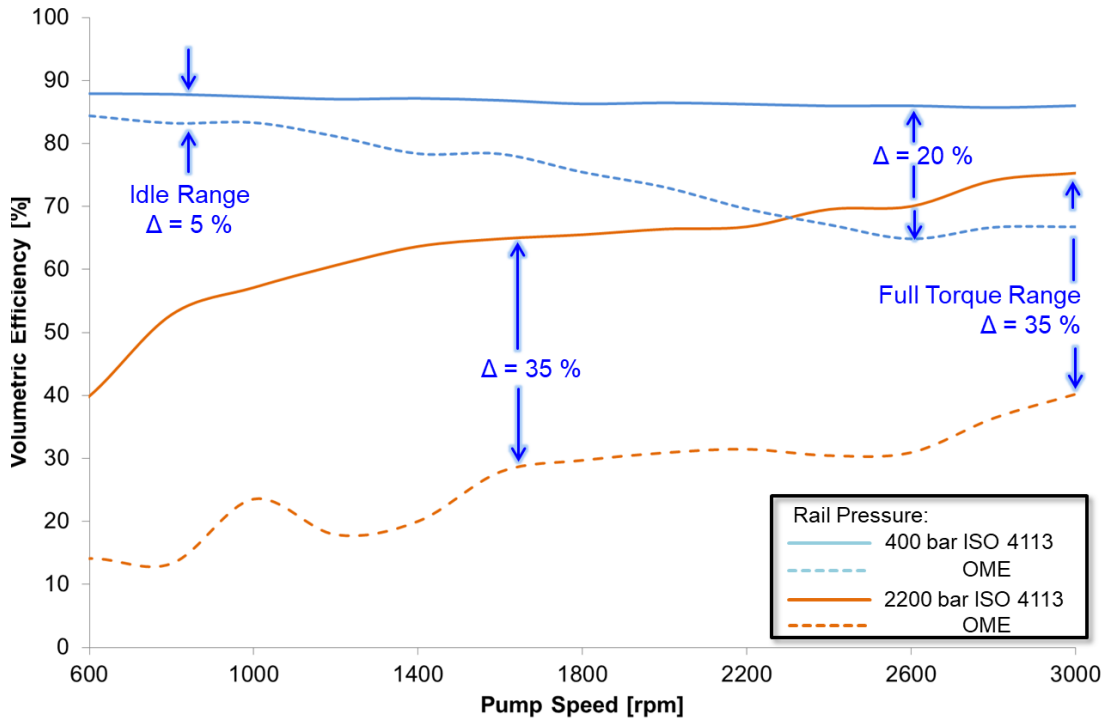
Figure 68: Volumetric efficiency impact by OME vs. ISO4113 diesel test fluid on Continental DHP1 OME

As most obvious observation, volumetric efficiency decreases by increasing rail pressure levels. Anyhow, *Figure 68* shows increasing loss from 5 % to 20 % difference at higher pump speeds on lower rail pressure range, while higher rail pressure range difference has nearly steady values of 35% in range from 1600 rpm to 3000 rpm pump speed.

To complete analysis on OME impact to diesel high pressure pump performance, a total efficiency analysis becomes mandatory.
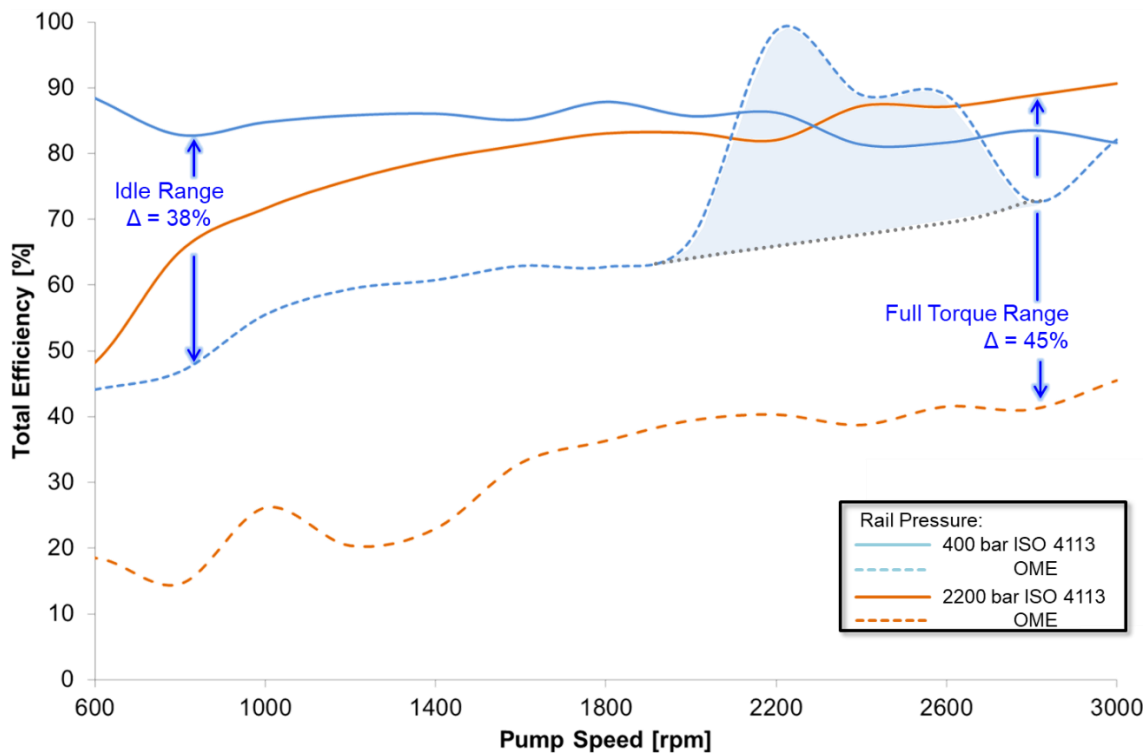
Figure 69: Total efficiency impact by OME vs. ISO4113 Diesel test fluid on Continental DHP1 OME

In same manner as *Figure 68, Figure 69* displays increasing reduction of total efficiency for OME. Within this range especially total efficiency range increases up to 38%, with decreasing impact by rising pump speed. The unexpected difference from typical pump characteristics appears in speed range below 2200 rpm and 2800 rpm. The deviation seen here from straight characteristic line include three measurement points (2200 rpm, 2400 rpm and 2600 rpm). All measurement values are in the automated measurement protocol in reasonable range, which may indicate a physical effect causing this phenomenon.

To clarify this phenomenon, a cross check measurement with a second pump type becomes also mandatory, as supportive action for analysis. Therefore, a Bosch CP4s1 high pressure pump pressurizing OME in same system build up was utilized for this cross check.
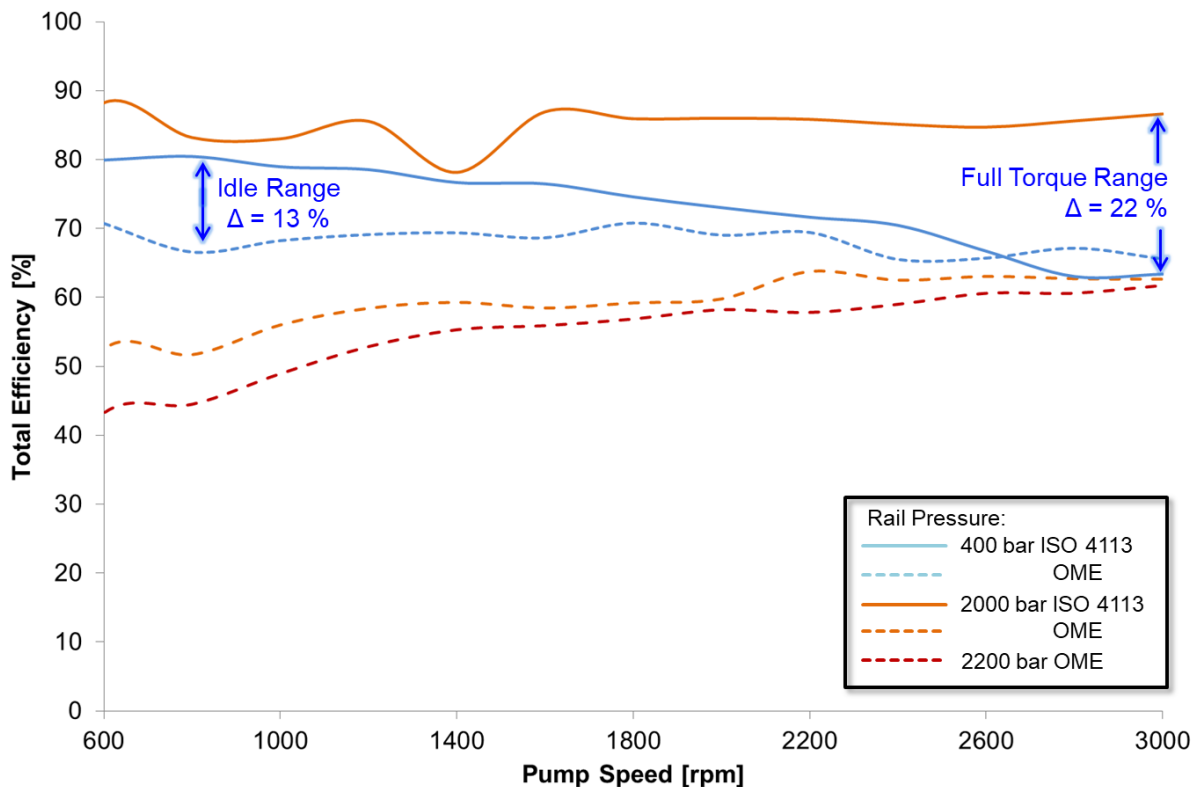
Figure 70: Total efficiency impact by OME vs. ISO4113 Diesel test fluid on Bosch CP4s1

In principle most of the before mentioned observations in *Figure 69* have at least similar characteristics for Bosch CP4s1. Values in *Figure 70* differ over total range, starting from idle range differing 13% from ISO4113 measurement to OME measurement up to 22% for 2000 bar measurement line. Since the utilized Bosch CP4s1 is designed for 2000 bar maximum comparison range keeps within this boundary. The shown line for 2200 bar rail pressure is a target value by controller, but achieved pressure of ~ 2100 bar follow the maximum capability of high pressure pump sample. Therefore, the line is included for uniformity to the measurement in *Figure 69*.

The root cause for second measurement as cross check (the unexpected total efficiency increase from speed range 2200 rpm up to 2800 rpm at 400 bar rail pressure) cannot be verified on this sample. Furthermore, the total efficiency approaches to 60 % when OME is pressurized. This impact is more significant for high load operation, since high pressure area at higher speed range meet often calibration situation in real road engine duty operation. As example the mentioned "full torque" operation point, where the high pressure pump typically

requires the highest calibrated delivery rate, but obviously the rated power operation point will be influenced by this change in total efficiency between OME and diesel fuel.

4.1.4. Measurement results of diesel high pressure pump for commercial application

The operation principle between passenger sized and commercial sized high pressure pumps does not differ. Furthermore, commercial engines utilize higher torque and higher power output. Thus, a high pressure pump usually has larger displacement per rotation and therefore has a larger geometrical volume, typically realized via multiple plungers with higher volume. In addition, different speed ratio between engine and high pressure pump are also feasible.

The measurement results refer to the Denso HP4 Diesel High pressure pump as well as friction modified derivate in order to achieve comparability (see chapter 4.1.1). Most remarkable difference to before mentioned Bosch CP4s1 remains in Denso HP4's delivery by larger displacement and plunger count. As analysis procedure before, first analysis contains total efficiency analysis.
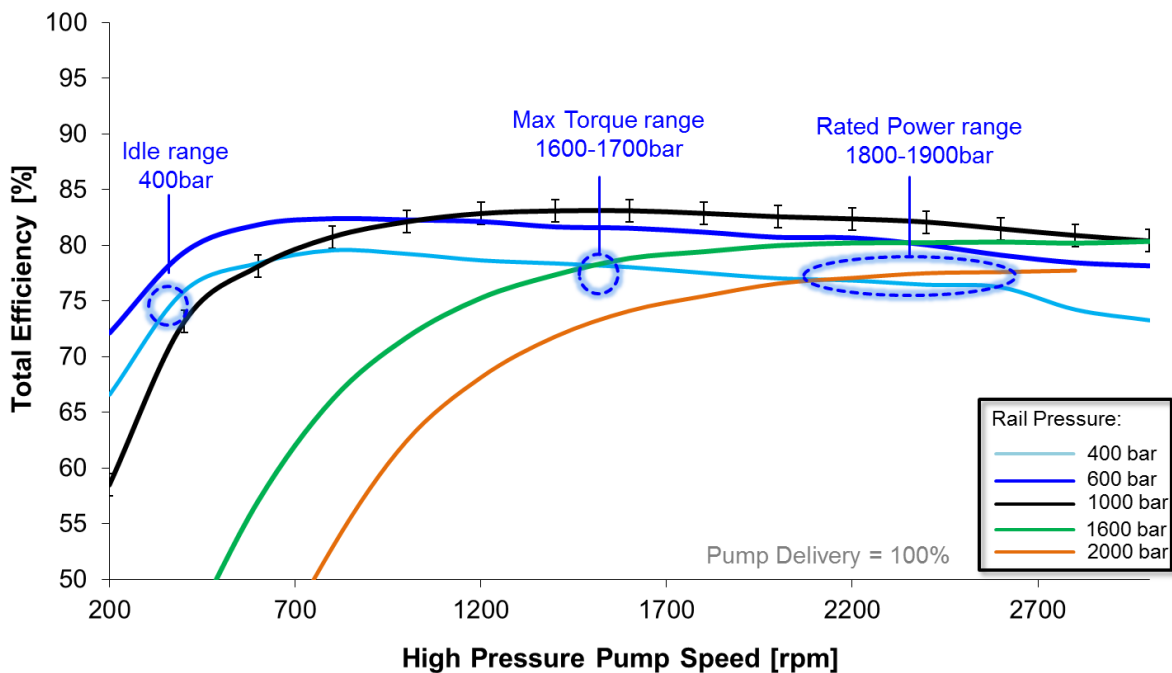
Figure 71: Denso HP4 total efficiency mapping in consideration with HMC G-Engine demands

The operation point marks shown in *Figure 71* differ from the orientation marks for smaller diesel high pressure pumps as well as GDI high pressure pumps. Reason remains in different duty cycles of their targeted engine applications. Typically, engines in heavy duty and commercial application have to endure absolute and relative higher loads as engine application for passenger cars. A truck running with full load uphill on highway will reach its engine maximum torque operation point frequently. The encountered total efficiency levels stay within this perspective in range between 75% and 80%. The displayed error bars are intended for overview and reminder on the measured process stability. Important information again remains in mechanical power consumption.
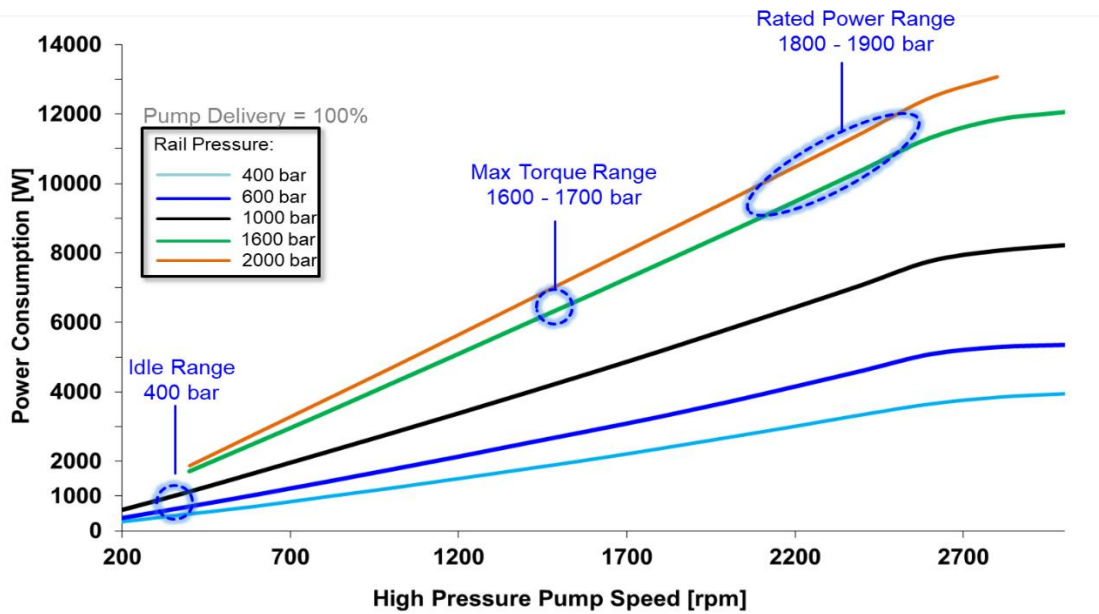
Figure 72: Power consumption of Denso HP4 high pressure pump for HMC G-Engine

The mechanical power consumption in *Figure 72* reaches levels of 12,5 kW and higher in full delivery state of ~190 ltr./h at 2000 bar as maximum possible. Since commercial application often runs in high load ranges by its nature of application, even lower rpm ranges as rated power still have high rail pressures as well as high mechanical power consumption by FIE. Also strategies in commercial areas often utilize 400 – 600 bar range for idle and start duty areas in range of 1000bar, while passenger car application commonly do not reach rail pressure levels of 600 bar over average in driving cycles (e.g. WLTP).

The increased fuel delivery to serve higher engine demands is the root cause for this high power consumption. In addition, the dynamic torque has to follow this high mechanical power consumption.
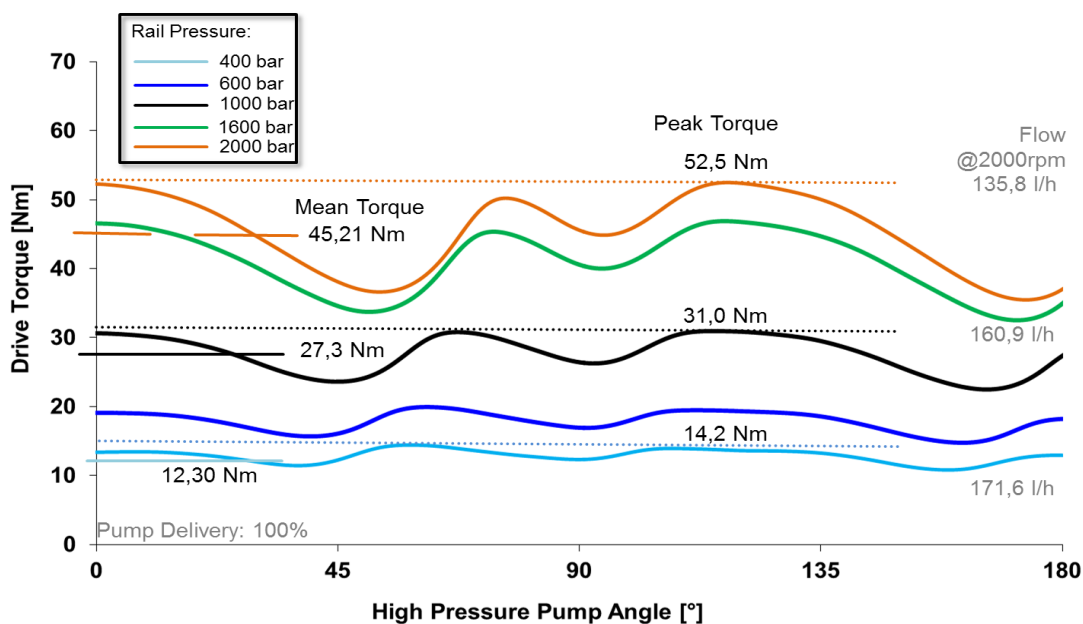
Figure 73: Drive torque of Denso HP4 in full delivery for HMC G-Engine

87

Two major geometrical boundaries differ in the here shown *Figure 73* from the drive torque of the passenger vehicle sized Bosch CP4 (see *Figure 62*): the number of plungers and their larger displacement. The most significant influence is the higher number of plungers on drive torque performance. While not two lifts per rotation (360°) becomes visible, in total six distinguished peaks appear. This follows by the summation of all single plunger dynamic torque waveform [45]. But larger displacement causes higher peak torques as well as higher mean torques. Also the ratio between mean torque and peak torque is lower than in single plunger case. As the Denso HP4 has a peak torque of ~115% of mean torque, the Bosch CP4s1 as single plunger pump has a peak torque of ~300% of its mean torque.

In order to achieve lower mechanical power consumption by the high pressure pump without changing the specific pump type, a friction reduced pump sample type has been prototyped and measured. Details to the friction reduced Denso HP4 are listed in *Table 17*. Following analysis demonstrates most significant differences in pump performance compared to serial produced Denso HP4.

As obvious impact, friction reduction measures have significant influence on total efficiency performance, as the *Figure 74* illustrates.
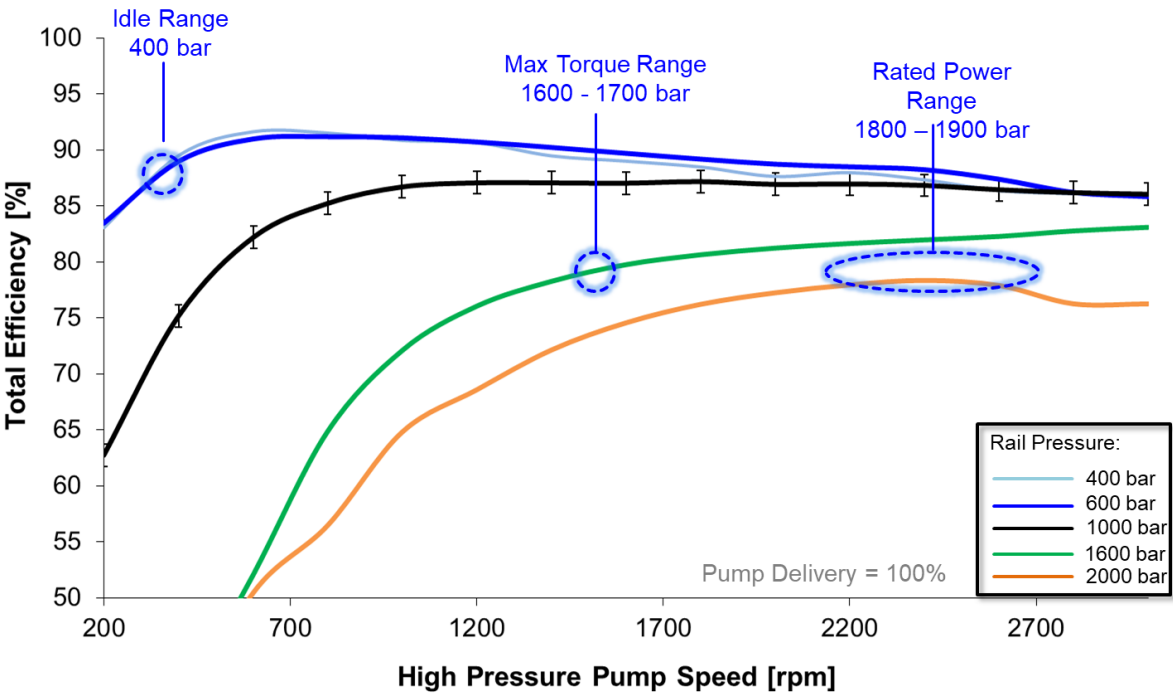
Figure 74: Friction reduced Denso HP4 total efficiency mapping in consideration with HMC G-Engine demands

The friction reduced version of Denso's HP4 achieves total efficiency levels of 78% in rated power range and 88% in idle range, while highest achieved total efficiency reaches level of 91%. Also pressure level of highest total efficiency moves to 600 bar instead of 1000 bar for the serial version of the Denso HP4 (see *Figure 71*). This total efficiency improvement results from a reduction of mechanical power consumption by same hydraulic performance. Therefore, power consumption reached in this are values of 11,5 kW. Thus also drive torque performance differs from its serial produced version.

4.2. Measurement results of high pressure pump in chain drive

As not only the component but also its integration into engine mechanics determines later system power consumption and therefore losses of the entire powertrain, the interaction between high pressure pump and engine needs to be analyzed. Therefore, a chain drive setup, which can be installed on the FIE test bench has been utilized. By integrating of an HMC R-Engine chain and valve architecture onto a test frame, a high pressure pump performance as close as possible to an engine assembly can be determined. The measurement setup is described in chapter *3.1.*

In order to determine high pressure pump specific contribution to engine friction, the crank shaft measurement requires separation of cam shaft impacted torque and high pressure pump impacted torque. Whereas a total drive torque, including the cam shafts, shows a "full picture" of crank shaft close to operating conditions. The "pump only mechanics" shows the influence of the high pressure pump to alone on the whole drive chain. The test procedure follows the same approach as used for diesel engine high pressure pump performance measurement. This includes the rail pressure as well as the pump speed range, with exception of limiting the maximum speed to 3000 rpm due to safety reason. Since the ratio between high pressure pump and crank shaft is 1:1, the pump speed is equal to engine speed.
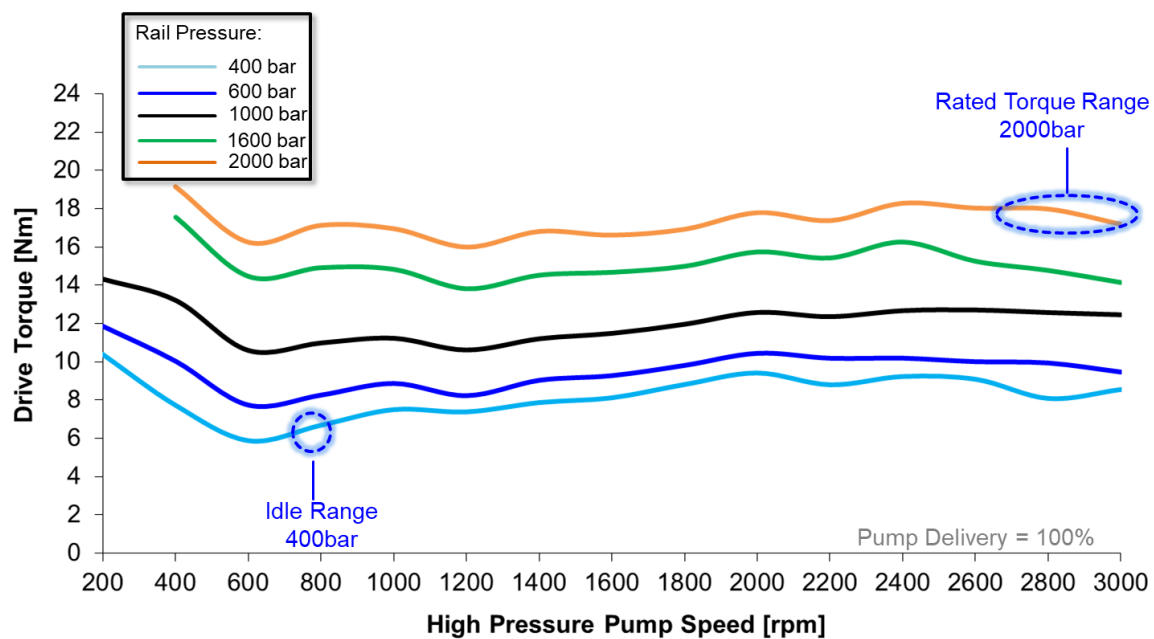
Figure 75: Chain integration impact of Bosch CP4s1 on R-Engine in chain only configuration

Reflecting drive torque of high-pressure pump and chain drive, drive torque reaches level of 6,7 Nm at idle similar condition and up to 18 Nm at rated torque condition, as *Figure 75* shows. In comparison to the prior measured drive torque of the same Bosch C4s1 pump alone (see *Figure 62*), increase of losses from 4 Nm at 400 bar (pump alone measurement: 2,8 Nm in idle similar condition) up to 6 Nm at 2000 bar (pump alone measurement: 12,5 Nm at full torque condition). Since highest mean torque values appear on 2800 rpm and decreasing tendency with higher speed range, the decreasing performance as in *Figure 61* visible, reduces the required torque by high pressure pump.
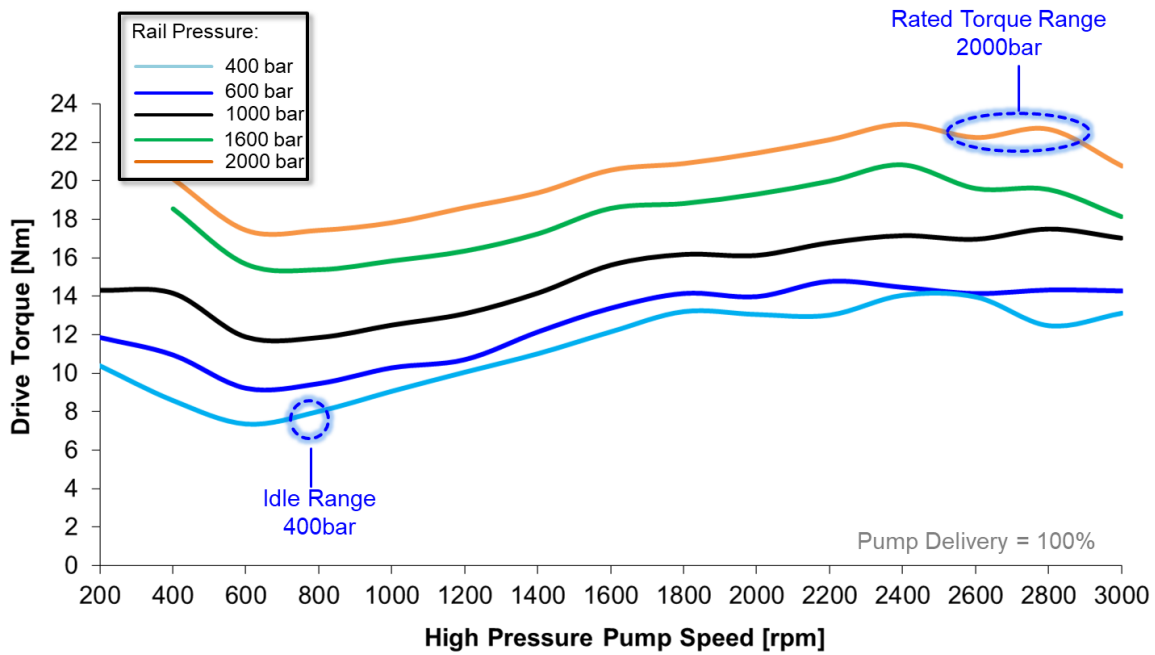
Figure 76: Chain integration of Bosch CP4s1 on R-Engine in total cam shaft mechanics

The extension to a measurement in full setup has similar performance as the setup without cam shafts working. *Figure 76* differs in absolute measured drive torque level, but shows minor changes in characteristic. The speed range has most significant impact, as values differ between ~2 Nm and up to 4 Nm as visible in 400 bar rail pressure line. Remarkable is the similar drive torque consumption of 400 bar and 600 bar in speed range of 2400 rpm to 2600 rpm. Anyhow, to understand nature of the resulting mean drive torque, detailed dynamic drive torque analysis becomes mandatory.
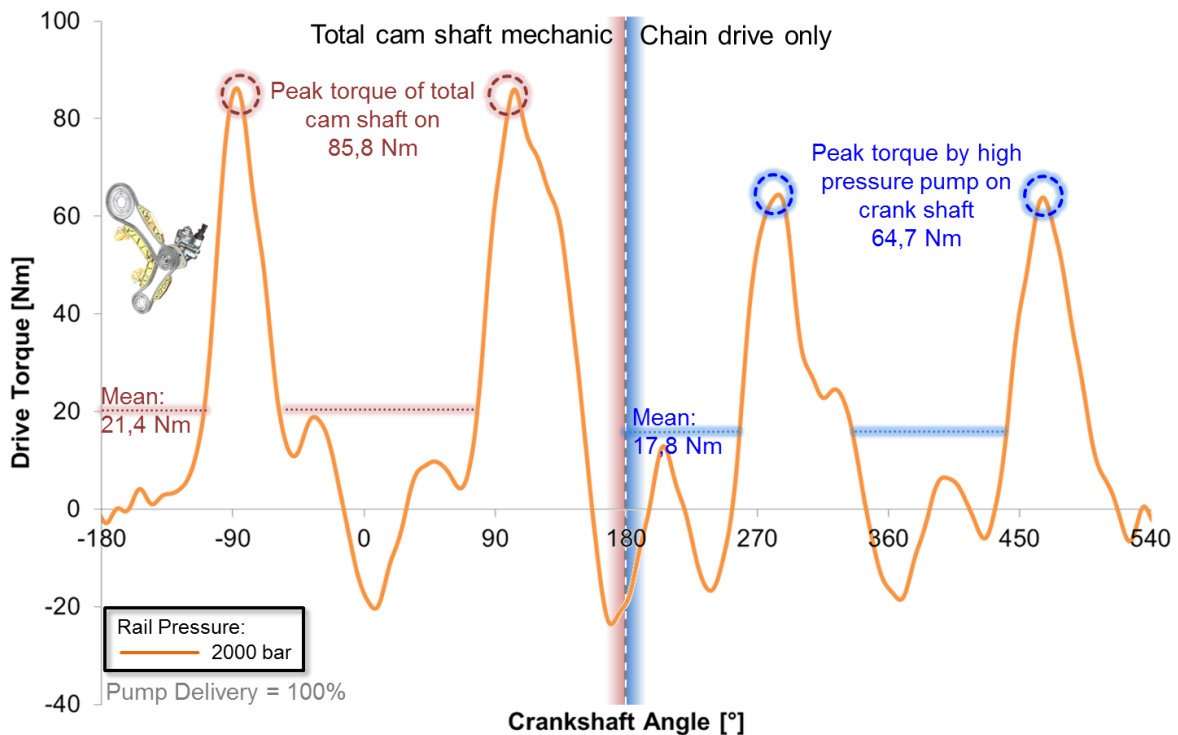
Figure 77: Dynamic drive torque impact on chain drive by Bosch CP4s1 pump at 2000bar and 2000rpm engine speed on R-Engine chain with and without mechanical cam shaft application

As described in chapter *3.3* the displayed results respect to combined measurement of "pump only" configuration in range from -180° to 180° angular position of crank shaft and full applied cam shaft, respective to 180° to 540° angular crank shaft position. Therefore, *Figure 77* shows detailed impact of high pressure pump on crank shaft and therefore to engine performance. Two major differences become directly visible: the peak torque in the "pump only" configuration is more than 20 Nm lower than in full mechanical configuration while mean torque shows similar results. In this case, the mean torque is 3,6 Nm higher for a fully applied cam shaft.

On second view, the combined frictional impact of high pressure pump and chain determines physical impact of high pressure pump to engine. Therefore, not only the measured dynamic torque as visible in *Figure 62* of 38,1 Nm peak torque and 12,54 Nm mean torque at 2000bar, but also the influence by chain and bearing itself reflects in the range of-180° to 180° crank shaft angular position.

4.2.1. Influence by part load delivery on engine's mechanical performance

Since fuel delivery in full load condition remains a rare case in typical engine duty, part load analysis becomes mandatory for understanding engine performance. As most obvious case, engine idle condition has therefore strongest impact, since fuel dosing differs most significantly from full load. Therefore, an analysis in this particular operation point shows the most significant results for engine performance.
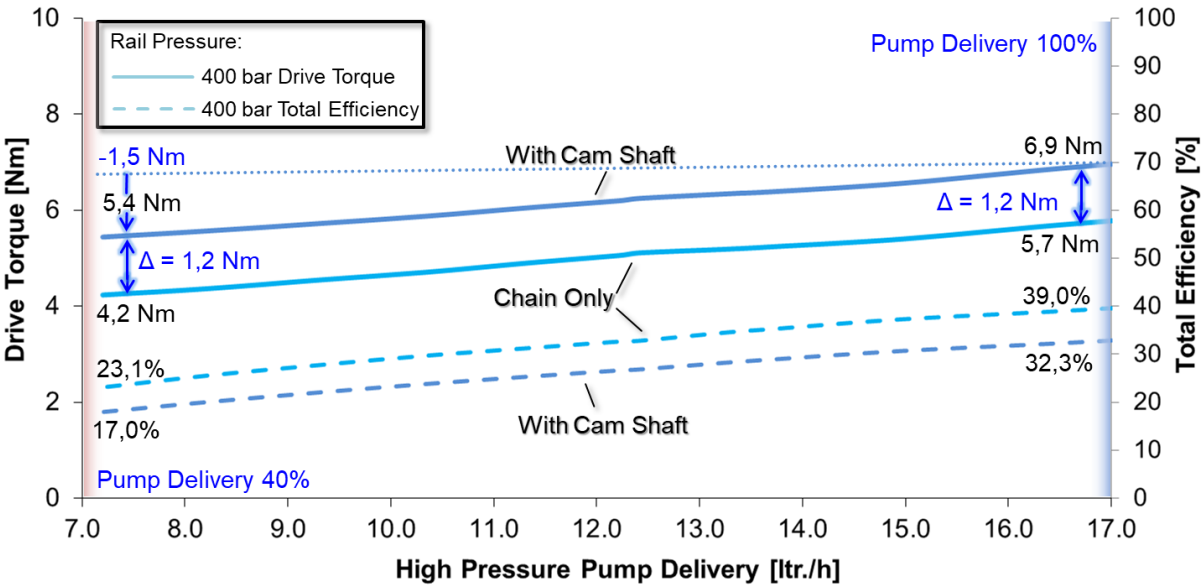
Figure 78: Part load operation of Bosch CP4s1 in idle similar condition (400 bar and 800 rpm engine speed)

The part load operation of Bosch CP4s1 high pressure pump, as shown in *Figure 78*, demonstrates impact on total engine friction. Reduction by 60 % flow rate reduces drive torque in both cases by 1,5 Nm or 22 % of highest total chain drive torque. In different view, total high pressure pump efficiency, measured at crank shaft, drops to 17% in this particular frame. Since the typical idle fuel demands by the engine is lower than 2 ltr./h, fuel flow below 5 ltr./h are often not applied in practice due to bad controllability in lowest delivery area as described in chapter *2.2.1.*

Also here, a deeper analysis of the dynamic drive torque performance becomes mandatory for evaluation of total friction.
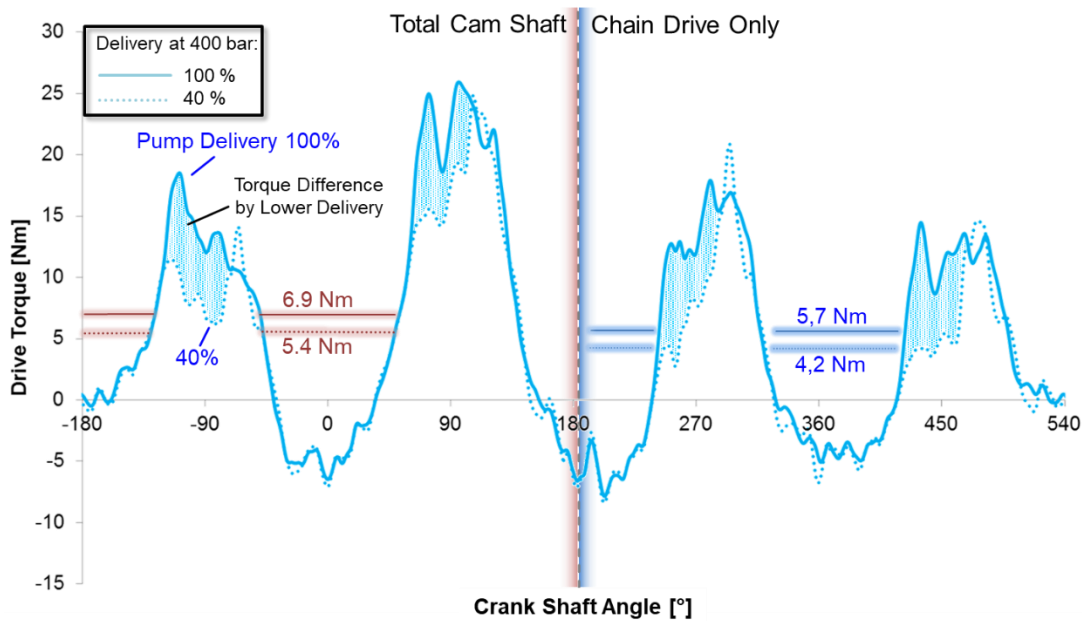
Figure 79: Dynamic drive torque of metered Bosch CP4 at 800 rpm engine speed and 400 bar

Figure 79 shows that the resulting dynamic drive torque in "pump only" and total engine mechanical build up is reduced by part load operation. Only a few spikes have locally higher value in part load delivery than in full delivery. As second minor impacted range by high pressure pump delivery is the area close to 0 Nm and at negative drive torque. In this area of energy retaining no difference becomes visible. As this area is not impacted by pressurization process, the friction of the entire system becomes the major parameter for its performance.

As a consequence, to demonstrate lowest possible friction of the entire drive train, the high pressure pump has to be disabled. For this measurement, the pumps MeUn has been actuated to fully close and the tappet has been removed. This leads to a pump with frictional abilities, but no pressurization capacities.
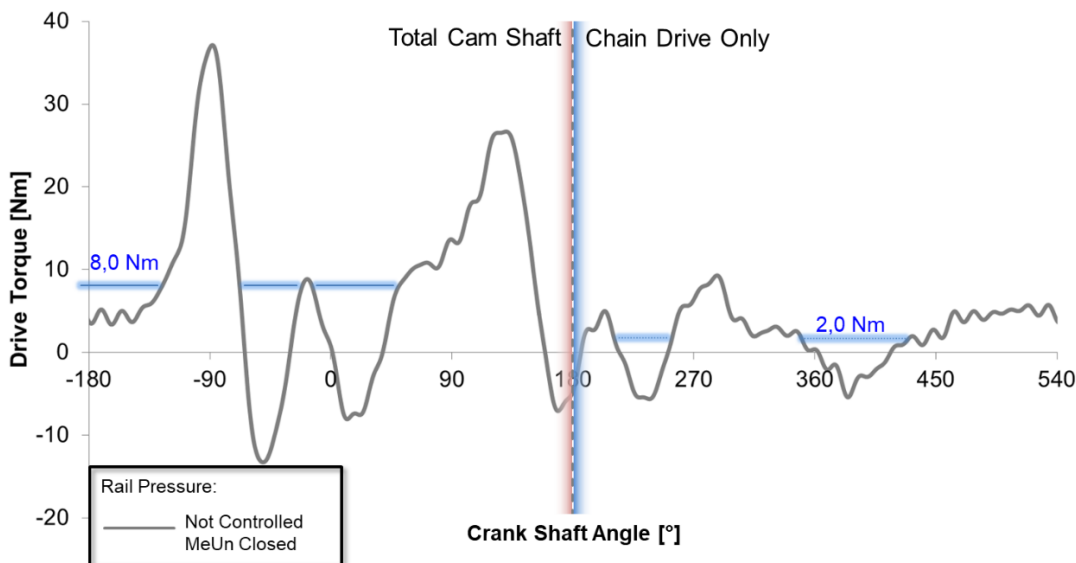
Figure 80: Dynamic drive torque of Bosch CP4 at 2000 rpm engine speed and closed metering unit (= 0% flow)

92

The scenario of the high pressure pump without any fuel delivery shows clearly interaction within total chain. Therefore, at no delivery state and without high pressure pumps spring support, the frictional reaction increases. Therefore, as *Figure 80* shows, drive torque demand for total cam shaft mechanics increases up to 8 Nm, while only chain related friction drops at this particular measurement point down to 2.0 Nm.

Also, a difference in peak torque by type of actuated valve on cam side can be distinguished. The highest peak torque of above 25 Nm is caused by air intake valves, while exhaust side reaches a peak torque level of 10 Nm. In contrast to that, the peak torque levels without actuation by valves has flattened characteristic within a range between -5 Nm and +5 Nm.

4.2.2. Influence by pump friction on total chain drive performance

For the analysis, frictional information by bearing type within high pressure pump itself is the next logical target for measurement. As mentioned in chapter *2.5* the high pressure pump integrates deeply into engine and even in HMC R-Engine configuration, builds a particular component in engine timing chain. In this circumstances, the high pressure pumps bearing and friction becomes a part of the engine main bearing system.

Since HMC HEFP Gen 2 utilizes needle bearings instead of bush bearings as Bosch CP4s1, a friction impact analysis of the entire chain is expected to have most significant results. As shown in *Figure 79* and *Figure 80* the influence on drive torque for the crank shaft, has to split into the influence on pressurization and the influence on the friction.
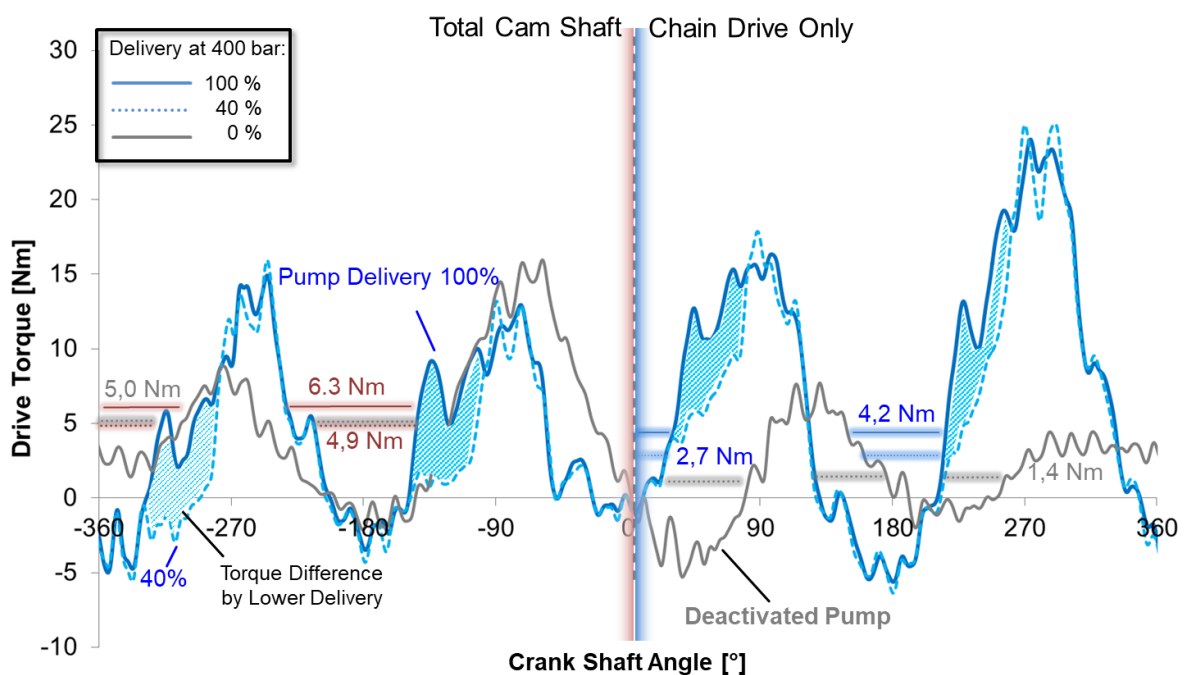
Figure 81: Chain drive integrated HMC HEFP Gen.2 in full load, 40% flow at 400 bar and deactivated at 800 rpm engine speed each

Despite already known performance in peak torque and mean torque, especially high frequent oscillation appears over the total measurement of *Figure 81*. In both cases of full cam shaft and chain only measurement, the mean torque performance is reduced between 1,4 Nm to 1,5

Nm: from 6,3 Nm to 4,9 Nm for total cam shaft and 4,2 Nm to 2,7 Nm for chain drive configuration.

In same way as for the Bosch CP4s1 high pressure pump, also the influence of part load operation needs to be validated up to full delivery.
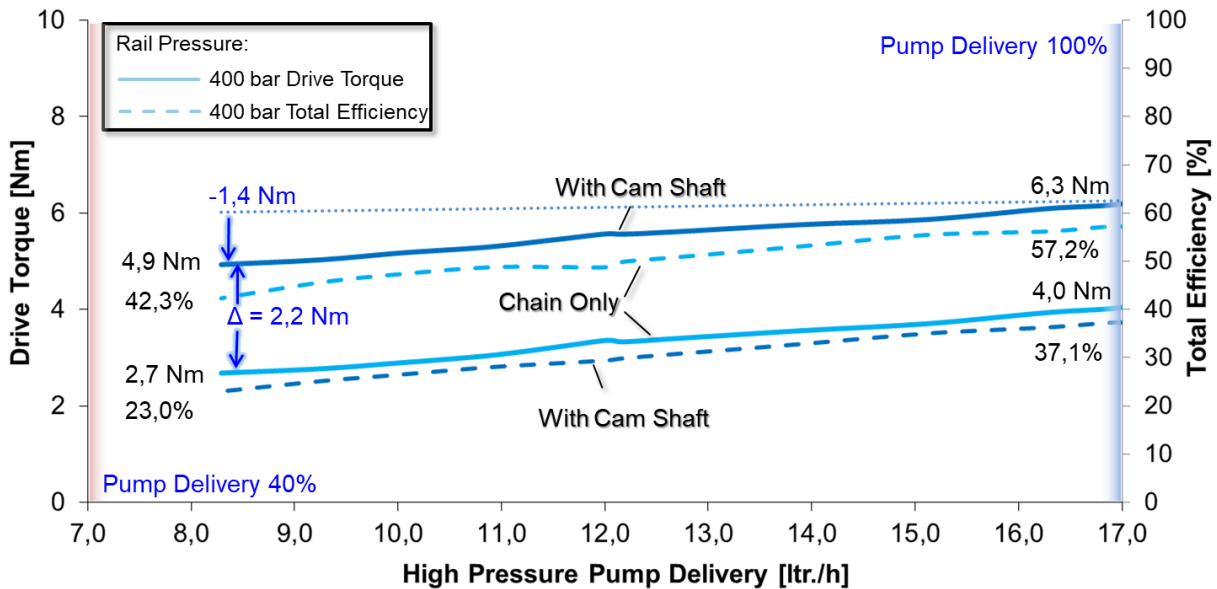
Figure 82: Part load operation of HMC HEFP Gen.2 in idle similar condition (400bar and 800 rpm engine speed)

Also in this particular frame a difference in mean torque demand becomes visible. Also known values from *Figure 81* are transferred into the displayed *Figure 82*. The total efficiency performance remains as additional information, indicating levels from 42,3% to 57,2% in "chain only" configuration and 23,0% to 37,1% in total cam shaft configuration. By type of inlet dosing, the dosing capability of HMC HEFP Gen.2 only allows metering down to 8,2 ltr./h due to higher fuel higher supply pressure than demanded. A constant supply pressure level of 3,5 bar relative was selected for total range comparability: the intended metering concept of HEFP Gen. 2 bases on metering via supply pressure control as its impact is described in chapter *4.3*. The HMC HEFP Gen.2 also has capability to control high pressure fuel flow via Metering Unit for higher vehicle integration compatibility.

As next step, an overview on total engine operation range has to be performed. In particular, an HMC HEFP Gen.2 integrated into the chain drive system with full applied cam shaft and full delivery in similar configuration as in *Figure 76* has to be checked for macroscopic differences.
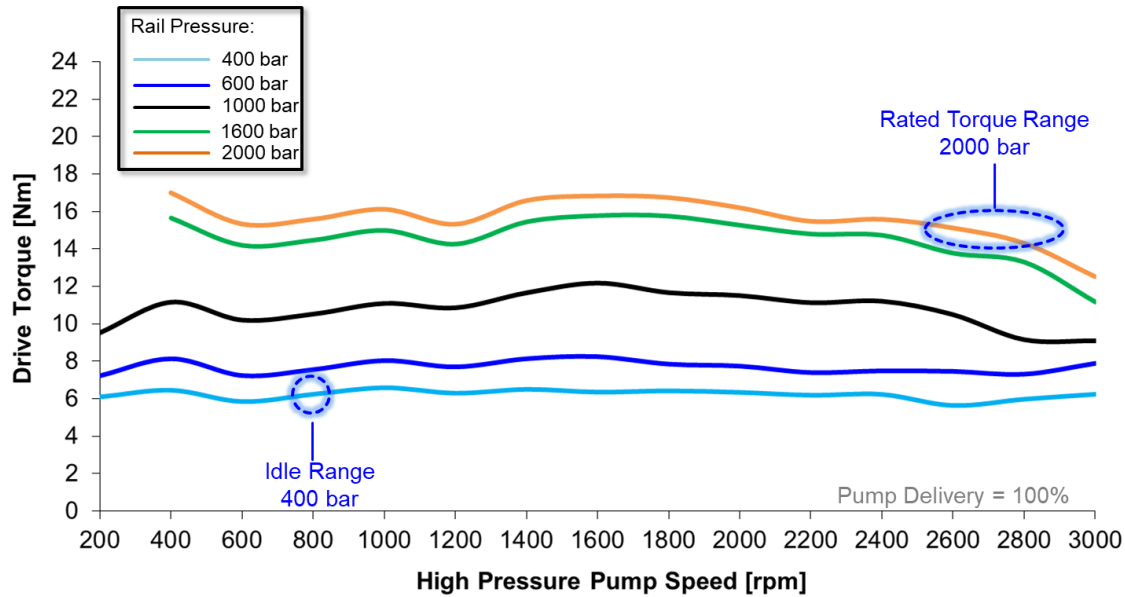
Figure 83: Chain integration of HMC HEFP Gen.2 with needle bearings on R-Engine in total cam shaft mechanics

In range for total engine operation, highest mean torque values reach levels of 17 Nm for rail pressure levels of 2000bar, as *Figure 83* visualizes. In case of idle operation, already known values of 6,3 Nm are measured and remain nearly steady over the complete engine speed. This feature remains in higher rail pressure levels of 600bar with corresponding higher mean torque levels. In range of 1000 bar rail pressure, higher engine speeds lead to an increase of torque in range from 1400 rpm to 1800 rpm and decrease with higher speeds. This tendency increases with higher rail pressure levels.

The measured rail pressure levels are limited for safety reason, due to mechanical layout of chain drive which has been made for maximum of 2000bar rail pressure, while installed high pressure pump has capability to reach pressure levels of 2500bar and higher.

4.3. Supportive fuel injection equipment component measurement

As mentioned in chapter *2.2* the architecture of an FIE contains more components than high pressure pumps. The before discussed high pressure pump delivers high pressurized fuel to the injector for injection. In most cases, a supply pump delivers fuel to the high pressure pump. Thus, the injector builds in this configuration the consumer and the supply pump the supporter.

Since both components have significant impact to power demand of total FIE, analysis in both cases becomes mandatory. While the low pressure pump in its supportive function in feeding the high pressure pump, the leakage of servo-hydraulic actuated diesel injector require more attention. Anyhow, in order to accomplish the task to identify FIE power consumption and therefore entire vehicle fuel consumption impact, information on both components are required.

The chapter *4.3.1* focuses on the analysis of the low pressure pump and especially its electrical power demand for operation.

The chapter *4.3.2* focuses on an exemplary measurement of injector leakage by a servo-hydraulic actuated diesel injector. Since the variety in this field is very wide, a standardized

leakage model by simulation will later be used in order to achieve a generic applicable model. The shown measurement in this chapter shall give an overview on principles of servo-hydraulic actuated injector leakages. In case of GDI commonly applied direct acting injectors, leakages can be ignored due to its operation principle.

4.3.1. Low pressure supply pump measurement results

In most cases the supply pump locates within vehicle fuel tank. As state of the art, two concepts are utilized in modern vehicles: steady flow concept with constant pressure and flow over complete duty cycle and demand controlled concept via pressure control. Both concepts utilize electrical power for pressurizing fuel and delivering sufficient quantity to the high pressure pump. Therefore, the battery of the vehicle is the common energy source for all types [66].

As an exception, commercial diesel engines often utilize mechanical pumps attached to the high pressure pump for feeding the high pressure pump (see *Table 17*). As they technically combine to one single device, its specific power consumption integrates into this type of systems high pressure pump.

To measure the electrical power consumption of the supply pump, setup and calculation follows as in chapter *3.4.* Also in this case total efficiency mappings of the low pressure pump remain as tool to identify power consumptions in total vehicle.
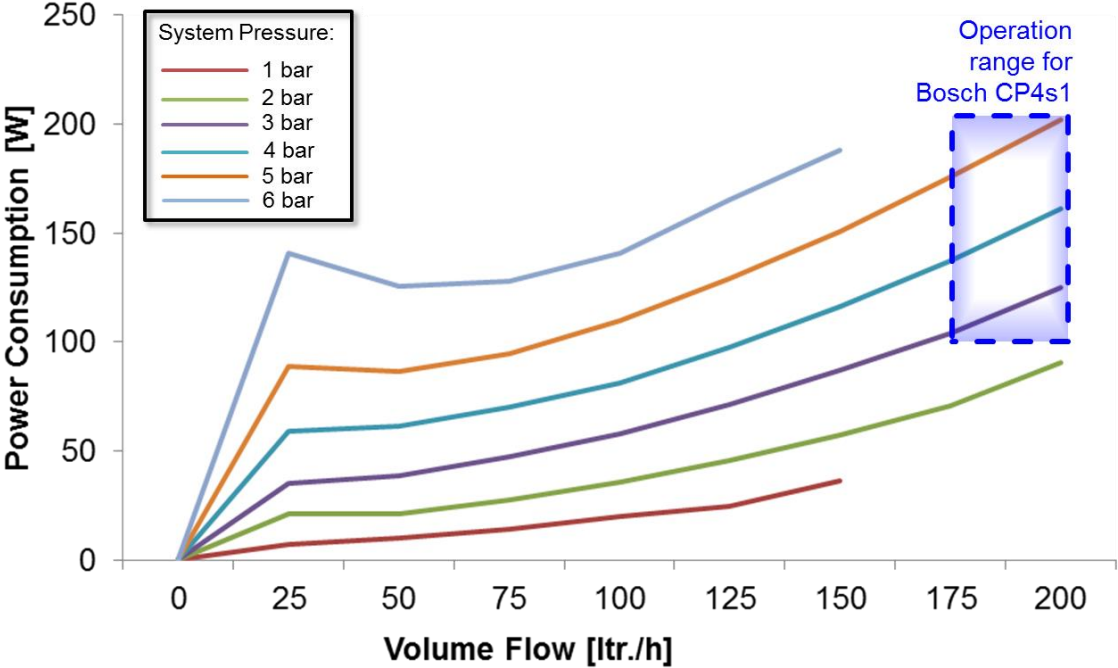
Figure 84: Low pressure supply pump power demand for HMC R-Engine configuration in total supply line to high pressure pump [64]

As the low pressure supply pump has to meet the specification of the high pressure pump installed on system side, specific duty areas have higher significance for total vehicle CO_2 emission. In particular, in *Figure 84* mentioned area meets to in Bosch's CP4 specified duty area. As visible, the low pressure pump consumes between 100W and 200W within this area. Within total operation range, pressure levels show most significant influence on power consumption. Therefore, the highest measured difference in power consumption appears at

150 ltr./h between 1 bar relative pressure difference an 6 bar relative pressure difference. Within these specific boundaries measured electrical power consumption shows values of 153 W. [64]

4.3.2. Injector leakage measurement of a servo-hydraulic actuated injectors

To characterize the injector as major consumer for high pressurized flow, information on total fuel flows required for function are required. This is especially required as described in chapter *2.2.3* for servo-hydraulic actuated injectors as typically utilized in diesel engine. Therefore, detailed measurement of diesel injectors become mandatory to determine correct quantities as for leakage and injection. Due to the injector variety of this particular type, a standardized leakage model by simulation will later be used. Anyhow, the shown leakage measurement shall give an overview.

As following figure demonstrates injection splits into injection itself and leakage by injectors servo-hydraulics actuator. In first simplified attempt, leakage can be assigned to injection timing and pressure, as it is done for injection in same way.
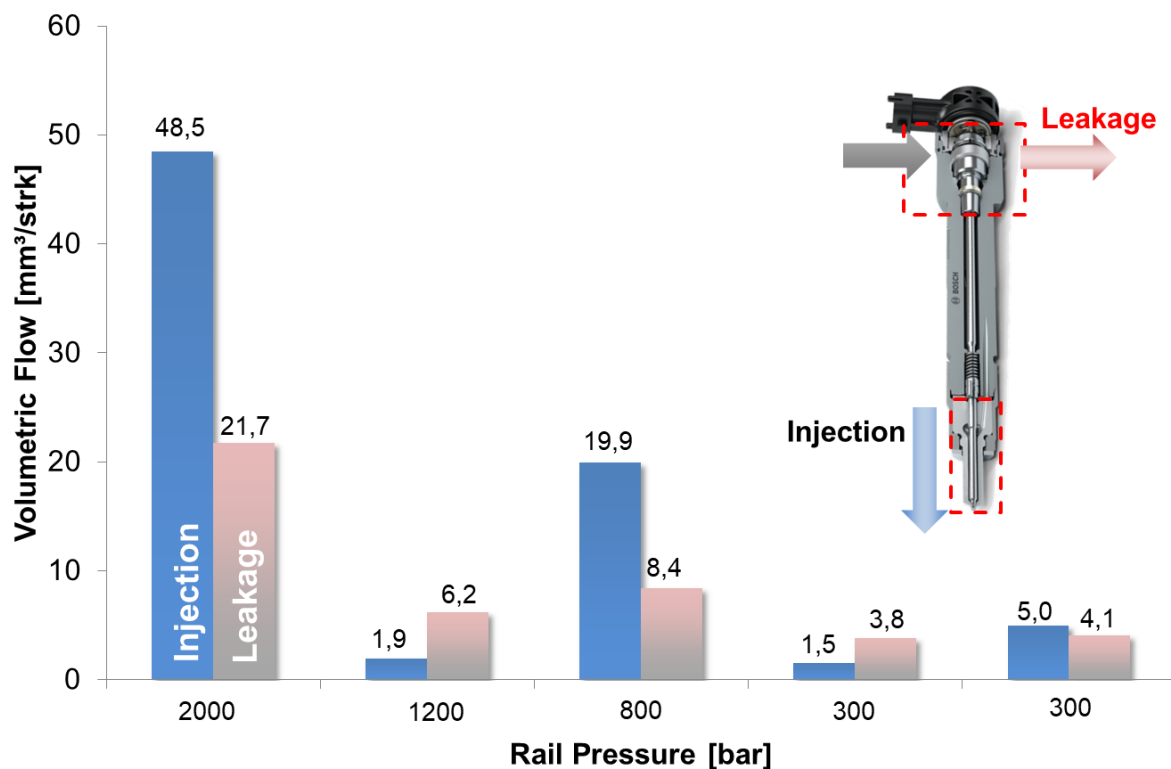
Figure 85: Selected injection and leakage share of Bosch CRI 2.20 injector for HMC R 2.0 ltr engine

Two major relations reveal within *Figure 85,* as it displays for R- Engine 2.0 ltr. serial injector performance. Injector leakage increases by injection time (or injected quantity), but lower than injection itself. In particular, measurement at 2000 bar and 800 bar have, compared to other three displayed results, a significantly higher share in injection. As second phenomena, rail pressure influences leakage ratio as visible comparing both measurements below 2 mm³/stroke. With rail pressure increasing, the leakage amount also increases, up to more than three times of the injected volume.

As this performance depends on internal injector build ups, as well as definition and manufacturing of internal hydraulic circuit, a generic assumption is not feasible. Furthermore,

to determine individual performance during engine operation in unknown state, large measured front load data is mandatory. Alternatively, simulation models which display such performance can close up also for unknown configuration during development processes.

4.4. Full engine measurement results

Engine measurement is mainly used during development process before existing and possibly even before vehicle prototyping. Therefore, test mode on engine test bench does not refer to all encounterable effects of entire powertrain or vehicle, but direct impact on engine base can be distinguished, despite lowest load condition. Also, due to typical high power and torque range of engine test benches, smallest differences are hardly measureable.

Also, the final fuel consumption and therefore CO_2 emission certification utilizes testing on entire vehicle on chassis dyno. Next chapter *4.5* presents therefore results based on such test mode of total vehicles. Anyhow, in case of commercial engines, chassis dyno test remains often not suitable. Also certification of commercial on road application proceeds in engines dyno operation, in "World harmonized transient cycle" (=WHTC). Also off-road application, whereas duty cycles often not mileage based, have to follow legislation limits, such as TIER. Major reason for this certification mode is the low availability of chassis dyno for commercial applications. Also often is an engine within this purpose not intended for a mobile application. In respect to this and for overview purpose, engine and vehicle analysis will follow the certification rules: commercial engine analysis will be done on engine test bench, the passenger vehicle analysis on chassis dyno. One exception has to be made, due to its status in development. Analysis of 1000bar GDI system is only available as engine dyno result.

Following bar chart demonstrates impact by high pressure pump variation in Hyundai G-engine with 6.3l displacement described in detail in chapter *2*. Details by high pressure pump results on FIE test bench are illustrated in chapter *4.1.4*.
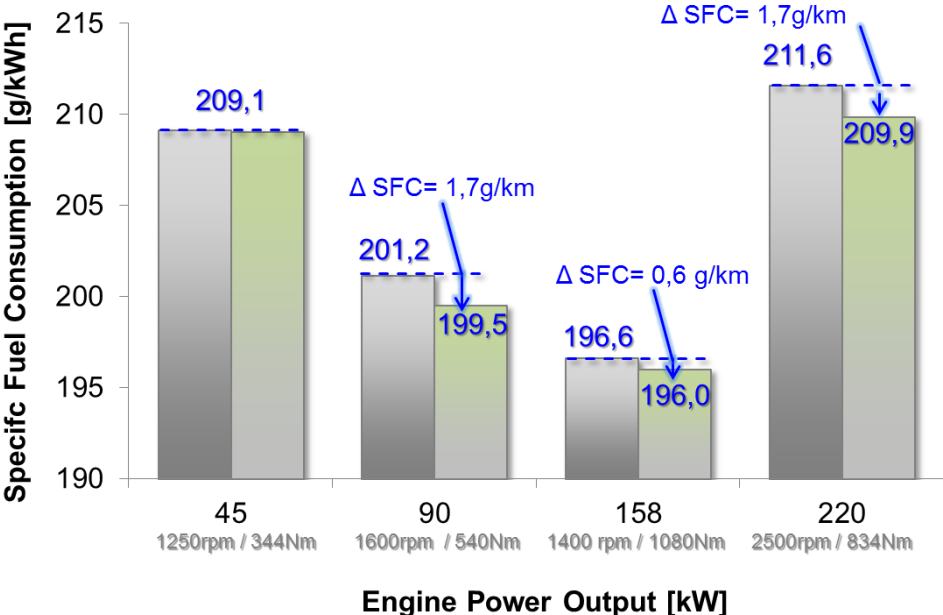
Figure 86: Specific fuel consumption (SFC) impact by high pressure pump modification on HMC G-Engine

Figure 86 shows four points of 13 WHSC point and demonstrate impact range on high pressure pump on entire engine fuel consumption. In lower load area for commercial application of 45 kW measurement determines minor impact in no measureable range and 1,7 g/kWh (or 0,8%) for high load area of 221kW and 90kW engine power output. The area of 158kW shows lowest specific fuel consumption and lowest improvement by exchanging or modifying the high pressure pump. Anyhow, trucks typically encounter in all day situation higher loads than passenger engines due to type of application. Thus, especially high load situations are in focus for evaluation and also for certification.

Typical fuel pressure levels in state of the art mass produced engines, equipped with direct injection system, often do not reach high levels in power consumption. Thus, measurement on engines dyno does not lead to high measurable influence. Anyhow, also pressure levels in GDI system rising as technology proceed to higher ranges. As mentioned in chapter *1.3* future pressure levels may target areas of 1000bar for pollutant emission reasons. Since power consumption by such increasing pressure levels also increase, an analysis in specific fuel consumption (SFC) impact becomes mandatory for the later prediction of the additional effort for cleaner combustion.
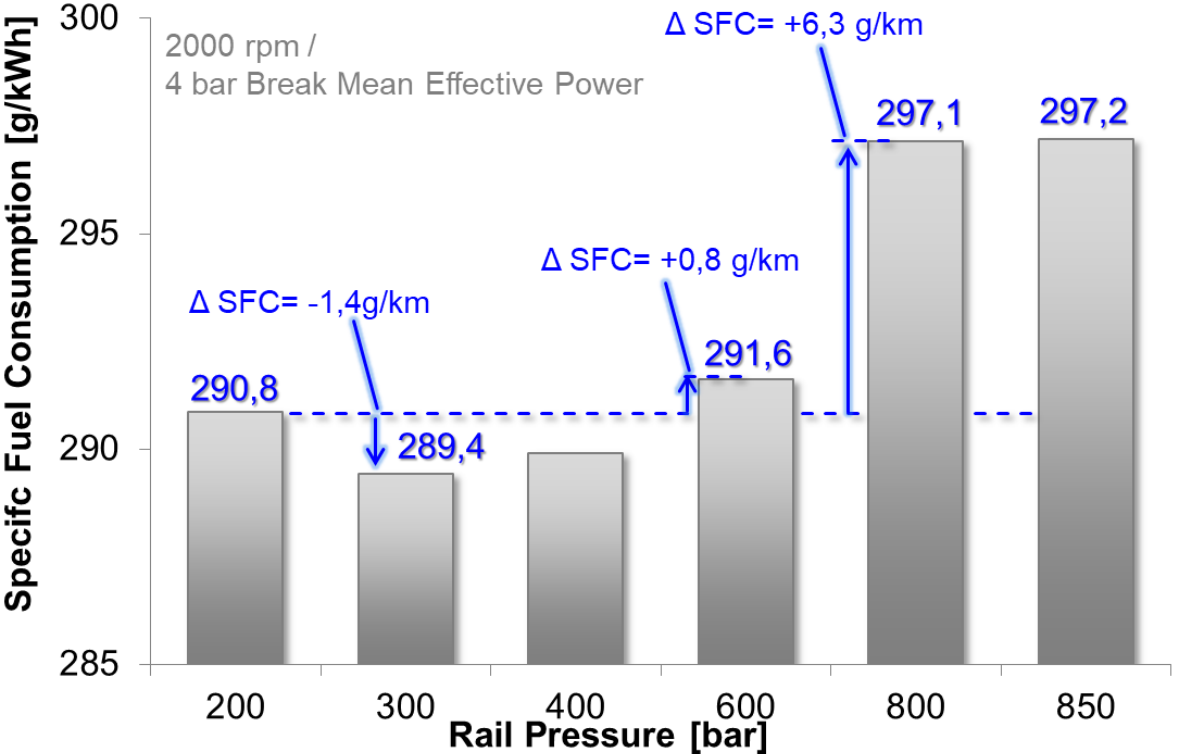
Figure 87: Rail pressure impact on GDI full 1.5ltr. HMC Gamma engine 1000bar injection system equipped

Utilized engine for this system pressure application remains by today state as prototype engine for impact analysis. The todays applied GDI system of HMC Gamma 1.5ltr. was removed and replaced by Magneti Marelli system mounted on exhaust cam shaft. The utilized measurements at 2000 rpm engine speed and 4 bar Brake Mean Effective Pressure (=BMEP), the here shown SFC results of *Figure 87* represent not a best point, but with low engine calibration modification to maintain stability at this point in a rail pressure sweep. As initial measurement value of 290,8 g/kWh impact in first rail pressure steps even slightly improve engines SFC up to 400 bar. Shown best mentioned point within this configuration means in

physical values an emitted torque of 45,6 Nm (= 9,94 kW) and measured fuel consumption of 2,88 kg/h or 3,88 ltr./h.

With starting 600bar rail pressure and increasing, SFC shows demerits between +0,8 g/kWh and +6,3 g/kWh. The highest increase per segment has the step from 600 bar rail pressure up to 800 bar rail pressure. Herein, SFC increases +5,5 g/kWh in a 200 bar step. Later following steps of 50 bar remains SFC in a nearly steady state value. In last mentioned measurement point, engine emitted drive torque reached value of 45,9 Nm (=10,0kW) and fuel consumption of 2,97 ltr./h or 3,99 ltr. /h. In other words, even when engine out torque increased by 0,6% fuel consumption increased at this specific point by 3,1%.

4.5.   Full passenger vehicle measurement results

Measurements on total vehicle have two options for execution, as also recognized by state of the art regulation as EURO emission legislation. Tests today within European Union consider, depending on emission legislation level, tests in New European Driving cycle (=NEDC), World harmonized light duty cycle (=WLTC) and Real Driving Emission (=RDE). The measured CO_2 emissions and therefore fuel consumption utilizes test in NEDC and WLTC on chassis dyno test for fair and equal measurement conditions [89]. Popular press instead utilizes often averaged values on predefined routes. In contrast, commercial on-road applications mostly certified in engine dyno evaluation, due to lag of test capability for such high average power out, weight and size [89].

For detailed analysis purpose of the FIE, the NEDC cycle remains more adequate than WLTC, since its long stabilization time allows identifying and comparing engine impacts to total vehicle more clearly. Anyhow, all vehicles mentioned represent for evaluation selected vehicles.

Name (detailed Type)	Kia Stinger (CK Pilot 1)	Kia Sportage (QL Pilot 1)	Hyundai iX35 (EL Pilot 2)
Fuel Type	Gasoline	Diesel	
Engine / FIE System	„Theta" 2.0 TGDI 255 BHP 200 bar GDI	„R-Engine" 2.0 CRDi 150 BHP 2000 bar Common Rail	
Legislation level	EURO 6	EURO 6	EURO 5b
Transmission	8 speed Automatic	6 speed Automatic	6 speed manual

Table 19: For evaluation selected vehicles test on chassis dyno at HMETC

Utilized vehicles focus on same displacement and have similar architecture. All vehicles therefore have 2.0 liter displacement, utilize direct injection system in common rail principle and were certified in NEDC.

4.5.1. Gasoline passenger vehicle test results

The test vehicle for all chassis dyno measurements to determine fuel consumption of a GDI vehicle and therefore CO_2 emissions is a Kia Stinger with 2.0 TGDI with 8 Gear automatic transmission on rear wheel drive (HKMC internal code: CK G4FII HP EU6) as described in chapter *3.5* .

A typical analysis – depending on emission level - respects for certification final value of averaged pollutant emissions. Therefore, majorly given information for CO_2 emissions is a final value at the end of a test. As OEM, especially the possibility to have insight into ECU states allows a deep dive understanding of vehicle results comparability. Also it allows application of different modes, suitable for analysis purposes only and often not practical for real driving behavior such as utilizing a steady vehicle battery discharging to avoid impact by alternator or electric system on measurement.

Anyhow, in case for gasoline passenger emission reduction analysis, the utilized Kia Stinger, performed analysis in battery charge mode. In this particular mode, engines alternator will always charge the vehicles battery, independent of its state of charge (=SOC). Since battery system remains as a 12 V only solution, charge distribution between batteries (such as 48V system) does not affect the measurement.

Of major interest of this analysis is the CO_2 influence by parameter optimized high pressure pump on entire vehicle performance. As an entry, a KIA Stinger (CK 2.0TGDI) has been tested. The car has no changes to serial application, but for test stability modified engine management software including battery charge mode, high pressure fault system deactivation and modified rail pressure control calibration for improved robustness, as described in chapter *3.5*.
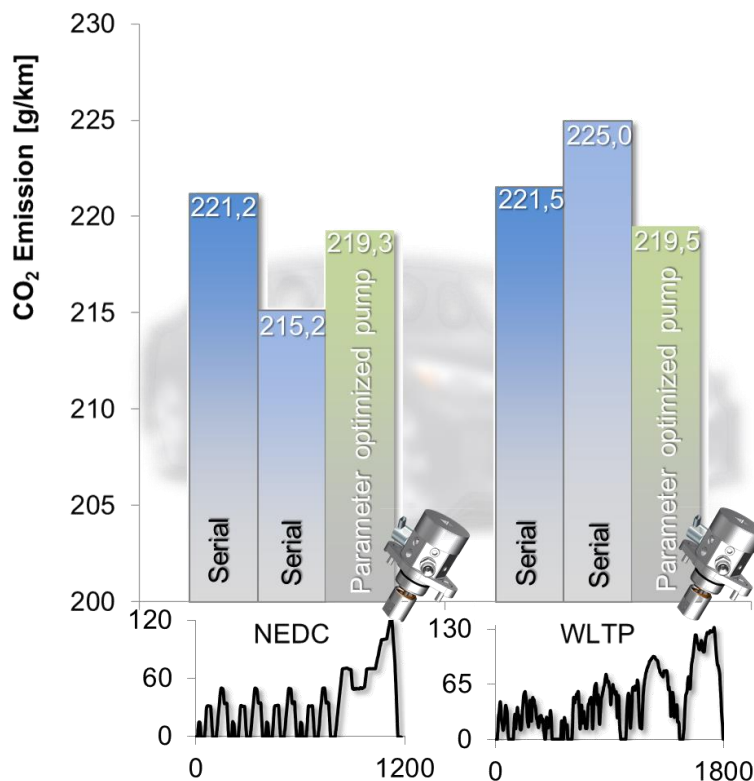
Figure 88: NEDC & WLTP CO2 results of Kia Stinger 2.0 TGDI on chassis dyno in serial FIE system vs. parameter optimized pump

Despite length and difference in dynamic, results between NEDC test and WLTP does not differ in high range by absolute value. In *Figure 88* shown uncorrected values in NEDC concentrate in range of 215,2 g/km to 221,2 g/km CO_2 emission and 219,5 g/km to 225,0 g/km CO_2 emission WLTP, whereas the parameter optimized pump shows in WLTP best value. To have a fair comparison, all tests shown here fulfil EURO6 emission legislation level, as the vehicle is calibrated for and the tests do not differ in engine calibration. This means in particular the rail pressure mapping remains the same 200bar system mapping as in serial calibration for both high pressure pump tests.

Anyhow, the vehicle tests have been executed in battery charge mode. Thus, a battery charge correction becomes mandatory in order to perform a fair comparison. For this particular vehicle, each percentage of SOC increase has an increasing effect of 2,04g/km CO_2 emission in NEDC. Since database for this in EURO6 b calibrated vehicle (=NEDC) data remains not sufficient for SOC correction in WLTP, a correction in WLTP is not possible. In this case average value of all tests remains suitable for analysis.
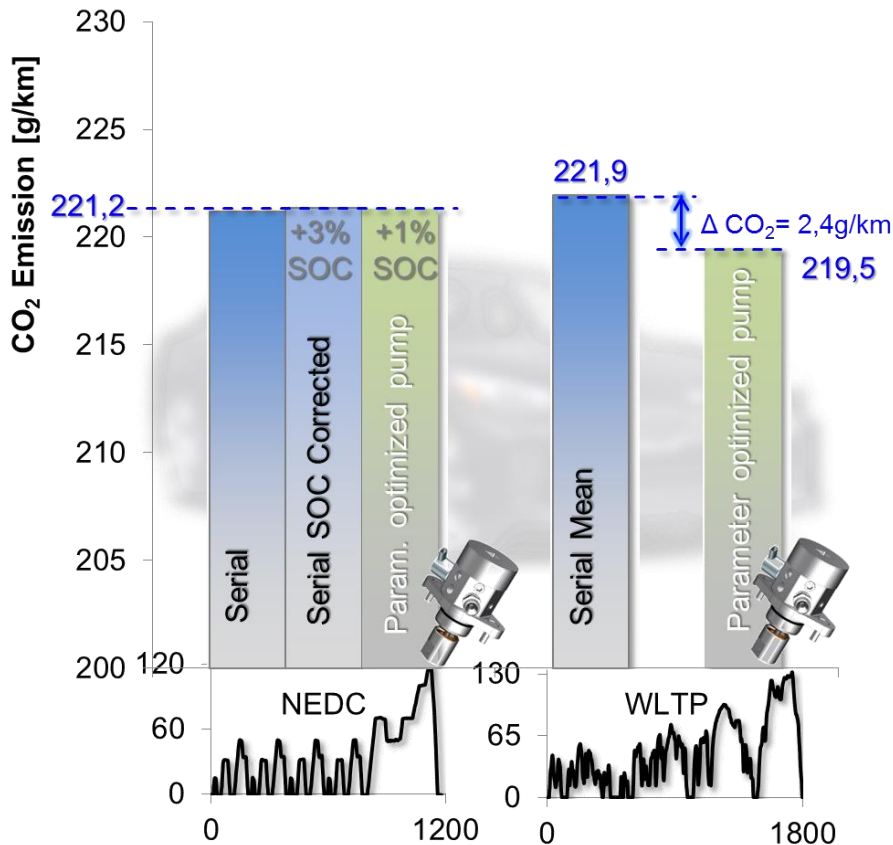
Figure 89: Corrected NEDC and WLTP results of Kia Stinger 2.0TGDI on chassis dyno in serial FIE system vs. parameter optimized pump

In NEDC case, all values enclosed within same range by utilizing battery correction for CO_2 emission, as *Figure 89* demonstrates. Also parameter optimized pump reaches nearly same range. Different as in WLTP case, whereas parameter optimized pump still has lowered CO_2 emission of 2,4 g/km, which is in scale of the demonstrated vehicle in range of 1,0%.

4.5.2. Diesel passenger vehicle test results

As displacement equivalent engine in HMC engine portfolio, the 2,0 ltr. R-Engine vehicles such as Hyundai Ix35 with Euro 5b emission level or Kia Sportage in Euro 6 application, generate a solid foundation for analysis CO_2 impact by FIE. Especially those two vehicles run in sum more than 100 tests in different FIE related modifications. Herein the NEDC cycle was used in most of those tests, due to its better abilities for this purpose. Due to this background high data availability, the following result will mainly focus on NEDC test results. Both vehicles are equipped with before mentioned R-Engine 2.0 ltr. The Hyundai iX35 with internal nomenclature EL 2.0 CRDi has a 6 speed manual transmission, while as test driver follow shift tables according to legislation. The Kia Sportage (internal QL 2.0 CRDi AT) is equipped also with 2.0 ltr R-Engine and 6 speed automated gearbox.
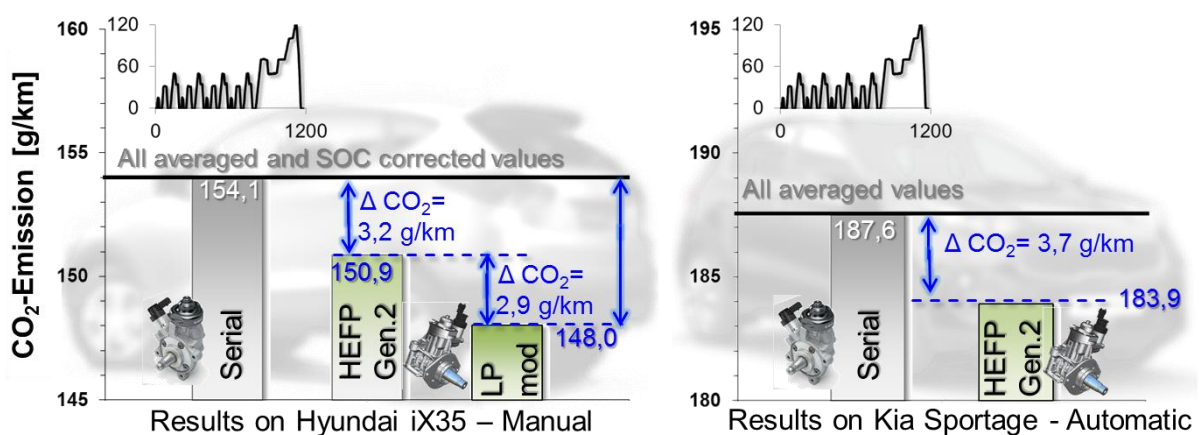
Figure 90: NEDC test results executed by Hyundai Ix35 and Kia Sportage equipped with R 2.0 CRDi in base and FIE modified variant

Both shown test vehicles demonstrate impact by changes on Diesel FIE infrastructure. While in case for exchanging high pressure pump (HEFP Gen.2 result bar) and lower friction pump ("LP mod" result bar), both results reduce CO_2 emission in range of 2,0% - 2,7%, as *Figure 90* illustrates. By applying modified low pressure system and therefore different rail pressure control concept as described in chapter *2.2* reduces additionally 2,9 g/km CO_2 emission. In summation a total CO_2 reduction of 6,1 g/km or 4,0% can be measured for cold NEDC. In similar attempt, difference reduces in hot NEDC to 4,9 g/km CO_2 emission.

Besides measurement by external sources, which chassis dyno itself provides, also sensor data by engine control unit can be reviewed. As mentioned at the begin, the NEDC has benefits for analysis, since its comparable long static phases allow review of engines direct reaction.
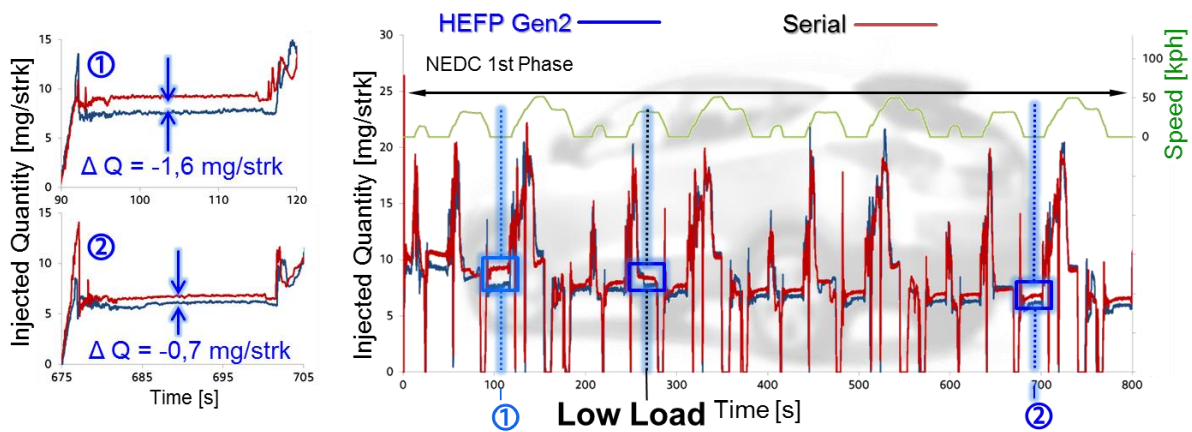
Figure 91: Engine control unit calculated injected quantity during NEDC of Hyundai iX35 2.0 CRDI in serial configuration and HEFP Gen.2

Insight to engine management data allows to review engine specifc reaction to changes. As the injected quantity per engine cycle or stroke (=strk) determines engine's fuel consumption and therefore CO_2 emission, impact in power consumption reduction as the injected quantity. As in *Figure 91* shown, ECU recognizes lower power consumption and therefore reduces the range of 0,7 mg/stroke to 1,6 mg/stroke the injected quantity. Those differences majorly impact engine idle area. Areas in "low load" such as 30 kph have also benefit by HEFP Gen.2 require lower injected quantity. During stabilization at 50 kph and during acceleration differences can hardly be distinguished. For illustrative reasons and the lowered significance by high pressure pump influence on calculated injected quantity, 2nd phase of NEDC Is not shown in this figure. The tendency of high pressure pump influence on engine's power consumption shows, by comparison of mark ❶ and ❷, the impact of engine oil temperature. Especially in idle, the friction reduction is driven by entire oil temperature. Considering this effect, the difference between at mark ❶ with 1,6 mg/strk. and mark ❷ with 0,7 mg/strk. is logical.

5. Analysis and evaluation of the performed measurements

To identify the impacting parameters of the fuel injection equipment (=FIE) on the total engine power consumption and therefore CO_2 emission, as first step an evaluation on hydraulic power consumption requirements to realize duty and further on detailed knowledge on power consumption by main demanding components is necessary. In this direction, as from source to "effect", first results of high pressure pump, as the component with highest impact on total power consumption (see to chapter *2.4*) will be evaluated.

Therefore, the chapter *5.1* evaluates the impacting parameters on high pressure pump performance which is a novel aspect. Since the mechanical influence of an exchanged high pressure is not measureable in vehicle (see chapter *4.5.1*) and a complete evaluation has not been performed in given literature (e.g.[32]), this particular evaluation is simplified and shall be mentioned for the "complete picture". The focus of the entire work is on evaluation on vehicle impact on CO_2 emission, which will then be evaluated more intensively. Anyhow, especially fuel properties have most significant influence on high pressure pump performance, a special deep evaluation on fuel impact will be shown. Of more relevance, especially in focus for changing markets, the influence of fuel on the high pressure pump performance has to be evaluated in deeper level. The chapter *5.1.2,* therefore focus on diesel high pressure pump performance, in special consideration of their performance when pressurizing alternative fuels. As last step for a "complete picture" high pressure pump parameters, the detailed impact by mechanical modification of a commercial high pressure pump is in focus. The chapter *5.1.3* discusses herein this particular content with a special focus on characterizing, how much performance can be improved by modified high pressure pumps. Due to the significant high mechanical power consumption reduction, an entry on relating the engine fuel consumption will be done.

The chapter 5.2, as next step in process, is the evaluation of vehicle performance. Herein, the mechanical influence on the engine performance in test cycle is in focus. As start in the simplest configuration, the chapter 5.2.1 evaluates the influence of a GDI system on entire vehicle performance. Herein, also the simulative support will be used the first time, in order to calculate the hydraulic boundaries for GDI mechanical power consumption evaluation. The next step due to increasing system complexity is the evaluation of diesel vehicles in chapter *5.2.2.* Due to its complexity of the system, also the simulation support increases. Herein, the simulation gives information on actual demands by the high pressure system.

After evaluation of measured effect, a knowledge is applied to predict the effects and features of novel and possible future application. Therefore, the chapter 5.3 focus on prediction of fuel based impact on the FIE and therefore the entire vehicle. The chapter *5.3.1* in particular focuses on the impact on GDI systems, while the chapter *5.3.2* focuses on diesel engine influence.

As last step and to finalize the task of showing potential for CO_2 reduction by FIE, novel applications for GDI and diesel applications will be shown in chapter *5.4*. In particular, the chapter *5.4.1* analysis and predicts the impact by novel injection systems and combustion approaches to their CO_2 potential. The chapter 5.4.2 shows a new method on handling alternative fuels within a FIE. This allows a new "virtual" sensor for fuel type.

5.1. Analysis of pump performance impact on engine performance loss

A first step in evaluating the performance impact and therefore an entire vehicles CO_2 emission impact is to focus on the major component for FIE power consumption. The high pressure pump samples have been analyzed from simple performance differences to significant changes. By transferring effects on measured vehicles, a significance in parameters become visible. This means that influence on state of the art GDI vehicles was low, barely recognizable, compared to common rail diesel (see *Figure 89*).

Still, this is a result of this analysis and needs at least to be mentioned. Therefore, the chapter *5.1.1* evaluates, to support a complete picture, the root cause for this result. More of interest is the performance influence of alternative fuel on high pressure pump performance. Herein, the analyzed performance differed significantly from diesel fuel. The chapter *5.1.2* evaluates intensively the impact on high pressure pump performance by alternative fuel. The last chapter *5.1.3* evaluates deeply the mechanical impact on commercial high pressure pumps and its influence on entire engine performance. Since the resulting performance difference between optimizations and the direct influence on engine performance is significant, it is a good entry to deeply evaluate the impact of the diesel high pressure pump on engine fuel consumption.

5.1.1. Gasoline direct injection high pressure pump performance spectrum

The analysis of entire measurement results as in chapter *4.1.* demonstrates, which total scale power consumption of modern FIE may reach. While gasoline high pressure pumps for a 2.0 TGDI engine has power demand levels up to 800 Watt (see *Figure 54*), a high pressure pump for 2.0 ltr. Common Rail Diesel has power consumption levels on component level up to 4400 Watt (see *Figure 63*) and increases up to levels of roughly 12000W as shown in *Figure 72*. As adequate tool for evaluation, the total efficiency for high pressure pumps gives proper information between high pressure pumps on how efficient the required hydraulic energy is utilized. Since the hydraulic energy demand has to supply all demands by combustion targets, such as injection strategy, this demand can be seen as fix in terms for component selection (see chapter *2.4.2)*.

As a starting point, the gasoline direct injection engines often mix the fuel injection components suppliers. This gives a practical reason to start an evaluation on this engine and pump configuration. Reasons for component mixing differ hereby from cost aspects up to performance or also legislation aspects. Referring to comparison between GDI pumps as in *Figure 53,* all samples have different best and worst operation points. This effect reflects impact between different pump types. Even though as the Kia CK vehicle (as shown in *Figure 89*) utilizes a serial applied high pressure pump and a specialized parametric designed and optimized high pressure pump. Herein, the NEDC does not show after all required correction, especially battery discharge correction, difference in CO_2 emission, WLTP case ranges benefits of 2.4 g/km lower CO_2 emissions by modified GDI high pressure pump. Starting point for understanding is high pressure pump performance difference.

For an overview purpose, evaluation will focus on comparison between the in chapter *4.1.1* described high pressure pump samples, in particular Hyundai-Kefico 250bar and the HMETC parameter carrier pump. To start the evaluation, the possible performance differences between two tested pumps have to be understood.
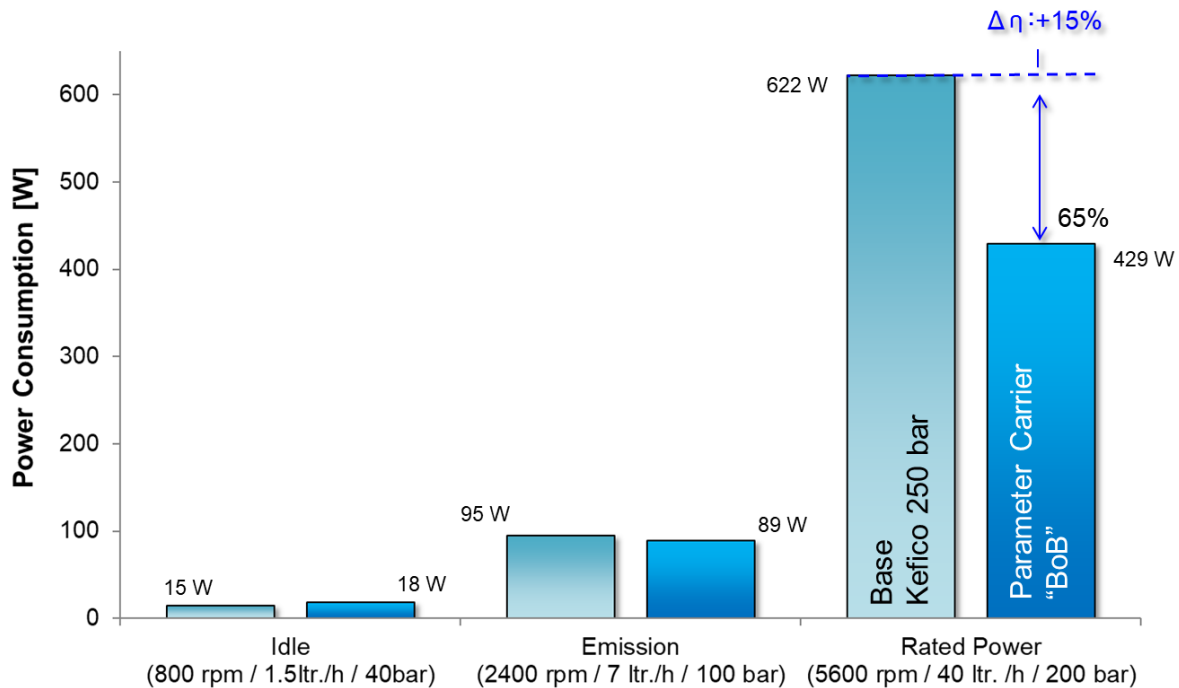
Figure 92: GDI high pressure pump power consumption differences at example engine operation points

The range of power demand during pump operation is wide for a GDI pump. As the *Figure 92* shows, a GDI high pressure pump requires in its major range of operation (here shown as from idle to emission) between 15 W and 95 W. The difference between both pumps is very low, compared to the power consumption demand difference in rated power. As an assumption, the mechanical influence on entire vehicle fuel consumption is in case for GDI high pressure pumps of less significance. The hydraulic power demand itself has a higher significance for the fuel consumption. In order to evaluate this effect, entire vehicle cycle have to be evaluated for their hydraulic power consumption. This will be done in chapter *5.2.1*.

5.1.2. Diesel high pressure pump performance analysis

A major difference between diesel and gasoline high pressure pumps remains in design for higher pressure levels. Even though, todays development and first serial approach targets "Diesel-like" rail pressure levels of 800bar to 1000bar, still rail pressure levels for gasoline systems are below 2000 bar and higher, for modern common rail diesel systems. Second major difference bases on the abilities by pressurized fuel type. This leads to difference in lubrication systems.

As the results for total efficiencies within chapter *4.1.3.* shows, total efficiency reaches roughly levels of 80% to 90% at 2000bar, depending on high pressure pump type, or has in best operation point levels of 85% to 95%. Anyhow, since total efficiency describes itself as product of all efficiencies, partwise analysis of each efficiency class become mandatory for power consumption optimization. Nevertheless, multiplication of volumetric efficiency with hydro-mechanical efficiency builds total efficiency as described in chapter *2.4.2.* Therefore, hydro-mechanical efficiency is in given situation [64]:

$$\eta_{hyd} = \frac{\eta_{tot}}{\eta_{vol}} \qquad (32)$$

η_{hyd}: hydro-mechanical efficiency; η_{tot}: total efficiency;
η_{vol}: volumetric efficiency;

Following given equation *(32)* including all calculation for volumetric and total efficiency as in chapter *2.4.2* including equation *(12)* and equation *(13),* especially highly pressurized condition reach hydro-mechanical efficiency levels of above 100%.

Values taken from Bosch CP4s1 as in chapter *4.1.3*			
Rail Pressure At 1600rpm pump speed	Volumetric efficiency	Hydro-Mechanical efficiency	Total Efficiency
400 bar	92,6 %	84,3 %	80,1 %
1000 bar	85,2 %	95,9 %	81,7 %
1600 bar	78,1 %	102,2 %	79,8 %
2000 bar	73,4 %	107,4 %	78,1 %

Table 20: Selected efficiency shares in geometrical bound efficiency calculation

As the pressure level increases, so also does hydro-mechanical efficiency. Within *Table 20* shown efficiencies of above 100% occur especially with coherent drop in volumetric efficiency. Thus, review of the volumetric evaluation method becomes mandatory. Since high pressure causes altering of density, the compression or bulk modulus for fuel needs to be included into calculation.

$$V_{bulk} = \frac{V_0 * \Delta p}{E} \qquad (33)$$

V_{bulk}: Bulk modulus corrected pump volume (displacement);
E: Bulk modulus of pure fuel; Δp: pressure difference during pressurization;
V_0: geometrical pump displacement

When considering the change in density by utilizing the fuel values given for diesel fuel between 1,6 GPa to 3,2 GPa as bulk modulus, mentioned in literature [70], volumetric efficiency at 2000bar increases to 74,7 % by using of equation *(33)*. As shown in chapter *2.4.1,* an solution is given by equation of Huang and O'Connel (see to *(10)* and *(11)*), which contains required parameter that are often not given for engineering evaluation. Different approach is in separation of fluid content and intruded air as void content. Therefore, the calculation approach calculates isotherm compression for fuel and polytope compressions for gas in each volume shares.

$$V_{cor} = R_{Fuel} * V_0 - \frac{V_0 * \Delta p}{E} + R_{Air} \frac{Vo}{\kappa \ln \frac{p_{rail}}{p_0}} \qquad (34)$$

V_{cor}: Corrected pump volume (displacement); R_{Fuel}: Ratio "pure" fuel;
E: Bulk modulus of pure fuel; Δp: pressure difference during pressurization;
V_0: geometrical pump displacement; R_{Air}: ratio "pure" air; κ: isentropic exponent;
$\frac{p_{rail}}{p_0}$: ratio of rail pressure to initial pressure during pressurization

Despite hydrocarbon gases, air is the most obvious solvent gas for fuel and builds a foundation for using equation *(34)*.
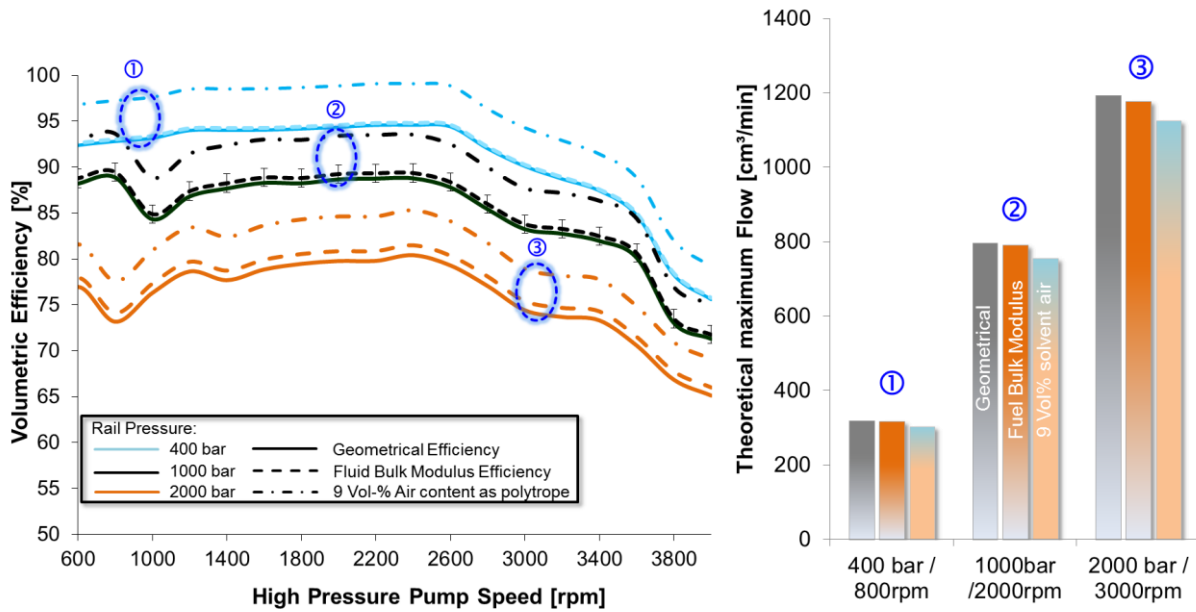
Figure 93: Impact of different approach in volumetric efficiency calculation

The difference in volumetric efficiency and its reflecting theoretical maximum pump flow shows impact when including solvent air into the analysis. The bulk modulus of pure fuel has an impact in range of 0,3% at 400bar rail pressure to 1,1% at 2000 bar rail pressure for selected operation condition (see *Figure 93*). Thus, also the volumetric efficiency mapping changes by calculation of the change in maximum theoretical pump delivery in same range, but too low to overcome 100%, listed in *Table 20,* listed exceeding hydro-mechanical efficiency.

By applying the fuel bulk modulus and solvent air calculation, values for theoretical volume reduce to a range of 6,2% at 400 bar and 7,7% at 2000 bar as representative for 9% solvent air. Within this value mentioned for petrochemical products for solvent air [27], volumetric efficiency does not reach 100% and reduces all hydro-mechanical efficiency below 100%. In terms of "handling", compared to the approach of Huang and o'Connels, wherein at least eight fluid properties have to be gathered, only two well-known properties are required.

As an "engineering approach" for petrochemicals products, the equation (34) builds the frame to analyze not "conventional" fuels, also novel fuels or unknown mixtures fuels can be analyzed deeper as shown in chapter *4.1.3.2* by application on OME fuel pressurizing high pressure pump. In current field of development, a major focus is the identification of alternative fuels. As one object of research, the differences between diesel and OME fuel and its application have high priority today, herein especially delivery differences to ensure rated power performance. Therefore, the difference in volumetric efficiency can be used as a maximum performance indication.
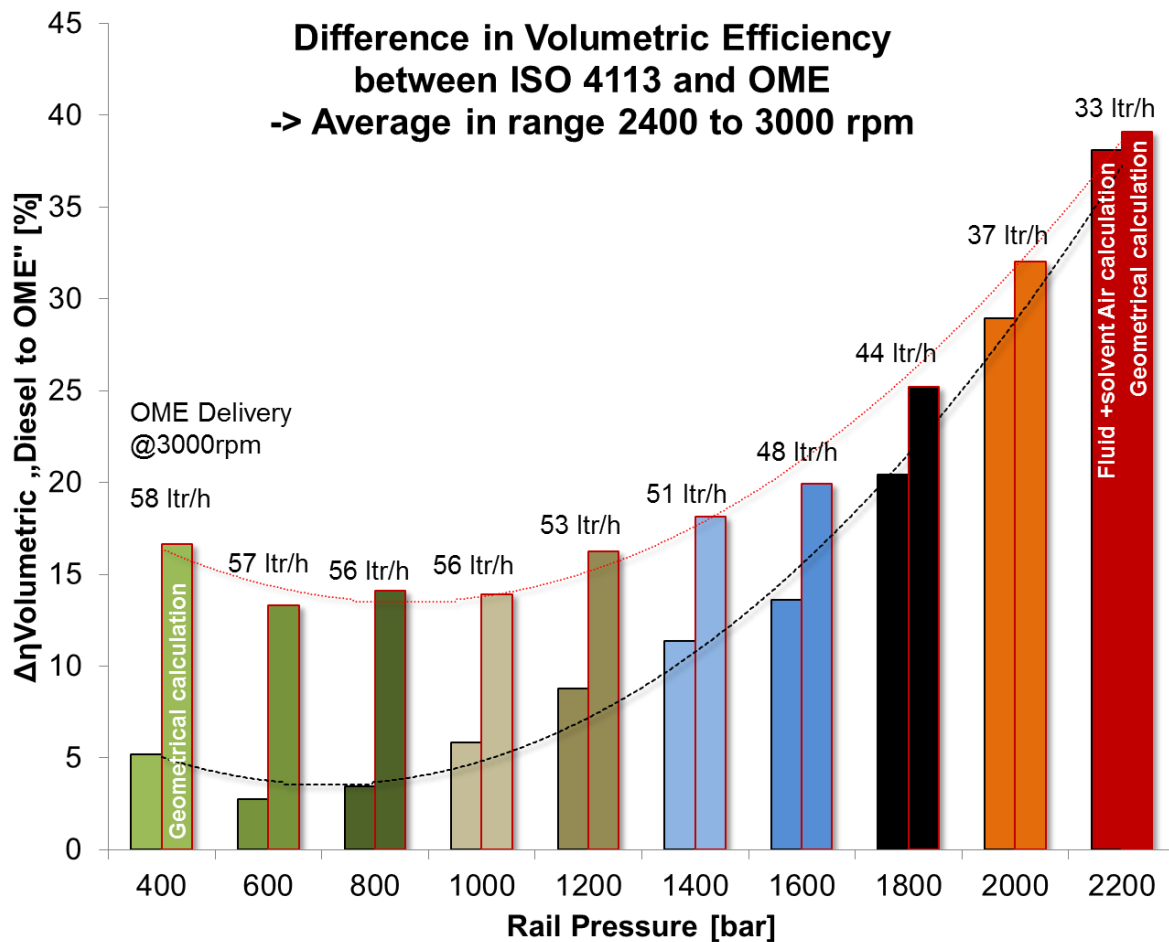
Figure 94: Volumetric efficiency difference of Continental DHP1 OME between Diesel and OME in respect to volumetric efficiency calculation modulus

As shown before in *Figure 93* geometrical based volumetric efficiency calculation and based on fluid bulk modulus and solvent air calculation differs up to 7.7% especially in high pressure levels. Analyzing the difference impact as well as absolute quantities by high pressure pump sample as visible in *Figure 94*, especially the high difference in fuel impact becomes obvious. While in respect to geometrical boundaries, flow reduces to minimum of 13 % and decreases to 39% for maximum capable pressure by this pump type of 2200 bar.

The appearing volumetric efficiencies and flow rates between 400 bar to 1000 bar can be assumed to be impacted by an altering DIV pre-control mapping for rail pressure stability. As referring to this assumption, to a high flow instability encountered in the mapping shown in *Figure 68*Figure 68: Volumetric efficiency impact by OME vs. ISO4113 diesel test fluid on Continental DHP1 OME and *Figure 69.* Whereas, the occurrence in 400 bar starting in range of 2400 rpm pump speed and remains until end of measurement range. In contrast, the difference in lower range between the theoretical volume flow of both fluids has a higher compensation and leads to lower difference in volumetric efficiency "estimation". Since the difference in calculated volumetric efficiency reduces to a lower bandwidth by a mathematical approach, a mandatory adaptation of a controller for alternative fuels becomes feasible. On increasing pressure levels, both calculation models converge, but still with a reduced difference by the shown mathematical approach.

Also, this results leads to the assumption to utilize for OME maximum pressure levels of 1600bar. A moderate displacement increase by ~20% between Diesel and OME can be utilized in production. In addition, by lower heat value of OME but higher density, an increased displacement of 34,2% is required. As detailed summation of 54,1% for total increased displacement, 34,2% is required to maintain engine power by fuel properties, 13,6% to encounter fuel compression abilities and 6,3% depend on increased leakage losses.

5.1.3. Commercial high pressure pump performance

As with diesel high pressure pumps for passenger vehicles, high pressure pumps for commercial applications are designed to reach rail pressures of 2000 bar and above. Herein, a difference to their "smaller brother" is the application in on- and off-road application and matching engine type. Especially the duty cycles of commercial engines differ from passenger vehicle duty: load collective of commercial application have higher grades than passenger. Therefore, the pumps for commercial application operate most of the time in close to full load operation. Fitting delivery layout as shown in *Figure 5* become a mandatory check for each engine, also over extended lifetime to meet customer expectations and nevertheless maintain functionality. Anyhow, also power consumption and high load area have significant influence, since every saved g/kWh on engine specific fuel consumption (=SFC) has impact on the so called "cost of ownership". But durability and the possibility to repair in field has a higher priority for customers.

The evaluation of a high pressure pump performance for commercial application differs from passenger application not only by size, but also by typical load collective and higher pressure levels. A commercial application targets in typical configuration higher performance targets in On- and Offroad application by higher demand on torque or power output then vehicle. As trucks run most of the times on highway, reaching speed levels heavily loaded close to legislation border, high load collectives in pressure ranges of above 1000 bar to maximum pressure capability in given system configuration have major priority for analysis. In case of HMC G-Engine Euro 6 maximum pressure levels reaches 1900 bar. As a first step in evaluation, a comparison of power demand between the two in chapter *4.1.1* shown pumps and their measurement results in chapter *4.1.4* provides first information.

Despite total efficiency levels between both shown version of Denso HP4 high pressure pump for G-Engine, also power consumption in each point differs from 106W up to 1988W for high points. In addition *Figure 95* illustrates power consumption range FIE system high pressure maximum power consumption of 13.320W. Anyhow, both pumps reach pressure and flow levels, but the required operation condition alter by pump modification in this particular point too much for fair comparison, but shall demonstrate potential improvement ranges. Also, the shown pump sample achieves its best performance shortly before a worn pump state. This state is for this experimental pump reached after 50 hours of run time. Thus, a second sample with same modification was utilized for the engine dyno tests.
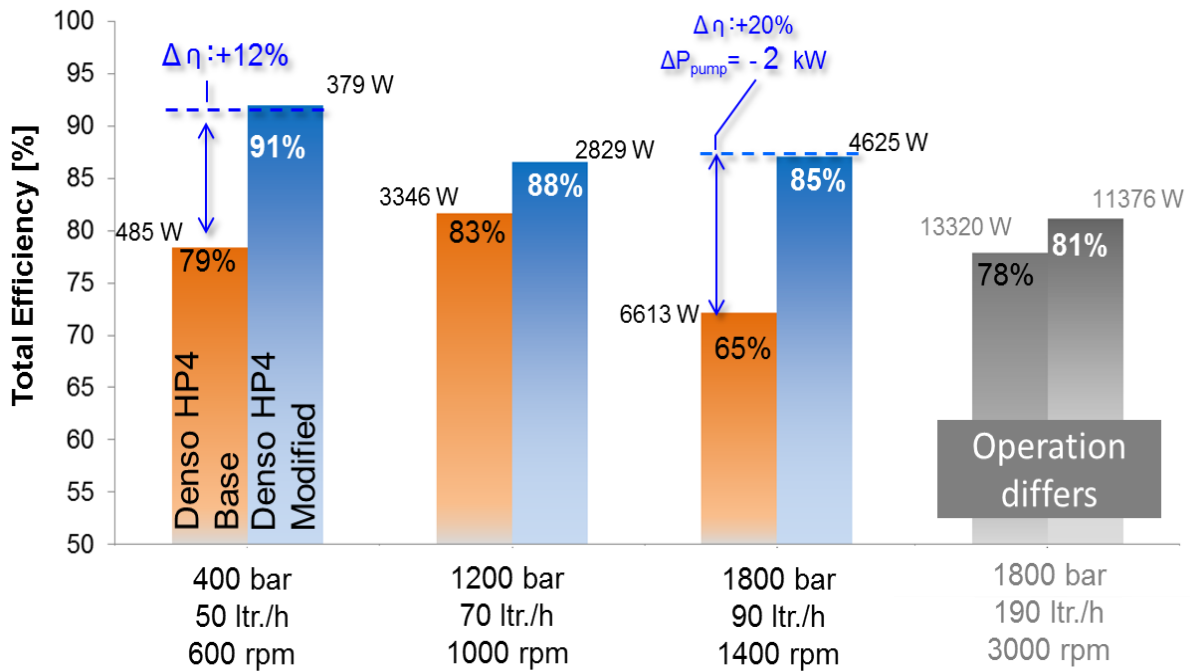
Figure 95: Denso HP4 performance impact on friction reduction after 50h run time vs. base G-Engine pump

Compared to engine operation states from test bench or engine calibration information, pump power consumption differs by state of operation to mapping tested condition. Since the nature of analysis intends to evaluate the pumps in any engine operation, engine operation points can be interpreted as unknown during measurement operation. Therefore, a matching of the measurement data to engine operation has been performed (see chapter *3.2* and chapter *3.5*).
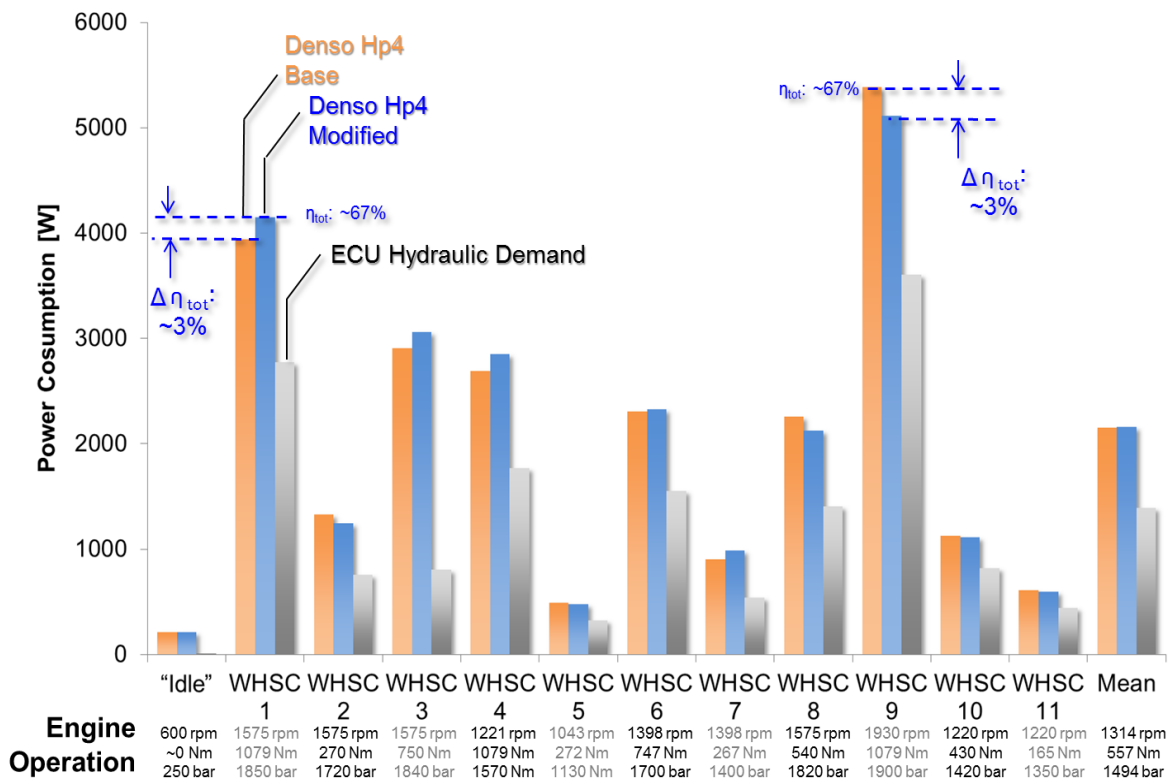
Figure 96: High pressure pump power consumption performance calculated in WHSC for HMG G-Engine in unranked weighting

In unranked analysis in *Figure 96* of high pressure pump power consumption, the mean result of "Base" Denso Hp4 and "Modified" Denso Hp4 are nearly equal, despite point by point analysis differs in range of total efficiency difference by 3% from one sample to another sample. Also "hydraulic demand" as ECU requests is listed within this chart. Herein given information shows impact by high pressure system total efficiency on power consumption itself. As detailed examples: while the mean power consumption in WHSC differs in range of 770 W, the power demand in operation points as "WHSC 9" differs up to 1785 W, while engine output at this point is 218 kW. As a result, the high pressure system losses at this specific point are 0.8% of engine output.

Duty cycles do not have equally distributed shares of run time of each specific condition, but have a changing run time share in each point. Therefore, the mean pump performance impact differs by each specific share.
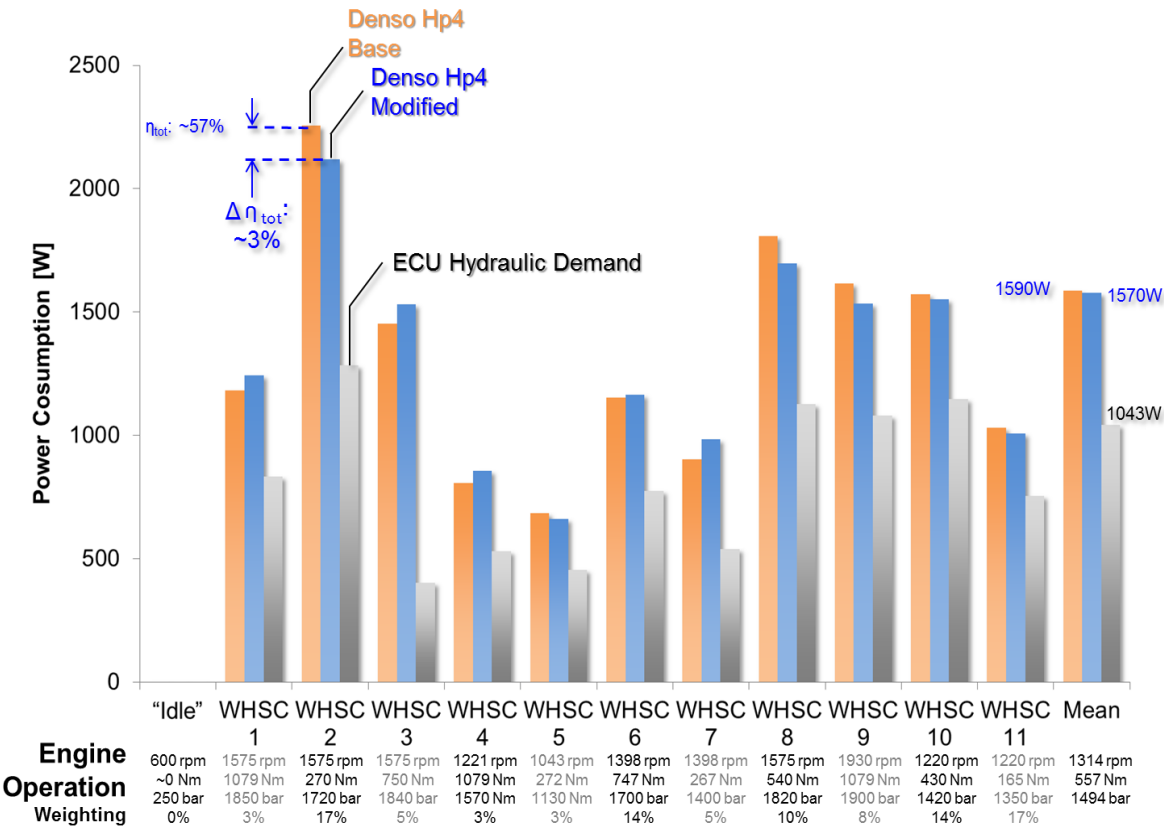
Figure 97: WHSC weighted high pressure pump power consumption performance calculated for HMG G-Engine

By multiplying all load points with their specific contribution to WHSC, especially lower load areas increase in significance, as increase of the bars relative "height" in *Figure 97* demonstrates. This represents share of typical operation point duration application by customers, such as high load acceleration and long static run time on highway. Herein WHSC 2 has grown in significance to the major share, while WHSC 9 as former highest load point reduces to medium range of significance. In average, the modified high pressure pump achieves a slight benefit of 20 W over total cycle. This information refers to WHSC for HMG G-Engine EURO6 (On-road application for vehicle with total weight of 7.5 tons).

In order to determine on engine fuel consumption, verification on exemplary points becomes mandatory to utilize for future analysis. Therefore, the following measurement is performed on

HMG G-6.3 Engine on engine test bench on HMC internal "four point" evaluation cycle. As mentioned, full cycle may suffer by experimental state of high pressure pump due to the fast worn bearing system, but shall represent a possibility for improvement. Herein included specific fuel consumption prediction based on serial configuration measurement and reduced flow as well as power consumption by changed high pressure pump.
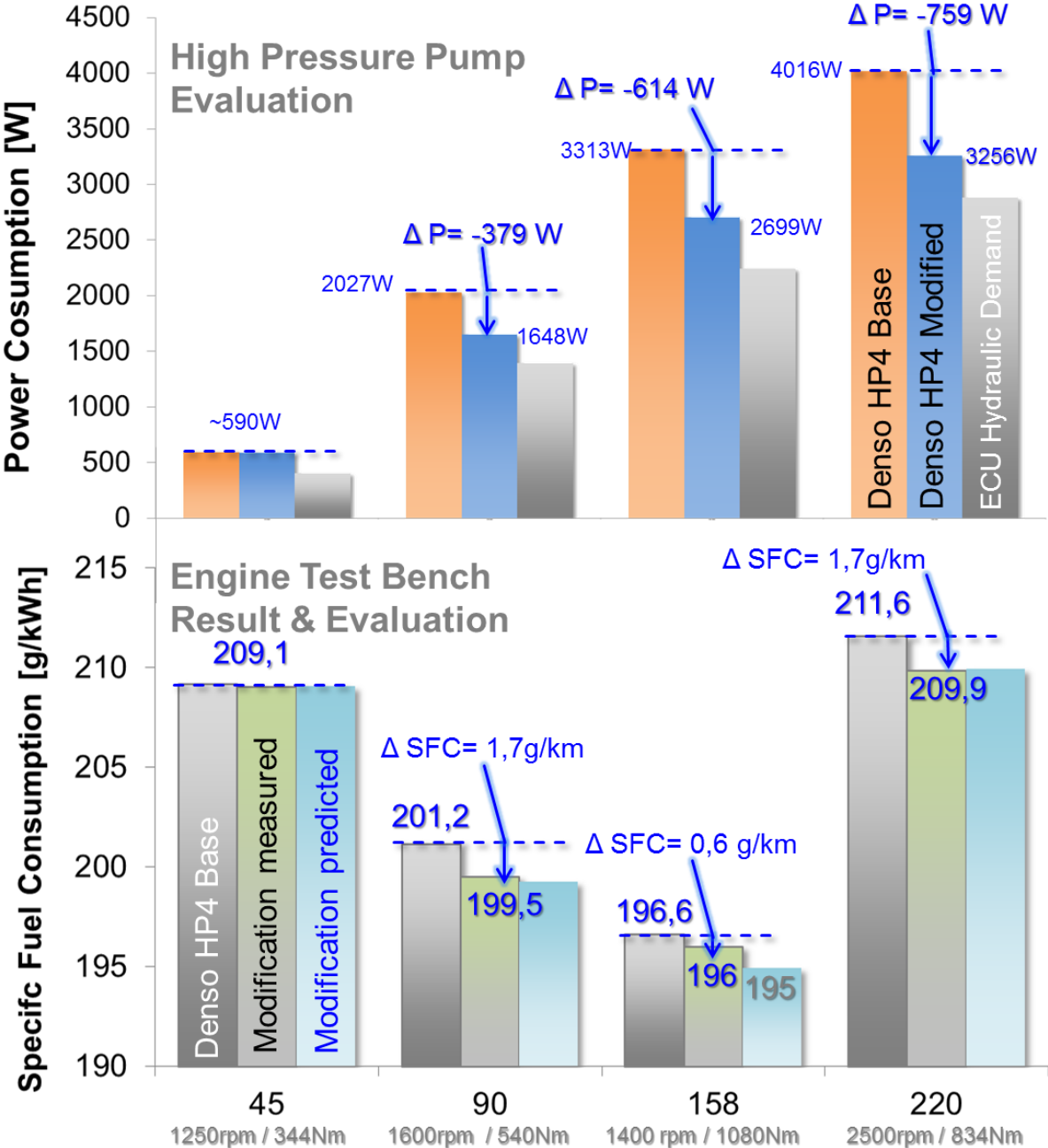
Figure 98: Engine test bench result with modified Denso HP4 on HMG G-Engine in relation to pump performance measurement and system state simulation

When analyzing in the same approach as the WHSC result (see *Figure 86),* high pressure pump demands needs to be calculated initially. In those particular cases, the power consumption differs between both high pressure pump variants from nearly 0 W to 759 W, which represents total efficiency benefit as shown in *Figure 95*. Anyhow, the lowest load point in duty cycle, with 45kW engine output, does not show benefit in high pressure system power

consumption. Neither does engine test bench measurement. Furthermore, prediction based on friction loss by high pressure pump shows in 3 of 4 cases matching results in difference below 15% relative to measured difference and below 0,1% on total SFC-scale. As exception, the operation point with 158kW engine output therefore differs from measurement to prediction by 1.0 g/kWh in specific fuel consumption in right direction. In addition, the engine test bench is not setup to run for quasi static hydraulic demand, as it cannot be for fuel consumption impact, but for static engine performance and torque levels. Since utilizing base measurement on engine for calculation, one major assumption for application of this approach is quasi static combustion. In other words, combustion effects cannot be covered. Thus, combustion simulation iteration becomes a possible extension to achieve higher prediction accuracy. Obvious case for such application is the evaluation of dynamic test cycles based on ECU data.

5.2. Total vehicle hydraulic demands based on simulation

Targeting a full high pressure pump analysis, a "first" layer of analysis is the effect on entire powertrain, including engine and total vehicle. Therefore, the determination of actual operation conditions within duty cycle builds the background for analysis to evaluate for accurate demands. Due to its highly dynamic and interacting nature, this step requires a 1D-Simulation. Therefore, to determine all required situations, a generic 1D FIE model can generate required front load. Generic system models mean in particular, that component and type wise difference are erased and only system function required are given and parametrized to fit for an application. In other words, this simulation does not deliver enough information to perform a combustion simulation by afterwards 3D-CFD, but is adequate to pre-layout systems before prototyping and to analyze upcoming required precautions. Detailed description of this generic simulation approach is shown in chapter *3.6.1.*

5.2.1. Gasoline vehicle hydraulic demand calculation

One major driver for FIE demands remains in its physical requirements on hydraulics demand. As in chapter *2.4* described, several relevant losses have to be fulfilled in order to have a functional system. Most obvious, beside injected quantity itself, is injector leakage. In same matter as rail pressure control direct leakage or pressure wave impacts, such losses are a system and situation specific.

Anyhow, as background information in chapter *2.2.3* shows, the typical utilized direct acting gasoline injector does not contain servo circuit. As Figure 99 shows, a leakage value cannot be assumed.

The content of chapter *3.6,* which also concludes the shown *Figure 99*, explains the principle of generic models for injector and their focus. In respect to this and the GDI high pressure pump function, such as rail pressure control via digital inlet valve (=DIV), functional leakages, such as from servo-actuator and rail pressure control, can be ignored for state of the art GDI systems. As last remaining simulative item, hydraulic pressure waves inside common rail remains as an energy demanding effect. Also in this case exception can be made: since rail pressure controller without leakage would lead to increasing pressure levels by pumping high amplitude, following pumping event would lead to reduced pump flow. Therefore, high pressure pump fuel flow can be assumed as in mean constant. This has to be assumed anyway by

measurement mode of high pressure pump via component test bench and Coriolis mass flow meter as described in chapter *3.1.*
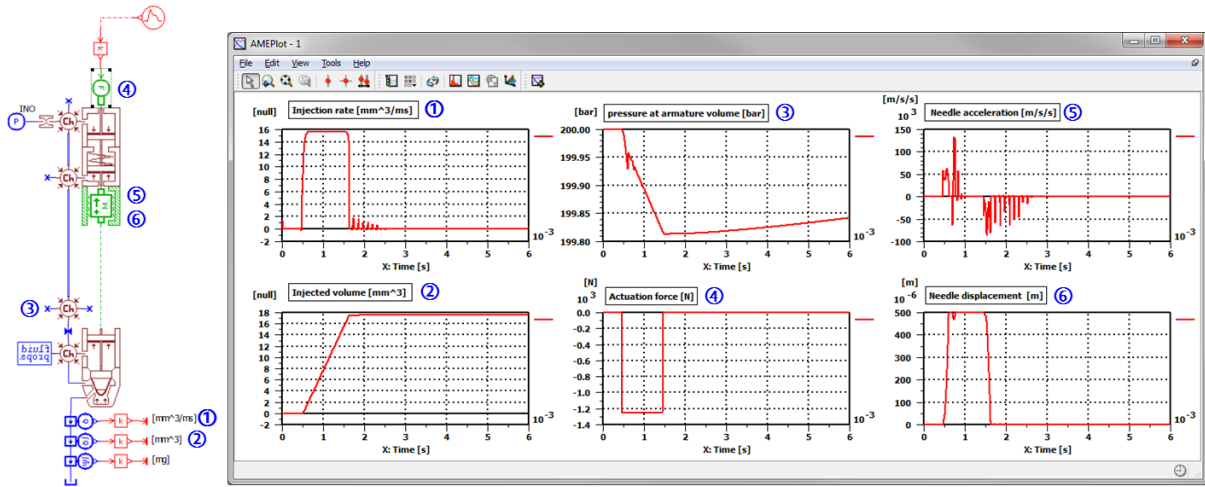
Figure 99: Example simulation results of generic injection model by AmeSim

In order to achieve a proper close up, known calibration data or (in best way) vehicle measurement serve as required background. Hydraulic power demand then in principle according to equation (4)

$$P_{hyd\_total} = \left[\frac{\dot{m}_{total}}{\rho_{Fuel}}\left(p_{supply} - p_{tank}\right)\right]$$
$$+ \left[\frac{\dot{m}_{Fuel} + \dot{m}_{Injector\_leak} + \dot{m}_{Rail\_control}}{\rho_{Fuel}}\left(p_{rail} - p_{supply}\right)\right]$$

(35)

P_{hyd_total}: entire FIE hydraulic power demand; p_{supply}: supply system pressure;
$\dot{m}_{total}$: entire FIE fuel mass flow; p_{tank}: atmosphere pressure in fuel tank; ρ_{Fuel}: fuel density;
$\dot{m}_{Pump\_leak}$: fuel mass flow for high pump leak and coolant;
$\dot{m}_{Injector\_leak}$: fuel mass flow for injector servo circuit actuation;
$\dot{m}_{Rail\_control}$: fuel mass flow for rail pressure correction leakage;

Following equations from chapter *2.4*, also change in density has to be reviewed for high pressure system of the GDI system, as in equation (9).

$$P_{Pump\_comp} = \dot{V} * \left(p_{rail} - p_{supply}\right) - \frac{\dot{V}}{E} * \left(p_{rail} - p_{supply}\right)$$

(36)

P_{Pump_comp}:Compression corrected hydraulic power demand; $\dot{V}$: geometrical volume flow;
E: elastic modulus;

In case of known (or measured) frontload data from ECU, a spreadsheet software, such as Microsoft Excel or IMC Famos, serves well for hydraulic power calculation. For other cases, a cycle simulation as front load data is required. For illustration and as entry in evaluation of cycle data, the ECU monitors basic data within a test cycle to calculate hydraulic power demand.

Major parameters for analysis within shown *Figure 100* are the mean values for fuel flow – or fuel demand- rail pressure, engine speed and resulting value for hydraulic power consumption. For overview purpose, selected values for NEDC show the spreading of hydraulic power

116

demand. While a spreading from below 10 W to values up to 135W are visible, the average over total cycle remains with 19,4 W in low range. Rail pressure controller instability has also a comparably low effect in this application of 200bar GDI system effect. In particular, average rail pressure deviation from target to measure value as detected by ECU sums up to 0,87 bar higher rail pressure as target, which is 1,4% of average rail pressure, while over total cycle maximum measured deviation appears in range of 25,7 (at this point target of ~35bar, without injection) higher pressure to - 6,3 bar (at target of ~82 bar) lower rail pressure as target.
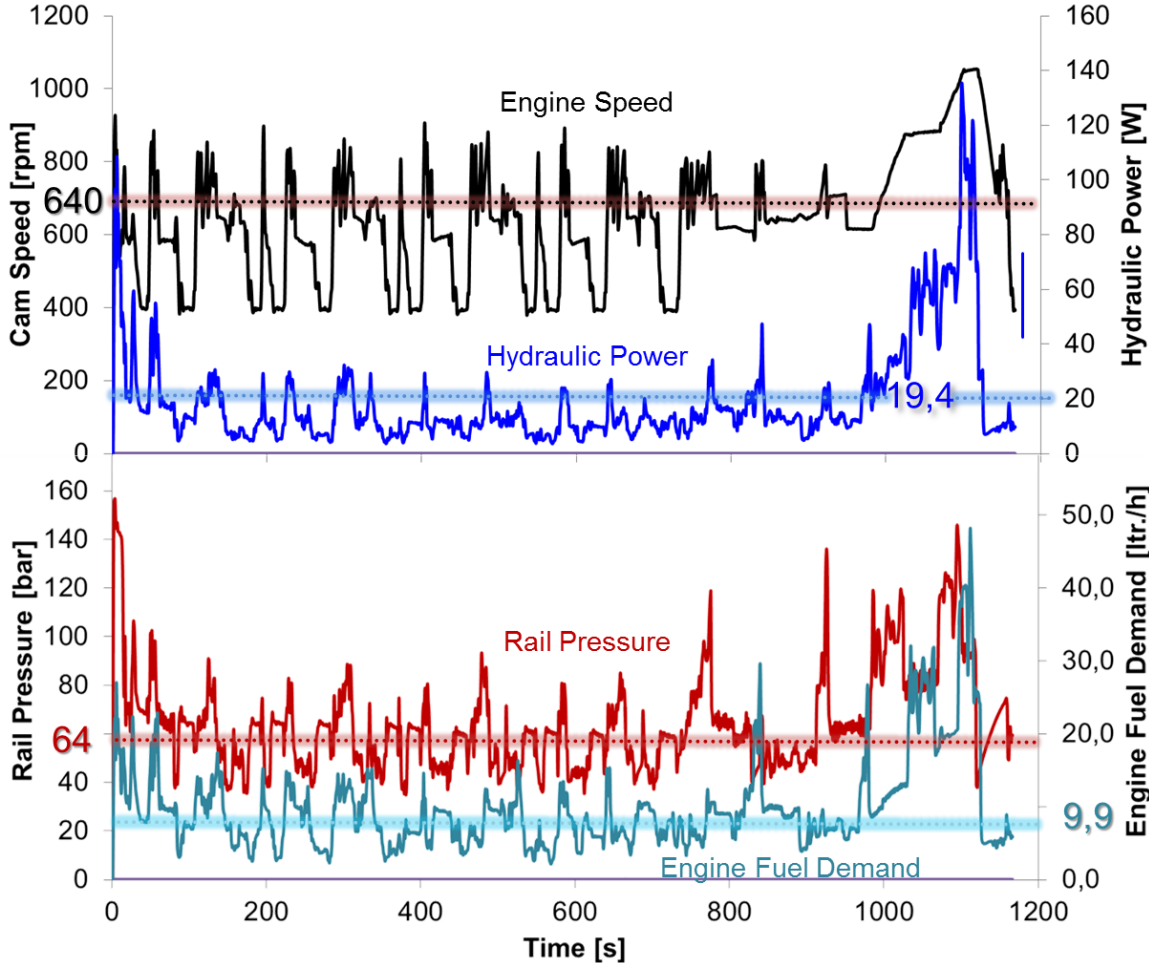
Figure 100: Hydraulic power consumption based on engine control unit monitored data of high pressure fuel injection equipment in KIA Stinger 2.0TGDI driven NEDC

Reviewing hydraulic power consumption and its major areas of high demands, two areas reach higher consumption levels of 80 Watt and higher: at engine start, whereas rail pressure target values reach also levels above 100bar, and during highway mode of NEDC, whereas vehicle speed reaches 100kph and higher. Both cases of higher power consumption have comparably small contribution to the total power consumption levels, due to small time range of high power demand (20 seconds of in total 1200 seconds above 90 W).

As a result, major areas for evaluating hydraulic data of the vehicle separately from idle range in steps of 30 kph, 50 kph, 70 kph, 100kph and 120 kph. Following simulative results show specific impact on mentioned engine load stages.

1D Simulation Results of Generic Gasoline Direct Injection System									
Engine Data & Calibration						Simulation			
Engine Operation Point	Engine Speed [rpm]	Engine Torque [Nm]	Injection Pattern Pilot2-Pilot1-Main-Post [mg/strk.]	Rail Pressure [bar]	Injected Quantity [mm³/cycle.]	Injector Leakage [mm³/strk.]	Control Leakage [mm³/strk.]		Rail Pressure During pumping [bar]
"Idle"	800	0,1	7	40	33,1				41
Max Torque	3000	365	82	180	325,2				192
Rated Power	5600	320	72	200	303,9				211
„30 kph"	1000	50	11	45	43,2				49
„50 kph"	1300	62	14	45	48,7	Not given by technical appraoch			54
„70 kph"	1280	89	20	65	78,8				71
„100 kph"	1900	116	26	82	106,8				90
„120 kph"	2090	138	31	94	126				103
„50-70"	1230	142	32	63	126				72
„70-100"	1750	187	42	82	166,8				92
„100-120"	2100	205	46	126	180,8				149

Table 21: Simulated hydraulic demands of gasoline direct injection system

By system architecture, GDI systems do not have leakage for control or injector actuation, therefore these are not represented in *Table 21.* Despite this loss, a GDI high pressure pump's pressure deviation appears. The injection itself profits by closed-loop quantity control due to lambda control and does not, in case of proper calibration, impact as loss in this particular analysis modulus. Herein, the physical approaching pressure within the high pressure pump chamber increases depending on injected volume and engine speed in higher level as targeted. This higher demand is required to realize calibrated condition for combustion. Since this system react sensitively on pressurization, small deviations in digital inlet valve control delivery angle changes pressure within the rail significantly.
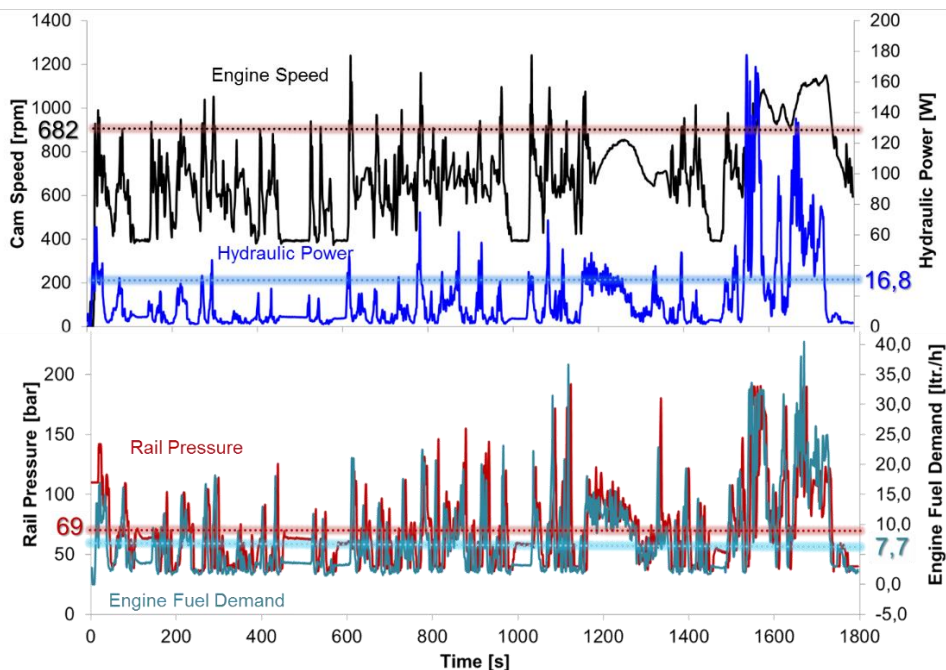
Figure 101: Hydraulic demand in WLTP cycle by GDI high pressure system of Kia Stinger 2.0TGDI

118

Anyhow, the acceleration phase especially shows increased hydraulic demand. These particular areas require higher flow and pressure for establishing minimum requirement of dynamic. As a more dynamic cycle, WLTP cycle test impacts on GDI system.

Referring to NEDC (*Figure 91*), major and averaged values do not differ much. Higher requested dynamic behavior leads to higher rail pressure, as shown in *Figure 101*, in the same time engine speed and therefore camshaft speed decrease. As a result, hydraulic power demand within WLTP cycles is slightly reduced by especially lower fuel flow demand. Comparing maximum achieved values, especially maximum achieved values reach higher levels as in NEDC, leading to a wider spreading of encountered states. Thus, high load request impact the total result. The highest total achieved hydraulic demand increases therefore from 135W in NEDC to 177W, while also maximum pressure levels increase from 157 bar to 190 bar. By this higher spreading, calibration variance will lead to stronger impact than for NEDC, with increasing tendency for larger vehicles with smaller engines. Anyhow, in this particular reviewed case, difference between NEDC and WLTP are comparably small. Not only for FIE but the entire vehicle, as the similarity of both results as illustrated in *Figure 88.*

5.2.2. Diesel vehicle hydraulic power demand simulation

In same way as for GDI systems, also diesel FIE hydraulic demand calculation can be applied. State of the art common rail diesel application contribute higher system complexity by servo hydraulics, two-governor rail pressure control and higher system pressures (see chapter *2.2.*). In addition, diesel fuel quality and mixture effects have higher contribution on FIE performance than gasoline fuel, as explained in chapter *2.3.* For achieving reliable front load data for analysis, not only measurement becomes mandatory, also simulation needs to be performed. As illustrative support, the following figure are based on described 1D simulation as described in chapter *3.6.3.*
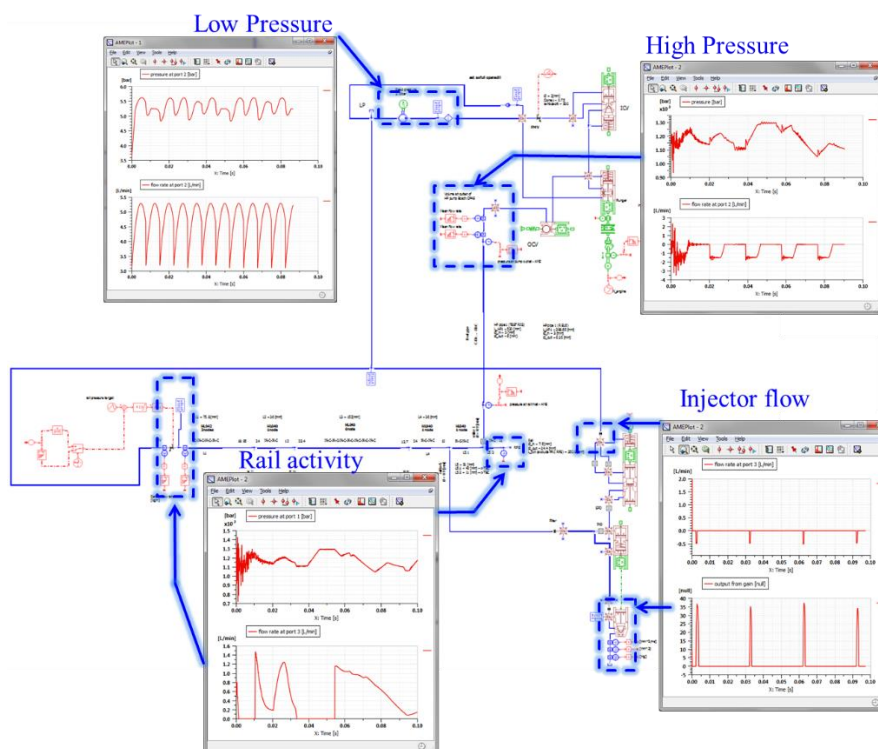
Figure 102: Illustration of 1D simulation provided front load data for hydraulic demand calculation

All major and minor hydraulic impacts become accessible to deeply understand specific interaction. Thus, the analysis position shown in *Figure 102* does not represent all evaluated simulated items, but those with at least significant impact- depending on duty cycle. In particular, this figure shall serve as illustrative overview. For analysis purpose, selected engine duty points based on HMC R-Engine calibration have been simulated in total system setup.

1D Simulation Results of Generic Diesel FIE											
Engine Data & Calibration					Simulation				Hydraulic flow share		
Engine Operation Point	Engine Speed [rpm]	Engine Torque [Nm]	Injection Pattern Pilot2-Pilot1-Main-Post [mg/strk.]	Rail Pressure [bar]	Injected Quantity [mm³/cycle.]	Injector Leakage [mm³/strk.]	Control Leakage [mm³/strk.]	Rail Pressure During pumping [bar]	Injection [%]	Leakage [%]	Control [%]
"Idle"	800	0.1	1,5 – 1,5 - 5	300	23,9	12,8	55,5	380	26	14	60
Max Torque	2000	410	0 – 1,5 – 72,9	1350	284,1	35,6	1	1364	89	11	<1
Rated Power	3750	347	0 - 1,5 - 65,4	1900	258,9	33,7	0	1950	88	12	0
„30 kph"	2000		1,5 – 1,5 – 3,9	640	25,1	14,3	225,4	598	10	5	85
„50 kph"	2000		1,5 - 2 - 5,9	660	35,9	16,4	201,1	592	14	7	79
„70 kph"	1750		0 – 1,5 - 10	630	43,9	14,7	201,5	567	17	6	77
„100 kph"	2000		0-3- 13,5	840	66,1	17,7	161,4	774	27	7	66
„120 kph"	2400		0 – 4,4- 16,8	1100	90,2	20,3	0	1147	82	18	0

Table 22: Simulated hydraulic demands based on R-Eng ECU monitoring of HMC EL Vehicle

Since drive cycles typically show highly dynamic behavior, especially when monitored during real road driving, the determination identical points to compare conditions or even microscopic "results" becomes hard and may even only be possible by usage of a engine test bench. But also engine test bench measurement has demerits of not exact mechanical interaction, leading to higher deviation from entire vehicle results especially in low load conditions. In same manner as before on GDI vehicles, NEDC builds still a good background for comparison due to long stabilization time. Results listed in *Table 22* show engine states monitored in stabilized condition and their specific results in hydraulic condition as simulated by 1D-Simulation (described in chapter *3.6.3.*). For illustration purpose, the simulation results show final values for mentioned area over one entire engine cycle (720° Crankshaft). All simulation and control parameters are setup for realizing desired quantity at desired rail pressure with lowest high pressure pump inlet flow.

The shares within each condition give two directions for hydraulic demand calculation. The injector leakage (even though here shown simulation contains dynamic leakage and no static leakage) usually has close range of ~ 12.5mm³/ cycle to ~ 20mm³/ cycle. By generic nature of mentioned simulation, values from real system application will differ but as results of chapter *4.3.2.* show, effects in reality lead into similar direction. Also the rail pressure controller "leakage" may have significant impact on hydraulic demands and increase in some operation points to the highest flow consumer during one cycle. Within this two controller concept utilization, the high pressure pump inlet flow to the high pressure head reduces in order to a lowered pressurized fuel flow. Anyhow below certain pressurized flow levels, final pressurized amount has a borderline controllability. Therefore, inlet control opens in higher flow direction to pressurize small amount above target (in ideal case) to have to minimize hydraulic losses. With an increasing pressure levels and flow demand by combustion, parasitic losses for rail pressure control reduce until reaching no loss. Anyhow, compared to high pressure pumps maximum flow capacity, above mentioned values are in lower range. The associated simulated

high pressure pump has over monitored time frame total capacity of ~800mm³/cycle, whereas above mentioned range at ~250 mm³/ cycle flow demands.

The rail pressure during pumping event describes the actual pressure at the moment of pressurization activity in the high pressure pump chamber. The high pressure system contains an accumulator, leading to dynamic reaction as pressure waves. By nature of high pressure systems, deviations in this particular range may lead to a high power consumption at comparably low flow. As in idle condition: pressure levels inside high pressure rail deviate from calibration given target by lowest demand but required rail pressure stability. As results, the high pressure pump does not encounter pressure of lower than 300 bar (as target) but 80 bar higher (+26%).

The last two mentioned points depend in technical approach strongly on utilized control method and calibration. Therefore, low flow controllability for high flow demanding systems may lead to high parasitic losses or require additional technical effort. Digital inlet valves as different flow control approach pressurizes based on the radial height of plunger and reach therefore higher control accuracy. On the other hand, such systems require a higher calibration effort as the number of parametric labels with ECU's software show, and have a higher sensitivity on aging, due to increased sensitivity on angular position deviation by engine mechanics.

Feasible impact in direct hydraulic demands, meaning combustion fuel flow and target rail pressure, as well as physical appearing hydraulic demands illustrates next figure based on total NEDC and calculated hydraulic demand. Again, the NEDC cycle data are selected for illustration purpose.

As in *Table 22* shown for selected points in engine duty, major difference of pressurized flow to ECU calculated fuel demands (and also external measured fuel consumption) leads to higher hydraulic power demands. Within *Figure 103* shown values of hydraulic power as monitored by ECU allows vs. simulated data differ in hydraulic power consumption when comparing stabilized operation points from 43 W to 116 W. Compared to total engine power demands, the portion of hydraulic losses towards engine side still remains on minor scale. By average engine power consumption, based on fuel consumption measurement, the vehicles engine receives an input of ~48 kW (based on fuels heat value) and average output power of 7kW. The calculated difference of 192W is a portion of 0,5% of total engine losses. Anyhow, on today's hunt for lower CO_2 emission, also those losses are more in focus for optimization. In addition, passenger diesel applications are in smaller range of diesel engine, whereas larger engines, such as commercial heavy duty on- and off-road application, demand higher fuel flows.
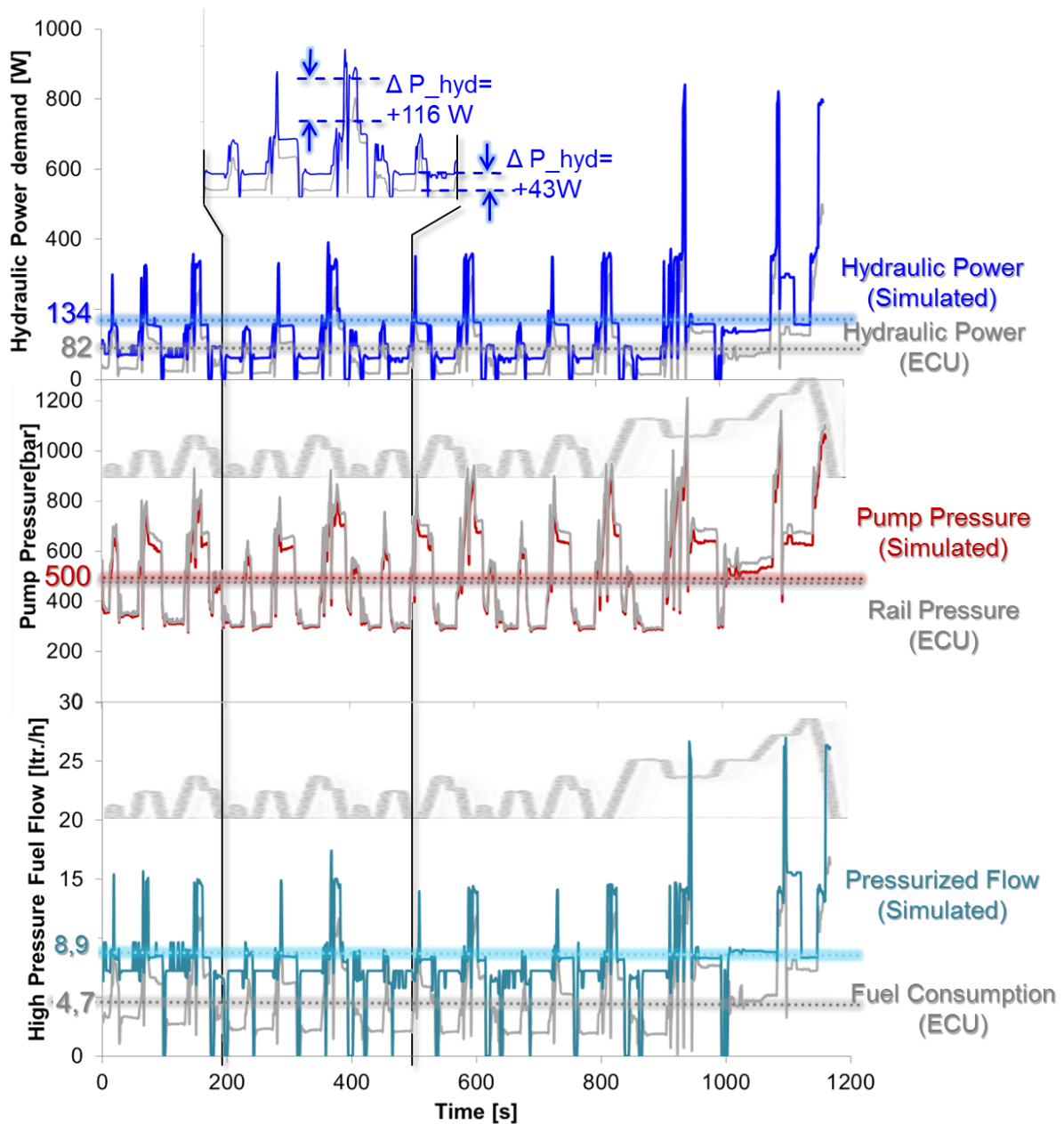
Figure 103: ECU monitored hydraulic demand(s) vs.simulation based high pressure flow determination

With available information on actual hydraulic system state in each operation point of hydraulic system, a calculation of high pressure system power demand based on high pressure pump mechanics power consumption is possible. The calculation of conditions in each point follows the method according to chapter *3.3*. This allows furthermore to evaluate impact on total vehicle fuel consumption during cycle. As described in chapter *3.5* selected pump samples Bosch CP4s1 and HEFP Gen.2 shall be compared in terms of impact on vehicle performance.
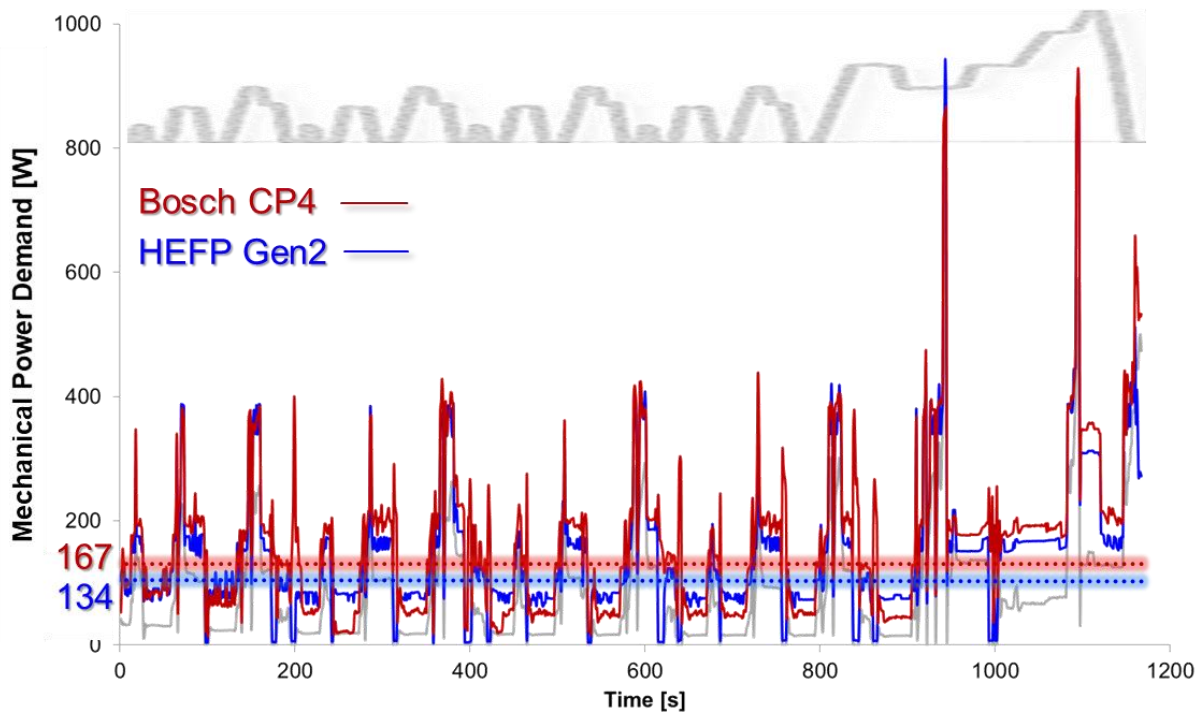
Figure 104: Power consumption of high pressure pump on Hyundai iX35 (EL) equipped with R-Engine in NEDC

The power consumption in NEDC by high pressure pump alters herein especially in high pressure pumps efficiency. In direct comparison of Bosch CP4s1 and HEFP Gen.2 (see *Figure 104*), which differs in bearing concept as well as hydraulic concept, average power consumption shows a benefit of 33W over total cycle. Difference in power consumption in detail does not only interact by total efficiency, but as a function of total efficiency at state of high pressure pump delivery. Therefore, the changed bearing system allows a wider range of high total efficiency than bearings of Bosch CP4s1 (see *Figure 66*), leading to higher comparable benefit with lower load and flow condition, which has major share in NEDC as averaged simulated flow within high pressure system is 8.9 ltr./h. Since hydraulic demand remains low, also total power consumption remains low. Small peaks in higher demands also leads to an increasing gap between both pump types, even though their relative difference decreases.
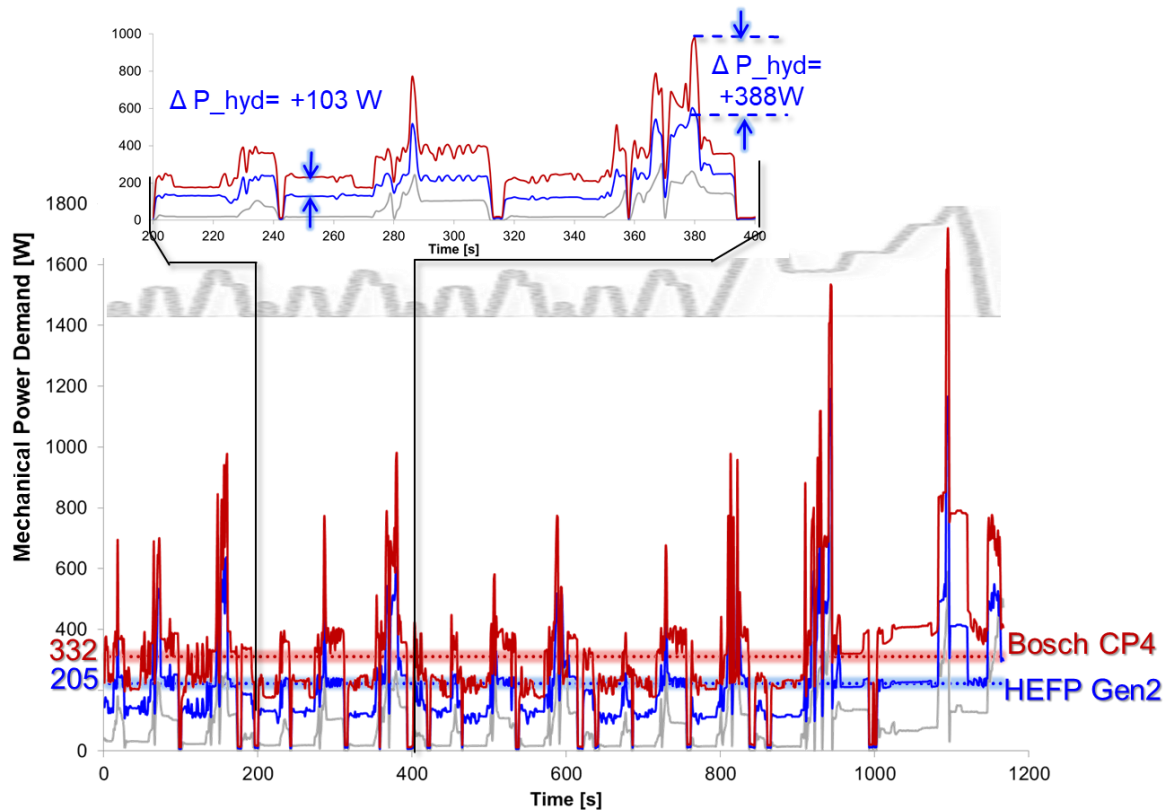
Figure 105: Mechanical power consumption of high pressure pump with chain embedded lossesby Bosch CP4s1 vs. HEFP Gen.2

As demonstrated in this particular case, also the high impact by high pressure pump on engine mechanics itself. In particular, *Figure 79* in comparison to *Figure 81* states differences between Bosch CP4s1 to HEFP Gen.2 in range of 0,5 Nm to 1,5 Nm.

Within these boundaries, mechanical power consumption of the high pressure system increases. In addition, the frictional impact by the high pressure pump increases the losses at each sample. Thus, the difference between Bosch CP4s1 and HEFP Gen.2 increase, as shown in *Figure 105*. This difference varies in shown illustrative detailed range from 103 W for idle operation up to 388 W for short time during an acceleration to ~50 kph vehicle speed. In summation over a total cycle, the average power consumption in engine mechanical integration increases from 71 W to 205 W for the HEFP Gen.2 and 165 W to 332 W for the Bosch CP4s1 sample.

In this perspective the mechanical power demand reaches high levels for an engine auxiliary, but compared to the engines power output, the demand still remains in a low range. For a detailed impact of fuel consumption share in given configuration, the fuel consumption determination requires a base configuration including SFC consumption measurement. Since the HMC R-Engine utilizes the Bosch CP4s1 high pressure pump measured and analyzed before, a fuel consumption prediction by HEFP Gen.2 high pressure pump becomes possible.
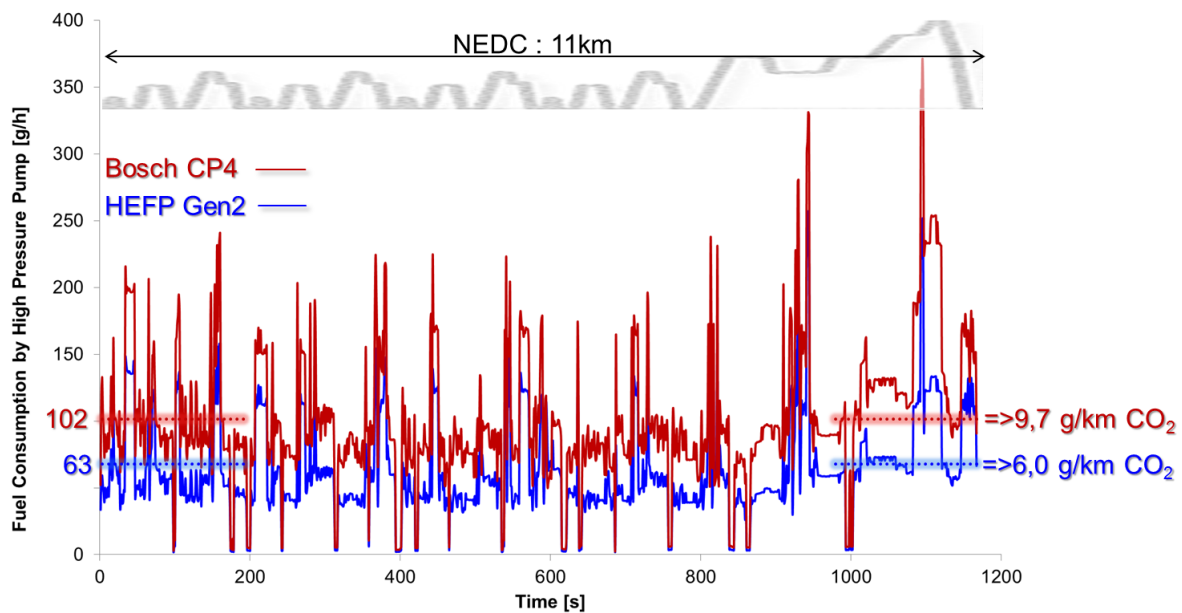
Figure 106: Fuel consumption of Bosch CP4 vs. HEFP gen2 in NEDC referring to HMC R-Engine data and following CO₂ Emission

When analyzing the power consumption of the high pressure system to an engine specific fuel consumption, also herein covered effects show a significant impact on the engine performance: a calculated difference of 3.7 g/km in CO_2 emission by a changed high pressure pump, as above shown Figure 106 shows. Remarkable is the increasing impact of flow and pressure. In relation, especially the low flow area reaches high impact on engine losses and therefore fuel consumption. The final calculated difference and mentioned behavior fit nearly perfectly into illustrated results from *Figure 90* and engine details from *Figure 91.*

The last direct impact, which has to be analyzed, remains in FIE supply system itself. Whereas high flow demands have to be covered by low pressure supply pump to serve not only high pressure system, but also to cool the high pressure pump and maintain supply pressure to fill high pressure head. Therefore, a system review becomes mandatory by the specific component selection and usage. As by major OEM's in serial production, most common used configuration utilizes an approach to drive low pressure supply pump in constant delivery. As noted in chapter *4.3.1*, the particular use case has a nearly constant power consumption of 153 W electrical power for a typical Bosch CP4s1 configuration. In this calculation electrical is assumed as draining of vehicle battery. Recharging by alternator and its specific losses are not included in this review.

As the HEFP Gen.2 high pressure pump allows regulating pressurized volume via low pressure system pressure control without damaging high pressure mechanics, analysis of low pressure system power demand has to be executed in a way to determine all states during engine operation. In a full vehicle setup for serial production, a pressure sensor inside low pressure line would most probably be skipped to reduce later product cost. In this case, the pressure control therefore receives its feedback from the rail pressure sensor monitored value, compared to a calibrated set value. This represents the setup of *Figure 90*. As visualization, an overview on hydraulic power in low pressure line and respective low pressure system power demand, has to be applied.
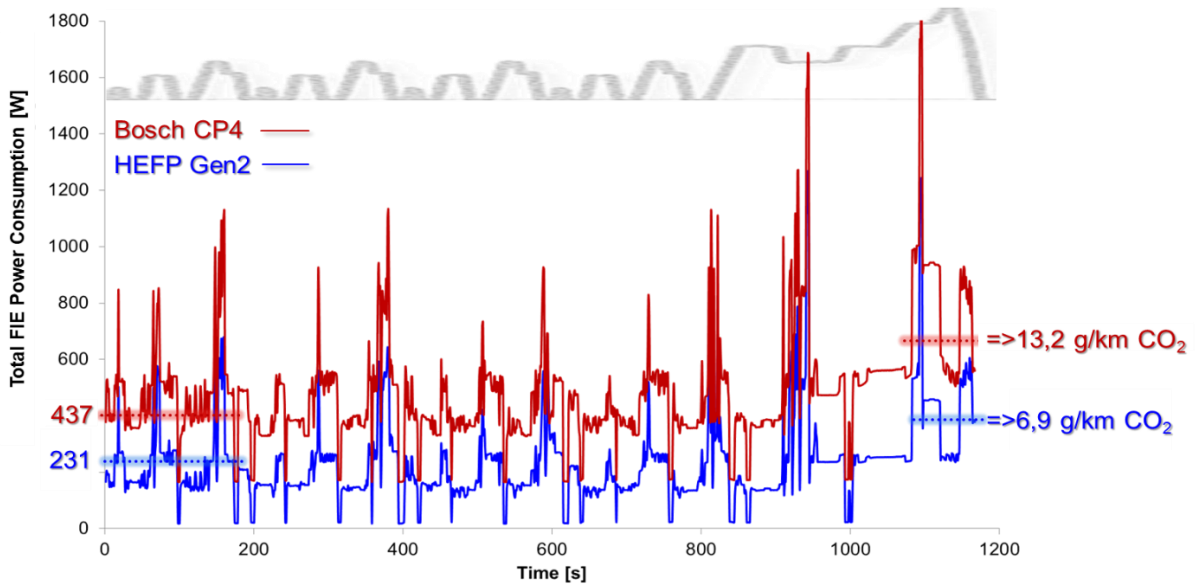
Figure 107: Total FIE power consumption of Bosch CP4s1 serial production vs HEFP Gen.2 with low pressure system adoption in NEDC cycle

With the low pressure system adopting to the coolant pressure and flow demands of HEFP Gen2, high pressure pump shows a lowered increase in power consumption over total NEDC as shown in *Figure 107*. The assumption for the Bosch CP4s1 supply demand utilizes a constant supply system, as it is installed on iX35 and also Kia Sportage test vehicle. This leads to difference between both setups in total to 6,3g/km CO_2 or 206W. The top value of 486W for Bosch CP4s1 reflects the entire loss for the engine including integration, which also includes losses in timing chain drive. Compared to the ECU demand, total efficiency of above mentioned wattage reaches 15,6% for Bosch CP4s1 and 28,0% for HEFP Gen.2. This indicates given room for further improvements.

In conclusion, a double check by measurement becomes mandatory. *Figure 90* in particular demonstrates such analysis. Therefore, a comparison of shown analyzed data on entire vehicle performance and its measurement is the next logical step.
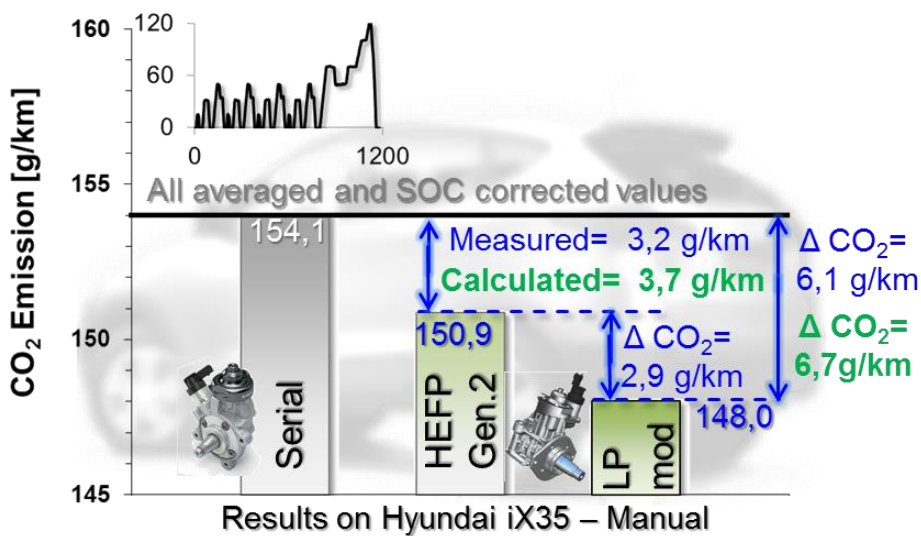
Figure 108: Comparison of calculated CO_2 impact vs. measured CO_2 impact in entire vehicle on chasses dyno

126

Although the measured values show comparably high impact on total vehicle at first glance, also mathematical approach combined with component measurement and FIE state simulation results in close range, as visible in *Figure 108.* By having the possibility to calculate states in each operation point, a system optimization or detailed impact calculation become feasible. In particular, this evaluation respects also mechanical and interaction performance and hydraulic performance as well. Thus, as shown by total efficiency, also mechanical and controller setup leads in summation to measurable power consumption and therefore fuel consumption.

5.3. Fuel properties' impact on engine consumption performance

Not only the system architecture and calibration strategy defines hydraulic losses of the high pressure system, but also fluid properties have influence. Since the density defines volume of the fuel flow, the timing chain drive losses may be seen as constant for this evaluation. Today's variety of fuel types or country specific fuel qualities rises up to a major concern for functionality items, as described in chapter *2.3.*. Anyhow, fuel consumption impact constitutes a secondary item for analysis: due to focus on customer satisfaction in terms of range or cost on one hand, as well as engine and mechanical layout during design phase on the other hand.

5.3.1. Fuel properties impact on GDI fuel injection equipment power consumption

When analyzing "classical" (fossil) fuels and their quality mix as shown in *Figure 29*, parameters are given which contribute to hydraulic boundaries and demands. With the given results of *Figure 101*, the impact on state of the art gasoline systems is expected to be low. As example for a high difference, a calculation of utilizing diesel fuel instead of gasoline results in altering power consumption of 34,9 Wh, while total base GDI system demands 35,1 Wh in average. The given scenario has in today's possible technological approaches has no fiel of application, but shall demonstrate the range of expectable impact.

Parameter	Gasoline (E5)	LPG [27]	DMC [22]	Ethanol [26]
Density [kg/m³]	747,5	540	1079	789,3
Kinematic Viscosity [mm²/s]	0,7 @20°C	0,4 @20°C	0.625 @40°C	1,5 @20°C
Heat Value [MJ/kg]	43,6	46	22,4	26,8
Pressurization Loss at 200bar	3,7%	0,9%	4,9%	6,4 %
Total System Efficiency (with ideal low pressure pump)	44,5%	65,7%	74,7% WLTP critical	74,2% WLTP critical
Power Consumption [W]	35	34	36	37

Table 23: Impact by alternative gasoline based fuels on FIE power consumption

To complete this frame with gasoline application, the *Table 23* lists expected power consumption impact. Background fuel quality and properties are listed in chapter *2.3.*

When considering the target of a future CO_2 reduction, alternative fuels also gain higher importance. Thus, the impact of alternative fuel properties moves into focus of ongoing

research and development activities. As such alternative fuel often require a combustion optimization research for optimal emission quality, the further listed evaluation of FIE power consumption adopts the same combustion as base GDI application by Kia Stinger 2.0TGDI EU6. This means in particular, mass flows match in heat release to base configuration. Total system power consumption result in altering hydraulic fuel properties, such as density, viscosity and fuel bulk modulus.

In general, the power consumption does not show a significant change on the given engine configuration with a 200bar pressure GDI system. The details in *Table 23* show a picture of importance for hardware design as well as precautions, which have to be taken into account for higher pressurized solutions. This means for example, while the predictions of DMC and ethanol fuel indicate a non-fitting geometry to meet WLTP cycle requirements, also the pressurization losses define the dead volume by the fluid's properties. By transferring the information of today gasoline E5 vs. ethanol fuels for a 1000 bar application, losses increase furthermore to 7,2% for ethanol and 4,1% for gasoline E5 fuel. This does not necessarily mean, that it implicates higher losses in linearity. Since compression in a simplified analysis acts as a spring, "energy" remains stored in the fluid and is released by a driving force on pumps cam shaft. This tendency increases by increasing pressure levels. Therefore, next mandatory evaluation focuses for diesel system pressure levels and system architectures.

5.3.2. Fuel properties impact on Diesel fuel injection equipment power consumption

As described in the chapter before, an increase of pressure levels leads to a higher impact by fuel abilities on the fuel injection system components. The following analysis utilizes front load data of a Kia Sportage EU6 in WLTP cycle and the fuel properties as described in details in chapter *2.3*.

In today's field usage of vehicle and engines in any kind, especially the fuel quality differences are seen as a blurring of development research. In daily activity such blur often encountered with the unwritten law of $\pm$ 1g/km CO_2 dispersion tolerance, from tank filling to tank filling.

Diesel Fuels Data base:2014	Germany	Finland	USA (Midwest)	South Korea	India	Brazil
Density@15°C [kg/m³]	836	802	844	823	832	847
Viscosity [cSt]	2,68	2,12 @40°C	2,62	2,61	2,57	2,8
HFRR [µm]	250	341	378	328	432	198
Pressurization Loss at 2000bar	6,6%	9,6%	6,4%	6,8%	6,4%	6,5%
Total System Efficiency (with ideal low pressure pump)	18,5%	18,3%	18,4%	18,7%	18,6%	17,3%
Mean Power Conusmption [W]	90	93	90	91	90	95

Table 24:Impact on FIE system performance by fuel quality

By variance on power consumption by the high pressure system and its supply system, a diesel common rail system is more influenced, also in absolute value, as shown in *Table 24*. In this attempt to determine fuel quality impact, the power consumption with idealized low pressure pump shows difference of 5 W from best to worst in average power consumption over total WLTP. While the fuel from Germany, USA, South Korea and India perform in similar range from efficiency point of view and pressurization losses, fuel from Finland and Brazil differ. Both fuel origins show within their properties affiliates in density or viscosity and lubricity. The root cause in both cases is the difference in crude oil mixture as well as additives used in these particular regions. Beside, two effects are not encountered with this analysis. First one is the combustion impact on fuel quality. Such detailed impact prediction on combustion is also part of modern research activities and requires more than a generic approach by today's available tools, such as 3D CFD combustion simulation. The second effect is in utilization of an idealized low pressure pump with efficiency levels of 100%. The reason is the high sensitivity by this particular low total efficiency of below 25% and lower. Small differences would lead to in high deviation, but reviewing with new or better low pressure pump would alter above mentioned calculations significantly. Anyhow, as this analysis targets defining impact of fuel qualities, detailed assumptions for today or future applications can be done according to shown method.

As in case for future applications of new fuels required, an analysis and evaluation for "alternative" fuels also becomes mandatory. Not only to replace conventional fuels in today's given engines, but also for upcoming possible solution for future mobility. The shown approach allows an estimation for alternative fuel applications. Since the equations focus on FIE impact, combustion effects are not represented. In particular, heat release by heat values is adopted, but combustion quality impacts are not considered.

Parameter	B7 Diesel EN 591	OME-3 [24]	BtL (HVO) [51]
Density [kg/m³]	835	1070	780
Kinematic Viscosity [mm²/s]	2,68 @40°C	0,71@40°C	3,0 @40°C
Heat Value [MJ/kg]	43,8	22,5	44
HFRR [µm]	260	278 @20°C	<460 @60°C
Pressurization Loss at 2000bar	**6,6%**	**16,5%**	**5,8%**
Total System Efficiency (with ideal low pressure pump)	**24,0%**	**22,1 Test 20,7 % Calc.**	**19,1%**
Mean Power Consumption [W]	**164**	**232 (test) 249 (calc.)**	**179**

Table 25: Mechanical impact by alternative fuel on FIE in WLTP cycle

The shown impacts in *Table 25* for two selected alternative fuel variants, demonstrate expected range for difference in FIE performance. Since the mechanical data background utilizes Bosch CP4s1 performance mapping data and HMC R-Engine infrastructure, the estimated performances differ by application to different engine types. Nevertheless, results differ mostly due to an increased volume flow, required by lower heat value or lower density. The highest effect shows in this analysis Oxymethylenether (OME), in terms of power consumption. Especially a lower heat value and higher pressurization losses are driving the power

consumption to higher levels (see for pressurization losses chapter *4.1.3.2).* When utilizing those data as front load for OME, the difference in power consumption compared to B7 diesel over total WLTP is 6,9%. In relation, utilization of required power demand based on ECU hydraulic data increases power consumption from 45 W for Diesel to 68W for OME. The prediction and simulation of hydraulic consumption increases from 114W to 158W (+38%) in average for entire cycle, while above mentioned over total system increase states a difference of 69W or 42% for tested condition.

For analyzing plausibility and capability of high pressure system prediction by a fuel properties analysis, a detail analysis over an entire cycle becomes mandatory to understand differences.
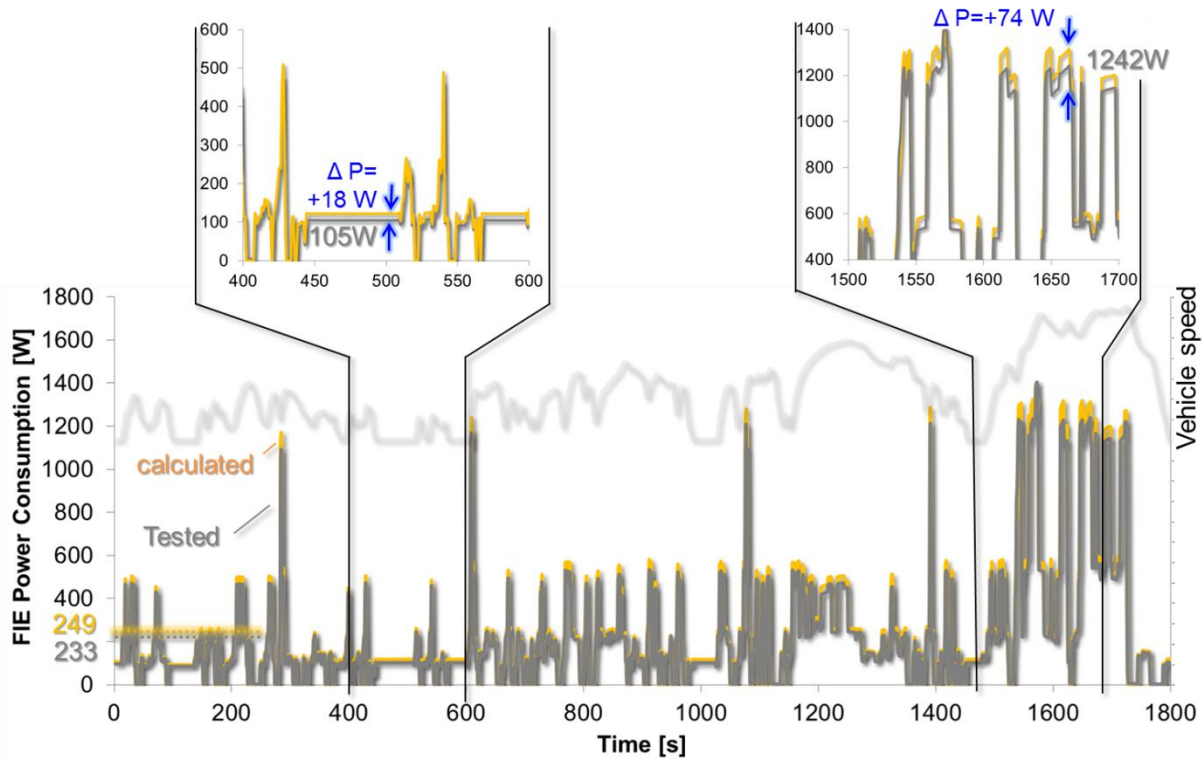
Figure 109: WLTP power consumption by high pressure pump pressurizing OME based on calculated and measured pump data

As the total result of a calculated pump mapping as well as the fuel tested pump mapping differs as mentioned before, also detailed operation point analysis act in a similar way (see *Figure 109*) . On the entire mapping, both methods differ for human eye in "line thickness", as the total difference of 16W (~6,9%). Zooming into particular areas of short time stabilization, range of drift becomes visible in this phases. Thus, values range from 18W (~17%) difference in idle (left zoom in *Figure 109*) to 74W (~6%) in high acceleration load (right handed). This indicates a good prediction capability, when approaching pump loses by fuel abilities. Anyhow, measurement for highest accuracy with real fuel remains necessary, as required to finalize a serial calibration. This tendency intensifies with lowered consumption by FIE.

5.4. Potential for future optimization

Today's concentration of research and development procurement bases on analysis of potential, and their connected cost. Novel technologies with substantial benefit do not enjoy a deep dive optimization to get last percentage of performance. In both cases an idealized

assumption based on mathematical approach supports definition of maximum achievable benefit. As modern society generates high effort to reduce CO_2 emission, new combustion approaches as well as new "alternative" fuels enjoy a higher focus.

As the variety of technology increases from day to day, not all possibilities can be discussed at once. Therefore, following potential analysis focuses on today's recognized development, representative for technology field of GDI engines, passenger diesel application and heavy duty application.

5.4.1. Gasoline direct injection system pressure level increase

Compared to a diesel engine, which reaches pressure level of nowadays 2000 bar and higher, gasoline direct injection engines utilize pressure levels of 200 bar and higher. In further development, gasoline engines shall reach higher pressure levels for improved combustion efficiency. Two approaches in particular are in focus of modern combustion development: lean combustion, which is targeting spark controlled compression ignition and homogenous charge compression ignition, whereas homogeneous fuel air mixture shall auto ignite. Both methods often recalled in public as combination of diesel and gasoline engines. Both approaches require as a mandatory feature higher pressure levels.

Since GDI system in its architecture should remain steady as today, future GDI system should also contain comparable cost attractive parts, such as direct acting injectors, integrated unit pump and one governor concept for pressure control. From today's perspective some items do not justify reasonable technical effort, which leads in first hand to higher cost and secondary to leave given path of today GDI system architecture. As starting point for such analysis on fuel injection system side, the following figure describes estimated impact on fuel consumption over entire cycle by utilizing higher system pressure. As efficiency approximation, mechanical properties of today system technology are extrapolated to represent a possible future state of technology.
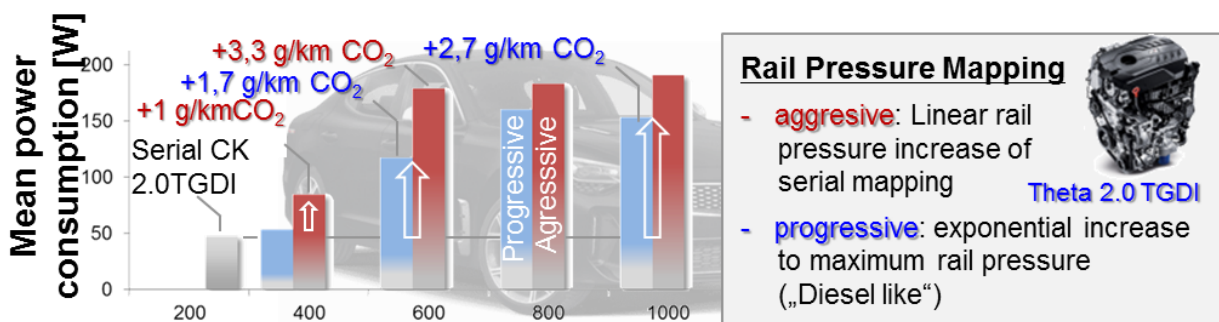
Figure 110: Estimated WLTP cycle CO_2 emission in Kia Stinger 2.0 TGDI without combusiton improvement
(engine and vehicle illustration from [92]

Increasing rail pressure to higher levels may follow, depending on different strategies. As two selected possible application scenarios, herein called "aggressive" and "progressive" shown in *Figure 110,* illustrates that the pressure increase also depends on calibrated pressure mapping. In a linear mapping (="aggressive"), high rail pressure levels are reached relatively fast. Thus, part load with 50% of engine output within its specific speed range leads to approximately 50% of maximum pressure level. In contrast (="progressive"), higher rail

pressure demanded late in its mapping. Thus 50% rail pressure levels is reached at 80% of engine load levels, which represents a calibration close to today's often used diesel engines.

This difference in rail pressure control logic differ CO_2 emission significantly. In general, aggressive rail pressure mapping reach higher CO_2 demerits as progressive strategies. Herein maximum reached difference states 1,6 g/km at achieved maximum rail pressure levels of 600 bar. Beyond this rail pressure levels, demerit for aggressive strategies does not change significantly, while progressive strategies still show increasing demerits. Referring to *Figure 87,* this performance impact in particular can be revised in engine performance as well, and fits well between calculations and engine measurement.
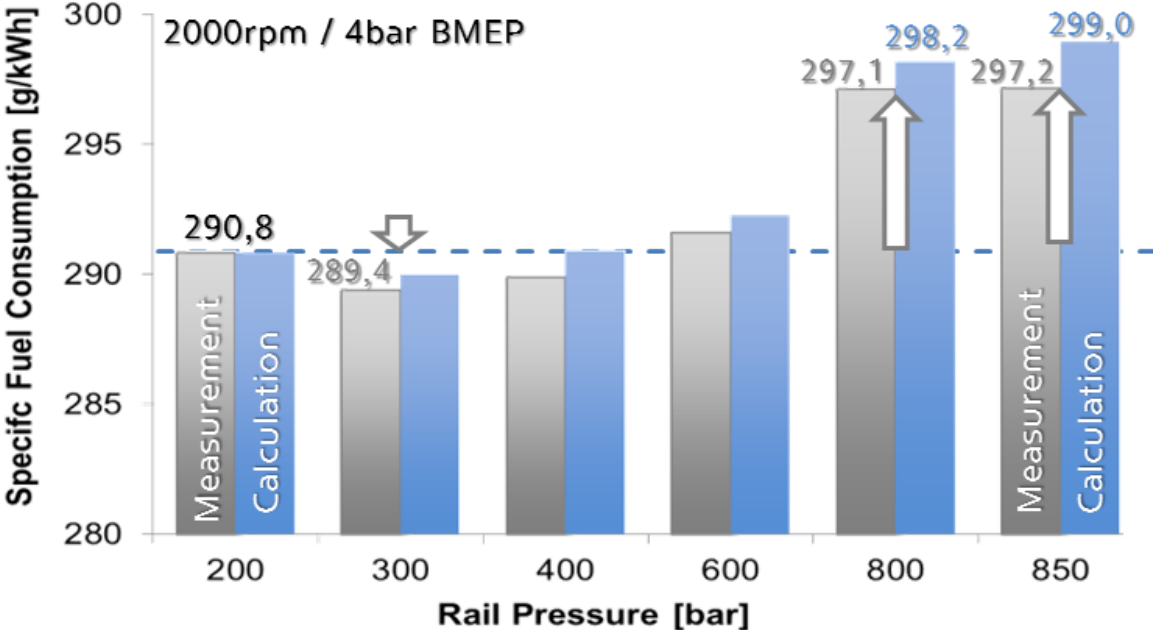
Figure 111: Comparison of measured engine specific fuel consumption and calculated engine specific fuel consumption on HMC Gamma engine

The predicted SFC matches to engine test bench result within below 1% in absolute value. Relatively to predicted difference, highest alteration reaches level of 10.8% at 850 bar, whereas prediction always has higher values than measurement. In both cases, for this particular operation point in *Figure 111*, specific fuel consumption receives firstly reduction and then increases significantly at 800 bar rail pressure. Since hydraulic power consumption should increase proportionally in idealized assumption, increasing losses can be explained by high pressure pump efficiency and engine interaction. Therefore, a deeper analysis supports understanding of the measured occurrence.

In this particular analysis of losses at 800 bar rail pressure or 600 bar difference to 200 bar as in serial calibration, it separates into three different impact causes. The first and most obvious one is the impact of increased hydraulic demand. By assumed constant flow, pressure increase remains as major driver. Second impact is efficiency and mechanical losses by high pressure pump. In this particular operation point, those losses show highest contribution to total CO_2 emission demerit by 4,2 g/kWh. In principle, those losses have potential for improvement and therefore show the limit for feasible improvement. On the other hand, combustion benefit by higher pressure already utilizes benefit for SFC, but cannot be covered by analyzing fuel injection system only. In this particular case for homogenous combustion, former analysis by

Karlsruher Institut für Technologie pointed out a beneficial combustion impact by 600 bar pressure difference of 1 g/kWh [93].
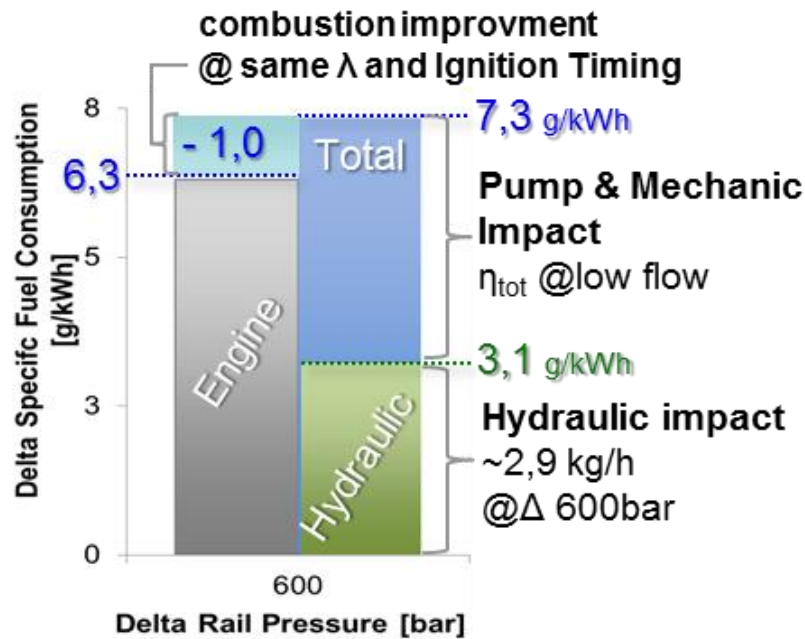
Figure 112: Impact summation of 800 bar rail pressure at 2000rpm and 5 bar BMEP operation point

Finally, the predicted losses and its related engine impact match on same value. By following this, three actions for improvements become visible: at first improvement by advanced combustion principles is required to overcome mentioned increased losses by FIE and the second is open potential in mechanical improvement. This includes pump as well as engine interaction, as results from Diesel engines within entire chain drive (see chapter *4.2.2.*) proves. As third approach for future optimization, an energy optimization to avoid low efficiency operation ranges would also lead to fuel consumption benefits over entire cycles. This requires an independent pressure generation and different approach for rail pressure controller setup.

5.4.2. New fuel application for today's engine

The utilization of new fuels impacts predominanly the diesel engines. Herein, most variety for passenger vehicles is under discussion to push forward to carbon neutral mobility concepts. Diesel engines therefore have today most possibilities to run with alternative fuels, as number of fuels and their different crude stock shows. Since nowadays applied FIE bases on diesel fuel within narrow corridor of specification, for alternative fuel tailored systems may receive further improvements leading to lower fuel consumption in general. This becomes most obvious when reviewing mentioned differences in total efficiency on Continental DHP1 pump and Bosch CP4s1 high pressure pump between ISO 4113 (or diesel substitute) and OME fuel (see to *4.1.3.2)*. Herein mentioned difference at 400 bar reaches levels of 13% to 38% difference between both fluid types. This require in particular a redesign of the mechanical components and an optimization to match the current design with new fuel abilities.

In spite of the hardware itself, a matching of calibration parameters to fuel boundaries leads also to a benefit in fuel consumption. As explained in detail on OME, especially compression

abilities impact on total efficiency and flow rate significantly. This is shown in particular in *Figure 94* and related chapter *5.3.2.*

Difference in Volumetric Efficiency between ISO 4113 and OME -> Average in range 2400 to 3000 rpm
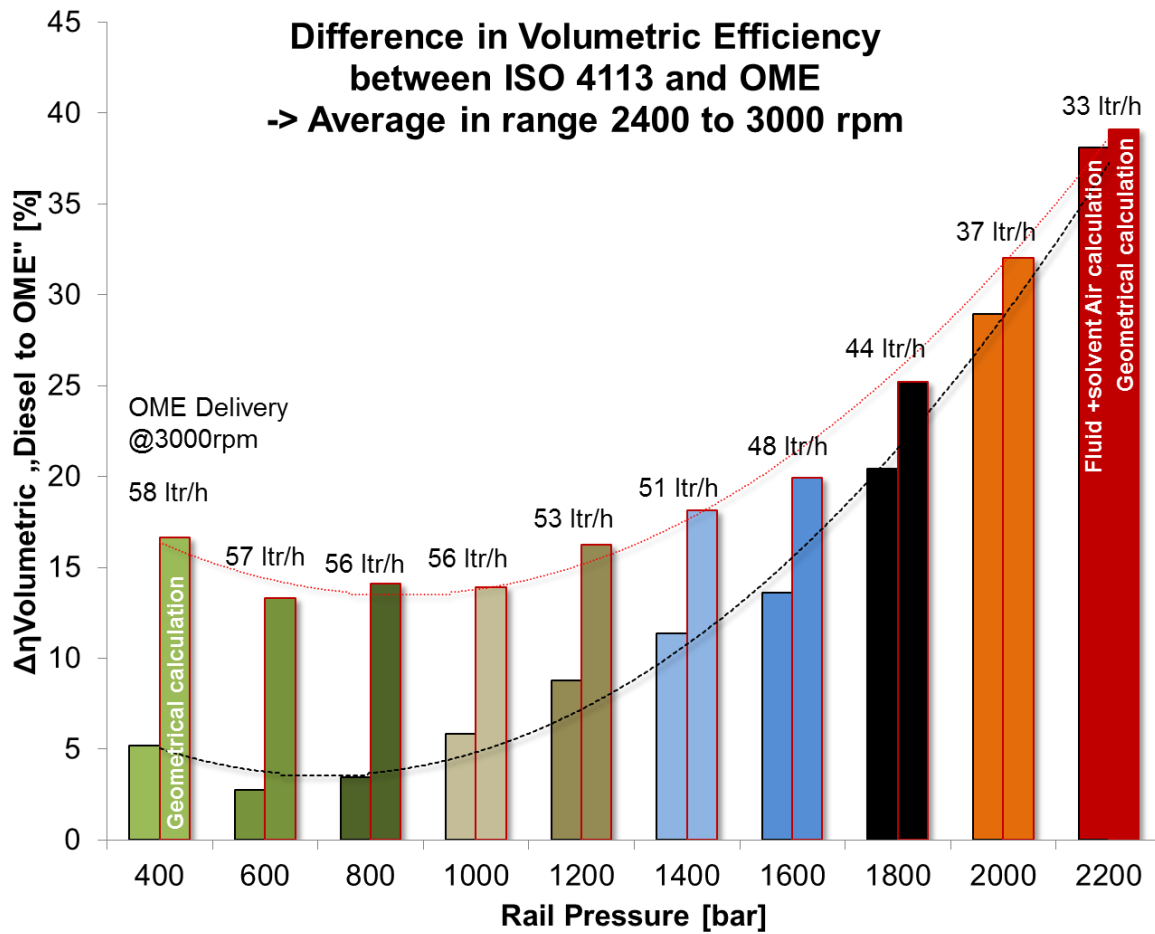
Figure 113: Volumetric efficiency difference of Continental DHP1 OME between Diesel and OME in respect to volumetric efficiency calculation modulus

When analyzing this particular *Figure 113* (former *Figure 94*) in retrospective for future improvements, especially significantly decreasing high pressure flow with increasing pressure shows a start for improvement. In a first attempt, the maximum pressure should be limited to a fuel suitable limit. Since 20% difference in volumetric efficiency to ISO 4113 or diesel fuel marks the point of strong increasing, keeping pressurization level up to a maximum 1600 bar and below initiate countermeasures against higher fuel consumption of system. It also supports retrofit applications to maintain power output level without major changes of FIE system.

Another detail showing an opportunity for fluid based loss reduction. By assumption for enclosure of fuel properties during compression by dividing into isotherm and polytrope compression, which assumes fuel as partwise gaseous behavior, reduction of "solved gas content" would improve volumetric efficiency significantly. This does not exclude "classical" fuels from achieving this benefit also.
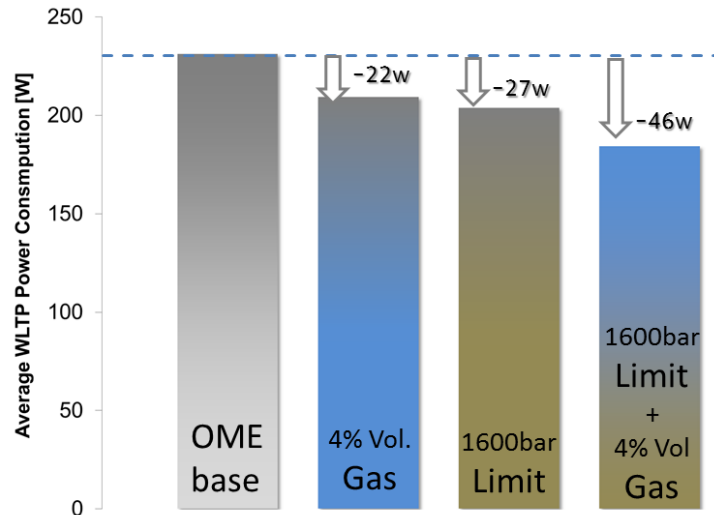
Figure 114: Prediction on OME FIE power consumption by compressibility related counter measures in WLTP

The evaluation of the given possibilities shows a close effectiveness by reduction of gaseous content and limitation of rail pressure limit, and a possible combination of both effects. The missing information in this particular evaluation remains in combustion effects, as well as power consumption by "De-gasing" measures. Today's feasible approach for on board solution would be a high frequency oscillation cell within fuel line. Since 22 W achievable benefit from this particular case lies in comparable range for power consumption of high frequency cells, a final benefit may be very low or not given. Other option by fluid properties may require substantial effort for industrialization. As remaining option, a fuel properties fitting rail pressure limitation shows for this particular case a potential benefit of 27 W. This assumes a linear rail pressure decreasing to find former 2000 bar calibration in a 1600 bar calibration.

In addition, a possibility as on board and online optimization remains in using pump drive torque analysis for compressibility, as *Figure 67* shows. Since characteristic of pump itself as well as fluid properties are reflected in its physical appearance of drive torque, physical equilibriums in different stages become understandable. Therefore, top dead center (=TDC) clearly defines one position within a dynamic drive torque waveform, whereas drive torque switches from positive to negative values. Second position is the negative peak in drive torque, in other words drive torque's minimum. In assumption of not losing contact between tappet and roller to cam shaft, resulting torque and therefore force results only by spring and fluid residual pressure.

$$F_{effective(\delta)} = F_{Spring(\delta)} + F_{Pressure(\delta)} = \frac{T_{min}}{r_{(\delta)}} \qquad (37)$$

$F_{effective(\delta)}$: effective force by plunger on cam shaft related to shaft angle δ;
$F_{Spring(\delta)}$: force by spring;
$F_{Pressure(\delta)}$: force by actual pressure; T_{min}: minimum torque (negative peak) in high pressure pump drive torque characteristic; $r_{(\delta)}$: effective radius at pump angle δ (see equation *(38)*);

135

In addition, the angular position between before mentioned TDC and position determines the discharged displacement by considering pump geometry. The angle δ describes in this circumstances the angle of minimum torque ("negative peak torque") and the drive torque of 0 Nm.

$$r_{(\delta)} = f(cam\ lift) + r_{base\ crcle} \tag{38}$$

$r_{(\delta)}$: effective force by plunger on cam shaft related to shaft angle δ;
$f(cam\ lift)$: cam lift at shaft angle δ;
$r_{base\ crcle}$: base circle of applied cam shaft

And

$$F_{Spring(\delta)} = c_{spring} * (r_{(\delta)} - r_{base\ crcle}) + F_{Spring0} \tag{39}$$

$F_{Spring(\delta)}$: force by spring: effective force by plunger on cam shaft related to shaft angle δ;
c_{spring}: spring stiffness;
$F_{Spring0}$: initial spring load in bottom dead center

Consequently follows

$$p_{comp(\delta)} = \frac{F_{pressure(\delta)}}{A_{plunger}} \tag{40}$$

$p_{comp(\delta)}$: pressure in high pressure chamber related to shaft angle δ;
$F_{pressure(\delta)}$: force by actual pressure;
$A_{plunger}$: pressurized surface on plunger

And

$$V_{comp} = r_{plunger}{}^2 * \pi * (l - r_{(\delta)}) \tag{41}$$

V_{comp}: discharged displacement from TDC to shaft angle δ;
$r_{plunger}$: radius of pressurized surface on plunger;
l: Maximum lift of plunger from camshaft centerline

As last required state for compressibility calculation, initial pressure information needs to be obtained. With assumption residual amount at TDC has rail pressure, all information is given.

$$K_{est} = \frac{P_{rail} - p_{comp}}{V_{comp}} = \frac{P_{rail} - \dfrac{\dfrac{T_{min}}{r_{(\delta)}} - c_{spring} * (r_{(\delta)} - r_{base\ crcle}) + F_{Spring0}}{A_{plunger}}}{r_{plunger}^2 * \pi * (l - r_{(\delta)})} \qquad (\,42\,)$$

K_{est}: estimated fuel compressibility at rail pressure;
P_{rail}: pressure level in high pressure rail; T_{min}: minimum torque (negative peak) in high pressure pump drive torque characteristic; $p_{comp(\delta)}$: pressure in high pressure chamber related to shaft angle δ; V_{comp}: discharged displacement from TDC to shaft angle δ; $r_{plunger}$: radius of pressurized surface on plunger; l: Maximum lift of plunger from camshaft centerline; $A_{plunger}$: pressurized surface on plunger; $F_{Spring0}$: initial spring load in bottom dead center; c_{spring}: spring stiffness; $r_{base\ crcle}$: base circle of applied cam shaft; $r_{(\delta)}$: effective force by plunger on cam shaft related to shaft angle δ;

The shown equation (42) requires information from high pressure pump geometry, as well as sensor values by rail pressure. In addition, it requires a one plunger radial piston high pressure pump and dedicated measurement technology for analysis. Multiple plunger on one shaft will lead due to summation of dynamic drive torque to not clearly detectable conditions. On the other hand, filling and operation condition has impact minor, since dead volume at TDC is a hard design parameter of each high pressure and crates initial conditions. To clarify the approach, following illustration demonstrates the application of equation (37) to (42).
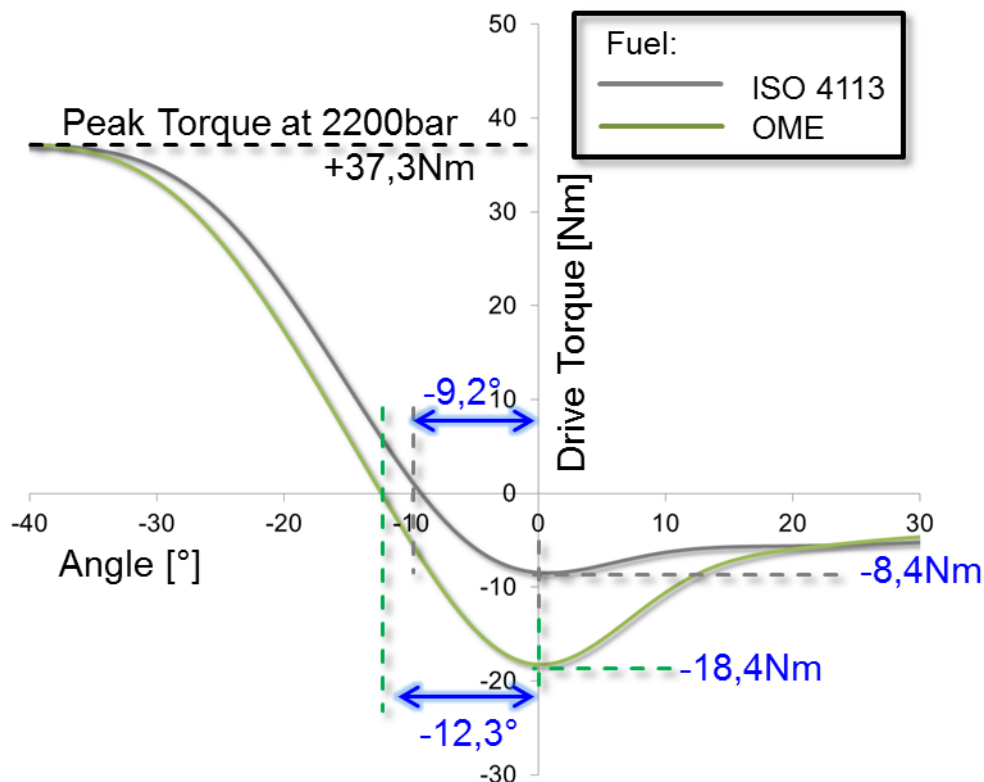
Figure 115: Discharge stroke of Continental DHP1 at 2200 bar and 2000 rpm pressuziing ISO 4113 and OME

Since applied high pressure pump for ISO 4113 and OME does not change, the effects shown in *Figure 115* on same 2200bar operation point display impact by fuel properties. As described, minimal torque as well as its related position to TDC differs to each fuel type. Utilizing equation *(37)* to *(42)*, the resulting compressibility states values of 2.8 GPa for ISO4113 and 1.3 GPa

for OME. For reference, simulated data states based on Bosch adiabatic diesel measurement compressibility of 3.3 GPa at 2200bar, while also shown approximation by isotherm and polytrope compression (see chapter *5.1.2* in particular equation *(34)*) results in a value 2.9 GPa compressibility.

In conclusion, fuel type utilized has significantly impact pump and high pressure system performance. Not only does it impact on fuel flows as they change for combustion and heat release, also their specific properties impact in hydraulic performance and also may limit application boundaries and parameter ranges. It is also shown, that fuel system can detect physical properties of the fuel on its own. As a possible application example, fuel type detection via compressibility and speed of sound over a pressure mapping, allows a clear fuel type detection on board. Modern processing tools as artificial intelligence can use these data to operate in several ways for a full matching to changing fuel type on on-road application.

6. Conclusion

Automobile industry and global mobility will change within the next decade. The focus in global activity remains as years before on the hunt for CO_2 reduction. While battery electric vehicle gain higher importance in markets, combustion engines play and will play several years in the future a major role for mobility and also several industrial applications. Based on this role, combustion engines contribute in CO_2 reduction not only in optimization for higher efficiency, but also increase flexibility to run with non-fossil ("alternative") fuels.

Since the fuel injection equipment (=FIE) of every engine has a significant share on the engine performance, detailed analysis has been executed to establish a deep dive knowledge. Therefore, the major injection system variants have been analyzed by own measurement approaches to determine performances in every engine operation state. With power consumption performance and efficiencies in focus, also driving cycle impacts become feasible. In total, analysis of FIE on engine CO_2 and frictional performance bases on measurements on three vehicles, five different engines types, eleven high pressure pumps types including self-made samples. In addition, an own designed generic simulation system, to determine operation condition of FIE during engine duty, supports up to fuel consumption prediction and optimization approaches.

Herein, a "tool" also for novel combustion principles has been established to analyze in higher accuracy. While combustion impact determination of new fuels or combustion impact is often known, the mechanical impact on engine has often no reference at all in such analysis. Furthermore, a simplified approach to receive fluid properties and their impact on FIE system performance has been generated. All results match between calculation and measurement, from engine operation points up to entire vehicle CO_2 emissions. This provides insights into the high impact of high pressure system modification on the entire vehicle performance.

6.1. Prediction and analysis of fuel injection equipment performance losses

As first step to achieve a deep dive analysis and to have an understanding in FIE interaction with all engine components, the mathematical equations for understanding of modus operandi are mandatory for a starting point. Herein knowledge of state of the art applied hardware and also well-defined measurement approaches contribute in total analysis procedure.

Therefore, first analysis and introduction to power consumption calculation reviews system specific hardware and related system architecture, as described in entire chapter *2.2.* Within this step, the analysis starts by general aspects such as direct acting or servo injector type, high pressure pump type, leading to rail and controller type and finally supply architecture build up including fuel type. This level of details follows significance for engine operation. As injector type defines interface between combustion and FIE, it has a major impact on engine performance, whereas high pressure pump demands power consumption for fuel pressurization to target pressure. The next step focuses in gathering frontload data. This requires not only engine operation conditions – from single test points to entire cycles- but also performance data by FIE. In today's development processes, the component or even a complete system is often not available in early state. In this situation generic system components based on 1D simulation generate first front load data. Unfortunately, high

pressure pump and also entire FIE system simulation gives good hydraulic approximation, but no mechanical useful information, despite peak torque for mechanical stress limit determination. Friction models differ from measurement and do not interact correctly with physical changes (see to *Figure 46* and *Figure 47*)*. Anyhow, a system simulation becomes mandatory to obtain the system's specific data such as controller and rail pressure reaction – also in the high pressure pump head. Therefore, the utilized generic simulation system is described in detail within chapter *3.6.*

The high pressure pump performance mapping builds a foundation for detailed power consumption analysis. Herein, the dedicated measurement principle of chapter *3.1*, in full load and part load operation. It may not be necessary to use a full hull curve and mapping for the entire pump, but the procedure will later lead to most precise result by applying a regression based operation to calculate for engine duty cycles. The other option remains in using a best fit operation with and extrapolation. This method is suitable for prototype pumps, whereas durability may not be given at certain point of development. In addition, a detailed injector hydraulic measurement of the injected volume and the leakage volume increases precision of the power consumption calculation. A frontload source selection for the injector performance depends mainly on the development state and target analysis. Depending on the principle of mechanical integration, it may be necessary to measure in entire chain or engine belt drive, as in chapter *3.3* and corresponding results of chapter *4.2* show. While gears, as applied typically in commercial engines, have typically a mechanical impact of 2- 7 %. In opposite, the results in chapter *4.2* shows, that the chain drive build in HMC R-Engine impacts in mean torque increase of up to 220%.

As a final step, all measured as well as simulated data or also static power data, as an "easy handling" approach for steady operated supply systems, have calculated according to engine data. In particular, simulated physical flows as pressures inside the FIE have to be reviewed for this step. In case of a state of the art serial produced 200 to 350 bar Gasoline direct injection (=GDI) engine, the analyzed differences are minor. Therefore, this step may be skipped and engine control unit (=ECU) values may be utilized as front load data. In other cases, approach depends on the selected operation and cycle. As on single operation points, such as in WHSC for commercial, every point may be simulated directly (see to chapter *5.1.3)*. In driving cycles or real road recorded driving cycles, a simulation of every operation cycle demands too much time. The simulation of base points and interpolation between these points ensures a time efficient close up. In opposite to nowadays typically used approaches in an engine development process, the simulation of the majorly occurring operation points within cycles for FIE has to be performed in outer boundaries of the cycle and for operation points "in the middle" of such cycle or mappings.

As utilizing this approach in its mathematical principle as described in chapter *2.4.,* the equation *(20)* is the base equation to the entire evaluation

$$\eta_{FIE} = \frac{\left[\frac{\dot{m}_{total}}{\rho_{Fuel}}*\left(p_{supply}-p_{tank}\right)\right]+\left[\frac{\dot{m}_{Fuel}+\dot{m}_{Injector\_leak}+\dot{m}_{Rail\_control}}{\rho_{Fuel}}*\left(p_{rail}-p_{supply}\right)\right]}{T_{mean}*2*\pi*n_{pump}+U_{Bat}*I_{LP\_Pump}} \qquad (43)$$

η_{FIE}: entire fuel injection equipment total efficiency;

Both pumps embedded in this equation *(20)* describe the entire power consumption at each specific operation. Anyhow, for an analysis of engine performance impact, FIE power consumption only is not enough. In particular, the engine specific fuel consumption at each corresponding point has to be set in relation to FIE power consumption. Herein a calculation of auxiliary specific fuel consumption becomes mandatory, as described in chapter *2.5.* in particular in chapter *2.5.3.*

Such analysis focuses on differences between the systems and their configuration and therefore supports in selection of fitting components or parameters. Herein, the required next step combines the already achieved results with the engine fuel consumption data. By this operation, component based fuel consumption as described in chapter *2.5.3* will be obtained. The equation (22) and the equation (23) perform this task.

$$\dot{m}_{fuel\_sub}\left(T_{Eng},n_{eng}\right) = b_e * P_{loss}\left(T_{eng},n_{eng}\right) * h\ [16] \qquad (44)$$

$\dot{m}_{fuel\_sub}$: sub-component fuel consumption share; P_{loss}: sub-component power consumption

$$\begin{aligned} m_{fuel} &= \sum \dot{m}_{fuel\_sub}\left(T_{Eng},n_{eng}\right) * X \\ &= \dot{m}_{fuel\_sub}\left(T_{Eng1},n_{eng1}\right) * X_1 + \dot{m}_{fuel_{sub}}\left(T_{Eng2},n_{eng2}\right) * X_2 \\ &\quad + [\dots] + \dot{m}_{fuel\_sub}\left(T_{Engn},n_{engn}\right) * X_n \end{aligned} \qquad (45)$$

m_{fuel}: total fuel consumption ; X_n: test point share to entire test

Respective to the utilized fuel type, the emitted CO_2 results by each type the specific CO_2 emission, which basically depends on its Carbon and Hydrogen ratio. In comparison to so calculated values, the counteract measured values in engines or total vehicles. The chapters *4.4* and *4.5.* shows all related results. A comparative evaluation and analysis shows results as in chapter *5.2,* in particular illustrated in *Figure 98*, in *Figure 108* and *Figure 111.*

These two selected engine test bench results in *Figure 116* demonstrate differential engines and operation modes, as well as power output, by running tests on an engine dyno and focus on FIE matching condition for both analyses. Herein, the mentioned results are described in chapter *5.1.3* and *5.4.1.* Also common for both of the illustrated comparisons are close prediction of SFC compared to its measurement. Anyhow, an obstacle for a fitting calculation lies within shown GDI measurement.
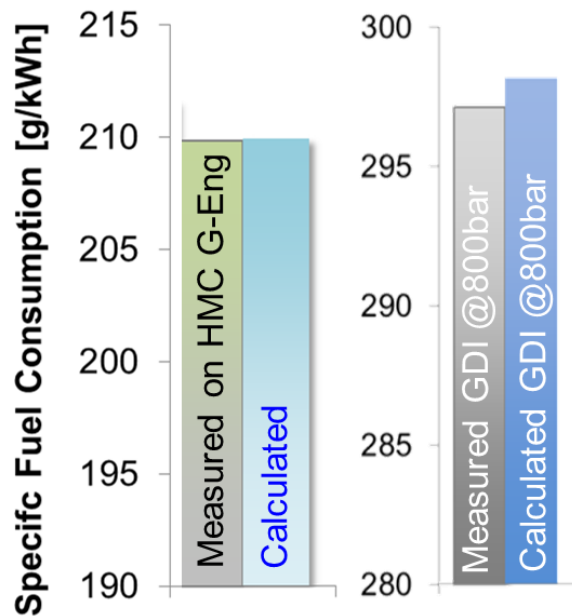
Figure 116: Summary of selected engine test bench results vs calculated results

Its detailed analysis follows the illustrated analysis in *Figure 112.* Herein the combustion improvement of modus operandi states SFC benefit of 1 g/kWh as former analysis performed. Thus, the combustion impact interaction needs at least as an iterative step a simulation model. Therefore, the shown method has highest potential for benefit in complete engine simulation models and may also be used as so called virtual testing, when novel fuels are applied. A shown parameter optimization or conventional evaluation for best fitting hardware, predicts matching results in tests and evaluation of three different vehicles. Since the achieved data for an entire cycle or real road driving are reliable, one single test generates enough frontload data to save time and money for variation and its prototyping. This states still as common improvement step between test based evaluation and virtual or simulation based evaluation.

6.2. Potential improvement for future fuel injection systems

The future combustion engine development and trends focuses on different topics at once. As foundation of nearly all approaches and also entire road maps, the direct injection under high pressure justifies as given or even mandatory. In some cases, the direct injection even plays major role within novel concepts. Thus the pressure increases by its entire system, fuel mixing or total new fuels are named in modern road map titles and papers as solution for clean and even CO_2 neutral concepts.

Herein mentioned information of increasing pressure levels, as nowadays the GDI system receives, increase also the importance of an efficient FIE increase by every evolutionary step. To "get a feeling" in possible dimension, an evaluation of today diesel common rail FIE power consumption level represents a fair starting point. As rough close up to this situation and to frame such scenario, the analysis of a theoretical increase from 200bar GDI today to a possible 2000bar GDI requires hydraulically factor 10 in power consumption, assuming same engine fuel efficiency. By technical reason of the injectors architecture and also possible injection accuracy requirement for this purpose, an exchanging of injector type to servo injectors becomes mandatory, which will lead in power consumption analysis to an entire increase of

factor ~1.5 to 2. In total, the hydraulic power consumption of such a vehicle would increase in range of 15 to 20 times from today status. Of course, this scenario does not include a combustion improvement, changed auxiliaries or an adaptation in rail pressure mappings over duty to operation. The resulting impact on engine changes on performance significantly. As *Figure 117* shows the impact on CO_2 emission on KIA Stinger by calculated pressure increase.
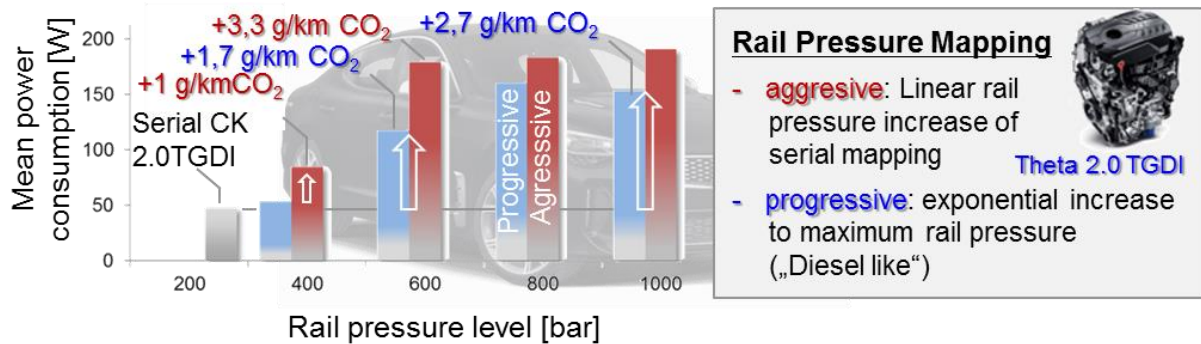
Figure 117: Estimated WLTP cycle CO_2 emission in Kia Stinger 2.0 TGDI without combusiton improvement
(Engine and Vehicle illustration from [52]

This particular evaluation illustrates an expected effect on state of the art technology. Despite the rail pressure strategies impacting on cycle results, direction of emission by pressure increase is set. Furthermore, the details are within mean power consumption, which states an increasing factor of loss by FIE of 3 to 4 from 200 bar today to 1000 bar GDI. As state of the art system technology for such usage is today on separation on "Diesel-like" approaches and GDI based approaches, the final system levels, lead by combustion development, will give target limits. Nevertheless, also novel fuel types and future mixtures will determine future pressure levels.

6.3. Impact of fuel quality and type on powertrain performance losses

As a major concern for future mobility, fossil fuels have today a negative stand by their direct impact in CO_2 emission. To overcome this situation, novel or alternative fuel has increasing focus in society as well as research and development. Since combustion abilities change by their molecular structure, all available fuel types have altering ideal combustion condition. This means also rail pressure level may vary by own calibration strategies.

As shown in chapter *5.3* and chapter *5.4.2* difference in average cycle power consumption depends basically on the systems components, in particular injector type, rail pressure governor, fuel type and pressure level. As a sum up *Figure 114* shows simplified impact by different fuel type.
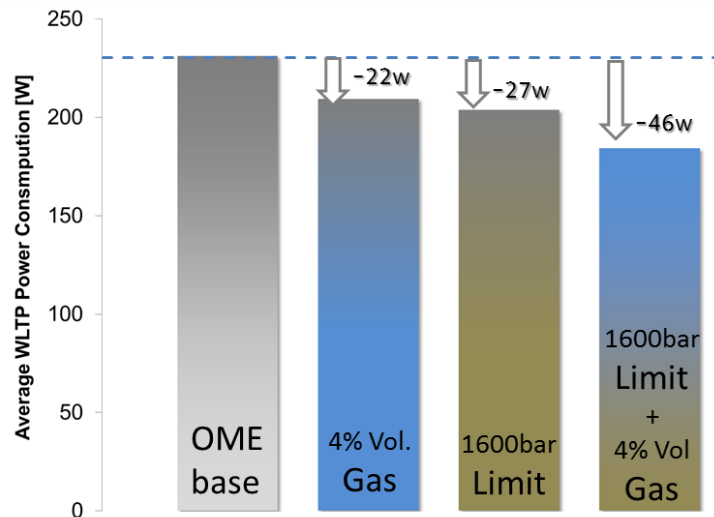
Figure 118: Prediction on OME FIE power consumption by compressibility related counter measures in WLTP

Since the CO_2 emission does not necessarily fit for alternative fuels as measurement value, power consumption gets more in focus for review. In case for such "CO_2 neutral" fuels, highest priority remains still on lower fuel consumption by economical reason. As herein shown impact by fuel abilities – as selected reduction of volumetric gas content in fuel mixture of OME- has also a significant impact on total FIE power consumption. In similar range remain calibration options as herein shown by 1600 bar rail pressure limit. Both case reach improvement levels in this particular case of 9% to 12%. Of course, alternative fuels require a certain analysis for each usage case.

In summary, two options for a future optimization for novel fuels remain with significant impact on entire performance: modification of fuel quality and abilities, as they are regulated today by norms as EN590, and a calibration approach fitting to the fuels abilities. The selection of one of these approaches -or a combination of both- require in future applications a dedicated analysis to select best solution.

7. Future possibilities in propulsion development

Independent from the question of which fuel type will energize future mobility, desired targets for future applications and utilization will remain on emission quality regulation. What emission in particular requires focus, will change by social or political reasons over the next years and differential for regions over the world. In combination by different upcoming fuel types, numbers in variety will increase. It is often the case that possible optimized points cannot be reached due to physical boundaries or other limiting factors. One typically used engineering approach removes boundaries to have an additional degree of freedom.

To match on fuel injection equipment, fix limiting boundary remains rotation speed connection of high pressure pump to engine. This leads to lowered operation efficiency as well as require a dosing method to control correct quantity for pressurization. Overcoming this challenge can solve a engineering "trade-off" and a focus pressure calibration to designated targets. In combination with a larger accumulator or pressure adjusting volume, a power consumption saving even at higher rail pressure becomes feasible. As alternative, a rail pressure configuration with energy saving modes can reduce average power consumption, with increasing effect by increasing pressure levels.

The herein shown equations and entire method bases on the calculation of efficiency at each point and to determine by that its precise impact on the engine performance. This is possible in a prior measurement of the entire system or by simultaneous calculation via power parameters, such as torque and rotation speed or electrical power. When the efficiency levels drop below a defined threshold, residual amount in accumulator can cover required amounts. Since efficiency levels reach typically in lowest load condition lowest efficiency levels, residual amount ensures longest as possible operation. In addition, when the rail is drained and operation becomes required, high load operation to charge the rail has a higher total efficiency. This gives also the opportunity to utilize higher rail pressures also in low load condition to improve the combustion quality.

This approach also impacts the fuel flexibility. A fuel with different combustion abilities leads to different rail pressures and flow for combustion. In case for state of the art direct mechanics connection, the pump displacement majorly fits to one setup for one fuel type. By independent pressurization, flow and pressure levels itself in an optimum as well as well rail pressure build up. Since a driver interacts still by his command of accelerator pedal, engine power output and therefore fuel demand will adjust. In addition, by utilization of in chapter *5.4.2.* mentioned approach for fuel property analysis, engine control unit has an additional feature to calculate also for altering fuels ideal combustion strategies.

In summation, by analyzing upcoming new opportunities and challenges for future mobility, the combustion engine as today will still remain as one major pillar for a mobile society. Moreover, future legislation for clean air and carbon neutral mobility will cause a change for next generation engines and propulsion concepts. The fuel has to conduct in this process; especially it has the possibility to "retrofit" in today's engines and lead to clean mobility without replacing all vehicles on the road and ensure a mobility for everyone.

A. Sources

[1]   Wikipedia article on Karl Benz, https://en.wikipedia.org/wiki/Karl_Benz, 17th .06.2017

[2]   Summary of "Climate Action Plan" by "Federal Ministry for Environment, Nature Conservation, Building and Nuclear Safety" of the Federal Republic of Germany as of 14th November 2016

[3]   M. Linder ;"Portfolio of powertrains for passenger cars – a fact based evaluation" ;   Presentation from 5th international environmentally friendly vehicle conference 2012

[4]   Y. Balk, R. Hensley, Pa. Hertzke and S. Knupfer, "Making electric Vehicles profitable", article   for   MicKinsey   on   8th   March   2019 https://www.mckinsey.com/industries/automotive-and-assembly/our-insights/making-electric-vehicles-profitable on 29.06.2019

[5]   H. Holdinghausen, R. Bauer, „Historiker über Autos" [German], Inteview in TAZ, 5th of February 2017 and   https://taz.de/Historiker-ueber-Autos/!5377474/ (on 16th of June, 2020)

[6]   H. Wallentowitz, "Handbuch Kraftfahrzeugelektronik", Vieweg und Teubner 2nd edition, 2011, P.97

[7]   S. Pischinger, J. Schaub, F. Aubeck, D. v.d.Put; "Powertrain Concepts for Heavy-duty Applications to Meet 2030 CO2 Regulations". ATZ Heavy Duty worldwide 13 (2020), P. 36–41

[8]   J. Dulac, "Global transport outlook to 2050", International Energy Agency 2012, p.12

[9]   J. Dulac, "Global transport outlook to 2050", International Energy Agency 2012, p.23

[10]   "Estimate of the Technological Costs of CO2 Emissions reductions in Passenger Cars", Report of the German Federal Environment Agency on 6th August 2008, p.19- 24

[11]   J Dulac, "Global transport outlook to 2050", International Energy Agency 2012, p.19

[12]   A Burkert, „ The fuel showdown", in „Motorentechnische Zeitschriften", March 2020, p.6-7

[13]   W Piock, „Delphi Technologies Next Generation GDi-System – improved Emissions and Efficiency with higher Pressure", paper and presentation at "Wiener Motorensymposium" 15th May 2019

[14]   US Legislation §86,1811-17 (eCFR) from 25th of October 2016 by US Environmental Protection Agency

[15]   F. Pischinger, "Handbuch Dieselmotoren", Springer Fachmedien Wiesbaden, 2017, p.278 f

[16]   K.H. Grote, „Dubbel-Taschenbuch für den Maschinenbau", Srpinger Fachmedien Wiesbaden, 21. Auflage;

[17]   Hyundai Motor Europe Technical Center Introduction Presentation, 2014

[18]   Technical Information on engine performance on https://www.hyundai.de/modelle/i30-n/ , 30th June 2020

[19]   "Problems in Hyundai Theta II Engines" website,

 https://medium.com/@phravinxavi.14/problems-in-hyundai-theta-ii-engines-ab971e5c16f3, 30th June 2020, engine illustration

[20]   MY Song ,"Hyundai Introduces New R-Diesel Engine"   www.hyundainews.com.
http://www.hyundainews.com/us/en/media/pressreleases/28779

[21]   Hyundai Truck and Bus, Technical Data to G-Engine on

http://trucknbus.hyundai.com/global/brand/technology/performance-and-safety-technology, 30th June 2020, picture and listed performance data

[22]   T Tzanetakis; M Sellnau; V Costanzo; M Traver; "Durability Study of a Light-Duty High Pressure Common Rail Fuel Injection System Using E10 Gasoline" SAE-Technical Paper 2020-01-0616; 2020

[23]   JE Johnson, SH Yoon, JD Naber, SY Lee, G Hunter, R Truemmer, T Harcombe; "Charactersitics of 3000 bar Diesel Spray Injection under Non-Vaporizing and Vaporizing Conditions, paper at 12th Trienial International Conference on Liquid Atomization and Spray Systems in Heidelberg, 2nd to 6th September 2012

[24]   U Pfisterer, „Erdöl, Raffenerieverfahren, Herstellen und Logistik von konventionellen Kraftstoffen", paper and presentation on „Kraftstoffe für Verbrennungsmotoren" UNITI Forum 13th of October 2016

[25]   U Pfisterer, "Ottokraftstoffe incl. Ethanol im detuschen Markt", presentation and paper on "Krafftstoffe für Verbrennungsmotoren" UNITI Forum 13th of October 2016

[26]   U Mayer „Dieselkraftstoff", paper and presentation on "Kraftsoffe für Verbrennungsmotoren UNITI Forum" 11[h] November 2010

[27]   ExxonMobil Jet Fuel Specification from 29th September 2021

[28]   R v Basshuysen, F Schäfer; „Handbuch Verbrennungsmotor: Grundlagen, Komponenten, Systeme, Perspektiven";Vieweg und Teubner; 5th edition, P. 890f

[29]   UNECE –Regulation No 101 – Revision 3 from 12th April 2013

[30]   UNECE- Amendments to global technical regulation No.15 on worldwide harmonized light vehicles test procedure from 3rd November 2015

[31]   "Prüfzyklen WHTC und WHSC" as seen on
https://www.emitec.com/technik/prueffeld-eisenach/rollenpruefstand-leistungsstarker/
on 29th May 2020

[32]   S Revidat, J Ullrich, HI Park; "Full Electric High Pressure Pump for Electrified Powertrains of the Future"; presentation and paper from Hyundai Motor Group Conference, South Korea, on 16th October 2019

[33]   A Settle, "Evaluation of 350bar GDI Pumps", Master Thesis, University of Applied Science Friedberg and Hyundai Motor Europe Technical Center GmbH 2017

[34]   Hirschvogel AG, Press Release illustration,
https://www.hirschvogel.com/fileadmin/editor/produkte/kraftstoffeinspritzung/produkte-kraftstoffeinspritzung-diesel-rail-banner.jpg, 30th of June 2020

[35]   Robert Bosch GmbH, press release illustration, on
https://www.bosch-mobility-solutions.com/media/global/products-and-services/passenger-cars-and-light-commercial-vehicles/powertrain-solutions/gasoline-direct-injection/fuel-rail/thumbnail_di-fuel-rail.jpg, 30th of June 2020

[36]   Liebherr   Common   Rail   System   11.2   specification   as   seen   on
https://www.liebherr.com/shared/media/components/images/injections-systems/common-rail-systems/liebherr-fuel-injection-system-engine-block-3d.jpg

[37]   "High-Performance and Fuel-Efficient Common Rail Systems by Liebherr", Advertisement and Datasheet by Liebherr in 2017 as seen on https://www.liebherr.com/external/products/products-assets/252089/liebherr-common-rail-systems.pdf

[38]   Internal documents of Hyundai Motor Europe Technical Center GmbH, Rüsselsheim Germany

[39]   Press Release for General Motors a thttps://gmauthority.com/blog/wp-content/gallery/gm-6-2l-v8-small-block-lt1-engine/gm-6-2-liter-v8-small-block-lt1-engine-04.jpg 30th June 2020

[40]   GDI parameter design pump schematics and volume data by Hyundai Motor Europe Technical Center

[41]   TD Spegar, SI Chang, S Das, E Norkin; "An Analytical and Experimental Study of a High Pressure Single Piston Pump for Gasoline Direct Injection (GDI) Engine Applications"; SAE-Technical paper, 2009-01-1504, 2009

[42]   R v Basshuysen, F Schäfer; "Ottomotoren mit Direkteinspritzung",   3rd edition; Springer Verlag

[43]   W Willems, M Pannwitz, M Zubel, J Weber, „Oxygenated Fuels in Compression Ignition Engine" in „Motorentechnische Zeitschrift" in March 2020, p.28

[44]   S Fitzner; „High Pressure Pump"; European Law Patent (Application) Form; EP3124783, date of filing 6th November 2015

[45]   "Bosch Mediaspace" (Press material published by Bosch as seen on 26th of June 2017)

[46]   S Fitzner, "Drive Torque Measurements of High Pressure Pumps", Diploma Thesis written at University of Applied Science Gießen-Friedberg October 2011

[47]   S Fitzner, Johannes Ullrich; "Unit Pump as solution for Cost Reduction in Diesel Engines"; presentation and paper on Hyundai Motor Group Conference 2014

[48]   A Wieland, E Achleitner, A Lyubar; "Raildruckbasierte Diagnosefunktionen für Benzin-Direkteinspritzsysteme"; presensation and paper on ATZ Expertenforum Powertrain 20th October 2020; p.2

[49]   "XL3 Injector" by Continental as seen on http://www.conti-online.com/www/iaa_com_en/general/2013/highlights_en/xl3_injektor_en.html on 27th July 2017

[50]   MA Shost, MC Lai, B Befui, P Spiekermann, DL Varble; "GDI Nozzle Parameter Studies Using LES and Spray Imaging Methods"; SAE-Technical paper; 2014-01-434, 2014

[51]   K. Aschmoneit, N. Iannucci, C.Yanik; "Mehrfacheinspritzung zur Vermeidung von Ölverdünnung"; presentation and paper on Expertenforum Powertrain 20th of October 2020; p.8

[52]   B Befrui, G Hofmann, P Spiekermann, WF Piock; "A comparative study of the fuel pressure and temperature effect on GDI Multi hole Spray", presentation and paper on "10. Tagung Benzin und Direkteinspritzung 2016"

[53]   "Common Rail System mit Magnetventilinjektoren" as seen on www.bosch-mobility-solution.de (as seen on 19th June, 2017)
        http://www.bosch-mobility-solutions.de/de/produkte-und-services/pkw-und-leichte-nutzfahrzeuge/antriebssysteme/common-rail-system-magnet/

[54] M Härtl; „Potenziell CO_2-neutrale Kraftstoffe für saubere Ottomotoren", in „Motorentechnische Zeitschrift" (MTZ), July 2017

[55] M Härtl; „Oxymethylether als potenziell CO_2- neutraler Kraftstoff für saubere Diesel Motoren, in „Motorentechnische Zeitschrift" (MTZ) February 2017

[56] U Pfisterer; "Ottokraftstoffe incl. Ethanol im deutschen Markt" from „Uniti Mineralölforum" on 11th October 2016

[57] K Wilbrand; „Anforderungen und Potential von gasförmigen Kraftstoffen" from „Uniti Mineralölforum" on 11th October 2016

[58] S Dörr; „Potential von Biokraftstoffen und Regularien" on behalf on Neste Oil on Uniti Mineralölforum on 11th October 2016

[59] H Aatola, M Larmi, T Sarjovara; "Hydrotreated Vegetable Oil (HVO) as Renewable Diesel Fuel: Trade-off between NOx, Particulate Emission and Fuel Consumption of a Heavy Duty engine" by of Helsinki University of technology and as shown in SAE paper 2008 – 01-2500

[60] G Richter und H Zellbeck; „OME als Kraftstoffersatz im PKW-Dieselmotor", in „Motorentechnische Zeitschrift" (MTZ) December 2017, p.66 -72

[61] A Konzack; "Latest Findings in Fuel Quality Around the World" by SGS from "UNITI Mineral Oil Congress" on 14th & 15th April 2015, p.6 ff.

[62] "Worldwide Winter Diesel Fuel Quality Survey 2014" by "Infineum International" in 2014 as seen on https://www.infineum.com/media/80722/wdfs-2014-full-screen.pdf on 25th December 2015

[63] HD Baehr; S Kabelac; "Thermodynamik", Springer-Verlag Berlin-Heidelberg, 21.Auflage,

[64] H Siegloch; „Technische Fluidmechanik", Springer Verlag Berlin-Heidelberg, 9.Auflage,

[65] BE Poling; "The properties of Gases and Liquids" ; 5th Revision; McGraw-Hill Companies; p. 154ff

[66] S Alhadou; "Evaluation of different fuel feed pump technologies for CR-Diesel Engines", Master-Thesis, Technical University of Darmstadt, 2015

[67] A Kapp; „CO2 Reduction of Diesel Powertrain by Consequent Optimization of Vehicle Subsystems" from Powertrain 3.0 on 14th of July 2014

[68] S Fitzner; "Hochdrucksystemoptimierung zur CO2-Reduktion", paper and presentation, from ATZ Reibungsminimierung im Antriebsstrang Conference on 28th of November 2016

[69] H Elmqvist, SE Mattsson, H Olsson, J Andreasson, M Otter, C Schweiger, D Brück; " Real-time Simulation of Detailed Automotive Models", paper on 3rd International Modelica Conference on 3rd November 2003, p.29ff

[70] T Fink, H Bodenstein; "Möglichkeiten der Reibungsreduktion in Kettentrieben", in "Motorentechnische Zeitschrift (MTZ)", p.72, July 2011

[71] Documentation to Bosch Moehwald Injection test rig CA4000 with EPS835

[72] S Fitzner; "Simulation based optimization of common rail injection systems for CO2 reduction in passenger vehicles", presentation and paper at "Vehicle Performance Conference" on 15th of April 2015

[73] Technical Bulletin No. 118 "HYD BOSCH FUEL PROPERTIES" for LMS Imagine.Lab Amesim by Siemens Industry Software from 2016

[74] Content LMS.AMESIM 15.2 (63896-58725) as published 2017 by Siemens Industry Software

[75] JC Wurzenberger, R Heinzle, A Schuemie, T Katrasnik; Crank-Angle Resolved Real-Time Engine Simulation –Integrated Simulation Tool Chain from Office to Testbed," SAE Technical Paper 2009-01-0589, 2009

[76] D Anguita, F Rivieccio, M Canova, Paolo Casoli, A Gambarotta; "A learning based method for the simulation of combustion process in automotive ICE", paper on "International Combustion Engine Division Spring Technical Conference" 12th May 2003

[77] Documentation to Seminar "Hydraulic components and systems" by Siemens Industry Software from 7.7.2016

[78] J Ullrich; „New method for early injector hardware qualification", presentation and paper on "Benzin und Diesel Direkteinspritzung" by Haus der Technik Berlin, 2016

[79] J Kahlert; "Simulation technischer Systeme"; Vieweg Praxiswissen, 1st edition, p.31 ff., 2004

[80] J Ullrich; „Technologies for injection quantity control in modern common rail diesel engines", presentation and paper on "International Engine Congress" in Baden Baden, 2016

[81] J Ullrich; „Diesel common rail fuel injection systems", seminar presentation at from Hochschule Darmstadt, 28th of May 2015, p.33

[82] S Fitzner, "Noise Reduction of 350bar Gasoline FIE", presentation and paper on Acoustic Society of Korea autumn conference on 1st of November 2018

[83] M Gleß, "Walzkontaktermüdung bei Mischreibung", dissertation, Otto-von-Guericke-Universität Magedburg on 9th of March 2009

[84] S Fitzner, "Simulation based optimization of common rail injection systems for CO2 reduction in passenger vehicles", presentation and paper at "Vehicle Performance Conference" on 15th of April 2015

[85] S Kraft, M Moser, C Büskens, M Echim; „Real-time capable combustion simulation of a dual-fuel engine for hardware-in-the-loop application", Conference Paper on "ATZ Heavy-Duty, On und Off-Highway Motoren 2018", published 13th April 2019

[86] Magneti Marelli press release on https://www.marelli.com/key-product-areas/powertrain/, 30th June 2020

[87] CAD-Data provided by Magneti Marelli of PHP7- GDI High Pressure pump with 1000bar pressure target as distributed on 4th of September 2018

[88] Continental Automotive, Product Information advertising booklet, Version 09/2015;

No. 46-03-0103EN

[89] "Common rail Components" at Denso hompage: https://www.denso-am.eu/products/automotive-aftermarket/diesel-components/common-rail-components/ 1st of April 2019

[90] M Bertsch, "Experimental Investigations on Particulate Number Emissions from GDI Engines", Dissertation at Karlsruher Institut für Technolgie on 9th of June 2016

[91] European Union Commission Regulation 2018/1832 of 5th November 2018 for the purpose of improving the emission type approval tests and procedures for light passenger and commercial vehicles

[92] Hyundai Kia Motor Group released press material

[93] M Schilling; "Betriebsstrategien zur Emissionsreduzierung beim Ottomotor mit strahlgeführten Brennverfahren", Dissertation, Karlsruher Institut für Technologie, 15th of November 2012

B. Nomenclature

BDC   Bottom Dead Center

BMEP Break Mean Effective Pressure

BoB   Best of Best (GDI High pressure Pump)

BtL   Bio(mass) to Liquid

CO   Carbon-monoxide

CO_2 Carbon-dioxide

DIV   Digital Inlet Valve

DMC   Dimethylcarbonat

FIE   Fuel Injection Equipment

IEA   International Energy Agency

GDI   Gasoline Direct Injection

HFRR High Frequency Reciprocating Rig

HIL   Hardware in the Loop

HMETC Hyundai Motor Europe Technical Center GmbH

HPP   High Pressure Pump

LPG   Liquified Petroleum Gas (Low Pressure Gas)

MeFo Methylformiat

NO_X Nitro oxide

NEDC New European Driving Cycle

PCV   Pressure Control Valve

MeUn Metering Unit

OEM   Original Equipment Manufacturer

OME   Polyoxymethylendimethylether

PLDV Passenger Light Duty Vehicle

PtL   Power to Liquid

RON   Research Octane Number

ROZ   Octane number

SFC   Specific Fuel Consumption

SGS   Société Générale de Surveillance

SOC   (Battery) State of Charge

SOH   (Battery) State of Health

Strk   illustrative shortage for Stroke

TDC   Top Dead Center

Tier1   Expression for first in supply chain

WHTC Worldwide harmonized Transient Cycle

WLTP Worldwide harmonized Light vehicles Test Procedure

C. Equation Character

$A_{plunger}$	Plunger area of pressurized surface	m^2
b_e	Specific engine fuel consumption	$\frac{g}{kWh}$
h	Time in hour (industrial established standard frame)	hour
h_{fuel}	Fuel specific enthalpy	$\frac{J}{kg}$
I_{LP_Pump}	Low pressure pump current	$A = \frac{W}{V}$
K	Bulk modulus	$Pa = \frac{N}{m^2}$
K_{est}	Estimated bulk modulus	$Pa = \frac{N}{m^2}$
$\dot{m}$	Mass flow	$\frac{kg}{s}$
$\dot{m}_{fuel}$	Fuel mass flow for engine duty	$\frac{kg}{s}$
$\dot{m}_{injector\_leak}$	Fuel mass flow of injector's servo circuit	$\frac{kg}{s}$
P_{pump_comp}	Hydraulic pump power in respect to fluid compression	$W = \frac{Nm}{s}$
$\dot{m}_{pump\_leak}$	Fuel mass flow for high pressure leak and coolant	$\frac{kg}{s}$
$\dot{m}_{rail\_control}$	Fuel mass flow for rail pressure regulation	$\frac{kg}{s}$
$\dot{m}_{total}$	Fuel mass flow for total fuel system	$\frac{kg}{s}$
n_{eng}	Engine speed	min^{-1}
n_{hullx}	High pressure pump speed at position x within full fuel…	min^{-1}
n_{pump}	Actual high pressure pump speed	min^{-1}
P	Power	$W = \frac{Nm}{s}$
p	Pressure	$Pa = \frac{N}{m^2}$
P_{eng_out}	Engine effective power output	$W = \frac{Nm}{s}$
P_{pump_mech}	Mechanical power consumption (high pressure pump)	$W = \frac{Nm}{s}$
P_{FIE}	Effective FIE power consumption	$W = \frac{Nm}{s}$

p_{inlet}	Pressure at pump inlet (general)	$Pa = \frac{N}{m^2}$
P_{hyd}	Hydraulic power	$W = \frac{Nm}{s}$
$P_{HP_{mech}}$	High pressure pump mechanical power consumption	$W = \frac{Nm}{s}$
P_{LP_hyd}	Hydraulic power demand in low pressure system	$W = \frac{Nm}{s}$
P_{pump_hyd}	hydraulic power consumption (high pressure pump)	$W = \frac{Nm}{s}$
P_{pump_mech}	Mechanical power consumption (high pressure pump)	$W = \frac{Nm}{s}$
p_{rail}	Pressure of common rail	$Pa = \frac{N}{m^2}$
p_{outlet}	Pressure at pump outlet (general)	$Pa = \frac{N}{m^2}$
p_{supply}	Supply pressure on high pressure pump inlet	$Pa = \frac{N}{m^2}$
p_{tank}	Pressure of fuel tank / storage	$Pa = \frac{N}{m^2}$
r_x	Regression factor to full fuel flow hull of HPP	[-]
s_{lift}	High pressure pump plunger lift	m
T_{Eng}	Engine effective torque output	Nm
T_{hullx}	Full load torque at position x within full fuel flow hull	Nm
T_{mean}	Mean drive torque of high pressure pump	Nm
U_{Bat}	Vehicle electrical infrastructure voltage	$V = \frac{Nm}{A\,s}$
$\dot{V}$	Volume flow	$\frac{m^3}{s}$
$\dot{V}_{fuel}$	Volume fuel flow of high pressure pump	$\frac{m^3}{s}$
$\dot{V}_{Geom}$	Geometrical volume fuel flow of high pressure pump	$\frac{m^3}{s}$
X_n	Proportional factor for measurement point significance	[-]
η_{FIE}	Total efficiency of complete FIE system	[-;%]
ρ	Density	$\frac{kg}{m^3}$

D. Appendix

D-1: Measurement reproducibility of component test bench

Results of executed CP Test for measurement reproducibility on applied measurement setup and entire method.

Repeating entire high pressure pump mapping 25 times with Bosch CP4s1. By drive torque characteristic worst know sample due to high dynamic peak torque). After each cycle, test bench stops for 15 minutes with simulated reinstallation of pump during working times, during night test bench stops for 15 minutes and continues. Tolerance field: 2,5 % (±1,25%) for volumetric and total efficiency as reached a CP value of higher than 1,33, which represents a deviation lower than 13ppm.
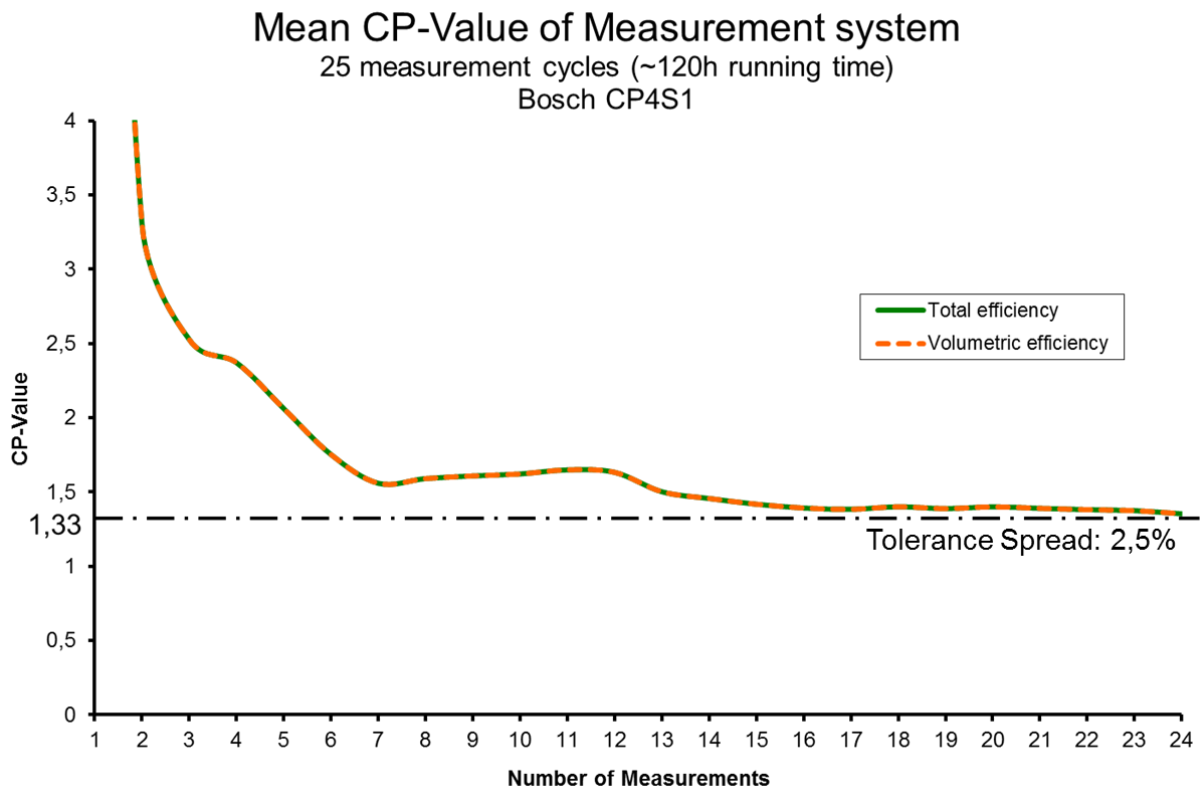

Figure A-01: CP value verification of the high pressure performance measurement system

Detailed analysis of major performance information (Torque and flow):
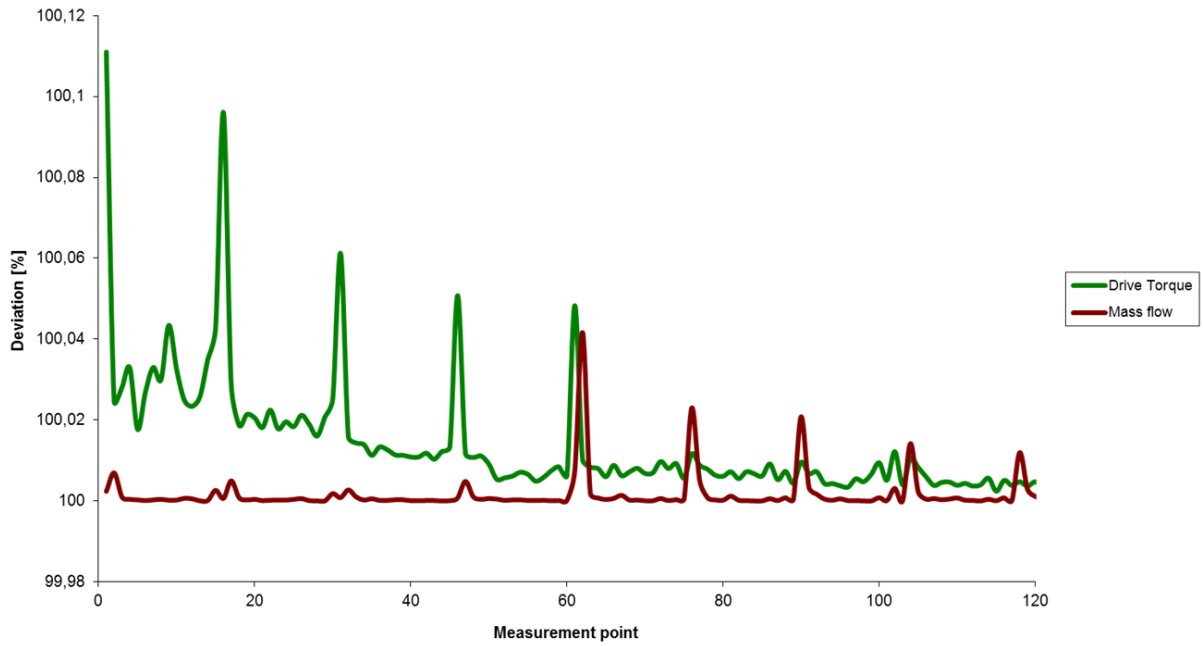
Figure A-02: Detailed CP-value verification of the major measurement parameters for total efficiency calculation

Relative deviation from each points average value shows at specific cycle points highest deviation of max. 0,1% for drive torque and max 0,04% for flow. Specific areas remain to rotation speed of 200rpm to 400rpm, which are not used for analysis purposes. Furthermore, those points represent "harsh" condition and represent a partial overload test for HMETC test procedure. Within for analysis purpose utilized area, torque deviation reach maximum 0,04% and 0,01%.
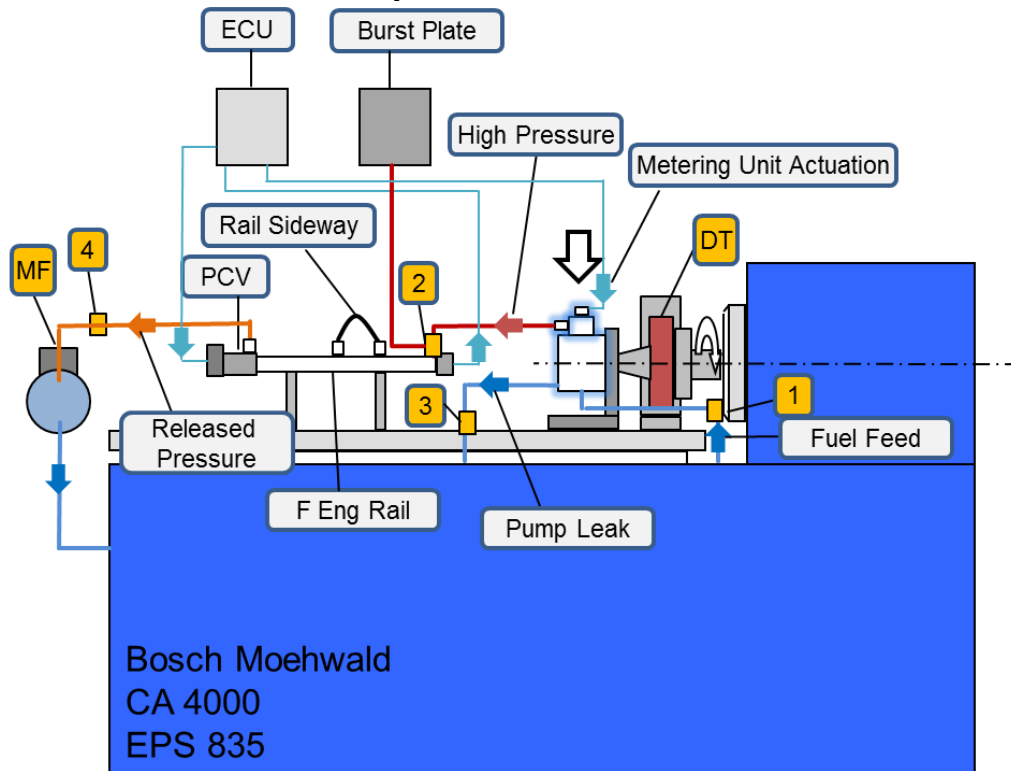
D-2: Detailed Test bench setup

Figure A-03: Schematics of the high pressure pump performance test bench at HMETC

Index	Type	Range
Fuel Feed	Supply Line for Pump Sample	Typical 3.5 bar relative, Changed when specified
Pump Leak	Return line of pump coolant flow	Direct to fuel storage
F-Engine Rail	High pressure rail equipped with Rail pressure sensor and pressure control valve (PCV)	Max. 4000bar Volume: (330 mm³) OR Kefico Kappa Rail for GDI Pump
Released Pressure	Flow after pressure control valve	Direct to Coriolis, up to 200°C
PCV	Pressure control valve	Max 2.500bar OR 3x GDI injectors
ECU	Engine Control Unit	Bosch EDC17 OR IAV FI2RE OR KEFICO HNB
Burst Plate	Safety System for pressure release	Depending on pump sample
High Pressure	High Pressurized Flow	2500 bar and higher
Metering Unit	Metering of high pressure pump	PWM Or Digital Inlet valve Energizing
DT	Drive Torque Flange	Kistler 4505B ±500Nm
MF	Coriolis Mass Flow Meter	Siemens Sistrans 0-150 kg/h
1	Inlet Pressure Inlet Temperature	0-10 bar -40 – 120°C
2	High Pressure Sensor	0- 3000 bar
3	Return flow temperature Return flow volume	-40 – 120° 0 – 250 ltr /h
4	Coriolis inlet Temperature	0 – 300°C

Table A-01: List of used sensors for high pressure pump performance measurement

D-3: Generic gasoline simulation system

Figure A-04: Total model overview for generic gasoline direct injection system in AmeSim

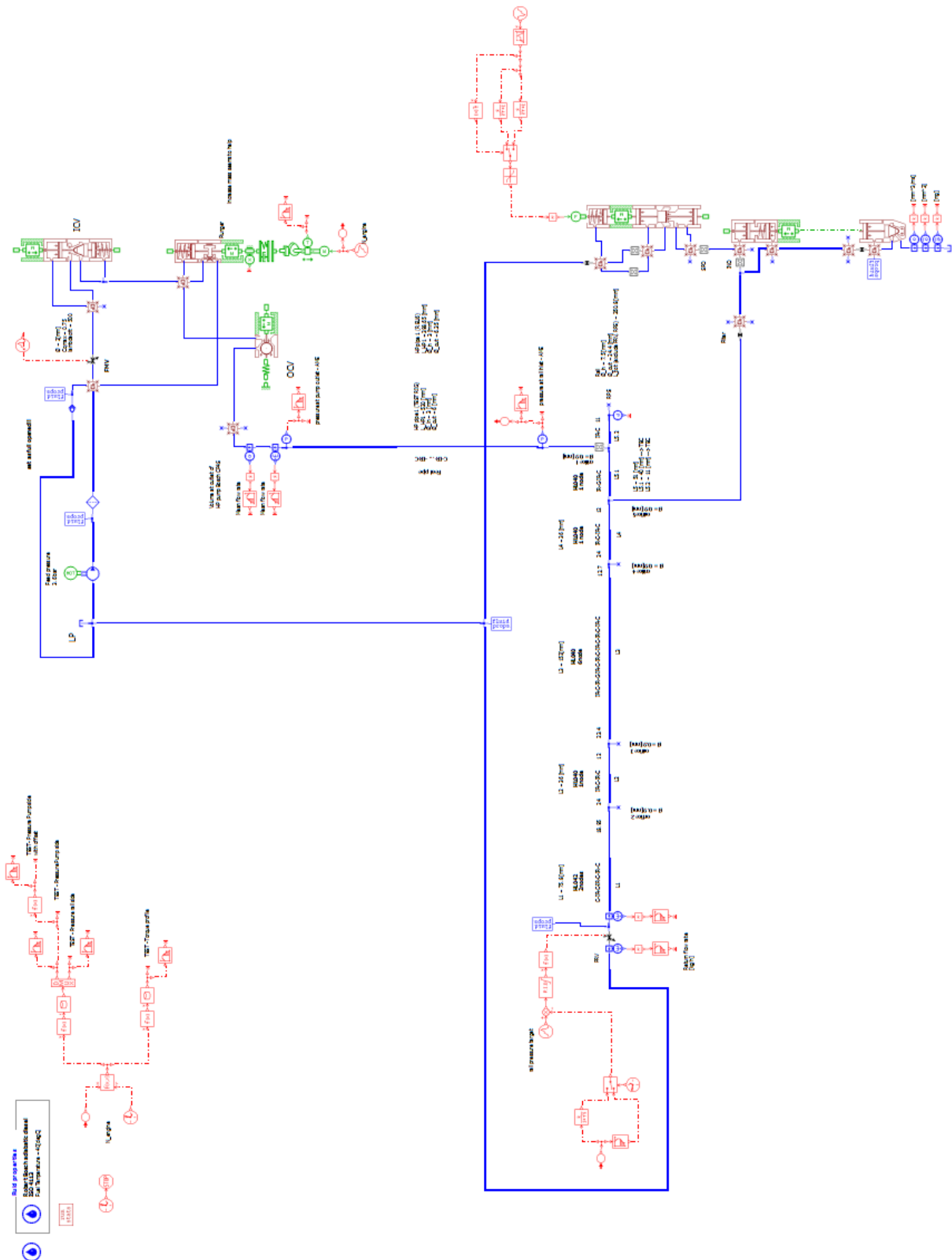## D-4: Generic common rail diesel simulation system

Figure A-05: Total model overview for generic common rail diesel system in AmeSim